A PROTEOMIC AND BIOCHEMICAL APPROACH TO UNDERSTANDING THE MODE OF ACTION OF A NOVEL CLASS OF INSECTICIDE

Thesis submitted in accordance with the requirements of the

University of Liverpool

for the degree of

Doctor in Philosophy

by

GERARD POWELL

SEPTEMBER 2008

Acknowledgements

I would like to express my thanks to everybody who has supported me throughout the duration of this project.

I would like to thank my supervisor Prof. Huw Rees for all of his help during this project and for sharing his wealth of scientific knowledge and expertise.

I would also like to thank Dr Deborah Ward and Mr Mark Prescott for their proteomics expertise, Dr Mark Willkinson for help with protein fractionation techniques, Prof. Mike White and Dr Dave Spiller for help with live cell imaging techniques and everybody in lab C for their help and good humour over the course of this project.

ABSTRACT

In order to control insect populations that are resistant to the currently used insecticides, new compounds with completely different modes of action need to be developed. One such novel insecticide is Pyridalyl; it shows high specificity towards lepidopteran pests, no phytotoxicity and it is capable of controlling lepidopteran populations that are resistant to the currently used insecticides. The main aim of this project was to elucidate the mode of action of Pyridalyl using biochemical and proteomic techniques.

A live cell imaging approach showed that Pyridalyl causes cytotoxicity in *Bombyx mori* cells in a dose-dependent manner, and also that pre-incubation with general cytochrome P450 inhibitors (1-ABT & PBO) protects the cells from the cytotoxic effects. In a complementary investigation using radiolabelled Pyridalyl, it was shown that the metabolism of Pyridalyl by *Bombyx mori* cells yields three major metabolites and that general cytochrome P450 inhibitors completely prevent the metabolism of the insecticide. This lead to the hypothesis that Pyridalyl is metabolically activated by at least one, possibly several, cytochrome P450s and without this metabolism the insecticide is incapable of causing cytotoxicity. Differences in the proteomes of Pyridalyl-resistant and –sensitive *Spodoptera frugiperda* cells were assessed using difference gel electrophoresis (DIGE) to possibly reveal leads as to the molecular action of Pyridalyl. Two members of the thiol peroxiredoxin family of antioxidant enzymes were up-regulated (2.3- & 1.9-fold) in the Pyridalyl resistant cell line. Further proteomic studies examining the effects of Pyridalyl on protein profiles in *B. mori* larvae and BM36 cells, showed an up-regulation of thiol peroxiredoxin, members of the Hsp70 family, and various subunits of the proteasome in Pyridalyl-treated insects and cells. Based on evidence that a P450 is involved in Pyridalyl action and that xenobiotics frequently up-regulate such proteins, the effect of Pyridalyl on a microsomal sub-proteome was examined by a 1D-PAGE coupled to an iTRAQ approach.

The up-regulation of antioxidant enzymes and the proteasome lead to the theory that Pyridalyl, following metabolic activation by a cytochrome P450, causes oxidative stress within treated cells, resulting in necrotic cell death. Attempts to measure the levels of reactive oxygen species within Pyridalyl-treated cells proved unsuccessful. However, the effects of oxidative stress, i.e. oxidative damage to proteins, was measured using the antibody based protein oxidation detection assay Oxyblot™. Using this assay, it was shown that Pyridalyl-treated cells exhibit a 1.6-fold greater level of oxidative protein damage than untreated cells.

Although no Pyridalyl-modulated cytochrome P450s were identified during this work, it was conclusively shown that the metabolism of Pyridalyl by a P450 is essential for the insecticide to show any cytotoxicity. Pyridalyl-resistant and –treated cells and larvae showed an up-regulation of antioxidant enzymes, the proteasome and general stress proteins. Also, Pyridalyl-treated cells showed greater levels of oxidative protein damage when compared to untreated cells. Thus, this work leads to the hypothesis that following metabolism by a cytochrome P450, a metabolite of Pyridalyl causes oxidative stress within treated cells, which leads to oxidative damage to proteins, lipids and DNA, that then ultimately leads to necrotic cell death.

CONTENTS

CHAPTER 1

INTRODUCTION

1.1 GENERAL

Insects (class Insecta) are a major group of Arthropods and are one of the most successful groups in the Animal Kingdom, with over a million described species. Insects may be found in nearly every environment on the planet; the possession of a hard chitinous exoskeleton provides protection from predators and water loss, enabling their survival in the most extreme environments. Insects can be beneficial to humans and the environment; bees, wasps, butterflies and ants, for example, play an important role in pollinating flowering plants. Insects produce many commercially important substances such as honey, wax and silk and scavenging insects, such as beetles, are important in the recycling of biological materials. Insects are important vectors of disease and plant pests, but their resilience and success has proven problematic in the ability to control those that are responsible for the spread of disease (e.g. mosquitoes) and ones that have a detrimental effect on agriculture (e.g. caterpillars and moths).

With the global population expected to reach 8 billion within the next 25 years and around 40% of those relying on agriculture for their livelihood, crop protection has become a major problem. Without the use of crop protection products, such as insecticides, around 40% of the worlds crops would be lost to insect pests. Of particular concern is the emergence of insecticide-resistant strains of crop pest. There is, therefore, an increasing demand for the development of new insecticides that work in different ways to existing insecticides i.e. having novel modes of action.

1.2 Lepidoptera

The order Lepidoptera is one of the largest orders in the class Insecta and contains both butterflies and moths. There are about 180,000 described species of Lepidoptera, around 10% of all described species of living organisms. Lepidopterans are members of the Holometabola and, as such, undergo complete metamorphosis, as part of a four-stage life cycle of: egg – larva (caterpillar) – pupa – butterfly or moth (Figure 1.1).

Lepidopteran larvae generally feed on the foliage and other parts of living plants and, consequently, can be in direct competition with man, requiring counter-measures and control. Some Lepidoptera are beneficial, many are aesthetically pleasing, and most, through their association with vegetation, reflect the ecological stability of natural environments.

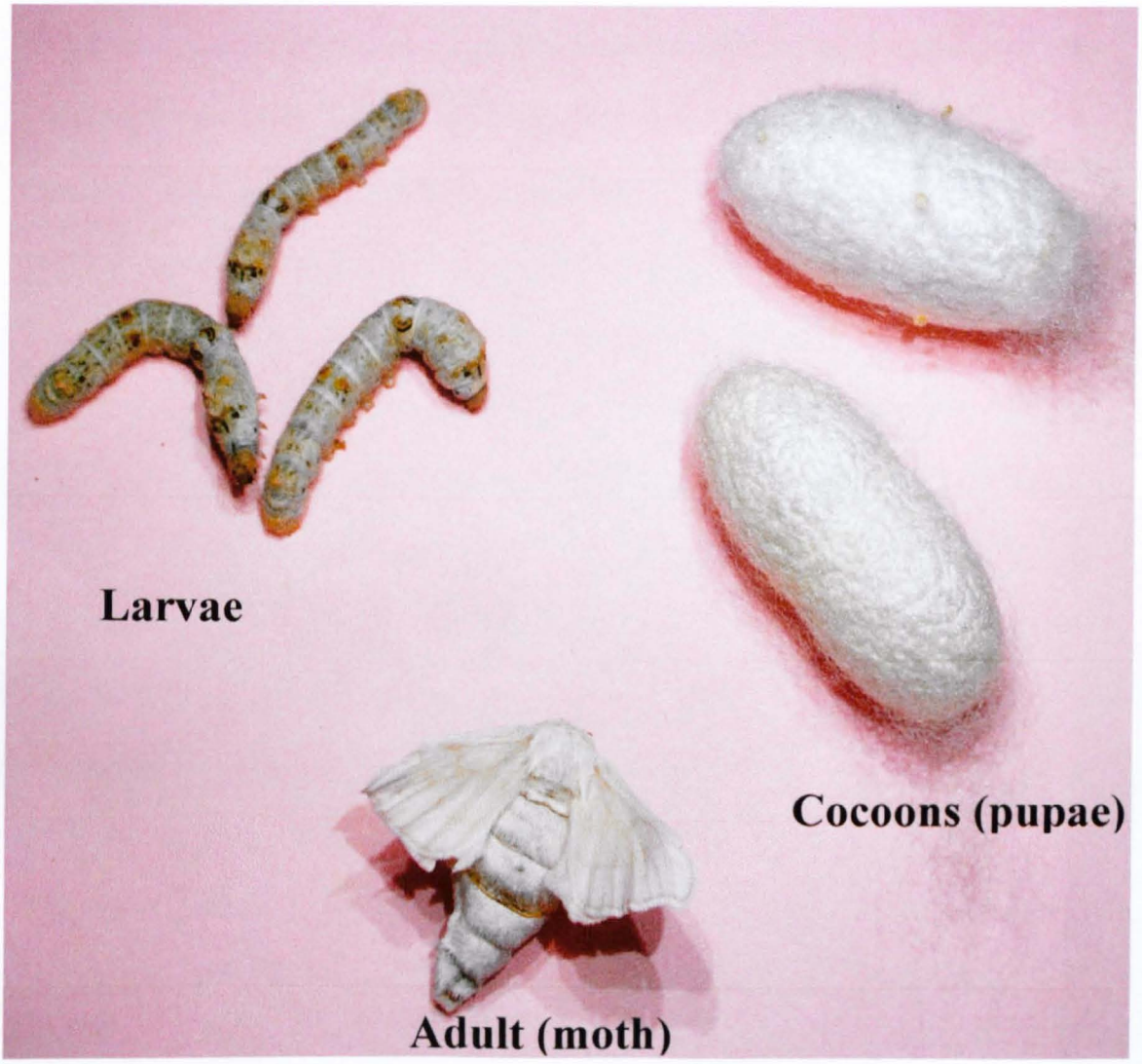

Figure 1.1 Stages in the life cycle of the Lepidopteran *Bombyx mori* (silkworm).

1.2.1 Beneficial lepidoptera

The adults of most Lepidopteran species make some sort of contribution to the pollination of flowering plants. Tobacco flowers are usually pollinated nocturnally by species of Sphingidae, such as the tobacco hornworm moth, *Manduca sexta* (Goyret and Raguso, 2006). Many Lepidopteran larvae spin silken cocoons within which they pupate. The cocoons of species in the superfamily Bombycoidea are especially well developed and have come to be exploited by man for their silk. The classical commercial silkworm is *Bombyx mori.* Lepidoptera themselves can be used as agents of biological control, the classic example being the use of the cactus moth (*Cactoblastis cactorum*) to control *Opuntia spp.* (prickly pear) in Australia (Raghu and Walton, 2007). Increases in human population combined with advances in technology have subjected the ecosystems of the world to pressures with which they were never adapted to cope. There is, therefore, a need to develop techniques to monitor changes in these ecosystems, one such technique being the use of indicator species. Insects, due to their diversity, rapidity of generation turnover and therefore susceptibility to change, are ideally suited to this task, particularly phytophagous insects such as Lepidoptera. Lepidoptera are particularly suited, as they can be readily sampled with light-traps and they have been relatively well collected and studied taxonomically (Holloway *et al.*, 1987).

1.2.2 Detrimental Lepidoptera

The majority of detrimental Lepidoptera are those with larvae that feed on foliage. In severe outbreaks by lepidopterous defoliators, crops and trees can be completely stripped of foliage, however, most outbreaks are minor but can severely affect the yields of crops either directly or indirectly, for example by the defoliation of shade trees for cash crops such as coffee (Beer *et al.*, 1997). A number of Lepidopteran

species as well as defoliating plants, compound the issue by scrolling leaf lamina or tying leaves together with silk to form protective cases; for example the cotton pest, *Syllepte derogata* (Ochou *et al.*, 1998). Some Lepidoptera have larvae that are small enough to feed between the upper and lower epidermis of leaves, these 'leaf-mining' pests are a major economic importance; it is estimated that the cocoa pod borer (*Conopomorpha cramerella*) caused the loss of 31% of the cocoa crop in 1994 (Teh *et al.*, 2006). Species from several different families have larvae that bore into the stems of plants, for example the maize borer (*Chilo partellus*) and tuber feeders, such as *Phthorimaea operculella* (potato tuber moth), which is a major potato pest and will also attack tomatoes. Several species will attack fruits, such as *Cydia pomonella* (common apple worm), which feeds on the fruits of apple and pear trees.

1.3 Existing Insecticides

Until the 1850s farmers relied on sulphur-containing compounds and petroleum for use as insecticides; an example of these early insecticides is the sulphur-containing sheep dip used to control sheep scab caused by the parasitic mite, *Psoroptes ovis* (Sargison *et al.*, 2007). One of the first commercially produced insecticides was Paris green (copper acetoarsenite), that was introduced to control the Colorado potato beetle (*Leptinotarsa decemlineata*). The birth of synthetic organic compounds as insecticides occurred in the 1940s with the introduction of p,p'-dichlorodiphenyltrichloroethene (DDT).

Of the world's total land area of 150 million km^2, 10% is under arable production, 55% supports meadows, pastures and forests and the remainder is not suitable for

agricultural use (Devine & Furlong, 2006). Since 1960, the global population has doubled to over 6 billion (UN, 1999), agricultural productivity has risen 2.6-fold, but the arable area under production increased by just 10%. This increased productivity is due, in part, to advancements in the field of crop protection, i.e. insecticides and herbicides.

Each year, around 3 billion kg of pesticides are applied to cash crops worldwide, with a purchase value of nearly £20 billion. Despite the application of pesticides at the recommended dosages, pests still manage to destroy 37% of all potential crops (Pimentel, 2005). In general, each pound sterling invested in pesticide control returns about £4 in protected crops.

1.3.1 Organophosphates

Organophosphates kill animals, both vertebrates and invertebrates, by inhibiting the enzyme cholinesterase. Subsequently, nervous activity is disrupted by the accumulation of the neurotransmitter acetylcholine at nerve endings (Pan & Dutta, 1998). Organophosphates were first recognised in 1854, but their toxicity was not established until the 1930s. Tetraethyl pyrophosphate (TEPP) was the first organophosphate insecticide and was developed in Germany during World War Two as a by-product of nerve gas production (Potter, 1949). Generally, organophosphates are among the most toxic pesticides to vertebrates, however, they breakdown relatively quickly in the environment due to their instability.

Organophosphate insecticides are produced by many of the major agrochemical companies, some of the main products are: Hostathion (triazaphos), Dursban

(chloropyrifos) and Sumithion (fenitrothion, Fig. 1.2). Organophosphates are often used due to the fact that they are cheaper than the modern alternatives.

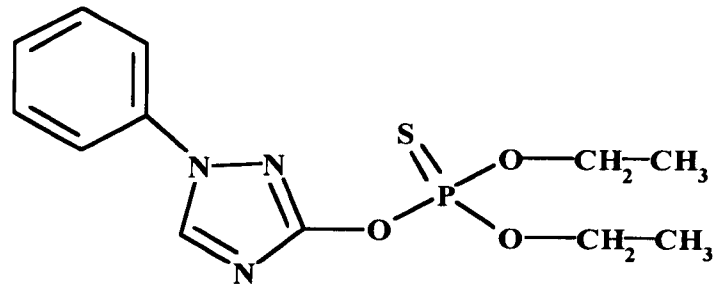

(a)

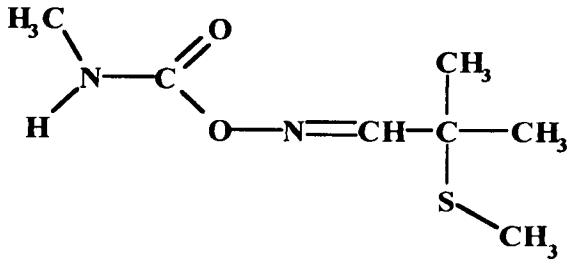

(b)

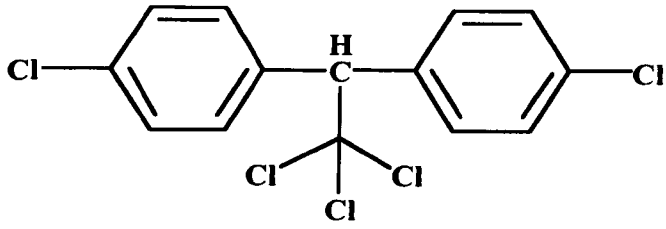

(c)

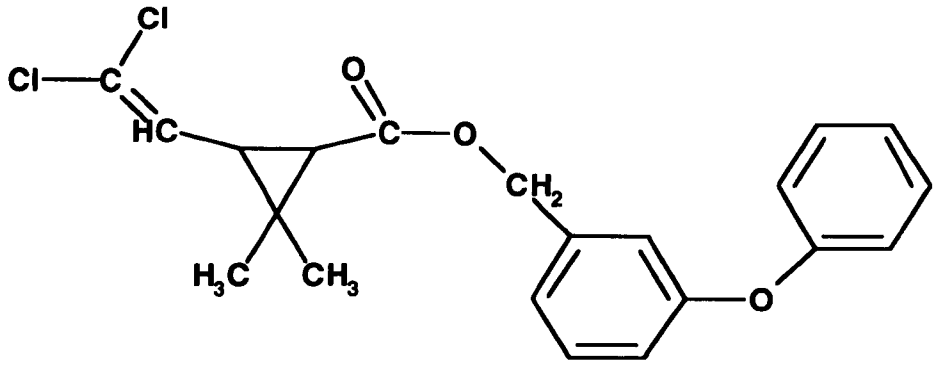

(d)

Figure 1.2 The chemical structures of four common insecticides. (a) triazophos, (b) aldicarb, (c) DDT and (d) permethrin.

1.3.2 Carbamates

The first carbamate, physostigmine (eserine), was isolated from the beans of the poisonous plant *Physostigma venenosum* in 1864. The structure was established in 1925 and was revealed to be an ester of carbamic acid. Its mode of action is similar to that of organophosphates i.e. it is a potent inhibitor of acetyl cholinesterase. Carbamates are mainly systemic insecticides. They are applied to the soil, absorbed by plant roots and distributed throughout their tissues, where insecticidal concentrations are achieved. Some carbamates are also contact insecticides (Gencsoylu *et al.*, 2004).

Carbamates reversibly inhibit acetyl cholinesterase by adding a carbamyl moiety to its active site, preventing interaction with acetylcholine. The carbamyl group is released from the active site by spontaneous hydrolysis, restoring nerve function. Commonly used carbamate insecticides include: Temik (aldicarb), Furadan (carbofuran) and Sevin (carbaryl, Fig. 1.2).

1.3.3 Organochlorines

This group of insecticides was discovered in 1939 when Paul Muller identified the insecticidal properties of the chemical p,p'-dichlorodiphenyltrichloroethane (DDT, Fig. 1.2). DDT also acts on insects' nervous systems, however, unlike organophosphates and carbamates, it doesn't act on acetyl cholinesterase. It causes the permanent opening of sodium channels in insect neurons, leading to continuous nerve stimulation, spasms and death.

DDT is highly fat soluble and tends to accumulate in the fatty tissues of insects and higher animals. As animals lower on the food chain are eaten by other animals higher up, DDT becomes concentrated in the fatty tissues of the predators. This bioaccumulation effect continues until reaching the primary predator of the food chain, which receives the highest dose of DDT. This was a particular problem amongst predaceous birds. DDT is metabolised to DDE, which causes eggshell thinning, making the eggs more susceptible to fracturing (Wiemeyer *et al.*, 1984). DDT is acutely toxic to fish and aquatic invertebrates at low concentrations and can persist 10 times longer in aquatic environments than on land. Other organochlorine insecticides include chlordane, aldrin and heptachlor.

1.3.4 Pyrethroids

Pyrethrin, a crude mixture of pyrethroids, is one of the oldest of the organic insecticides. However, due to its relatively inert nature towards mammals, synthetic pyrethroids are beginning to replace organophosphates and organochlorines as first choice insecticides. Pyrethrins occur in the seed cases of the perennial plant *Chrysanthemum cinerariaefolium*. Both pyrethrins and pyrethroids owe their insecticidal potency to a rapid pharmaco-functional disruption of the insects' neuromuscular system and secondary consequences of this rather than to any direct cytotoxicity (Ray & Fry, 2006). Similar in mode of action to the organochlorines, pyrethroids cause sodium channels in nerve cells to open and remain open, resulting in continuous nerve stimulation, spasm and death.

Mammals are three orders of magnitude less sensitive to the pyrethroids than insects, due to a combination of faster metabolic disposal, higher body temperature (pyrethroids show a negative temperature coefficient of action), and an inherently lower sensitivity of the analogous mammalian ion channel target sites (Vais, 2001). These characteristics have led to pyrethroids becoming the major insecticide class for agricultural and public health use eg pyrethroid-treated mosquito nets are helping to combat the transmission of malaria (Wiseman, 2003). Examples of pyrethroid insecticides currently in use include: Permethrin, Phenothrin and Allethrin (Fig. 1.2).

1.3.5 Insecticide resistance

Insecticide resistance is one of the major obstacles to the control of agriculturally and medically important arthropod pests. Resistance results in increased application frequencies, increased dosages, decreased yields, environmental damage and outbreaks of human and animal diseases (Scott, 1998). Resistance to organophosphate, organochlorine, carbamate and pyrethroid insecticides is conferred by a limited number of mechanisms in all insects analysed to date (Hemingway, 2000). The resistance mechanisms that have been found thus far predominantly involve either metabolic detoxification of the insecticide before it reaches its target site, or changes in sensitivity of the target site, so that it is no longer susceptible to inhibition by the insecticide. The most common resistance mechanisms involve esterases, glutathione S-transferases or monooxygenases (Hemingway *et al.*, 2004).

Esterase-based resistance to organophosphate and carbamate insecticides is common in a range of different insect pests. The major class of esterases involved

is the carboxylesterases, which are enzymes that hydrolyse carboxylic esters (Hemingway & Karunaratne, 1998). The carboxylesterase-based resistance mechanism has been reported for more than 30 different pest species and confers resistance to organophosphates, carbamates and pyrethroids. There are three general mechanisms by which detoxifying enzymes are associated with resistance to insecticides (Wheelock *et al.*, 2005).

(i) Firstly, resistance may arise in populations through selection for insects that possess and express multiple copies of a gene for a carboxylesterase i.e. gene amplification (Field *et al.* 1988). In this case, resistance conferred by carboxylesterases is due, not to an overall increase in catalytic efficiency as would be thought, but to the higher titer of enzyme present that serves as an 'insecticide sink' and delays or prevents interaction between insecticide and target site. Resistance due to this sequestration mechanism may be further heightened by the co-expression of target sites with reduced sensitivity to insecticides.

Carboxylesterase-mediated resistance also occurs through selection for and expression of mutant enzymes. Point mutations result in enzymes with an enhanced capability for insecticide metabolism (Oppenoorth & Van Asperen, 1960). Finally, metabolic resistance may be conferred through enhanced transcription of non-amplified, structural genes for insecticide detoxifying enzymes, i.e. mutations in regulatory genes result in the over-expression of carboxylesterases, and the capacity for insecticide metabolism is enhanced.

(ii) Secondly glutathione S-transferases (GST) can confer resistance to a range of insecticides by conjugating reduced glutathione to the insecticide or its primary

metabolites. As with esterase-mediated resistance, gene amplification leads to an over-expression of GSTs and the resulting enzyme titer results in higher overall activity. Also, mutations in individual GST genes can lead to the expression of enzymes that show increased activities (Grant & Hammock, 1992).

(iii) The final major method of insecticide resistance is the monooxygenase-mediated metabolism of the insecticide or its active metabolites (Scott *et al.*, 1998). Monooxygenase-mediated resistance is due to increased detoxification (or decreased activation, in some cases) of the insecticide (Scott, 1999); this can be due to a change in the catalytic activity of the monooxygenase i.e. due to point mutations and/or an increase in the expression levels of that protein (Oppenoorth, 1984). Monooxygenase based resistance is the most common type of metabolism based insecticide resistance, and unlike target-site resistance, metabolic detoxification has the potential to confer cross resistance to toxins independent of their target site. Increasing levels of insecticide resistance among crop pests have led to the requirement for new insecticides, one of which is Pyridalyl.

1.4 Pyridalyl

The discovery of insecticides with novel modes of action is vital for managing crop pest strains that have become resistant to existing products. Also, toxicological issues have limited the use of many of the main insecticides; therefore, it has become desirable to develop new insecticides that are active against resistant strains, inactive against non-target organisms and safe to humans and the environment. With this in mind, Sakamoto *et al.* (Sumitomo Chemical Co.

Ltd., Japan) synthesised novel compounds and screened for insecticidal activity (Sakamoto *et al.*, 2003).

Their work focused on two known insecticidal compounds, both of which contained a 3,3-dichloro-2-propenyloxy group. From these compounds, several compounds containing the 3,3-dichloro-2-propenyloxy group were synthesised, and 2-(trifluoromethyl)-4-phenoxyphenyl 3,3-dichloro-2-propyl ether was found to show weak insecticidal activity against lepidopteran larvae. These results prompted Sakamoto *et al.* to enhance the insecticidal activity of the lead compound by structural modification; optimisation led to the discovery of a second lead compound that showed increased insecticidal activity and ultimately the discovery of the insecticide, Pyridalyl (2,6-dichloro-4-(3,3-dichloroallyloxy)phenyl 3-[5-(trifluoromethyl)-2-pyridyloxy]propyl ether)(Fig.1.3).

Pyridalyl exhibited excellent activity against lepidopteran pests and thrips species by contact and ingestion. No cross-resistance was found in *Plutella xylostella* or *Heliothis virescense* between Pyridalyl and synthetic pyrethroids or organophosphates and the impact of the insecticide on various important beneficial arthropods was minimal (Saito *et al.*, 2004). Lepidopteran larvae treated with 100ng of Pyridalyl directly to the cuticle are killed within 6h. However, larvae treated with lower doses showed unique symptoms similar to burns at the site of application after moulting (Saito *et al.*, 2006).

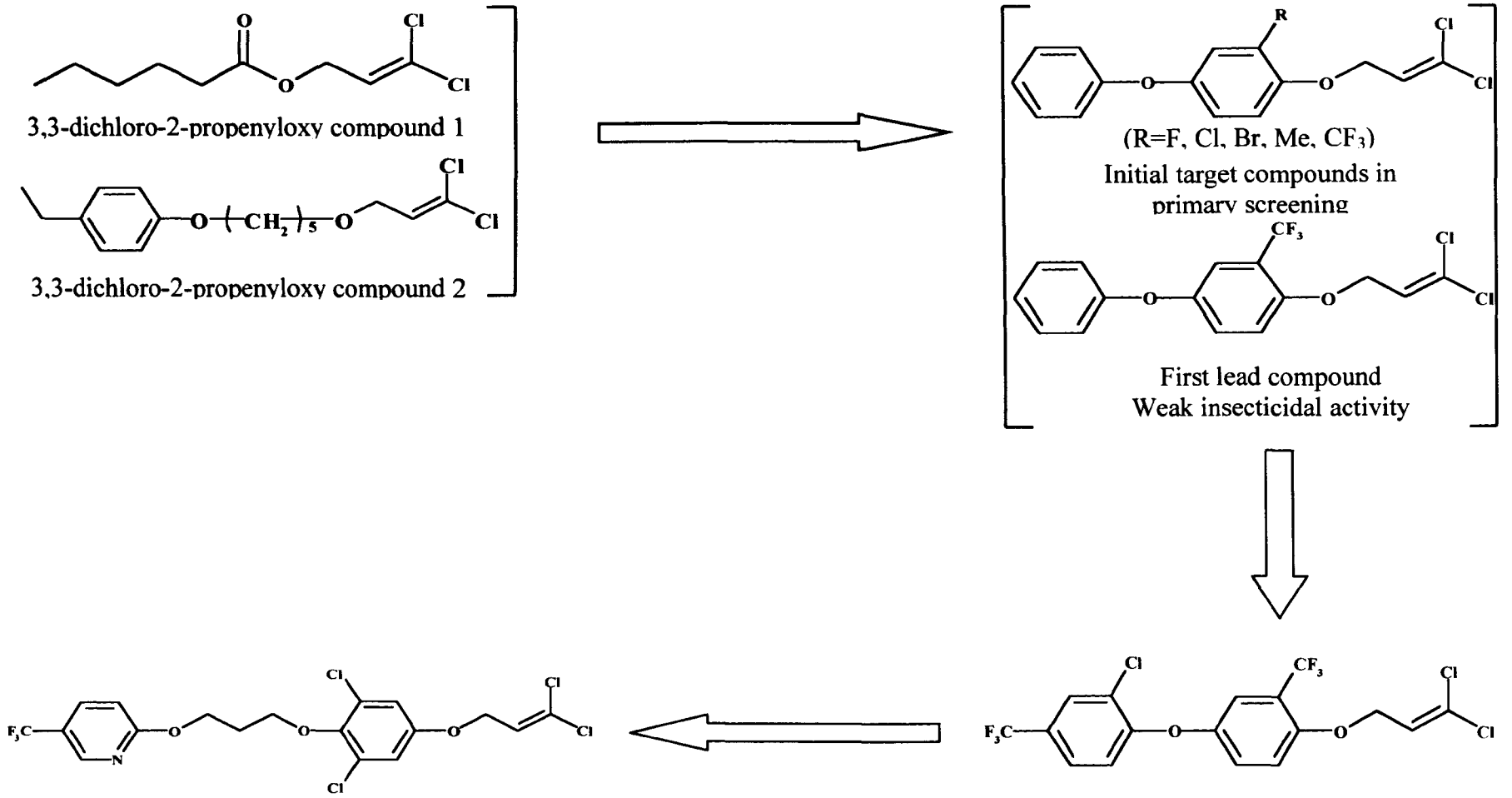

Figure 1.3 Discovery of lead compounds and optimisation to Pyridalyl (Sakamoto *et al.*, 2003).

It is believed that such symptoms are caused by interference with metamorphosis, suggesting that Pyridalyl would suppress populations of lepidoptera even at low doses i.e. toxic doses that would kill the insects outright are not necessarily needed to control lepidopteran populations, death can be brought about by interefering wil metamorphosis (Saito *et al.*, 2004). These unique insecticidal symptoms suggest that Pyridalyl has a novel biochemical mode of action.

Pyridalyl shows high cytotoxicity to insect cell lines (particularly Sf9 cells) and almost no cytotoxicity to mammalian cell lines (Isayama et al., 2005), therefore, Pyridalyl would make an ideal insecticide for controlling lepidopteran pests, as its impact on humans and the environment would be minimal. The effects of Pyridalyl were compared to the effects of several compounds that disrupt mitochondrial respiration (e.g. acequinocyl and rotenone) in Sf9 cells. Whilst compounds that disrupt mitochondrial respiration caused a rapid decrease in the ATP concentrations within the cells, Pyridalyl showed no such effects. It has also been demonstrated that Pyridalyl does not influence the respiration of mitochondria isolated from the lepidopteran, *Spodoptera litura* (Saito, 2005). Therefore, it can be concluded that the cytotoxic effect of Pyridalyl does not involve the direct disruption of mitochondrial respiration. Further experiments have also shown that RNA and protein synthesis are not disrupted by Pyridalyl (Saito, 2005a).

1.5 Cytochrome P450 monooxygenases

Cytochrome P450 monooxygenases form one of the largest superfamilies of enzymes and metabolise a diverse range of substrates including steroids, fatty acids and xenobiotics. The name cytochrome P450 is derived from the discovery of a liver microsomal pigment, which exhibited an adsorption peak at 450nm when reduced and saturated with carbon monoxide (Klingenberg, 1958). Cytochrome P450s have been found in all eukaryotic organisms and some prokaryotes. The recommended nomenclature designates all members of the P450 superfamily with the prefix CYP, followed by a family number, a letter for the subfamily and a number for the individual enzyme (Nelson *et al.*, 1996). For inclusion within a particular family, the amino acid sequence must possess at least 40% sequence homology with an existing family member and at least 55% sequence identity to be assigned to a specific subfamily.

Cytochrome P450s of eukaryotic organisms are all bound to the membranes of the endoplasmic reticulum or mitochondria, whereas most bacterial P450s are water-soluble. The biosynthesis of sterols (cholesterol in animals, ergosterol in fungi and phytosterols in plants) is dependent on P450-catalysed reactions; sterols are essential constituents of the plasma membrane in eukaryotic cells and their biosynthesis seems to be the most ancient role of P450s (Omura, 1999).

1.5.1 Mechanisms of P450 catalysed reactions

The principal function of cytochrome P450s is the monooxygenation of various substrates, which requires molecular oxygen and the supply of reducing equivalents from NADPH or NADH for the reactions. In eukaryotes, the electron

transport systems associated with the mitochondrial and microsomal P450 enzymes are different (Rees, 1996, Fig. 1.5).

In the mitochondrial system, two soluble components, an NADPH-linked flavoprotein and a ferredoxin type iron-sulphur protein, which was named adrenodoxin, catalyse the electron transfer from NADPH to mitochondrial P450s. On the other hand, the microsomal system consists of two membrane-bound components, cytochrome P450 and a cytochrome P450 reductase.

1.5.2 Insect P450 enzymes

The genome of every insect species may carry up to a hundred or so different P450 genes and the enzymes themselves are found in virtually all insect tissues. They participate in many processes: P450s are found in the biosynthetic pathways of ecdysteroids and juvenile hormones, which are at the centre of insect growth, development and reproduction (Feyereisen, 1999). P450 enzymes metabolise insecticides, resulting in bioactivation, or more often, in detoxification. It is well known that many cases of insecticide resistance are due to increases in levels of P450 enzymes or increases in the activities of the enzymes. The induction of P450s by xenobiotics is well established (Waxman, 1999). This is of interest in the agrochemical industry; a certain insecticide may induce a P450 that can metabolise it to a more active form.

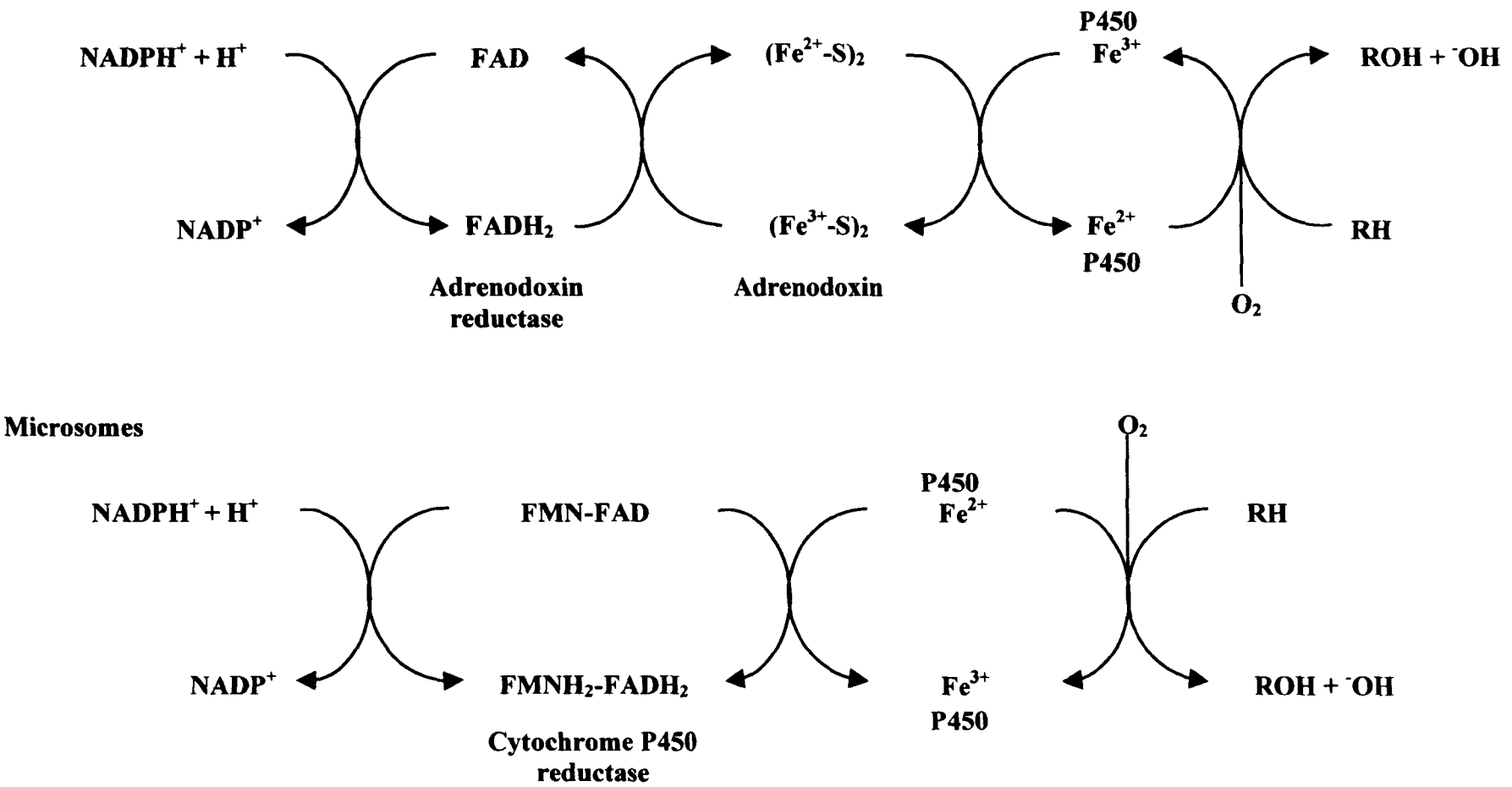

Figure 1.5 Cytochrome P450 electron transport systems (Rees, 1996).

1.5.3 Bioactivation of xenobiotics

The metabolism of xenobiotics, in this case insecticides, to less toxic metabolites is perhaps the best known feature of P450s in insects (Li *et al.* 2007), however, P450s will metabolise xenobiotics irrespective of the eventual fate of the metabolites. There are many cases where P450 enzymes act as anything but detoxification enzymes (Feyereisen, 1999). The metabolism of pesticides to more active toxicants has been at the basis of the action of phosphorothioate insecticides (the activation of P=S to P=O), cyclodiene insecticides (aldrin and heptachlor to their epoxides) and others (Feyereisen 1999).

A number of phosphorothionate triesters, such as parathion and fenitrothion are used as commercial insecticides, and, as with other organophosphorous insecticides exert their toxic action by inhibiting acetylcholinesterase (AChE). The parent phosphorothionates (P=S) are poor acetylcholinesterase inhibitors, however, metabolic activation by cytochrome P450s produces oxygen analogs (P=O), which are potent inhibitors of acetylcholinesterase (Levi *et al.*, 1988, Hodgson & Rose, 2006, Fig. 1.6).

Some P450s also metabolise insecticide synergists, in this instance the P450 enzyme metabolises a chemical to its reactive form which then goes on to inactivate the P450. This inhibition of the P450 prevents it from metabolically inactivating the insecticide. Insecticide synergists currently in use include (i) piperonyl butoxide, which after oxidative metabolism, forms an irreversible complex with the haem iron of P450s, and (ii) 1-aminobenzotriazole (1-ABT), which covalently modifies the prosthetic haem group following P450 metabolism (Feyereisen *et al.*, 1984).

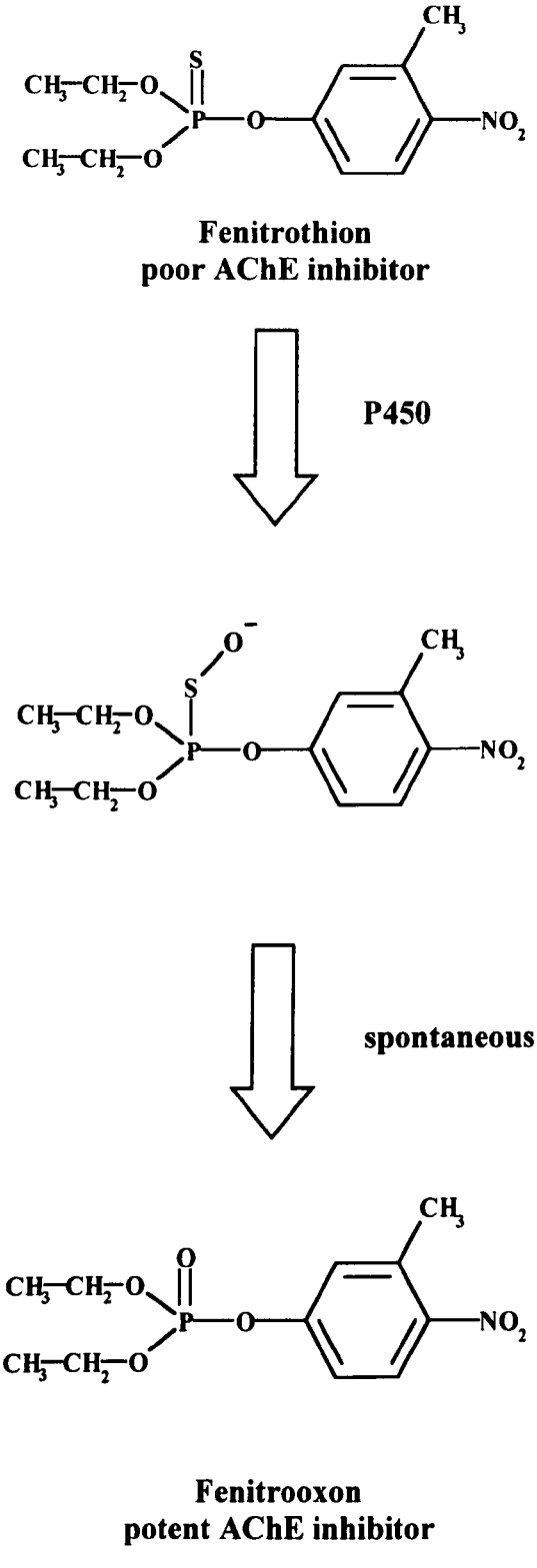

Figure 1.6 Metabolic activation of fenitrothion a organophosphate insecticide (modified from Sultatos, 1991 and Soranno & Sultatos, 1992).

1.5.4 P450 classification

Cytochrome P450s can be divided into four classes depending on how electrons from NADPH are delivered to the catalytic site. Class I proteins require both an FAD- containing reductase and an iron sulphur redoxin and include mitochondrial and some bacterial forms of P450 enzymes.

Class II proteins require only an FAD/FMN-containing P450 reductase for the transfer of electrons and include microsomal (endoplasmic reticulum) forms.

Class III enzymes are self-sufficient and require no electron donor. These enzymes are isomerases rather than monooxygenases and include thromboxane synthetase and prostacyclin synthetase, both of which are involved in the production of eicosanoids.

Finally, P450s from class IV receive electrons directly from NADPH. This classification of the interactions with redox partners is unrelated to P450 evolutionary history (Werck-Reickhhart & Feyereisen, 2000).

1.5.5 P450 structure

Cytochrome P450 enzymes form one of the largest superfamilies of enzyme proteins. However, pairwise sequence identity can be less than 20% across the superfamily and there are only three absolutely conserved amino acids that are shared by all P450 enzymes (Graham-Lorence & Peterson, 1996). Despite the low sequence identity, there is a high level of conservation in the general topography and structural fold among P450s (Graham & Peterson, 1999). Despite the presence of this conserved structural fold among P450s, the primary, secondary and tertiary

structures are sufficiently diverse to accommodate specific substrates and redox partners, and to target the protein to different cellular locations. Features of the primary structures of cytochrome P450 proteins are summarised in Figure 1.7.

In general, a P450 protein consists of four β-sheets and approximately 13 α-helices. The highest conservation is found in the structural core of the protein around the haem and reflects the common mechanisms shared by P450s, involving electron and proton transfer and oxygen activation (Werck-Reichhart & Feyereisen, 2000). The conserved core consists of a four helix bundle and these regions comprise: first the haem-binding loop, containing the most characteristic P450 consensus sequence (Phe-X-X-Gly-X-Arg-X-Cys-X-Gly), located on the proximal face of the haem (Fig. 1.8). The cysteine residue is absolutely conserved and serves as fifth ligand to the haem iron. There is a second conserved motif on the proximal side of the haem (Glu-X-X-Arg), which is probably needed to stabilise the core structure.

The less conserved or variable regions within the P450 structure are normally associated with substrate binding and recognition, redox partner binding or with either amino terminal anchoring or targeting of membrane bound P450 proteins. The substrate binding and recognition regions located near to the substrate-access channel and catalytic site are often referred to as substrate recognition sites or SRSs. These sites are described as being flexible, moving upon binding of substrate so as to favour the catalytic reaction. Other variations reflect differences in electron donors, reaction catalysed or membrane localisation. In eukaryotes, all cytochrome P450s are membrane-bound in either the ER or the mitochondrial inner membrane, and

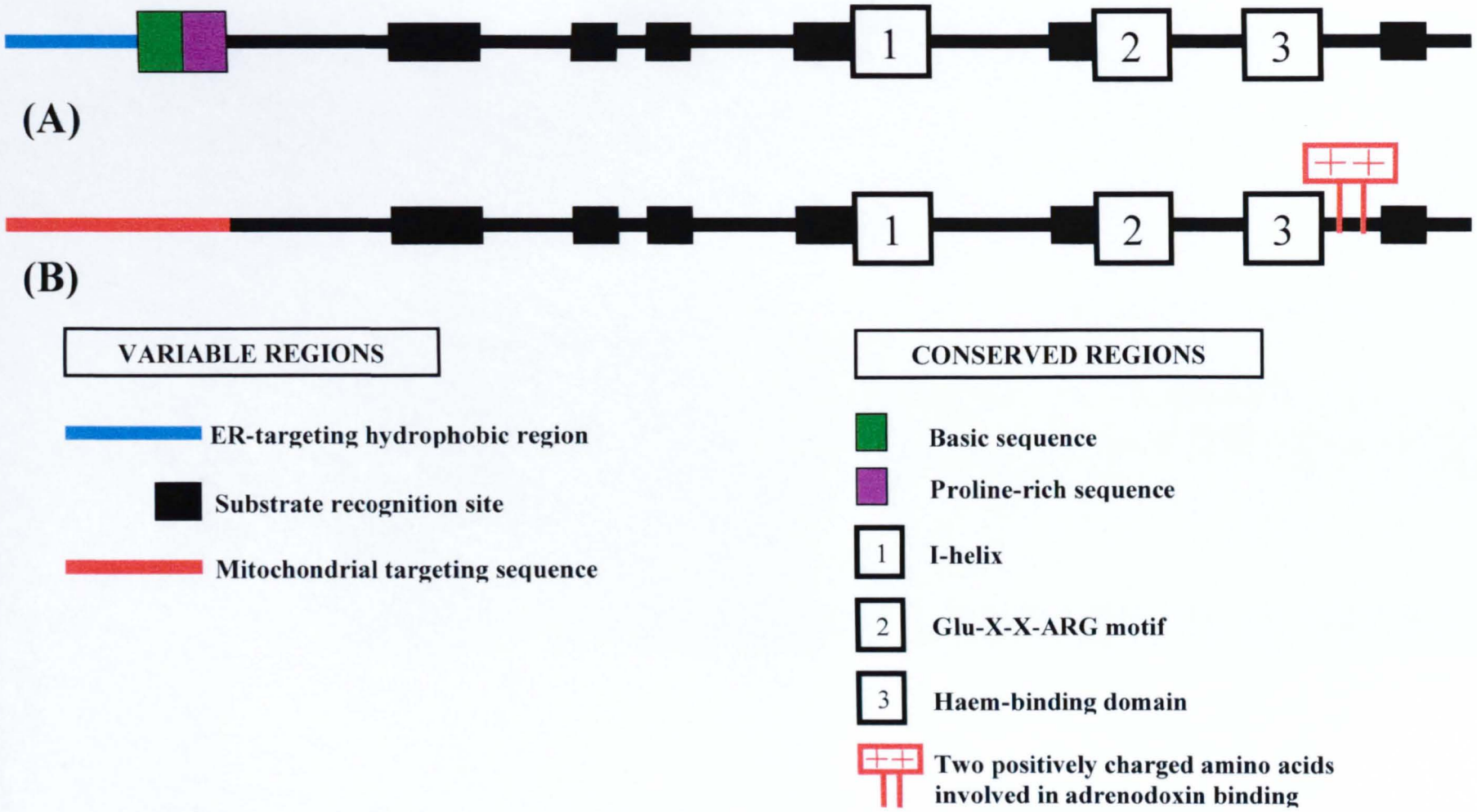

Figure 1.7 Schematic diagram of the primary structures of P450 proteins. Typical features of (A) ER-bound P450 proteins, and (B) mitochondrial-bound P450 proteins (modified from Werck-Reichhart & Feyereisen, 2000).

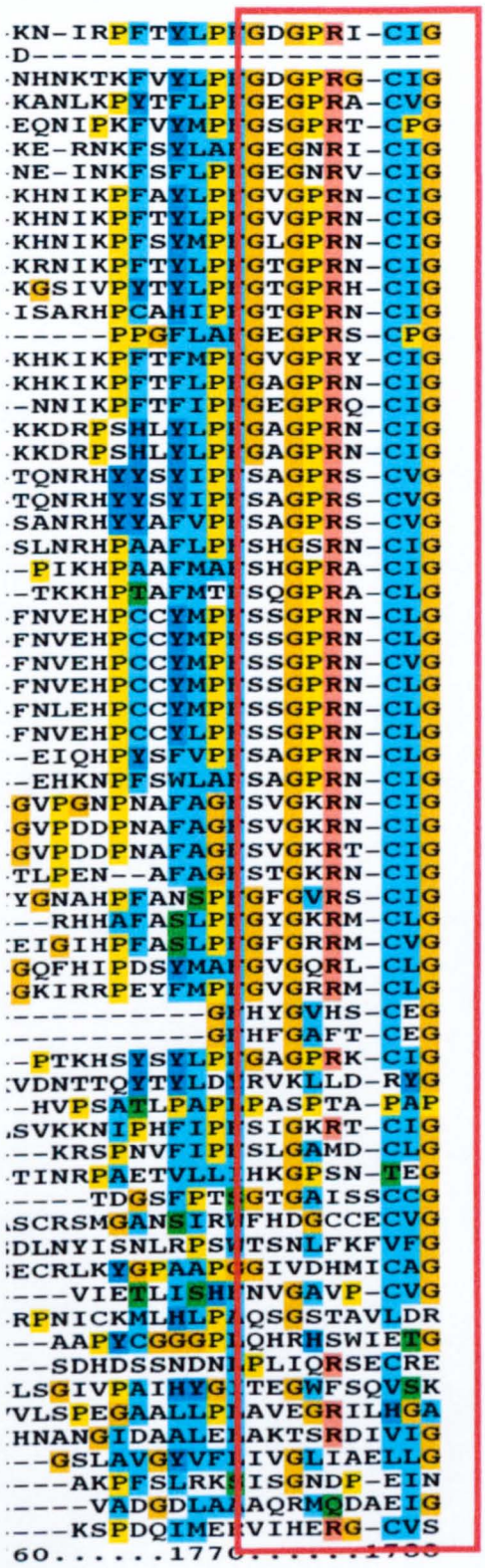

Figure 1.8 Alignment of *B. mori* P450 sequences in the region of the haem-binding loop. Alignment produced from P450 sequences identified from *B. mori* genome sequence.

comparison of the primary structures of microsomal and mitochondrial P450s reveals differences that can be used to predict the cellular location of a P450.

1.5.6 Differences in microsomal and mitochondrial P450s

Mitochondrial P450s are synthesised in the cytoplasm as water soluble precursors with an amino acid signal peptide that is proteolytically removed after import of the precursor into the mitochondria (Omura, 1999). Mitochondrial P450 enzymes also have a motif containing two conserved positively charged amino acids, either Arg-X-X-Lys or Lys-X-X-Lys, which are thought to be involved in adrenodoxin binding. Mitochondrial P450s are not phylogenetically related to bacterial cytochrome P450s (Werck-Reichhart & Feyereisen, 2000).

Microsomal P450s are synthesised on membrane-bound ribosomes of the ER and co-translationally inserted into the membrane (Bar-Nun *et al.,* 1980). They are attached to the ER by amino-terminal hydrophobic anchors. Microsomal P450s (class II P450 enzymes) are extremely diverse and almost all P450 xenobiotic metabolism is due to microsomal P450s (Omura, 1999, Feyereisen, 1999 and Werck-Reichhart & Feyereisen, 2000).

1.6 Aim and Objectives

The overall aim of this project is to elucidate the mode of action of the insecticide Pyridalyl using various biochemical and proteomic techniques.

Specifically, the aims include:

i. To study the metabolism of Pyridalyl by reversed-phase high performance liquid chromatography (HPLC) using radiolabelled Pyridalyl. Any metabolites that are detected will then be collected for later analysis by mass spectrometry.

ii. Differences in protein expression between Pyridalyl-sensitive and –resistant Sf21 cells will be examined using difference gel electrophoresis (DIGE). Differences in protein expression between these groups may give an indication as to the molecular action of Pyridalyl. Any protein spots that are found to be differentially expressed between the two sample groups in each experiment will be removed from replicate, preparative Coomassie blue stained gels. The proteins will then be digested by the proteolytic enzyme trypsin and short sequences will be obtained for the tryptic peptides using tandem mass spectrometry. These sequences will then be searched against several protein databases using various specialised search engines.

iii. The effects of Pyridalyl treatment on protein expression will be examined in two systems; Pyridalyl-treated and control *B. mori* larvae and Pyridalyl-treated and control *B. mori* BM36 cells. It is hoped that any differentially expressed proteins identified between the experimental groups may give clues as to Pyridalyl's mode of action. DIGE will be used in these experiments and any differentially expressed protein spots will be identified as above.

iv. To identify the effects of Pyridalyl on protein expression, with the aim of identifying, in particular, any cytochrome P450s that are induced by Pyridalyl (many xenobiotics have been shown to induce P450s) a sub-proteome from BM36 cells will also be investigated using the non-gel based proteomic technique, iTRAQ. This technique is especially well suited to identifying and quantifying hydrophobic membrane proteins such as cytochrome P450s, as many of the protein solubility problems that plague gel-electrophoresis can be bypassed.

v. In order to examine the effects of Pyridalyl at the whole cell level live cell imaging will be used to examine the effects of Pyridalyl on various insect cell lines. Fluorescent dyes allow us to measure levels of cell death after treatment with varying amounts of Pyridalyl and inhibitors.

CHAPTER 2

MATERIALS & METHODS

2.1 MATERIALS

2.1.1 Solvents

General solvents

Ethanol: redistilled; Department of Chemistry, University of Liverpool.

All other solvents were of AnalaR grade from VWR Ltd., Leicestershire, UK.

HPLC solvents

All HPLC solvents were of HPLC grade from VWR Ltd., Leicestershire, UK and were filtered and degassed under vacuum immediately prior to use.

2.1.2 Water

Water was purified using a Direct-Q System (Millipore Corp., Mass. USA). This system removes ions, bacteria and organic material present in tap water through a reverse osmosis cartridge, followed by an ion-exchange resin cartridge. As a final purification step, the water is passed through a 0.22μm filter as it is drawn from the system. The water produced has a resistivity of 18.2MΩ cm or greater. This water was used for all procedures, including proteomics and molecular biology experiments.

2.1.3 DEPC-treated water

Water used to prepare RNA was treated with diethylpyrocarbonate (DEPC) in order to inactivate ribonucleases. DEPC was added to water to give a 0.1% (v/v) solution, left to stand for 12 hours at 37°C and then autoclaved at 121°C for 15 minutes to remove residual DEPC.

2.1.4 Insecticides

Pyridalyl: technical grade.

[^{3}H]-Pyridalyl: (0.58TBq/mmol) technical grade. See below for position of radiolabel.

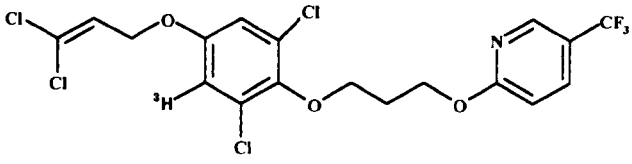

2.1.5 General Buffers

HEPES buffer: 0.037M *N*-(2-hydroxyethyl)piperazine-*N*-(2-ethanesulphonic acid (HEPES, Sigma), 0.3M sucrose (for isotonic buffer) or 0.05M sucrose (for hypotonic buffer), adjusted to pH 7.5.

2.1.6 Scintillation fluids

Optiflow Safe: Fisher Scientific, Loughborough, Leicestershire, UK. Used for on-line HPLC radioactivity monitoring.

Ultima Gold: Perkin Elmer, Beaconsfield, Bucks, UK. Used for static radioactivity counting.

2.1.7 Insects

Bombyx mori (silkworm) were cultured in the insectory from eggs obtained from Dr Silvia Cappellozza, Stazione Bacologica Sperimentale, Padua, Italy.

2.1.8 General reagents

All reagents used for general experiments were of normal laboratory grade and supplied by Sigma, unless otherwise stated. Molecular Biology reagents were usually of high purity or Molecular Biology grade. Proteomics reagents were of the highest purity available and supplied by GE Healthcare Ltd., Bucks., UK.

2.1.9 Culture media

TC-100 Medium containing 0.6g/litre L-Glutamine; Invitrogen Ltd, Paisley, UK.

2.2 GENERAL METHODS

2.2.1 Maintenance of B. mori *insect culture*

The eggs and larvae were maintained in an environment where temperature, relative humidity and photoperiod were controlled. The temperature was 25°C, relative humidity was 70-80% and the photoperiod was 16 hours dark: 8 hours light. Bed cleaning was performed once during the first, second and third instar stages at the end of the moulting period, twice in the fourth instar stage and daily in the fifth instar stage. Larvae were kept in plastic boxes of differing sizes according to their age and number and reared on an artificial mulberry leaf diet, obtained from Italy, according to Cappellozza (2005).

2.2.2 Dissection of insects

B. mori larvae were synchronised at the end of the fourth instar and resynchronised at the beginning of the fifth instar. Larvae were anaesthetised on ice for at least 15 minutes. The larvae were pinned to a wax dissection dish and after a ventral incision, the cuticle was cut open along the length of the larva and pinned back to expose the internal anatomy. The required organ/tissue was excised and rinsed in ice-cold isotonic Hepes buffer (0.037M Hepes, 0.3M sucrose, pH 7.5) prior to homogenisation in an appropriate buffer.

2.2.3 Treatment of B. mori *larvae with Pyridalyl*

The dose of Pyridalyl to be administered via the artificial diet was based on the results obtained for *S. litura* larvae i.e. μg Pyridalyl/g body weight (Saito *et al.*, 2004). Pyridalyl that was to be administered to *B. mori* larvae was dissolved in methanol and added to the artificial diet to give a final concentration of 2μg/g

(w/w). Each larva was given 5g of diet containing pyridalyl, resulting in a final dose of 10μg/larva.

2.2.4 Preparation of subcellular fractions from B. mori *tissues*

The required tissue of *B. mori* larvae was excised and homogenised using a Potter-Elvehjem homogeniser in ice-cold isotonic Hepes buffer. The homogenate was centrifuged at 1,100 x g for 10 minutes at 4°C and the supernatant was re-centrifuged at 12,00 x g for 20 minutes at 4°C. The resulting supernatant (S) was removed, the pellet resuspended in the same buffer and re-centrifuged at 12,000 x g to obtain the mitochondrial fraction. The mitochondrial pellet was washed twice with isotonic Hepes. The original supernatant (S) was centrifuged at 150,000 x g for 90 minutes to obtain a microsomal pellet and cytosolic supernatant. The mitochondrial and microsomal pellets were resuspended in a hypotonic Hepes buffer (0.037M Hepes, 0.05M sucrose, pH7.5) and stored at -80°C for later proteomic analysis.

2.2.5 High-Performance Liquid Chromatography (HPLC)

Reversed-phase HPLC (RP-HPLC) analyses of Pyridalyl and its metabolites was carried out on a Genesis C_{18} Column (15cm x 5mm, particle size 4μm; Jones Chromatography, UK) employing a linear gradient over 40 minutes of 20-100% (v/v) acetonitrile/30mM ammonium acetate at 1ml/min. Solvent was delivered using Gilson model 321 pumps and absorbance was monitored at 267nm on a Gilson model 152 UV/VIS absorbance detector. Radioactivity was detected by an on-line Flo-one/Beta Radiomatic Series A500 scintillation monitor (Canberra Packard).

2.3 Proteomics methods

2.3.1 Bradford protein assay

Protein concentration was determined by the method of Bradford (1976) using the Bradford Protein Assay Reagent (Bio-Rad). A series of protein standards were prepared from known amounts (0.1-1.5 mg/ml) of immunoglobulin G (IgG). 10µl of each protein standard was added to 1ml of Bradford Protein Assay Reagent, which had been previously diluted 1:4 (v/v) with water. 10µl of water was added to 1ml of reagent as a blank. The samples were allowed to equilibrate at room temperature for 10 minutes to allow colour development to occur. The absorbance of the samples was measured at 595nm using a spectrophotometer. A standard curve of absorbance versus IgG concentration was constructed to allow the amount of protein in unknown samples to be estimated from measured absorbance values.

2.3.2 Protein precipitation

The required volume of protein solution was mixed with 5 volumes of 10% TCA in acetone or 100% methanol, and incubated overnight at -20°C. Following centrifugation at 10,000 x g for 5 minutes, the supernatant was discarded and the protein pellet washed in 50µl of ether. The pellet was then centrifuged at 13,000 x g for 15 seconds and the ether removed. The ether wash was repeated before allowing the protein pellet to air-dry.

2.3.3 SDS-Polyacrylamide gel electrophoresis (SDS-PAGE)

A 10% (w/v) resolving gel for Tris-glycine SDS-PAGE was prepared as described by Sambrook *et al.* (2001). 15ml of resolving gel was sufficient for two 0.75mm minigels and was composed of 5.9ml sterile distilled water, 5.0ml 30% acrylamide/bis solution (Severn Biotech), 3.8ml 1.5M Tris (pH8.8), 0.15ml 10%

(w/v) SDS and 0.15ml 10% (w/v) ammonium persulphate. Polymerisation was initiated by the addition of 6µl TEMED (N, N, N', N'-tetramethyl-ethylenediamine; Bio-Rad). The mixture was rapidly but gently swirled and poured between the plates of the Mini-Protean III gel electrophoresis apparatus (Bio-Rad), leaving sufficient space for the stacking gel (the length of the comb teeth plus 1cm). The acrylamide solution was overlaid with isobutanol and left at room temperature for approximately 30 minutes to allow complete polymerization. After this time, the overlay was poured off and the top of the gel rinsed several times with deionised water to remove any unpolymerised acrylamide. The water was drained and any excess water was removed with the edge of a piece of filter paper. A 5% stacking gel was prepared by mixing 5.5ml sterile distilled water, 1.3ml 30% acrylamide/bis solution, 1.0ml 1M Tris (pH6.8), 80µl 10% (w/v) SDS, 80µl 10% (w/v) ammonium persulphate and 8µl TEMED. The mixture was quickly swirled and poured directly onto the surface of the polymerized resolving gel. A clean Teflon comb was immediately inserted into the stacking gel solution and the stacking gel was allowed to polymerise. Protein samples to be analysed by SDS-PAGE (1.0-10µg) were prepared by the addition of an equal volume of 2x SDS gel loading buffer [4% (w/v) SDS; 125mM Tris-HCl, pH6.7; 30% (v/v) glycerol; 0.002% (w/v) bromophenol blue; 2% (v/v) β-mercaptoethanol] and heated for 10 minutes at 95°C to denature the proteins, followed by centrifugation at 12,000 x g for 1 minute. Following complete polymerisation of the gel, the wells were rinsed with deionised water and mounted in the electrophoresis apparatus. Up to 20µl of each protein sample was loaded alongside 10µl of protein standards (PageRuler, Fermentas Life Sciences). The gel was run at 200V in Tris-glycine electrophoresis buffer (25mM Tris; 250mM glycine, pH8.3; 0.1% SDS) for approximately 45 minutes or until the bromophenol blue had reached the bottom of the resolving gel.

2.3.4 Two-dimensional SDS-polyacrylamide gel electrophoresis

The precipitated proteins to be analysed (100µg for analytical gel and up to 2.5mg for preparative gel) were resolublised in 320µl of rehydration solution (8M urea, 2M thiourea, 4% CHAPS, 0.2% Biolytes, 0.05% ASB14) by shaking at room temperature for 2 hours. The solutions were then centrifuged at 8,000 x g for 5 minutes to remove any insoluble material and then applied to the immobilised pH gradient (IPG) strip holder (Bio-Rad). IPG strips (17cm), pH 3-10 non-linear (Bio-Rad), were then placed over the protein solutions and overlaid with mineral oil. Isoelectric focusing was then performed using a Protean IEF cell (Bio-Rad); 10000V for 3 hours followed by 10000V to 60000V/hrs (linear ramp) was used to focus the proteins. Following Isoelectric focusing the IPG strips were allowed to equilibrate for 15 minutes, first in 2% (w/v) dithiothreitol (DTT) and then in 2.5% (w/v) iodoacetamide. A 12.5% or 10% resolving gel was then used for SDS-PAGE. 125ml of resolving gel was sufficient for the preparation of 2 gels and was composed of 52.5ml 30% acrylamide/bis solution (Severn Biotech), 15.6ml 3M Tris-HCl adjusted to pH 8.85, 56.85ml sterile distilled water, 1.25ml 10% (w/v) SDS and 1.25ml 5% (w/v) ammonium persulphate. Polymerization was initiated by the addition of 125µl TEMED. The mixture was poured between the glass plates of the Protean II xi cell gel electrophoresis apparatus (Bio-Rad), leaving sufficient space for the stacking gel. The acrylamide solution was overlaid with butan-2-ol and left at room temperature for 30 minutes to allow complete polymerization. After this time, the overlay was poured off and the top of the gel rinsed several times with water to remove any unpolymerised acrylamide. The water was drained and any excess water was removed with the edge of a piece of filter paper. A 4% stacking gel was prepared by mixing 2.2ml acrylamide/bis solution, 2ml 1.25M Tris-HCl adjusted to pH6.8, 15.4ml sterile distilled water, 200µl 10% (w/v) SDS, 200µl 5% (w/v) ammonium persulphate and 40µl TEMED. The mixture was poured directly onto the surface of the resolving gel, leaving sufficient space for the IPG strip, and overlaid with butan-

2-ol. Following complete polymerization of the gel, its surface was washed with water and the IPG strip placed directly on top. The IPG strip was then overlaid with 1% (w/v) agarose. The gels were then mounted in the electrophoresis apparatus and run at 60mA in glycine electrophoresis buffer (25mM Tris, 250mM glycine, 0.1% (w/v) SDS).

2.3.5 Silver staining

Gels were stained using a silver staining protocol (Yan *et al.*, 2000) that is compatible with mass spectrometric analysis. Gels were fixed overnight [10% (v/v) acetic acid, 40% (v/v) methanol in water]. The fix was aspirated, and sensitiser was applied [30% (v/v) methanol, 0.2% (w/v) sodium thiosulphate, 6.8% (w/v) sodium acetate in water] for 30 minutes. After three 5 minute water washes, silver nitrate solution was applied [0.25% (w/v) silver nitrate] for 20 minutes, followed by two 1 minute water washes. The silver nitrate was then removed and developer solution was added [2.5% sodium carbonate, 0.04% (v/v) formaldehyde] until spots appeared on the gel; when the required level of development had been reached, the developer was removed and stop solution was added [1.46% (w/v) EDTA]. The gel was left in stop solution for 10 minutes before a final three water washes were carried out. All solutions were freshly made, and all steps were performed with gentle shaking. After staining, gels were stored in a small amount of distilled water in large plastic bags at 4°C.

2.3.6 Coomassie Brilliant Blue staining

Immediately following electrophoresis, the gel to be stained was immersed in staining solution [0.1% (w/v) Coomassie Brilliant Blue R-250, 40% (v/v) methanol, 10% (v/v) acetic acid in water]. The gel was incubated at room temperature overnight. The following morning the staining solution was removed

and the gel was destained with a solution of 40% (w/v) methanol and 10% (w/v) acetic acid in water. The destain solution was changed several times, until the background of the gel had cleared. The stained gel was stored in water at 4°C. This method was used to visualise protein bands following SDS-PAGE.

2.3.7 Colloidal Coomassie staining

Following electrophoresis the gel to be stained was washed three times for 5 minutes with water to remove the SDS. ProtoBlue™ Safe Colloidal Coomassie staining solution (National Diagnostics Ltd) was then added to the gel. The gel was incubated overnight at room temperature with gentle agitation. The gel was then destained in water and stored at 4°C. This method was used to visualise protein spots on preparative 2D-PAGE gels.

2.3.8 Gel imaging

Gel images were acquired using a GS-710 Calibrated Imaging Densitometer (BioRad).

2.3.9 In-gel tryptic digestion and peptide extraction

Spots chosen for analysis by mass spectrometry were excised from a preparative Coomassie Blue stained gel using a spot-picking tool and transferred to individual microcentrifuge tubes. The gel plugs were destained by washing in 25mM ammonium bicarbonate, 50% Acetonitrile solution for 15 minutes at 37°C. Once all trace of stain had been removed, the plugs were dehydrated using 100% acetonitrile at 37°C. The gel plugs were then rehydrated overnight in 10µl 50mM ammonium bicarbonate containing 1µl of trypsin solution (0.1µg/µl trypsin in 50mM acetic acid; Promega). The following morning, the liquid was removed

from each gel plug and placed in clean tubes, taking care not to transfer any acrylamide as this can interfere with mass spectrometry.

2.3.10 Mass spectrometry of tryptic peptides

The peptide mixture was made up to a volume of 20µl with 0.1% (v/v) formic acid, before injection into the LC-MS/MS system. The system consisted of an UltiMate liquid chromatograph (LC Packings, Dionex, Surrey, UK) connected to a Q-Tof Micro™ tandem mass spectrometer (Micromass). The liquid chromatograph was set up with a C18 pre-column followed by a 3µm C18 column (15cm x 75µm internal diameter). The solvent system used was a linear gradient of 5% (v/v) solvent B [0.1% (v/v) formic acid, 80% acetonitrile in water] in solvent A [0.1% (v/v) formic acid, 2% (v/v) acetonitrile in water] to 100% (v/v) solvent B over 60 minutes at a flow rate of 200nm/min. The eluted peptides were monitored at an absorbance of 214nm.

Eluted peptides were ionised by electrospray ionisation (ESI). The mass spectrometer was set to perform Data Directed Analysis (DDA), where the quadrupole-MS performs a survey scan from 400-1500 (m/z), searching for doubly or triply charged ions, since these are most likely to be peptides. When such ions were detected, the spectrometer switched to MS/MS mode, and the ion of interest was fragmented in the collision cell. The time-of-flight mass spectrometer detected these fragments providing spectra characteristic of the amino acid sequences of the peptides.

2.3.11 Interpretation of mass spectrometry results

Tandem mass spectrometry spectra were analysed using MassLynx software (Waters, Mass., USA) and InsPect (Tanner *et al.*, 2005). Peptides of interest were selected from the chromatogram. Peptides of weak intensity and peptides of known contaminant masses such as trypsin and keratin were not selected. The fragmentation spectrum for each peptide of interest was smoothed, centred and any doubly charged ions were converted to their singly charged mass. This modified spectrum was then analysed using PepSeq software, by manually assigning amino acids to the intervals between peaks in the fragmentation pattern. The amino acid sequences obtained were then searched using several available search tools (BLASTp and FASTS), against the available protein database (*B. mori* genome database, a local database obtained from Prof. David Heckel, 2006).

2.3.12 Western blotting

Proteins to be analysed by Western blotting were separated by SDS-PAGE as previously described, alongside Prestained Protein Markers (New England Biolabs). Following electrophoresis, proteins were electrophoretically transferred to a nitrocellulose membrane using a Mini-Transblot transfer apparatus (Bio-Rad). The gel, a piece of nitrocellulose membrane (BDH Ltd.) cut to the size of the gel, two pieces of Whatmann 3MM filter paper and two transfer pads were soaked in pre-chilled transfer buffer (1 litre: 14.4g glycine, 3.03g Tris, 200ml methanol) for 30 minutes at 4°C. The cassette of the transfer apparatus was used to assemble a "sandwich" in the following order: transfer pad, filter paper, gel, nitrocellulose membrane, filter paper, transfer pad; it was ensured that each layer was saturated with transfer buffer and that all air bubbles were removed. The cassette was inserted into the transfer apparatus that had been filled with pre-chilled transfer

buffer and an ice pack to maintain a cool temperature. Transfer was allowed to proceed at 70 volts for 1h on a stirrer plate. Following completion of electrophoresis, the nitrocellulose membrane was immersed in blocking buffer [tris-buffered saline (TBS: 20mM tris-HCl, pH 7.5; 500mM NaCl), 5% (w/v) dried milk, 0.05% (w/v) sodium azide] and left stationary overnight at 4°C. The membrane was washed for 2 x 5 minutes with Tween-20 tris-buffered saline [TTBS: TBS plus 0.05% (v/v) Tween-20]. Immunoblotting was performed by incubating the membrane with a suitable primary antibody diluted in TTBS/1% (w/v) dried milk, at room temperature for the appropriate amount of time. The membrane was washed in TTBS for 4 x 4 minutes. The immunoblots were developed by incubation with an alkaline horseradish peroxidase (HRP)-conjugated goat anti-rabbit IgG, at a final dilution of 1:150 in TTBS/1% (w/v) dried milk, for one hour with shaking. The membrane was washed for 5 x 5 minutes with TTBS followed by 2 x 5 minutes with TBS to remove excess secondary antibody and Tween-20.

An equal volume of ECL (Enhanced Chemiluminescence) detection reagent 1 was mixed with detection reagent 2 to give a total volume sufficient to cover the entire membrane. Excess buffer was drained from the membrane and the ECL reagent applied to the side of the membrane with protein bound to it. After incubation for 1 minute at room temperature, excess ECL reagent was allowed to run off the membrane, which was then wrapped in 'Saran Wrap' and secured protein side up in a film cassette. The membrane was exposed to X-ray film (Fuji RX X-ray film) for varying amounts of time, depending on the strength of the signal produced.

2.3.13 iTRAQ

Following trypsin digestion, samples to be analysed by iTRAQ were dried under vacuum and resuspended in 70% (v/v) ethanol and 30% (w/v) triethylammonium bicarbonate (TEAB) before being sonicated to ensure that samples were fully dissolved. Each sample was then transferred to a vial of iTRAQ reagent (mass tags, 114-118; Applied Biosystems, CA, USA) and vortexed before incubating at room temperature for 1 hour. All labelled samples were then combined and diluted 1 in 10 with load buffer A (10mM KH_2PO_4 in 20% acetonitrile in water, pH 2.7). The pH of the sample mixture was then adjusted to between 2.5 and 3.3 by adding orthophosphoric acid drop-wise. Samples were loaded into a Poly Sulfoethyl cation exchange column [The Next Group, Southborough, MA USA (2.1mm x 100mm, 5μm, 200 Å)], attached to a fraction collector (Pharmacia, Uppsala, Sweden). The flow rate was fixed at 0.3ml/min, and the solvent system used was 100% (v/v) buffer A [10mM KH_2PO_4 in 20% (v/v) acetonitrile in water, pH 2.7] for 60 minutes, followed by 70% (v/v) buffer A in buffer B (buffer A plus 1M KCl) for 20 minutes and then 5% (v/v) buffer A in buffer B for 10 minutes, finishing with 100% (v/v) buffer B. A total of thirty peptide fractions were collected using the fraction collector. Eluted fractions were then analysed by LC-MS/MS as previously described.

2.4 Cell culture methods

2.4.1 Maintenance of Sf21 and BM36 cells

S. frugiperda and *B. mori* cells were grown at 27°C in an air atmosphere. Cells were grown in $25cm^2$ (area of flask base) cell culture flasks (TPP Techno Plastic Products AG, Helena BioSciences, Sunderland, Tyne & Wear) in TC100 1X Medium (Gibco BRL). The TC100 was supplemented with 10% (v/v) foetal calf serum (FCS; Gibco BRL, Sf21) or 20% FCS (BM36), which had been heat-inactivated for 1 hour at 65°C. Cells were subcultured two times a week, old medium was removed from the flask and the cells were dissociated from the flask surface by washing with fresh medium. The cell number was determined by counting the cells using a haemocytometer and cell viability was checked using Trypan Blue solution. Cells were seeded into new flasks containing 5ml TC100/10% FCS at a density of $1x10^5$ per 5ml flask.

2.4.2 Preparation of frozen stocks of Sf21 and BM36 cells

For freezing Sf21 cell cultures, a freezing medium was prepared by mixing (by volume) 70% chilled TC100 1x medium, 20% FCS and 10% DMSO (to maintain cellular integrity). Cells in mid-log growth were harvested by centrifugation at 1000 x g for 5 minutes. The cell pellet was resuspended in the freezing medium to obtain approximately $5x10^6$ cells/ml. 1 ml aliquots of cell suspension were transferred into sterile freezing vials. The cells were frozen by placing at -80°C overnight before being transferred to a liquid nitrogen storage bank.

2.4.3 Recovering frozen Sf21 and BM36 cells

5ml of TC100/10% FCS was added to a 25cm^2 cell culture flask for each vial of frozen cells to be thawed. A vial of cells was removed from liquid nitrogen storage and thawed by continuously swirling the vial in 30°C water. When only a small ice pellet remained, the vial exterior was sprayed with 70% ethanol and the contents were quickly transferred to the 25cm^2 flask. The cells were incubated at 27°C until adherent (typically 1-2 hours), and the medium was replaced with fresh medium to remove the DMSO from the cultures. Once the culture approached confluency, the cells were subcultured as normal.

2.4.4 Counting cells using a haemocytometer

A sample of cell suspension was used to prepare duplicate 1:2, 1:5 or 1:10 dilutions in trypan blue solution (0.4% trypan blue in PBS). A small volume of the stained cell suspension was withdrawn using a Pasteur pipette. The tip of the pipette was placed onto the slot of the haemocytometer (Hausser Scientific Company, Horsham, PA; USA) and the cell suspension was allowed to pass under the cover slip by capillary action. The average number of cells per large square of the haemocytometer was determined using a Nikon Diaphot inverted microscope. Cells that had stained dark blue were counted as non-viable. The viable cell number per ml was calculated by multiplying the average number of viable cells per large square by a factor of 10^4 (Hausser Scientific, 2001), followed by multiplication by the dilution factor. To determine the total viable cell number in the original cell suspension, the volume (ml) of the original suspension was multiplied by the viable cell number per ml.

2.5 Molecular biology methods

2.5.1 Isolation of total RNA

All equipment used for the isolation and purification of RNA was treated before use to inactivate ribonucleases (RNases). Diethyl pyrocarbonate (DEPC) is an inhibitor of RNase activity, inactivating RNases by covalent modification. Glassware, plasticware and homogenisers were treated with 0.1% DEPC in water overnight (12-14 hours) at 37°C and autoclaved at 121°C to remove residual DEPC. All solutions were prepared using water that had been treated with 0.1% DEPC and left to stand for 12 hours at 37°C. Solutions were then autoclaved at 121°C for 15 minutes to remove any traces of DEPC. For the preparation of tris buffers, water treated with DEPC was autoclaved before the addition of tris, since DEPC reacts with primary amines and, therefore, cannot be used directly to treat tris buffers.

Total RNA was isolated using Trizol Reagent (Gibco BRL), a monophasic solution of phenol and guanidine isothiocyanate, allowing one-step isolation of RNA. Cells from one 75cm^2 cell culture flask were homogenised in 1ml of Trizol Reagent. Addition of 0.2ml chloroform per 1ml Trizol followed by vigorous shaking and centrifugation (12000 x g for 15 minutes at 4 °C) resulted in the separation of the solution into an aqueous phase and an organic phase. The aqueous phase containing the RNA was transferred to a fresh tube and further purified by the addition of 0.5ml Trizol Reagent and 0.2ml chloroform. The samples were vigorously shaken and centrifuged at 12000 x g for 15 minutes at 4 °C. Following centrifugation, the aqueous phase was transferred to a fresh tube. The RNA was recovered from the aqueous phase by precipitation with 0.7ml isopropanol per 1ml of Trizol Reagent used for initial homogenisation. Samples

were incubated at room temperature for 10 minutes and centrifuged at 12000 x g for 10 minutes at 4°C. The resulting RNA pellet was washed with 75% ethanol and centrifuged at 7500 x g for 5 minutes at 4°C. The pellet was air-dried for 5-10 minutes and the RNA was dissolved in an appropriate volume of DEPC-treated water. The concentration and purity of RNA was determined by measuring the absorbance at 260nm (A_{260}) and 280nm (A_{280}) in a spectrophotometer. An absorbance of 1 unit at 260nm corresponds to 40μg of RNA per ml, whilst an A_{260}/ A_{280} value between 1.8 and 2.0, indicates that the RNA is relatively pure. Total RNA was stored at -80°C in DEPC-treated water.

2.5.2 First-strand cDNA synthesis

First-strand cDNA was synthesized from 1-5μg of total RNA using SuperScript II Reverse Transcriptase (Gibco BRL). First-strand cDNA synthesis was primed with 50ng of random hexamer primers (Roche). The RNA/primer mixture was adjusted to 12μl with DEPC treated water, the mixture was heated to 70°C for 10 minutes and quickly chilled on ice. 7μl of a preassembled mix was added to the RNA/primer mixture to give final concentrations of 1x first-strand buffer (50mM tris-HCl, pH8.3; 75mM KCl; 3mMMgCl_2; Gibco BRL), 10mM DTT and 0.5mM each of dATP, dCTP, dGTP and dTTP. The reaction mixture was gently mixed and incubated at 42°C for 2 minutes, followed by the addition of 200 units of SuperScript II reverse transcriptase. Reverse transcription was allowed to proceed for 50 minutes at 42°C, after which the reaction was inactivated by heating at 70°C for 15 minutes. The samples were then treated with 2 units of *E. coli* RNase H (Gibco BRL) for 20 minutes at 37°C, to degrade the RNA template. First-strand cDNA was stored at -20°C.

2.5.3 Polymerase Chain Reaction (PCR)

2µl of first-strand cDNA (one tenth of the first-strand reaction) served as template in PCR in which various primer sets were used (see section 3.2.2). PCR primers were synthesized by MWG-Biotech (http://ecom.mwgdna.com). The PCR amplification mixture was prepared in 0.5ml thin-walled PCR tubes on ice, in the following order, to give final concentrations of 1x PCR buffer (20mM tris-HCl, pH8.4; 50mM KCl; Gibco BRL), 1.5mM $MgCl_2$, 0.2mM of each dNTP, 1µM forward primer and 1µM reverse primer. 2µl of first-strand cDNA was then added to the PCR amplification mixture and the final volume was adjusted to 49.5µl with sterile distilled water. 0.5µl of *Taq* DNA polymerase (5 units/µl, Gibco BRL) was added. The tubes were transferred directly from ice to a thermal cycler, which had been pre-equilibrated to the initial denaturation temperature (94°C). The exact conditions used are given in the appropriate chapter. The PCR products were analysed by agarose gel electrophoresis.

2.5.4 Agarose gel electrophoresis

PCR products were analysed by electrophoresis on a 1.0% (w/v) agarose gel in 0.5x TBE buffer prepared by dilution of a 5x TBE stock (1 litre: 54g Tris buffer; 27.5g orthoboric acid; 20ml 0.5M EDTA, pH8.0). 0.5g of agarose (Sigma) was heated in 50ml of 0.5x TBE until fully dissolved. The gel was allowed to cool to approximately 60°C before being poured to a depth of 1cm in a gel tray. An appropriate volume of DNA loading buffer [6x DNA glycerol loading buffer: 5ml sterile distilled water, 1.5ml glycerol, 0.25% (w/v) bromophenol blue, 5µl 0.5M EDTA] was added to the DNA sample prior to loading. Gels were run at 50mA in 0.5x TBE. Following electrophoresis, the gel was stained in 0.5x TBE containing 0.5µg/ml of ethidium bromide to allow visualisation of DNA under an ultraviolet

transilluminator. The size of DNA was estimated using a DNA mass ladder ranging from 100bp-1000bp (GeneRuler 100bp DNA Ladder Mix, Fermentas).

CHAPTER 3

INVESTIGATION INTO THE EFFECTS OF PYRIDALYL ON INSECT CELLS

3.1 INTRODUCTION

The cytotoxicity of Pyridalyl towards lepidopteran cell lines has been investigated previously (Saito *et al.*, 2005) and is thought to occur through the same mechanism as its insecticidal activity. The action of Pyridalyl in lepidopteran cell lines is thought to be analogous to its action in whole insects, however this can only be proven through further thesting i.e. comparing the LD_{50} in insects to the LD_{50} in insect cells. Very little is known about the method by which Pyridalyl causes cytotoxicity, although it has been determined that Pyridalyl does not affect mitochondrial respiration (a common cause of cytotoxicity). The mode of cell death experienced by Pyridalyl-treated cells (apoptosis or necrosis) has never been determined.

It has been hypothesised that one, possibly several, cytochrome P450s, metabolically activate Pyridalyl and preliminary data to support this has been produced (data not shown). It has also been possible to to identify the major metabolite of pyridalyl, a possible product of oxidative metabolism by a P450.

With the aim of gaining an insight into the mechanism of Pyridalyl action on insect cells, the viability of Pyridalyl-treated cells was monitored using time-lapse confocal microscopy and the fluorescent viability stain, propidium iodide. Using

such an approach, the dose-response of Pyridalyl was examined, as well as the effects of inhibitors of caspases and of cytochrome P450s. Since caspases are involved in apoptosis (Blank & Shiloh, 2007), use of a caspase inhibitor should provide evidence as to whether apoptosis might be involved in Pyridalyl-triggered cytotoxicity. The uncleavable peptide pseudo-substrate, Z-VAD-FMK (Calbiochem, NJ, USA), was chosen, since it potently inhibits all caspases (Nicholsen & Thornberry, 1997). Since, as indicated above, there is some evidence that cytochrome P450(s) metabolically activate Pyridalyl, the effect of a fairly general cytochrome P450 inhibitor, 1-ABT, on the action of the insecticide was examined. 1-ABT has been shown to inhibit almost most P450 enzymes, in both the microsomal and mitochondrial systems (Dierks *et al.*, 1998). To complement the foregoing studies, the effects of the P450 inhibitors 1-ABT and PBO, on [^{3}H]Pyridalyl metabolism by *Bombyx* BM36 cells was examined over the same time-course as in the above experiments, by reversed-phase high performance liquid chromatography (RP-HPLC). These two complementary approaches should yield a better understanding of the way in which insect cells metabolise Pyridalyl and the way in which it causes cytotoxicity and, ultimately, give a better indication as to Pyridalyl's mode of action.

3.2 METHODS AND RESULTS

3.2.1 Live cell imaging

With the aim of examining the effects of Pyridalyl on lepidopteran cells a live cell imaging approach was used. $1x10^5$ BM36 cells in 2ml of cell culture medium were seeded into each of the wells of a 24 well plate (Corning) and incubated for 2 h at 27°C in an air atmosphere. The duplicate test wells were then treated with Pyridalyl dissolved in dimethylsulphoxide (20µl/well DMSO; Sigma) to give various final concentrations (0.5, 1.0 and 10.0µg/ml final concentrations) and the control wells were treated with DMSO alone. 1µl 1mg/ml propidium iodide was added to each well. Fluorescent images of the cells were taken every 15-30 min for 16h using an LSM510 laser scanning confocal microscope (Zeiss, Germany), where propidium iodide fluorescence was excited using a green helium neon laser (543nm) and detected through a 570nm long pass filter. Data capture and extraction was carried out using LSM510 version 2.1 software (Nelson *et al.*, 2001).

The nucleic acid stain, propidium iodide, is membrane-impermeable and is excluded from living cells, however, when cells die, propidium iodide can then enter them and intercalate with DNA and RNA causing the cells to appear red under the fluorescence microscope. The amount of red fluorescence in a given field is, therefore, proportional to the amount of cell death.

3.2.1.1 Effects of Pyridalyl concentration

A dose-response study of the effects of Pyridalyl on BM36 cells was undertaken. Fig. 3.1 shows images taken from a live cell imaging experiment comparing control cells (treated with DMSO) with Pyridalyl-treated cells (1.0μg/ml final concentration). Very few red cells appear in the control cell images, therefore, there is little cell death, and furthermore, the cells can be seen to divide suggesting that they are healthy. In the images of Pyridalyl-treated cells, red cells can be seen to appear indicating that these cells are dying, and furthermore, the cells have become small, granular and cannot be seen to be dividing. Rather than counting the absolute number of dead cells within a given field, the levels of red fluorescence within the field was used as a proxy for cell death mainly for convenience reasons.

The imaging data can also be plotted graphically; Fig 3.2 shows data from a BM36 cell Pyridalyl dose-response experiment. The data for the different treatments have different starting points due to varying amounts of background fluorescence in each of the wells. The important point to note, however, is the rate of increase in red fluorescence with time, as this can be directly compared between all treatments, whereas the absolute amounts of this fluorescence cannot be compared due to differing levels of background fluorescence. The control cells treated with DMSO, show little change in the amount of red fluorescence with time, therefore, there is very little cell death. The cells that have been treated with varying concentrations of Pyridalyl show increasing amounts of red fluorescence, indicating that there is a direct relationship between dose of Pyridalyl and the levels of cell death.

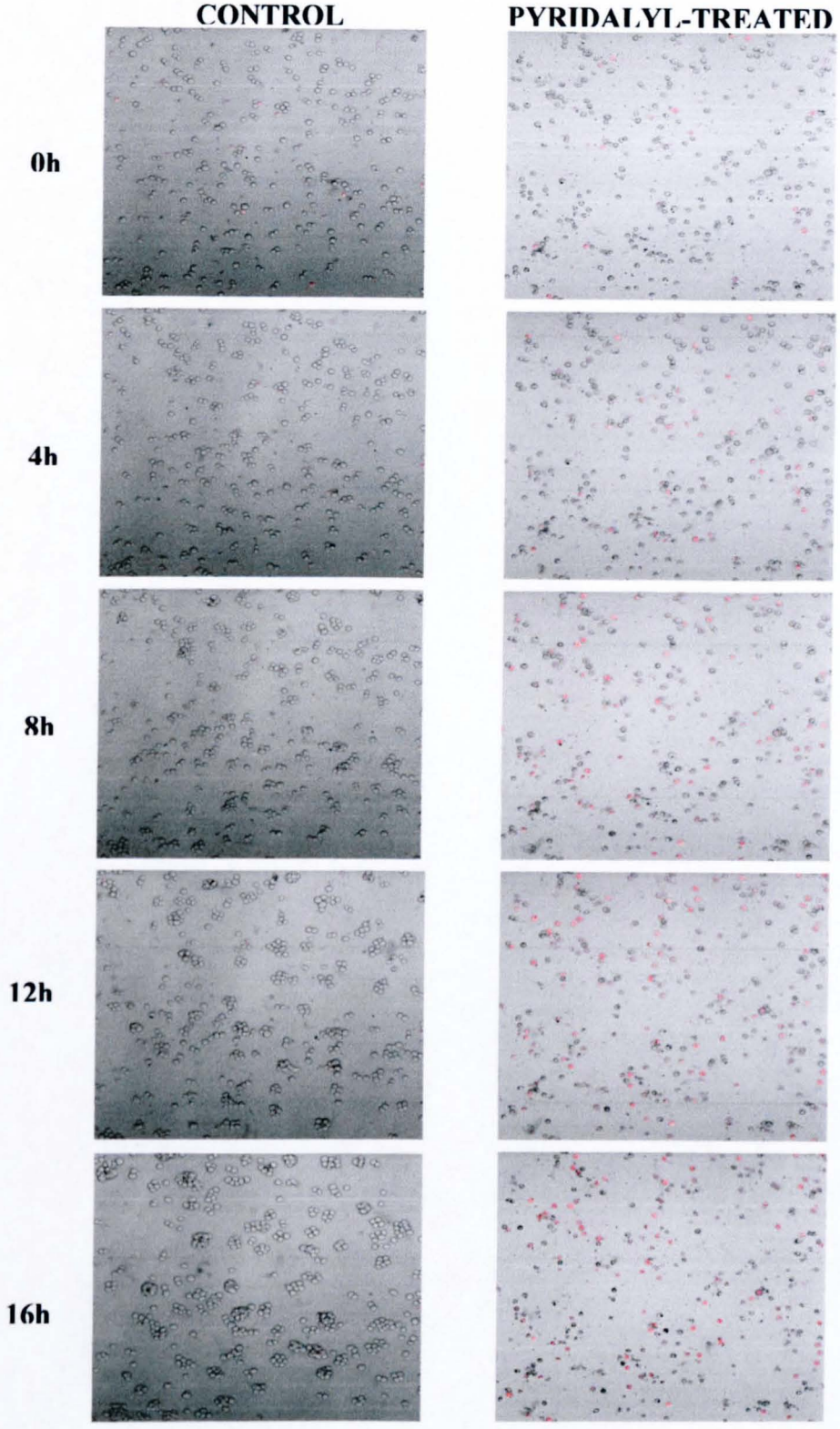

Figure 3.1. Live cell images of BM36 cells over a 16h period. Control cells (left) are compared to Pyridalyl-treated cells (right). Increasing levels of red fluorescence can be clearly seen in the treated cells.

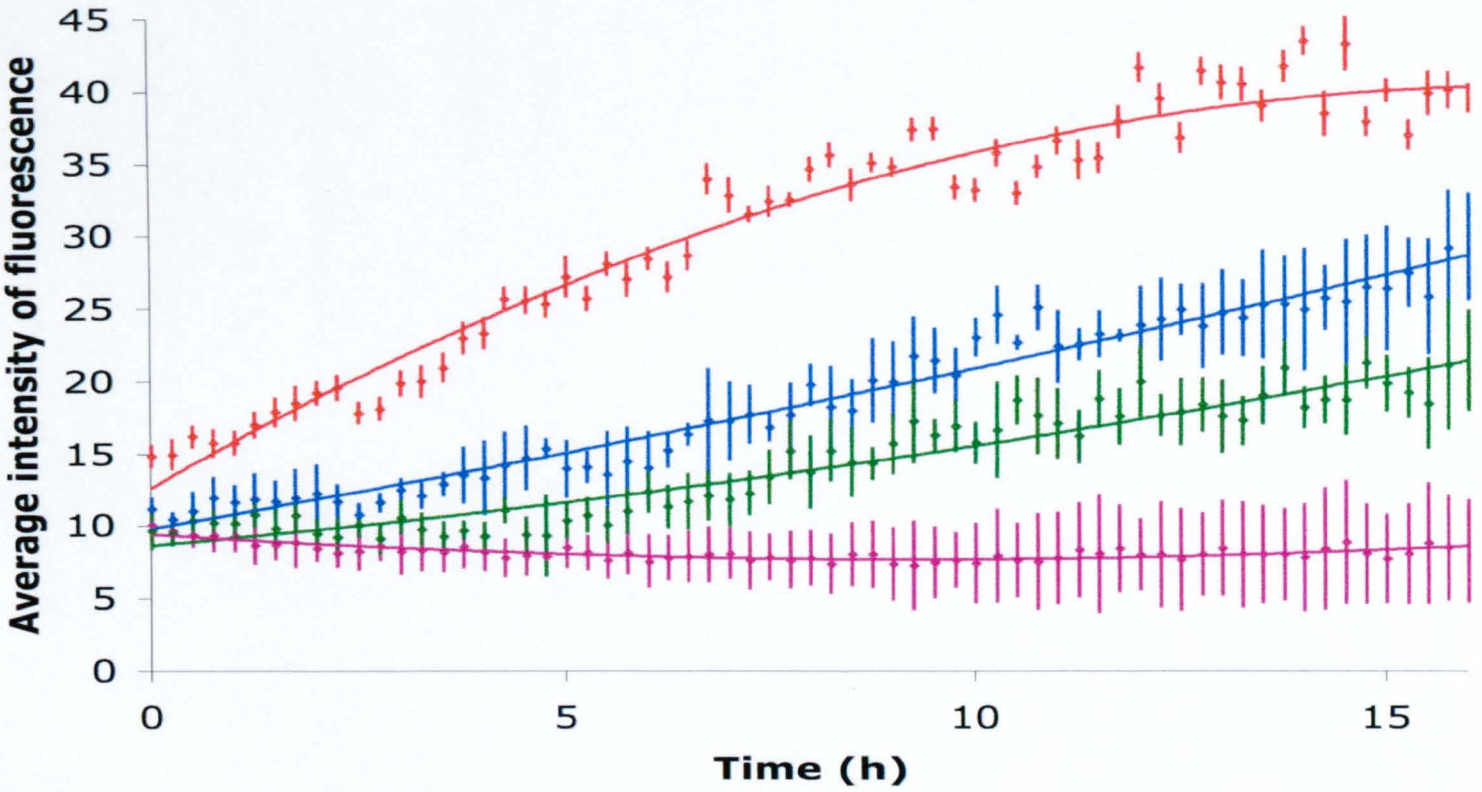

Figure 3.2. Live cell-imaging data showing the response of BM36 cells to varying doses of Pyridalyl.
Control ◆ 0.5µg/ml ◆ 1.0µg/ml ◆ 10.0µg/ml ◆ results are the mean of 3 independent experiments (± SEM).

3.2.1.2 Effects of inhibitors of caspases and cytochrome P450s

To assess the effect of inhibitors on the action of Pyridalyl in BM36 cells, a live cell imaging approach was used, where increased fluorescence over time revealed mortality. Four treatments were applied to cell cultures and the increase in fluorescence was measured over 17h: control; treated with DMSO (10µl) only; 1.0µg/ml Pyridalyl; 1.0µg/ml Pyridalyl plus 10mM Z-VAD-FMK (a general caspase inhibitor; Calbiochem, NJ, USA) and; 1.0µg/ml Pyridalyl plus 10mM 1-ABT (a general P450 inhibitor). To assess for differences, the slope of the response of *in situ* fluorescence (as a proxy for cell death) over time was examined, assuming a linear response over the incubation i.e. higher slope = more cell death. Replicate (n=6) incubations were conducted for each treatment (although mean and standard error were presented graphically; Fig. 3.3). Slopes were determined for each incubation over 17h and differences in effects of treatments were assessed by ANOVA (α=0.05). ANOVA was followed by Student-Newman-Keuls *post hoc* comparisons to determine differences between treatments (SigmaStat; Sysstat Software Inc., USA). The data were both homoscedastic and normally distributed (SigmaStat) making ANOVA possible.

ANOVA (n=6, α=0.05) revealed significant differences between treatments. Student-Newman-Keuls *post hoc* test revealed that mortality patterns of the treatments had the following pattern: Pyridalyl = Pyridalyl + VAD > Pyridalyl + 1-ABT = control (for details see Appendix 1). This indicates that VAD does not reduce Pyridalyl action, but 1-ABT does inhibit it.

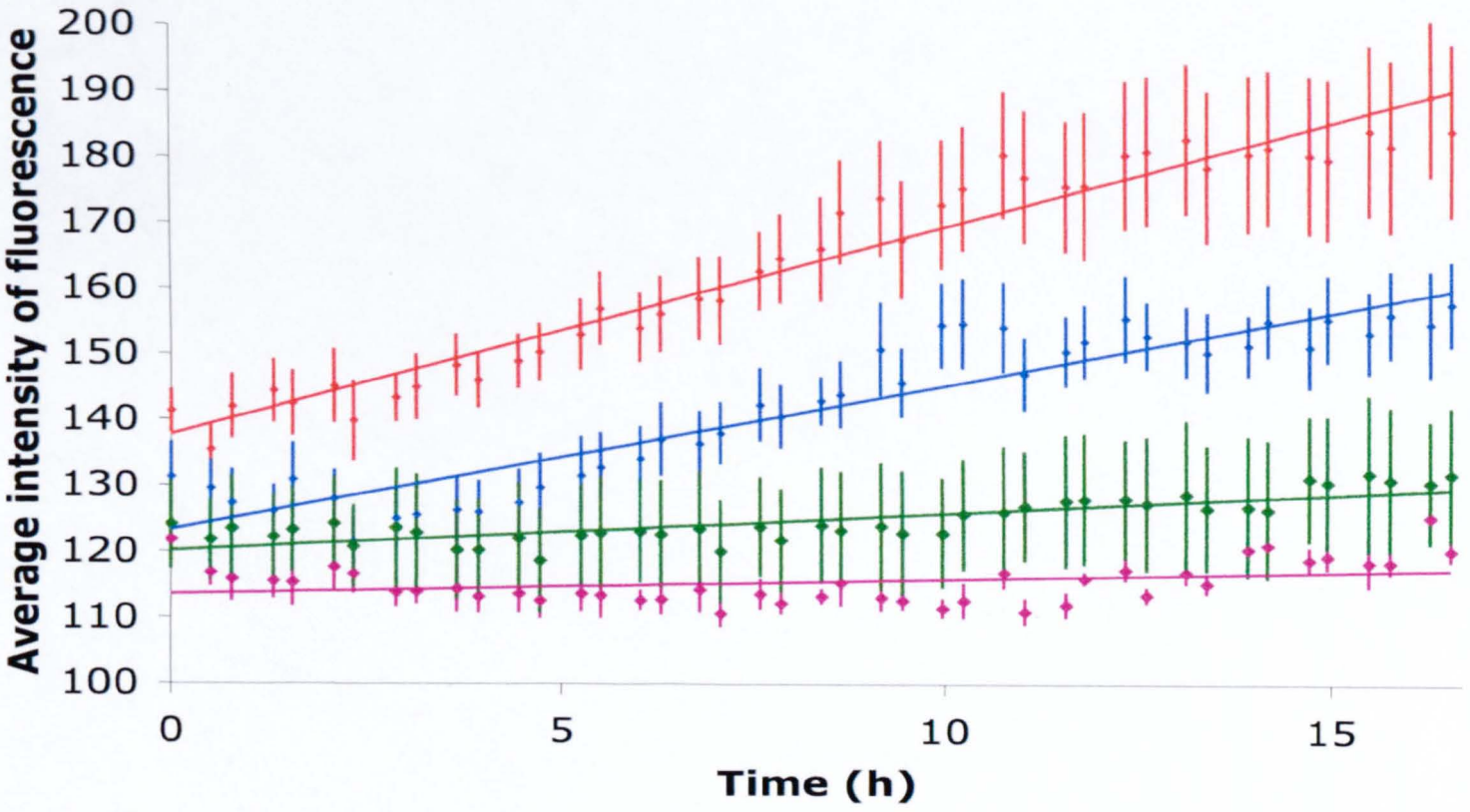

Figure 3.3. Live cell-imaging data showing the response of BM36 cells to Pyridalyl following treatment with various inhibitors. Control◆ 1.0µg/ml Pyridalyl plus 10mM 1-ABT◆ 1.0µg/ml Pyridalyl plus 10mM VAD◆ 1.0µg/ml Pyridalyl◆. Results are the mean of 3 independent experiments (± SEM).

3.2.2 Pyridalyl metabolism

To investigate Pyridalyl metabolism in insect cells, and the effects of P450 inhibitors on this, experiments were carried out using a small amount of radiolabelled insecticide ([^{3}H]Pyridalyl). BM36 cells from one 75cm^2 cell culture flask were centrifuged at 1300 x g for 10 mins at 4°C. The cell pellet was then resuspended in 1ml of fresh TC100 medium. 0.1μCi of [^{3}H]Pyridalyl and 10μg of 'cold' Pyridalyl was added to the concentrated cell suspension. The suspension was incubated at 27°C overnight (typically 12-14 hrs). The reaction was stopped by the addition of 1ml of ice-cold methanol and left overnight at -20°C. 250μl of the mixture was then centrifuged at 13000 x g for 10 mins, the resulting pellet was homogenised using an Eppendorf pestle, the homogenised mixture was then re-centrifuged and the methanolic fraction was then analysed by reversed-phase HPLC.

Reversed-phase HPLC (RP-HPLC) analyses of Pyridalyl and its metabolites were carried out on a Genesis C_{18} Column (15cm x 5mm, particle size 4μm; Jones Chromatography, UK) employing the following solvent system: linear gradient over 40 mins of 20-100% (v/v) acetonitrile 30mM ammonium acetate at 1ml/min. Solvent was delivered using Gilson model 321 pumps and absorbance was monitored at 267nm on a Gilson model 152 UV/VIS absorbance detector. Radioactivity was detected by an on-line Flo-one/Beta Radiomatic Series A500 scintillation monitor (Canberra Packard).

Fig. 3.4a shows the radiochromatogram obtained from 0.1μCi of radiolabelled Pyridalyl following incubation in TC100 cell culture medium; this was used as a

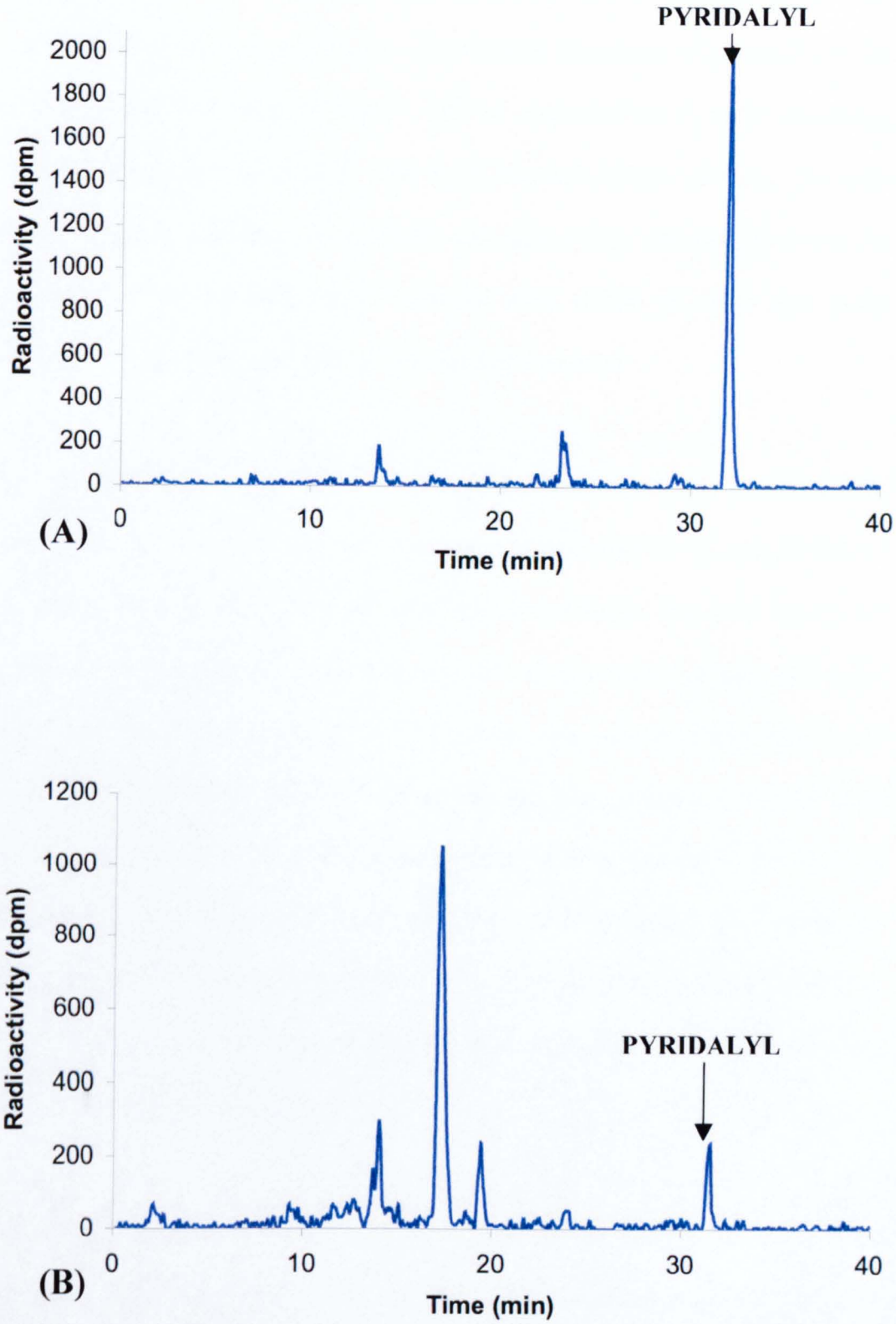

Figure 3.4. Radiochromatograms showing [^{3}H]Pyridalyl and its metabolites. (A) Radiolabelled Pyridalyl following overnight incubation with cell culture medium; this was used as a Pyridalyl standard. (B) Radiolabelled Pyridalyl following incubation with BM36 cells showing Pyridalyl and its three major metabolites.

Pyridalyl standard. The large Pyridalyl peak can clearly be seen, as can two smaller peaks due to impurities in the radiolabelled insecticide. Fig. 3.4b shows the radiochromatogram obtained from 0.1μCi of radiolabelled Pyridalyl following overnight incubation with BM36 cells in TC100 cell culture medium. The peak representing the radiolabelled insecticide can again clearly be seen, however, the size of the peak has been greatly reduced. Also visible are three new peaks corresponding to three more polar metabolites of Pyridalyl.

Data were available suggesting that cytochrome P450 inhibitors protected cells from Pyridalyl's action, however, it was not apparent whether the metabolism of the insecticide was affected in any way by the inhibitors. Fig. 3.5a shows the radiochromatogram obtained from 0.1μCi of radiolabelled Pyridalyl following incubation with BM36 cells in TC100 medium, again showing the three major metabolites of Pyridalyl. Fig. 3.5b shows the radiochromatogram obtained from the same amount of radiolabelled Pyridalyl after incubation with BM36 cells in TC100 medium, but this time in the presence of the general cytochrome P450 inhibitor, 1-ABT (10mM). Clearly, the presence of the P450 inhibitor has almost completely prevented the metabolism of Pyridalyl, however, a small amount of the major metabolite can be seen.

To confirm the previous results, a similar experiment was performed, but this time using a different cytochrome P450 inhibitor. The radiochromatogram obtained from 0.1μCi of radiolabelled Pyridalyl following incubation with BM36 cells in TC100 medium is shown again in Fig. 3.6a, with the three major metabolites being clearly

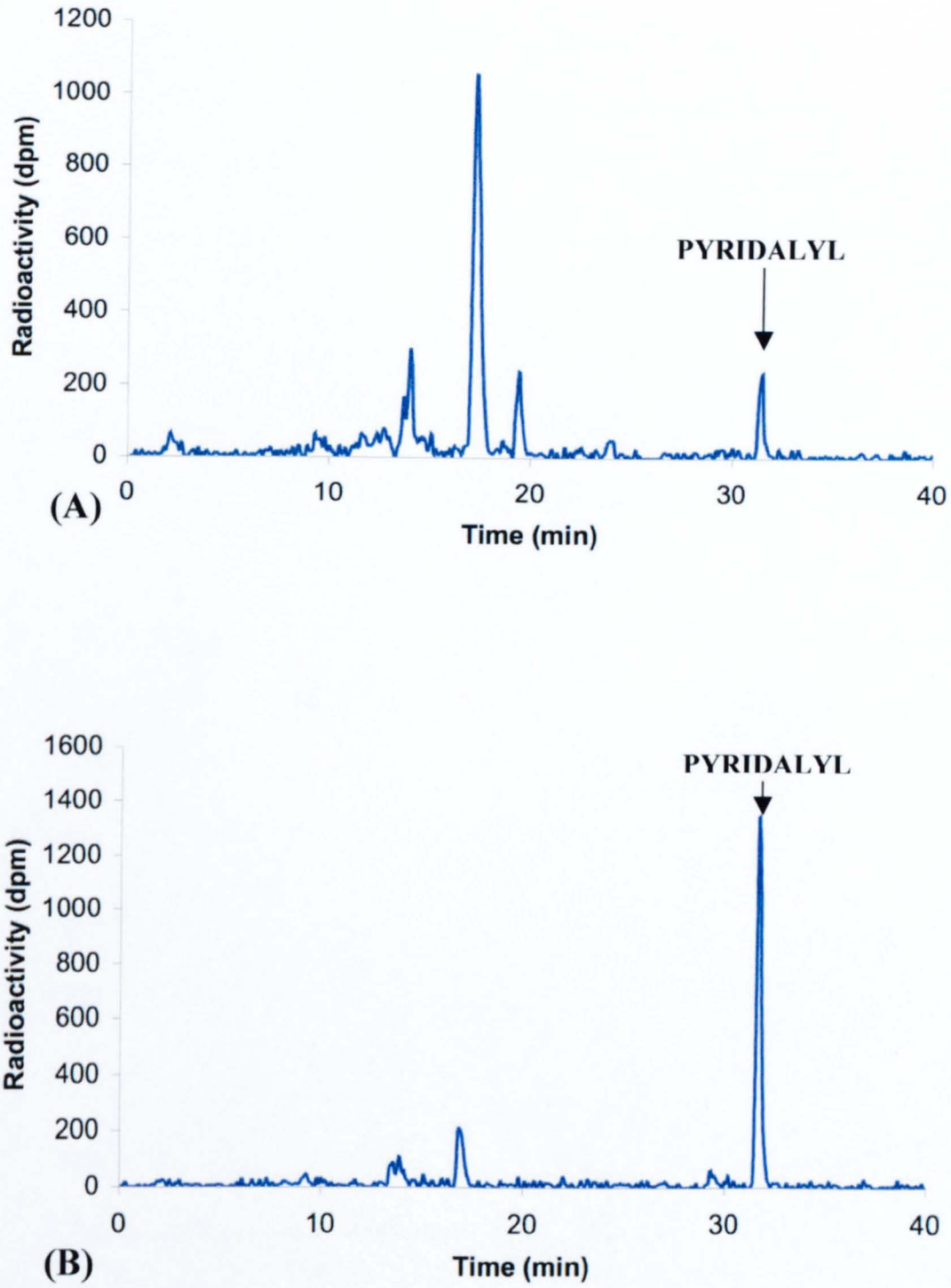

Figure 3.5. Effect of the cytochrome P450 inhibitor 1-ABT on [^{3}H]Pyridalyl metabolism. (A) Radiolabelled Pyridalyl following overnight incubation with BM36 cells, showing Pyridalyl and its 3 major metabolites. (B) Radiolabelled Pyridalyl following incubation with BM36 cells in the presence of the P450 inhibitor 1-ABT (10mM).

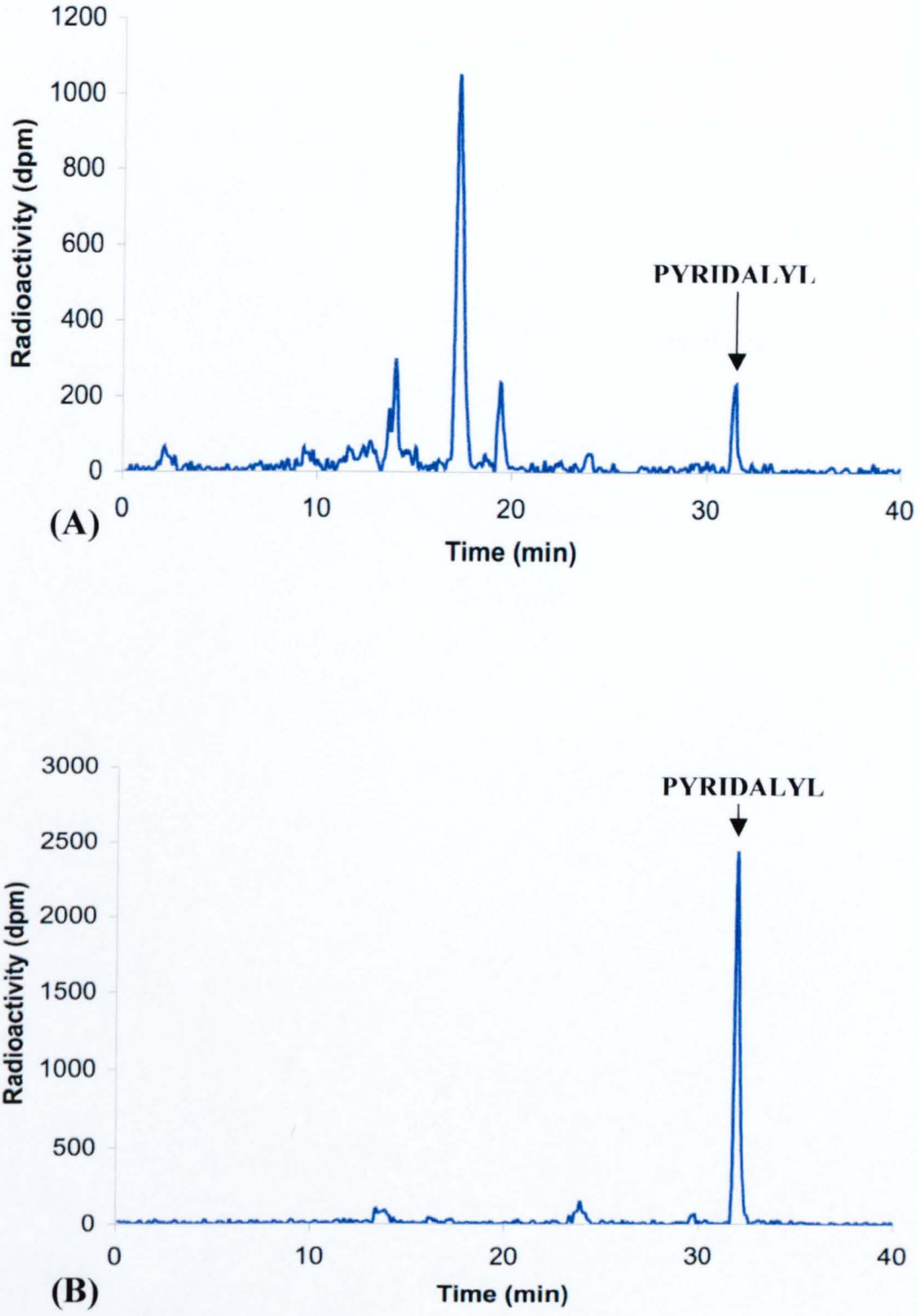

Figure 3.6. Effect of the cytochrome P450 inhibitor PBO on [^{3}H]Pyridalyl metabolism. (A) Radiolabelled Pyridalyl following overnight incubation with BM36 cells, showing Pyridalyl and its 3 major metabolites. (B) Radiolabelled Pyridalyl following incubation with BM36 cells in the presence of the P450 inhibitor PBO (10mM).

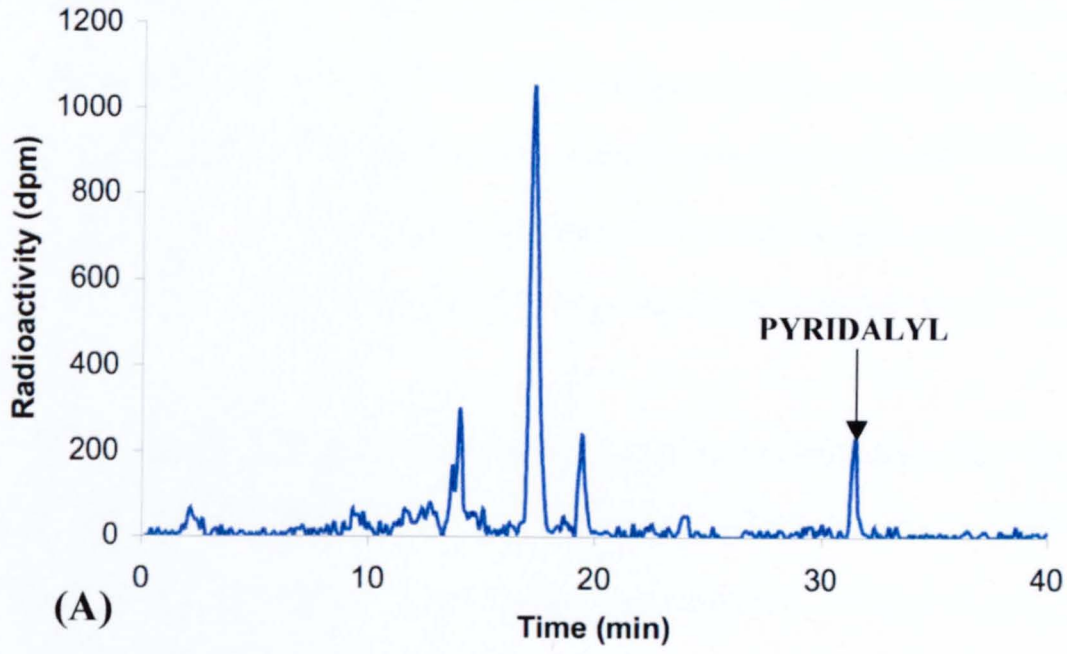

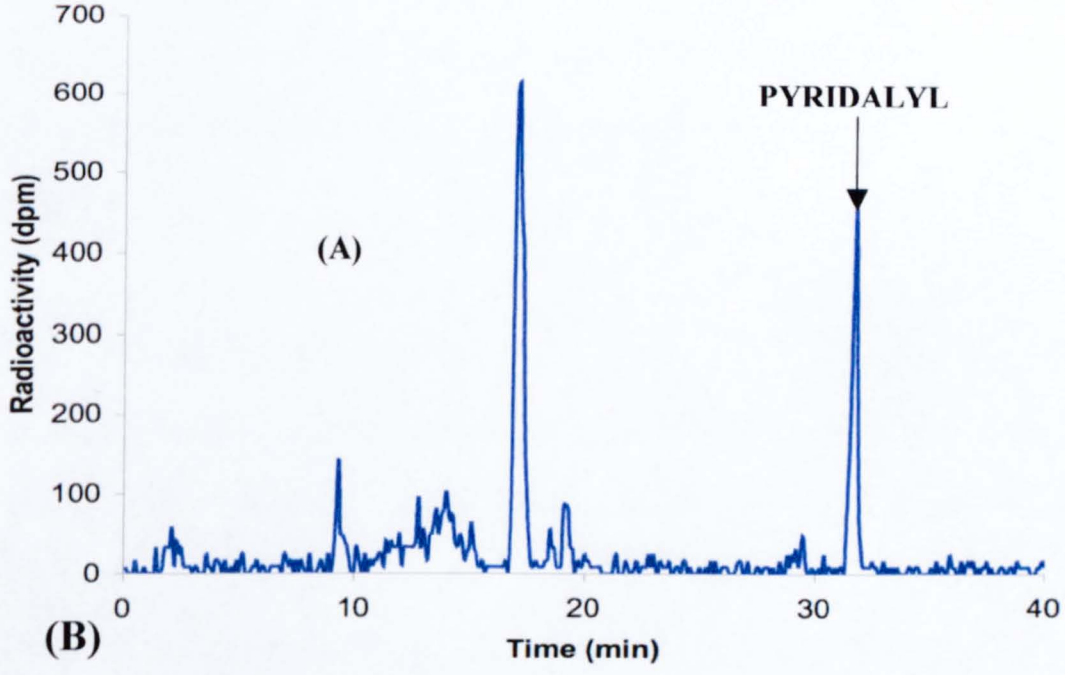

Figure 3.7. Effect of imidazole on [^{3}H]Pyridalyl metabolism. (A) Radiolabelled Pyridalyl following overnight incubation with BM36 cells, showing Pyridalyl and it's 3 major metabolites. (B) Radiolabelled Pyridalyl following incubation with BM36 cells in the presence of the P450 inhibitor Imidazole (10mM).

visible. Fig. 3.6b shows the radiochromatogram obtained from 0.1μCi of radiolabelled Pyridalyl following incubation with BM36 cells in TC100 medium in the presence of the general P450 inhibitor, Piperonyl butoxide 10mM (PBO, [Kumar *et al.*, 2002]). This inhibitor has completely prevented the metabolism of Pyridalyl i.e. only the large Pyridalyl peak and the two small peaks corresponding to the two impurities can be seen; the three major metabolite peaks are absent.

A third experiment using the P450 inhibitor, imidazole, was performed. Fig. 3.7a shows the radiochromatogram obtained from 0.1μCi of radiolabelled Pyridalyl following incubation with BM36 cells in TC100 medium, and once again the three major metabolites are visible. Fig. 3.7b shows the radiochromatogram obtained from 0.1μCi of radiolabelled Pyridalyl following incubation with BM36 cells in TC100 medium, in the presence of the P450 inhibitor, imidazole (10mM). The major metabolite of Pyridalyl can clearly be seen, however, a slightly different pattern can be seen with the other metabolites when compared to Fig. 3.7a, a previously unseen metabolite peak (A) is now present with a retention–time below 10 minutes.

3.2.3 Protein binding assay

Scintillation counting of precipitated protein from the Pyridalyl metabolism studies suggested that radiolabelled Pyridalyl and/or its metabolites become bound to proteins in the treated BM36 cells. With the aim of determining the number of proteins that bind Pyridalyl and/or its metabolites and their molecular weight, the proteins were separated by SDS-PAGE, the gel cut into slices and the amount of radioactivity present in each slice radioassayed.

For this, 10μg of BM36 whole cell proteins from the [^{3}H]Pyridalyl metabolism studies was precipitated overnight in acetone at -20°C, the following morning the precipitated protein pellet was washed three times in ether, allowed to air-dry and then solubilised in electrophoresis loading buffer. The proteins were then separated on a 10% SDS-PAGE gel, following electrophoresis the proteins were fixed and the gel cut into 1.5mm slices. The gel slices were dissolved in 1ml 30% (v/v) H_2O_2, scintillation fluid (1.5ml) was then added and the radioactivity was measured in a liquid scintillation counter.

Fig. 3.8 shows the results of the BM36 protein binding experiments, each gel slice represents 1.5mm of polyacrylamide gel lane, and increasing gel slice number corresponds to decreasing molecular weight. The initial high count at the top of the gel is due to insoluble material that was unable to enter the gel. Two distinct peaks of radioactivity can be seen, one of high molecular weight (greater than 170kDa) and one of low molecular weight (between 40 and 35kDa), suggesting that some protein binding does take place, specifically to at least two proteins. Other, small radioactive peaks were also apparent at approximately 80 and 52kDa.

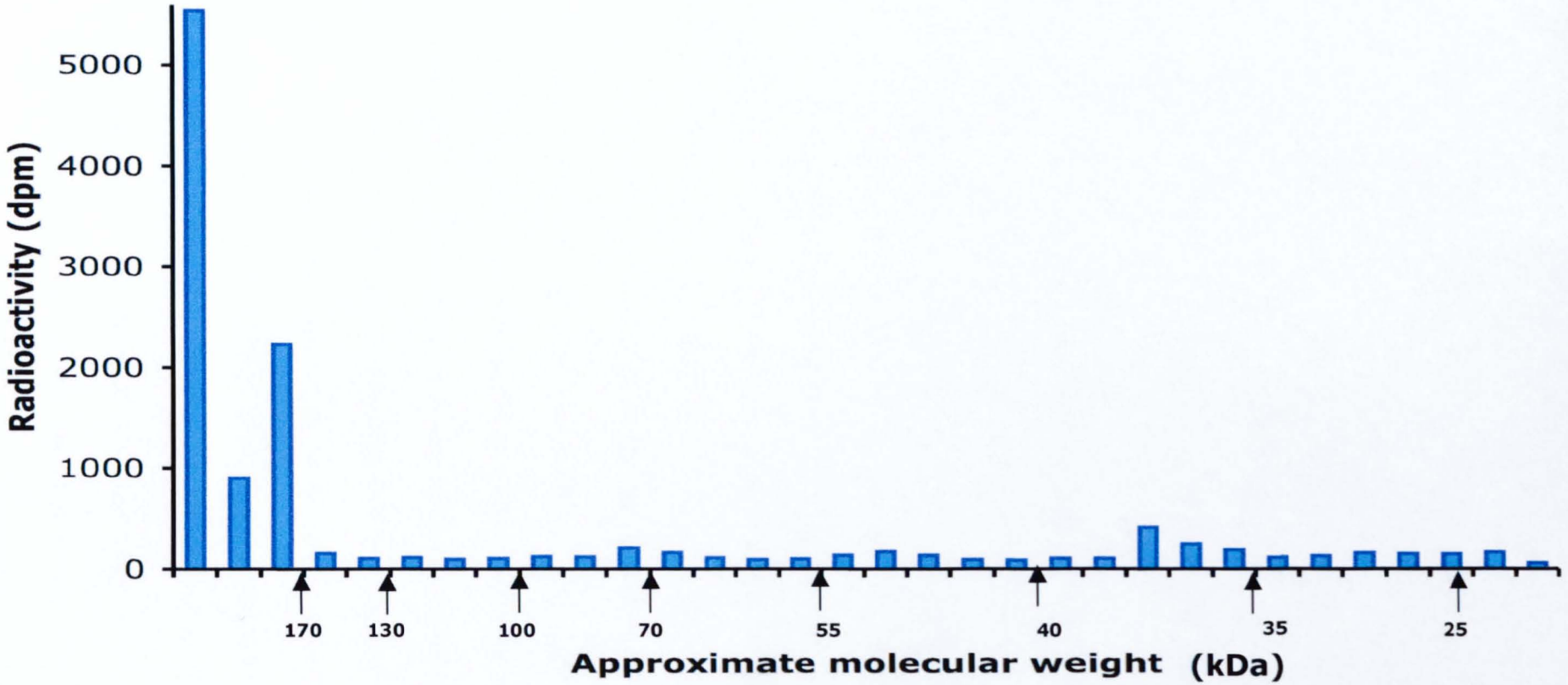

Figure 3.8. Radioactivity bound to BM36 cell proteins from studies on [^{3}H]Pyridalyl metabolism. Whole cell proteins from studies on [^{3}H]Pyridalyl metabolism were separated by SDS-PAGE, the gel was then cut into slices, solubilised in H_2O_2 and radioactivity measured by scintillation counting.

3.3 Discussion

The results have shown that Pyridalyl causes cytotoxicity in a dose-dependent manner. The metabolism of pesticides to more active toxicants by P450 enzymes has been shown to be the basis of the action of organophosphate insecticides and several others (Levi *et al.*, 1988). This also appears to be the case with Pyridalyl. The pre-incubation of BM36 cells with a general cytochrome P450 inhibitor (1-ABT or PBO) prevents the metabolism of the insecticide. The live cell imaging complements these results as it shows that pre-incubation with P450 inhibitors protects the BM36 cells from Pyridalyl's cytotoxic effects. The P450 inhibitors 1-ABT and PBO have been shown to inhibit most P450s, via suicide inhibition, without affecting the action of other haem-containing proteins i.e. other cytochromes such as cytochrome b_5 (Ortiz de Montellano & Mathews, 1981). These results, when viewed together, suggest that the metabolism of Pyridalyl by a cytochrome P450 is essential for its insecticidal activity, however, there is a possibility that the P450 inhibitors could also inhibit other haem-containing proteins although no evidence for this has been published it cannot be ruled out without extensive study. The inhibition of essentially all P450s prevents Pyridalyl metabolism and the formation of the active metabolite resulting in cell survival.

The P450 inhibitor, imidazole (Zhang et al., 2002), proved ineffective at preventing the metabolism of Pyridalyl and its insecticidal activity. The three major metabolites were all still present, however, a fourth previously unseen metabolite appeared. Clearly, unlike 1-ABT and PBO, imidazole was unable to prevent the bioactivation of Pyridalyl and the formation of its active metabolite. Which suggests that the metabolic activation of Pyridalyl does not involve the P450s that are inhibited by imidazole, which is a more specific P450 inhibitor.

The live cell imaging experiments allowed Pyridalyl-treated cells to be followed in real time as they died. Interestingly, none of the characteristic cell morphology changes associated with apoptosis (programmed cell death) could be seen i.e. cytoplasmic membrane blebbing (Vermes, 2000). This led to the hypothesis that Pyridalyl-treated cells die via some other mechanism, possibly necrosis.

Caspases are cysteine proteases that play an essential role in apoptosis. Once cell death has been initiated via apoptosis, caspases dismantle the cell in an orderly fashion by cleaving an array of intracellular substrates (Blank & Shiloh, 2007). Without this ordered dismantling, intracellular contents would be released and potentially harmful responses could take place. Inhibitors of caspases effectively prevent apoptosis completely (Chang & Yang, 2000) and when Pyridalyl-treated cells were incubated with the general caspase inhibitor, VAD, there appeared to be no significant effect on the levels of cell death that were observed. This, again, suggests that Pyridalyl-treated cells do not die via apoptosis; if they did, VAD should completely protect them from Pyridalyl's cytotoxic effects, however, it must be noted that due to a lack of a positive control i.e. treatment with a known apoptosis inhibitor, in this experiment this conclusion is provisional at best. The lack of observed blebbing of cell membranes following Pyridalyl treatment corroborates that the action of the insecticide is not via apoptosis.

The results of the protein binding experiments is consistant with the hypothesis suggesting that Pyridalyl and/or its metabolites binds to proteins in treated cells. Our results show that binding takes place to at least two proteins, however, this is all the information that we were able to obtain from these experiments, also, without a control experiment i.e. treating a cell lysate with [^{3}H]Pyridalyl it is

impossible to be entirely sure that the radioactivity observed in the gel slices has anything to do with binding to insect cell proteins. 2D-PAGE was attempted using proteins from the [^{3}H]Pyridalyl metabolism studies in an effort to get more information about the labelled proteins i.e. exact number of labelled proteins, isoelectric point, etc. These experiments ultimately yielded no further information about the labelled proteins, and since the radioisotope being used was ^{3}H, direct autoradiography was difficult. Prior to exposure to X-ray film, the gels were soaked in an enhancer solution, but the levels of radioactivity present in the gel were still too low to enable visualisation of any protein spots.

CHAPTER 4

A PROTEOMIC COMPARISON OF PYRIDALYL-SENSITIVE AND –RESISTANT *Spodoptera frugiperda* CELLS

4.1 INTRODUCTION

The term "proteomics" was first coined in 1995 and was defined as the large scale characterisation of the entire protein complement of a cell line, tissue or organism (Graves & Haystead, 2002). Proteomic studies as we know them today began with the introduction of 2D-PAGE, whereby, proteins are separated firstly on the basis of their isoelectric point and then on the basis of their molecular weight. Using this method, O'Farrell (1975) was able to separate over 400 proteins extracted from *Escherichia coli* (O'Farrell, 1975). 2D-PAGE has proven itself as being a powerful and reproducible separation technique; furthermore, it has become the major method for identifying differences in protein expression between two or more samples.

Whilst 2D-PAGE allows separation of complex protein mixtures, it does not identify the individual separated proteins. One of the earliest methods used for protein identification was microsequencing by Edman chemistry, to obtain N-terminal amino acid sequences (Edman, 1949). The use of Edman sequencing is waning in the field of proteomics, since mass spectrometry has recently become the major method of protein identification following 2D-PAGE. Compared with Edman sequencing, mass-spectrometric (MS) methods are far more sensitive, as

they do not require transfer to nitrocellulose membranes and can be used in high throughput operations (Graves & Haystead, 2002).

4.1.1 Difference gel electrophoresis (DIGE)

Whilst 2D-PAGE is a powerful technique enabling simultaneous visualisation of relatively large portions of the proteome, well documented issues of variation and lack of sensitivity and quantitative capabilities, have limited the use of this technique as a quantitative tool (Marouga *et al.*, 2005). Difference gel electrophoresis (DIGE) builds on this technique by adding a highly accurate quantitative dimension. DIGE relies on the pre-electrophoretic labelling of samples with one of three spectrally resolvable fluorescent CyDyes (Cy2, 3 and 5), allowing multiplexing of samples into the same gel (Van Den Burgh & Arckens, 2005).

CyDye DIGE fluors are *N*-hydroxyl succinimidyl esters, which react with primary amine groups, typically the terminal amino group of lysine side chains. Labelling reactions are optimised such that only 2-5% of the total number of lysine residues are labelled. The three fluors are mass matched, each labelling event adding 500Da to the mass of the protein. The fluors also carry an intrinsic charge of +1, such that the pI of the protein is maintained upon labelling (GE Healthcare website; www5.gelifesciences.com/aptrix/upp00919.nsf/Content/Proteomics+DIGE~proteomics_ettan_dige).

The experimental design for a typical DIGE experiment consists of labelling the samples to be compared with Cy3 or Cy5, whereas Cy2 is employed to label a pooled sample comprising equal amounts of each of the samples within the study,

and acts as an internal standard. The internal standard ensures that all proteins present in the samples are represented, assisting both inter- and intra-gel matching (Lilley & Friedman, 2004). Direct comparisons are made between the Cy3- or Cy5-labelled samples and the Cy2-labelled internal standard for that gel. These ratios are then normalised and compared with those generated for that particular protein from other gels.

For analysing the DIGE gel images, DeCyder (GE Healthcare), a software platform designed specifically for use with DIGE, is typically used. The DeCyder software package has a triple co-detection algorithm that allows simultaneous detection of labelled protein spots from images that arise from the same gel and increases accuracy in the quantification of standardised abundance (Alban *et al.*, 2003). The standardised abundances can then be compared across groups to detect changes in protein expression, regardless of whether the samples to be inter-compared have been resolved on the same DIGE gel (Lilley & Friedman, 2004). DeCyder is also capable of performing several statistical analyses on the data including a students t-test and 1- and 2-way ANOVA. The desirable design of a typical DIGE experiment to compare two samples, containing a minimum of four biological replicates, is shown in Table 4.1.

Gel	Cy2	Cy3	Cy5
1	Internal Standard	Control 1	Sample A1
2	Internal Standard	Sample B2	Control 2
3	Internal Standard	Control 3	Sample B1
4	Internal Standard	Sample B3	Sample A3
5	Internal Standard	Sample A4	Sample B4
6	Internal Standard	Sample A2	Control 4

Table 4.1 The recommended DIGE experimental set-up designed to derive statistical data between control and two treatment regimes A and B. For the control and two treatment regimes, four biological replicates are included (1-4). The internal standard (a pool of equal amounts from all samples; four controls and eight treated) is labelled with Cy2 and run on every 2D-gel. Two replicate control samples and two replicates of each of the treatments are labelled with Cy3 and the remaining two replicates are labelled with Cy5. This is to ensure that there is no preferential labelling that may influence the data.

4.1.2 Mass spectrometry

Mass spectrometry enables protein structural information, such as peptide masses or amino acid sequences, to be obtained. The proteins are generally subjected to protease treatment (usually trypsin), allowing analysis of the resulting peptides. For samples to be analysed by MS, the molecules must be charged. This is accomplished by ionising them using either electrospray ionisation (ESI) or matrix-assisted laser desorption/ionisation (MALDI). In both methods peptides are converted to ions by the addition or loss of one or more protons. Since only ESI was used in this project, this ionisation method will be discussed further.

In nano LC-ESI-MS, a liquid sample flows from a microcapillary tube into the inlet of the mass spectrometer, where a potential difference between the capillary and the inlet to the mass spectrometer results in the generation of a fine mist of charged droplets. As the solvent evaporates, the sizes of the droplets decrease, resulting in the formation of desolvated ions (Fenn *et al.*, 1989).

Following ionisation, the peptides are resolved according to their mass to charge ratio (m/z) in a mass analyser. There are three major types of mass analyser;

1. *Quadrupole mass analysers.* Here the ions are transmitted through an electric field created by an array of four metal rods, the quadrupole. A quadrupole can act to transmit all ions or as a mass filter to allow the transmission of ions of a certain mass to charge ratio.
2. *Time of flight (TOF).* A TOF instrument is one of the simplest mass analysers, and measures the m/z ratio of an ion by determining the time required for it to traverse the length of a flight tube. The 'time of flight' of a particular ion is proportional to it's mass. TOF mass analysers often include an ion mirror at the

end of the flight tube, which reflects ions back through the flight tube to a detector. By increasing the length of the flight tube in this way small energy differences amongst ions are accounted for and mass resolution is increased (Yates, 1998).

3. *Ion trap.* Ion trap mass analysers function to trap ions in a three dimensional electric field. In contrast to a quadrupole mass analyser, in which the ions are discarded before the analysis begins, the ion trap mass analyser allows ions to be "stored" and then selectively ejected, increasing sensitivity (Graves & Haystead, 2002).

In tandem mass spectrometry (MS/MS) two mass analysers are combined to achieve a combination of ion selection and ion determination. Tandem mass spectrometry determines the mass of each peptide from a sample and also the fragmentation pattern of each of the peptides. Tandem mass spectrometers contain two (or three) quadrupoles followed by a TOF mass analyser. Such mass spectrometers can be used in two different modes, scanning mode or MS/MS mode (Fig. 4.1). In scanning mode, the first two mass analysers simply transfer the peptide ions to the final mass analyser and detector, hence producing a list of possible peptide ions. The instrument can then be set to select ions of interest from this spectrum; usually, the ions are selected on the basis of their charge as most ionised peptides are doubly or triply charged, whereas contaminant ions are not. This process is known as Data Directed Acquisition (DDA). The chosen ions are selected by the electric field in the first quadrupole and passed into the second quadrupole. In MS/MS mode, the second quadrupole acts as a collision chamber. It fragments the ions in a process known as collision-induced dissociation (CID). These fragments then pass into the third mass analyser (either TOF or quadrupole),

and the m/z of each fragment is determined, producing a spectrum of fragment ions. This pattern of ions can then be interpreted and the amino acid sequence of the parent peptide determined.

In order to prevent all the peptides from the protein sample entering the MS/MS at once, it is common to subject the sample to some form of liquid chromatography (LC), generally nano-LC, prior to mass spectrometric analysis (nano-LC-MS/MS), that allows a steady flow of peptides into the mass spectrometer.

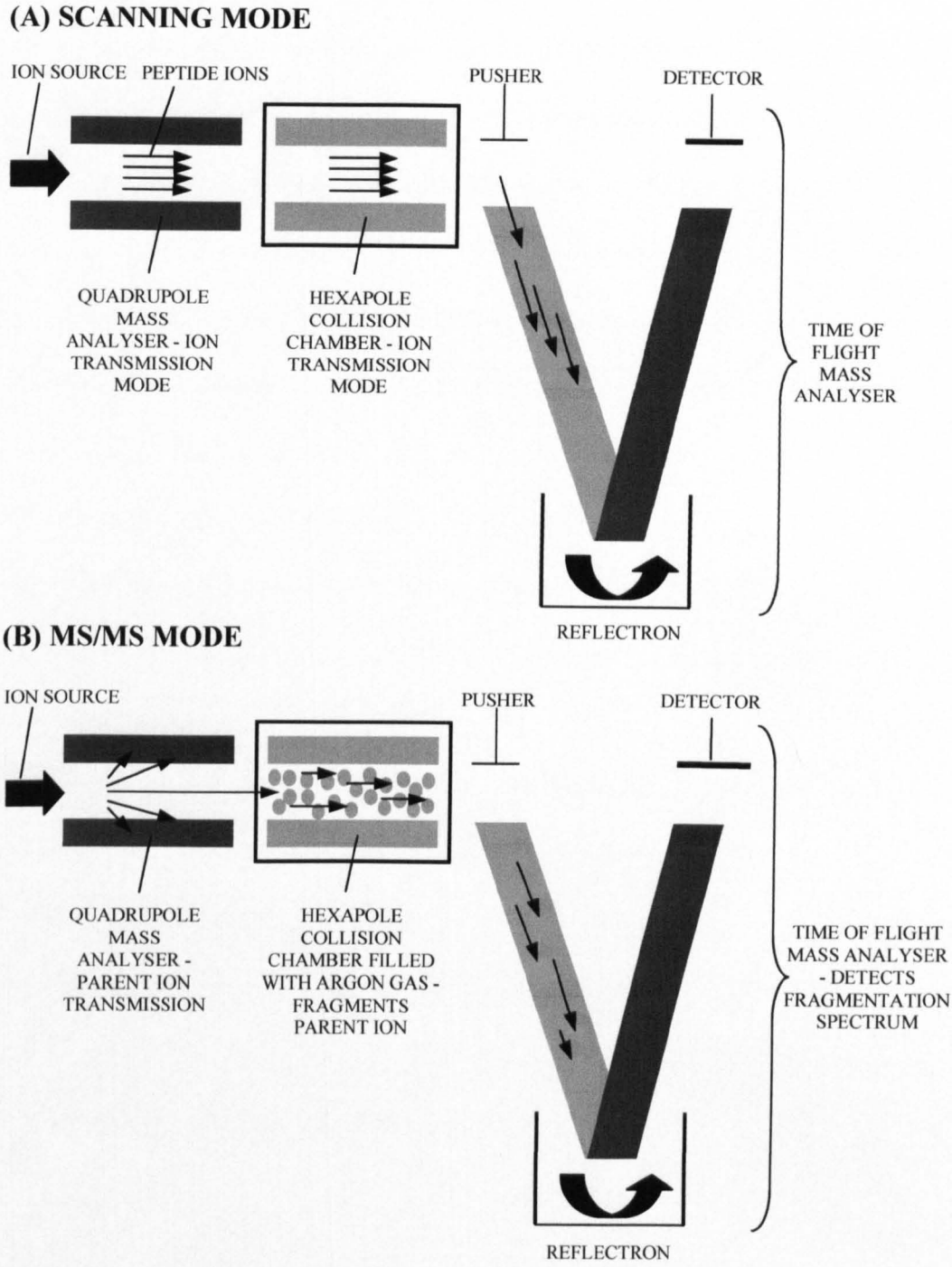

Figure 4.1. Conventional and MS/MS modes of analysis in a Quadrupole-Time Of Flight (Q-TOF) mass spectrometer. (A) In scanning mode, all ions within a certain m/z range are transmitted through the quadrupole and collision cell for mass analysis in the TOF analyser. From this spectrum, a parent ion is selected for fragmentation in the collision cell. The mass spectrometer then switches to MS/MS mode. (B) In MS/MS mode, the parent ion is selectively transmitted by the quadrupole into the collision cell and fragmented. The TOF analyser then resolves the resulting fragment ions.

4.1.3 Peptide sequencing

MS/MS generates fragmentation spectra, each of which can then be analysed in order to generate the (partial) sequence of the parent peptide ion. In general, using low-energy collisions in the collision cell causes peptides to fragment mainly along the peptide backbone. This generates six types of ion; a, b, c, x, y, and z (Fig. 4.2). The most common of these are the y ions, therefore these ions produce the most intense signals in the fragmentation spectrum. The intervals between each y ion fragment correspond to the mass of the amino acid residue lost after each fragmentation. By measuring the mass difference between each of the most intense peaks, it is possible to determine the amino acid sequence of the parent peptide (Fig. 4.3). Peptide sequencing software, such as the PepSeq module of MassLynx (Waters Ltd., Hertfordshire, UK) can be used to assist in this process.

Initially the partial sequences were used for database searching using a mass spectrometry-driven BLAST search (MS-BLAST; Shevchenko *et al.*, 2001) and FASTS, which compares a set of (presumably non-contiguous) short peptide sequences against a protein database (FASTS) or a DNA database (tFASTS) and is capable of maximising the information content of the minimal query data using a probability based scoring system (Mackey *et al.*, 2002).

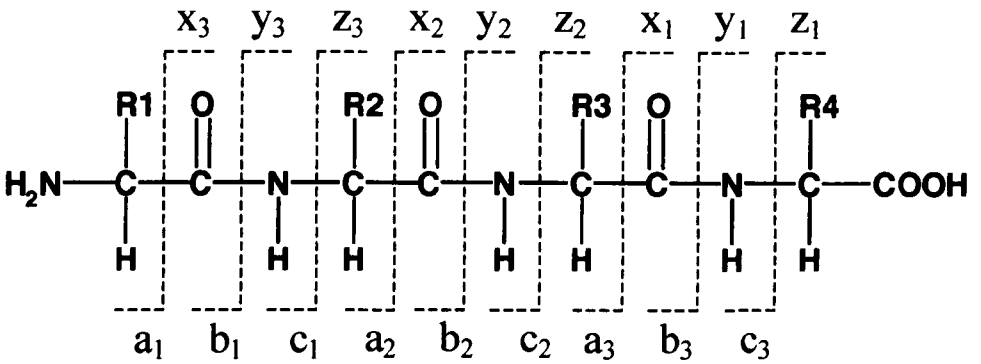

Figure 4.2. Common fragmentation ions generated in the collision cell of a tandem mass spectrometer. Fragments will only be detected if they carry a charge. If the charge is retained on the N terminal fragment, the ion is classed as either a, b or c. If the charge is retained on the C terminal, the ion is either x, y or z. A subscript indicates the number of residues in the fragment (modified from Roepstorff and Fohlman, 1984).

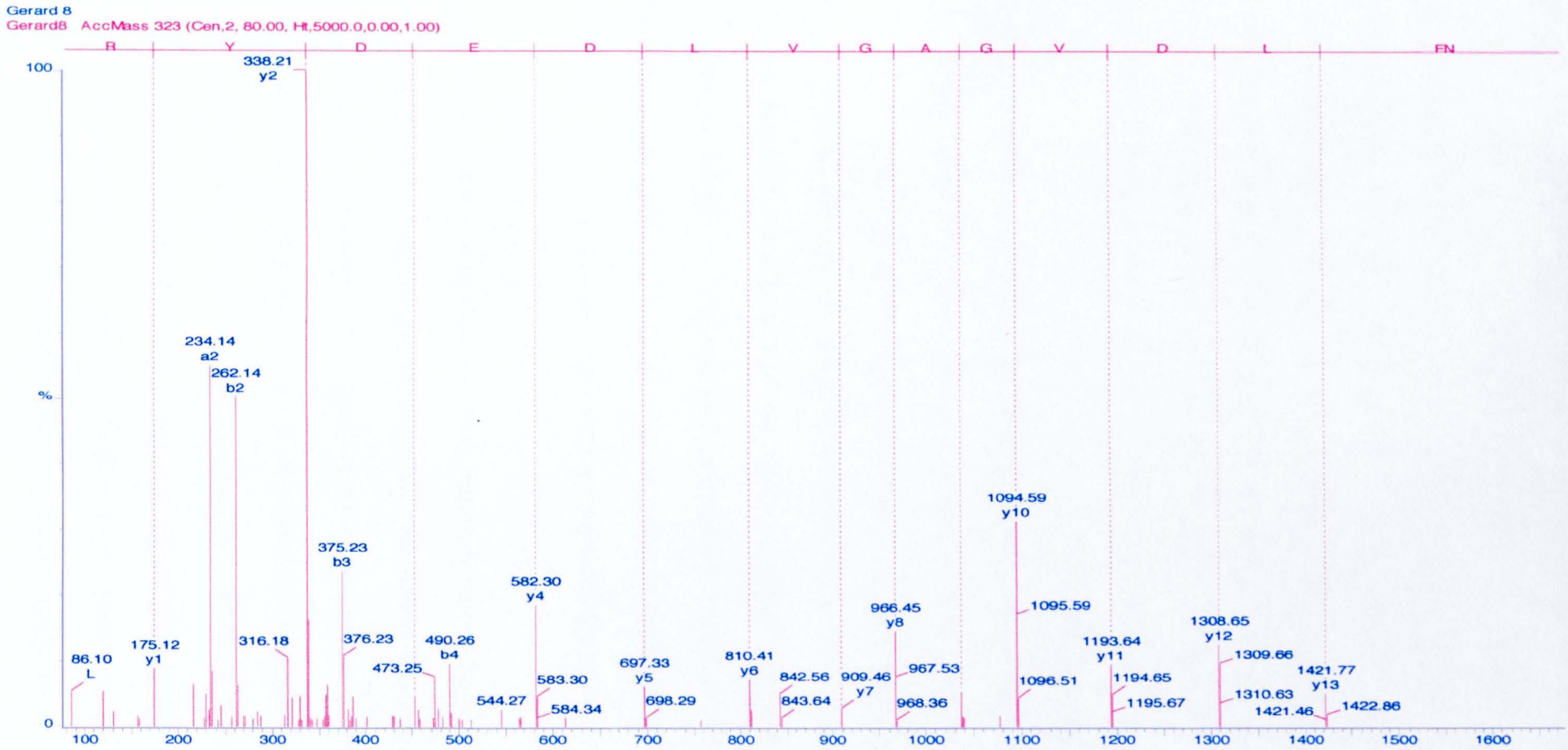

Figure 4.3. A typical MS/MS fragmentation spectrum. The fragmentation spectrum generated from the parent peptide ion at m/z 841 is shown. Interpretation of the y-ion series is shown.

Mass spectrometry data can also be analysed using 'ion searches' using software such as MASCOT. Experimental mass values for tryptic peptides are compared with calculated peptide mass or fragment ion mass values, obtained by applying cleavage rules to the entries in a comprehensive primary sequence database. By using an appropriate scoring algorithm, the closest match or matches can be identified. If the 'unknown' protein is present in the sequence database, then the aim is to pull out that precise entry. If the sequence database does not contain the unknown protein, then the aim is to pull out those entries that exhibit the closest homology, often equivalent proteins from related species (Perkins *et al.*, 1999).

4.1.4 MS/MS data analysis and database searching

Typical database searching does not deal well with the dynamic nature of the proteome. Post-translational modifications, alternative splicing and laboratory chemistry all affect protein behaviour and make spectrum interpretation more challenging. The automated tool InsPecT (Interpretation of Spectra with PT modifications) is an MS/MS database search algorithm specifically designed to address two crucial needs of the proteomics community: identification of post-translationally modified peptides search speed (Tanner *et al.*, 2006). It has the following features:

a. Tag-based filters using a novel *de novo* interpretation algorithm that works in the presence of modifications and poor spectral quality.

b. A fast trie-based search for scanning the database with sequence tags.

c. A dynamic programming technique to identify candidate peptides.

d. A scoring algorithm that reflects peptide fragmentation patterns and a novel quality based score based on several complementary features. (Tanner *et al.*, 2005).

The key feature of Inspect is that it uses peptide sequence tags (PSTs) to filter the database to be searched; it has an internal PST generator, PepNovo, which generates multiple tags for each spectrum to ensure that at least one of them is correct. These PSTs are extremely efficient filters, even in the context of up to a dozen post-translational modifications. A peptide sequence tag is a short amino acid sequence with a prefix mass value designating its starting position in the whole peptide. When used in filtering, PSTs are extremely efficient filters in reducing the number of candidate database sequences that need to be scored, even in the context of up to a dozen post-translational modifications. This increases accuracy, by reducing the number of candidates allowing for more accurate and less resource consuming scoring procedures to be used (Frank *et al.,* 2005). Unanticipated modifications are common in proteomics; InsPect implements the MS-Alignment algorithm for 'blind' spectral searches, with no bias towards anticipated modification types. This search has been applied to annotate heavily modified proteins such as crystallins (Tsur *et al.,* 2005).

Post-translational modifications need to be taken into account during peptide sequencing as even a single change in the peptide sequence due to a post-translational modifications or mutations shift spectral peaks significantly. InsPecT solves this problem by enumerating all possible mutations and modifications in the database (Tanner *et al.,* 2005). The output file generated by InsPecT provides p-values (a measure of match confidence) and match quality (MQ) scores for each of the peptides that it identifies, the match quality score indicates whether the match is correct or incorrect; a value of 1 and above indicates a correct match, whereas a value less than 1 indicates an incorrect match (Tanner *et al.,* 2005). Simply put, the match quality score separates true matches from false matches.

4.2 Methods and Results

With the aim of elucidating how Pyridalyl causes cytotoxic effects in lepidopteran cells, a proteomic investigation was undertaken using 2D-PAGE and DIGE to identify any differentially expressed proteins between a Pyridalyl-sensitive and –resistant *S. frugiperda* Sf21 cell line. Differentially expressed proteins may well reflect candidate target processes for Pyridalyl action.

4.2.1 2D-PAGE

Pyridalyl-sensitive and –resistant *S. frugiperda* Sf21 cells were grown until confluency in eight 75cm^2 cell culture flasks (~3x10^6 cells per flask), the cells were aspirated from the flasks, centrifuged for 10 min at 1500 x g and the culture medium was removed. The cell pellet was washed twice in ice-cold isotonic HEPES buffer before finally being resuspended in ice-cold hypotonic HEPES buffer (see section 2.1.5); both the wash and re-suspension buffer contained a protease inhibitor cocktail (Complete protease inhibitor cocktail tablets; Roche, Sussex, UK). The cells were then lysed by homogenisation followed by brief sonication (5 x 3 sec) on ice. The resulting homogenate was centrifuged for 10 min at 1500 x g to remove any cellular debris; the supernatant was removed and transferred to a clean tube and assayed using the Bradford method (see section 2.3.1). 2D-PAGE was then performed using the protein samples as in section 2.3.4. using pH 3-10 IPG strips and a 12% polyacrylamide gel. Initially, 100µg of each sample was analysed on separate gels in order to optimise the protocol and the gels were visualised by silver staining (Fig. 4.4).

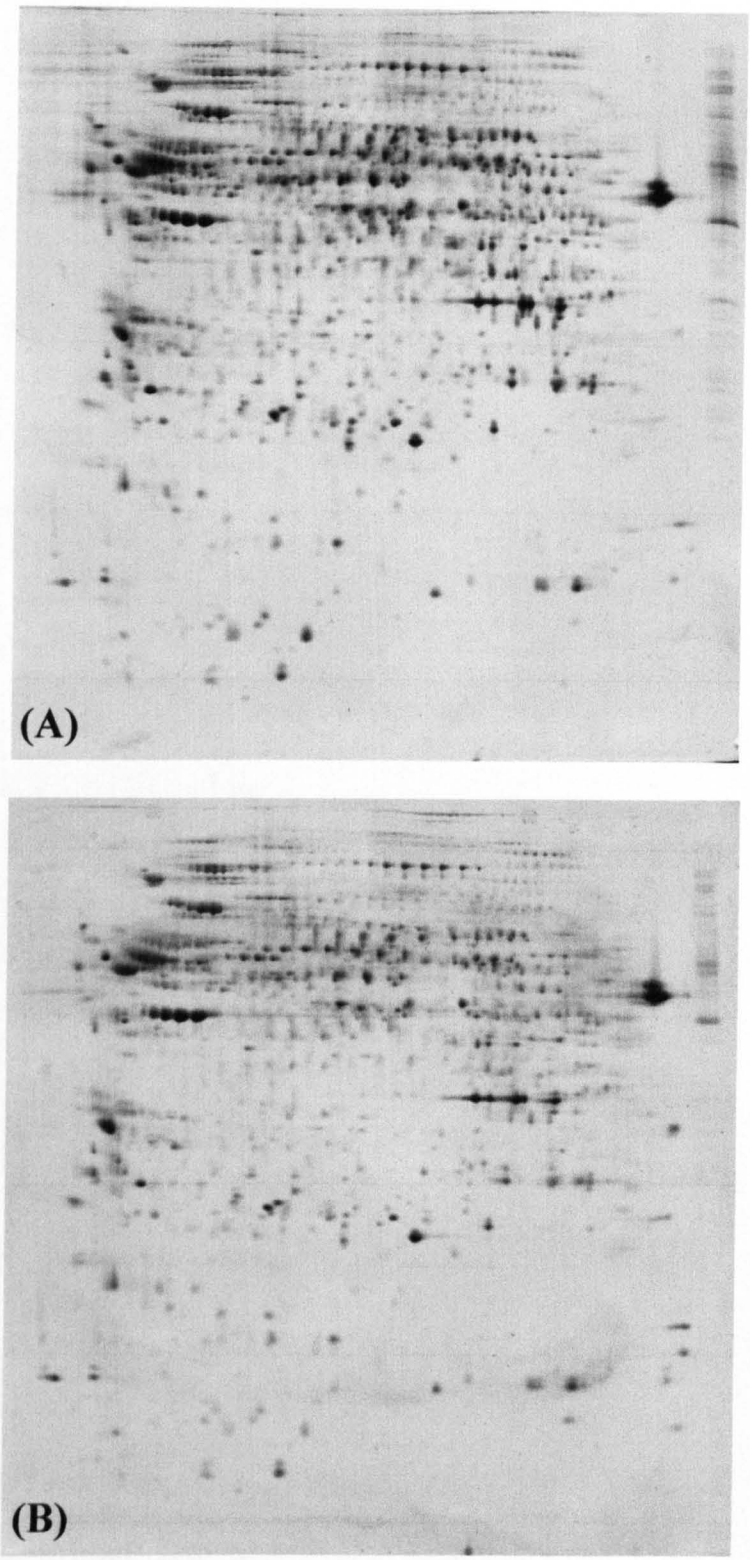

Figure 4.4. Silver stained 2D-PAGE gels showing whole cell proteins from Pyridalyl-sensitive (A) and –resistant (B) Sf21 cells. IEF was performed using pH 3-10 non-linear IPG strips (BioRad) and a 12% polyacrylamide gel was used in the second dimension.

4.2.2 DIGE

100μg of Pyridalyl-sensitive and -resistant Sf21 cell protein extracts, and 100μg of a 50/50 mixture of the two extracts, were precipitated in acetone at -20°C. The precipitate was then centrifuged at 8,000 x g for 5 min, washed twice with ether and allowed to air dry. The protein pellets were then dissolved in 10μl of lysis buffer (10mM Tris, 5mM magnesium acetate, 8M urea, 2M thiourea, 4% CHAPS adjusted to pH 8.5) and centrifuged at 13,000 x g for 5 min. 1μl of fluorescent dye (Cy2, Cy3 and Cy5; GEHC Biosciences) was added to each of the 3 supernatants (different dye for each sample, with Cy2 for the internal standard) and incubated for 30 min at 4°C in the dark. Unreacted linkers were then blocked by addition of 1μl 1mM lysine and incubated for 30 min at 4°C in the dark. The 3 samples were then pooled and an equal volume of 2x buffer [8M urea, 2M thiourea, 4% CHAPS, 0.2% (w/v) DTT, 0.4% (v/v) Biolytes] was added before incubation for 15 min at 4°C. Rehydration buffer (8M urea, 2M thiourea, 4% CHAPS, 0.2% Biolytes, 0.05% ASB14) was then added to a final volume of 320μl. Isoelectric focusing and SDS-PAGE were then performed as previously described. Unfortunately only 3 biological replicate were available for these experiments, which is not ideal, however, the labelling and separation was randomised as in Table 4.1 to eliminate the possibility of preferential labelling. The gels were then imaged using a Typhoon scanner (Fig 4.5, GEHC Biosciences) and image analysis performed using DeCyder software (GEHC Biosciences).

The DeCyder software matches all of the protein spots between all of the samples and, most importantly, all of the replicate gels. It then calculates relative expression levels for the protein spots between the experimental groups, in this case, sensitive and

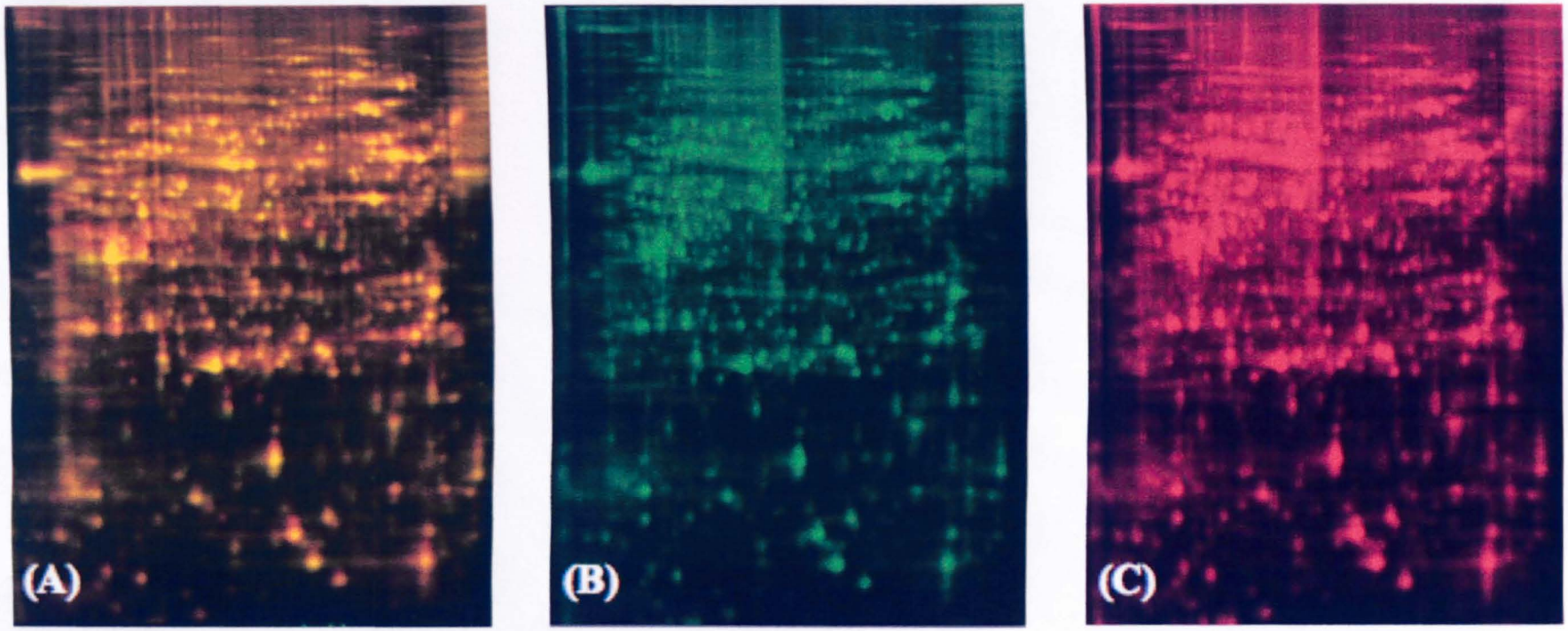

Figure 4.5. 2D-gel images of fluorescently labelled Sf21 whole cell proteins. (A) Internal standard (equal amounts of all experimental groups) labelled with Cy2. (B) Pyridalyl-sensitive cell line proteins labelled with Cy3. (C) Pyridalyl-resistant cell line proteins labelled with Cy5. Images were aquired using a Typhoon fluorescent gel imager (GEHC Biosciences).

resistant cell lines, and is capable of showing a graphical representation of the protein spots (Fig. 4.6). DeCyder can also perform statistical analyses on the data, including a students t-test and 1- and 2-way analysis of variance (ANOVA). The most statistically significant differentially expressed protein spots, i.e spots that showed greater than a 1.4-fold change and had t-test scores less than 0.01, are described in Table 4.2.

4.2.3 Spot excision, tryptic digestion and mass spectrometry

Proteins of interest were excised from four replicate, preparative 2D-gels (each loaded with 500μg of protein) stained with Colloidal Coomassie blue (Fig. 4.7, see section 2.3.7). Fig. 4.7 shows the region (blue box) where cytochrome P450s are likely to be located i.e. M.W. 45-65kDa and pI 7-10. The protein spots were excised using a spot-picking tool and expelled into a microcentrifuge tube. This produces a gel plug of approximately $1mm^3$. The proteins in each gel plug were then digested with trypsin and extracted as described in section 2.3.9. For each gel plug, this produced a 10μl solution of peptides. The samples were then analysed using a Q-Tof mass spectrometer as described in section 2.3.10.

4.2.4 Analysis of mass-spectrometric data and database searching

4.2.4.1 Database searching using the InsPect search engine

In order for the raw mass spectrometric data to be analysed by InsPect it must first be converted to an mzXML instance document using MassWolf software (NHLBI Proteomics Centre). The mzXML file was then analysed by InsPect and the results searched against an appropriate database (Fig. 4.8). The match quality score (MQ) indicates whether the identification is a true or false match. Positive values represent

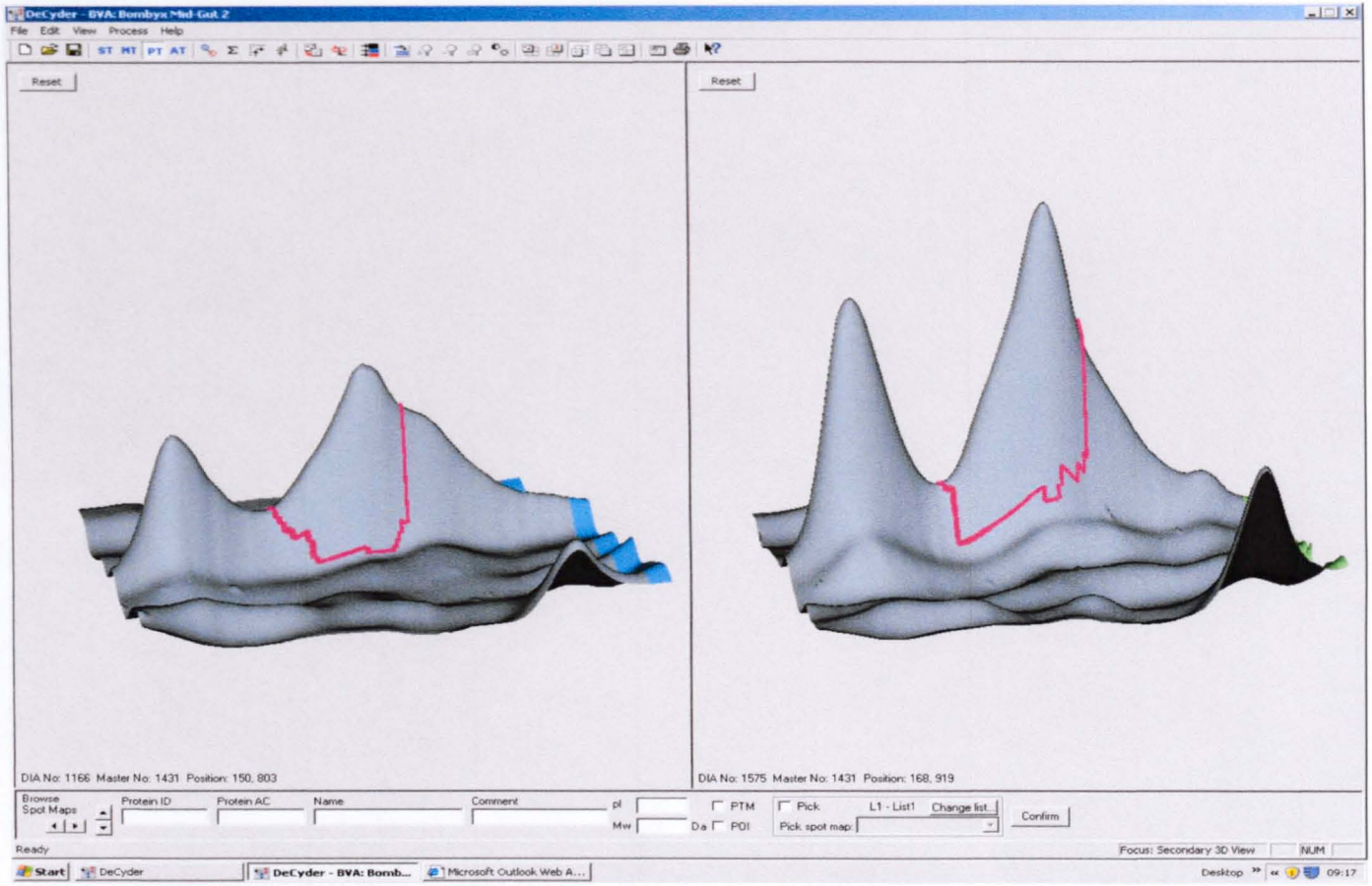

Figure 4.6. A screenshot from DeCyder showing a 3-dimensional representation of 2 protein spots. The same proteins from Pyridalyl-sensitive (left) and –resistant (right) Sf21 cells are shown. The proteins shown are clearly up-regulated in the Pyridalyl-resistant cell line i.e. the volume of the spot in question is an indication of the relative amount of that particular protein in the sample. The red outline highlights the current spot of interest, as detected by the software's spot detection algorithm.

Spot I.D.	Average Ratio of spot intensity Resistant/Sensitive ±S.E.M.	Students t test
321	-2.12 ± 0.03	$7.7x10^{-3}$
873	2.01 ± 0.08	$8.5x10^{-2}$
1043	2.09 ± 0.04	$3.8x10^{-2}$
1422	-2.12 ± 0.05	$9.3x10^{-3}$
1447	2.30 ± 0.02	$2.5x10^{-3}$
1466	-2.01 ± 0.03	$1.4x10^{-2}$
1480	1.92 ± 0.001	$1.0x10^{-3}$
1514	-2.37 ± 0.03	$4.8x10^{-5}$
1531	1.40 ± 0.001	$9.4x10^{-5}$
1567	-2.23 ± 0.005	$1.3x10^{-3}$

Table 4.2. The 10 most statistically significant differentially expressed protein spots between Pyridalyl -sensitive and -resistant Sf21 cells. Spot I.D. numbers are assigned automatically by DeCyder during spot matching between samples/gels starting from the top right corner of the gel. The average ratio of spot intensity, Resistant/Sensitive, represents the relative expression level of that particular protein i.e. an average ratio of 2.0 indicates that protein is upregulated 2.0-fold in the resistant cell line, conversely an average ratio of -2.0 indicates that the protein is down regulated 2.0-fold in the resistant cell line relative to the sensitive cell line. Values for the average ratios of spot intensities are the mean ± S.E.M. of 3 biological replicate samples run on 3 gels.

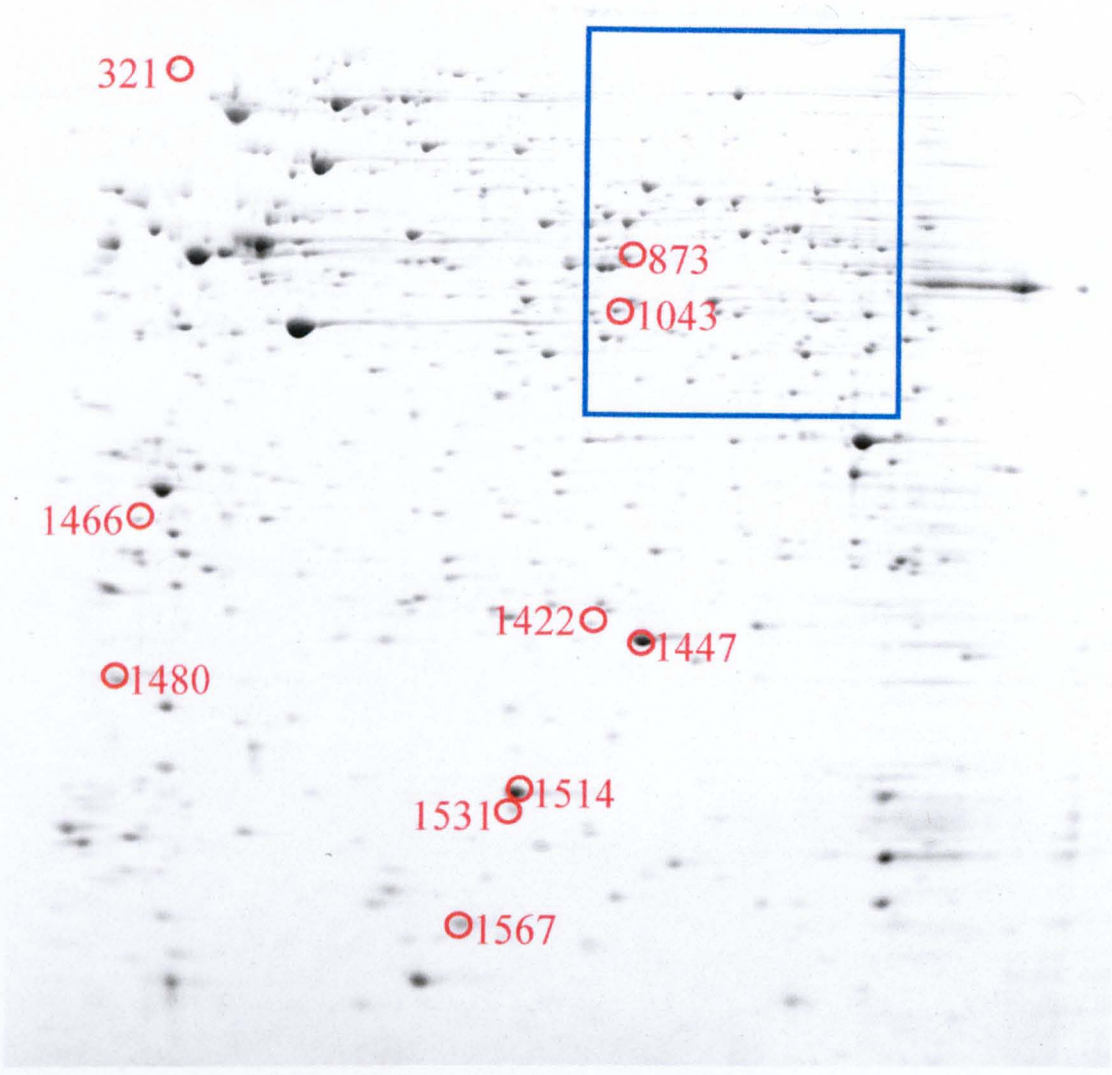

Figure 4.7. Colloidal Coomassie blue stained gel of Sf21 whole cell proteins. The 10 proteins of interest identified by DeCyder are highlighted along with their spot I.D. numbers. The blue box indicates the region of the gel where cytochrome P450s are likely to be located.

Bmb002691

2 peptides, 4 spectra, 14.3% coverage

```
  1 MPLQMTKPAP QFKATAVVNG EFKDISLSDY KGKYVVLFFY PLDFTFVCPT
 51 EIIAFSEKAD EFRKIGCEVL GASTDSHFTH LAWINTPRKQ GGLGPMNIPL
101 ISDKSHRISR DYGVLDEETG IPFRGLFIID DKQNLRQITI NDLPVGSSGP
151 VRCAACDRVW SNRPTADERL TKAGRRFASL SIIVPGSSQY TSAVMLVPFD
201 KKL
```

Residues	Total Spectra	Peptide	p-value	MQScore
90-105	3	K.QGGLGPMNIPLISDK.S	0.00290827164518	3.626
111-125	1	R.DYGVLDEETGIPFR.G	0.000829397773709	2.433

Figure 4.8. A typical InsPect output file for protein spot 1447. The amino acid sequence of the matched protein along with its accession number is shown; the peptides that were identified are shown within this in bold. The output also contains information about the number of peptides that the programme has identified and the number of spectra for each peptide along with p-values and match quality (MQ) scores for each of the peptides.

true matches whereas negative values indicate false matches, the higher the value the greater the likelihood of a correct match (Tanner *et al.*, 2005). As the genome of *S. frugiperda* has not been sequenced, the resulting peptide sequences from manual sequencing and from InsPect matches, were searched against the genome of the most closely related organism, in this case *B. mori*. As the *B. mori* genome is mostly un-annotated, once the peptides had been matched to a protein in the database it was necessary to perform a BLAST search (http://www.ncbi.nlm.nih.gov/BLAST/) to identify the parent protein (Altchul *et al.*, 1990). If, however, the identity of the protein cannot be found by BLAST, then a Conserved Domain Database (CDD) search can be performed to identify the function of the protein (McGinnis & Madden, 2004). The CDD is a compilation of multiple sequence alignments representing protein domains conserved in molecular evolution (Marchler-Bauer *et al.*, 2002) and allows putative annotation (putative function) of even completely un-annotated proteins. The proteins identified in this way from the spots of interest are described below and listed in Table 4.3:

- Two of the proteins were identified as belonging to the thiol peroxiredoxin family of antioxidant proteins.
- Karyopherin alpha 3; a protein involved in intracellular trafficking and secretion.
- Aldehyde dehydrogenase; a family of dehydrogenases that act on aldehyde substrates using NADP as a cofactor (Alnouti & Klaassen, 2008).
- Phosphoglycerate kinase (PGK); a monomeric enzyme which catalyzes the transfer of the high-energy phosphate group of 1,3-bisphosphoglycerate to ADP, forming ATP and 3-phosphoglycerate during glycolysis (Fothergill-Gilmore & Michels, 1993).

- Pop1-like nucleolar protein; an RNA-containing enzyme that generates mature tRNA molecules by cleaving their 5' ends (Lygerou *et al.*, 1994).

No identifications were obtained by Inspect or manual sequencing for four of the protein spots of interest, due to their low abundance.

4.2.4.2 Production of partial amino acid sequences from MS/MS data.

The tandem mass spectrometry spectra were, in part, analysed manually using MassLynx software (Waters, Mass., USA). This software generates three chromatograms containing all of the ions that DDA had selected for analysis in MS/MS mode. Three chromatograms are generated, as the system is capable of selecting and fragmenting three different ions simultaneously. Ions of interest were then selected from the chromatogram and their fragmentation spectra examined and the partial amino acid sequences derived. Ions of weak intensity and ions corresponding to peptides of known contaminant masses, such as trypsin and keratin, were not selected. The fragmentation spectrum for each ion was processed (smoothed and centred) and any doubly-charged ions were converted to their singly-charged mass. This modified spectrum was then analysed using the PepSeq module of MassLynx, by manually assigning amino acids to the intervals between the y-ion peaks in the fragmentation spectrum as previously described. The short peptide sequences obtained in this way were then used to search the *B. mori* genome database using search engines such as BLAST and FASTS. This method was, however, only used to supplement and confirm the analysis performed by InsPect.

Protein Spot Number	Peptides	Spectra	Average Expression Ratio Resistant/Sensitive	Protein Annotation	E value
Highly significant protein hits (low E values) obtained on database searching					
873	1	2	2.01	Aldehyde dehydrogenase	4×10^{-128}
1447	2	4	2.30	Thiol peroxiredoxin	2×10^{-85}
1480	1	19	1.92	Thiol peroxiredoxin	1×10^{-78}
Top protein hits observed that do not have significant E values					
321	2	5	-2.12	Karyopherin alpha 3*	0.14
1043	1	11	2.09	Phosphoglycerate kinase*	0.53
1466	1	2	-2.01	POP1-like nucleolar protein*	1.7

Table 4.3. Top BLAST hits of entire protein sequences, obtained using InsPect/*de novo* sequencing from the 10 DIGE spots of interest. The expect (E) value is a parameter that describes the number of hits that can be expected by chance when searching a database of particular size. Proteins marked by * indicate that only the function of a conserved domain in the protein could be assigned by CDD search.

4.2.5 Quantitative PCR analysis of Thiol peroxiredoxin transcripts in Pyridalyl-treated and –untreated Bombyx BM36 cells

DIGE spot 1447 was identified as belonging to the thiol peroxiredoxin (TPx) family of antioxidant enzymes. As differences were detected in the levels of TPx expression at the protein level between Pyridalyl-sensitive and –resistant Sf21 cells, ideally, any differences at the mRNA level should be investigated. As the genome of *S. frugiperda* is not sequenced, it was impossible to design PCR primers for the TPx gene in this species. As an alternative, primers for the equivalent TPx gene in *B. mori* were designed, as its genome sequence is known. The experimental design was then modified to investigate whether Pyridalyl treatment affects the levels of TPx transcription in Pyridalyl-sensitive *Bombyx* BM36 cells.

Reverse transcription PCR (RT-PCR) is the most sensitive method for the detection of low abundance mRNA, often obtained from limited tissue or cell samples (Bustin, 2000). Real-time, or quantitative, PCR (Q-PCR) allows the measurement of PCR products as they accumulate, or in 'real-time'. It is possible to measure the amount of PCR product at a point in which the reaction is in its exponential range (Ginzinger, 2002), thus eliminating the unreliability of end-point quantification.

Total RNA was extracted from $1x10^6$ BM36 cells that had been treated with Pyridalyl (10μg/ml final concentration) overnight, and from the same number of BM36 cells that had been treated with DMSO. This group represents the untreated control as Pyridalyl is added to the cell culture medium dissolved in DMSO. Reverse transcription was performed using Superscript™ II reverse transcriptase

(Invitrogen) and the resulting cDNA stored at -80°C for later use. The TPx gene was amplified from the cDNA derived from Pyridalyl-treated and –untreated BM36 cells using Q-PCR. Fig. 4.9 shows the sequence of the *Bombyx* cDNA. The primers used in the reaction were designed using the *B. mori* TPx cDNA sequence:

- **TPx-For** 5′-CATTCCTCTGATAAGCGACAAGTCGCACCG-3′
- **TPx-Rev** 5′-TGTCCGTGAACTGGAAGGCCTGCACCAGCC-3′

The primers were designed to have similar annealing and melting temperatures and also to produce an approximate 200bp PCR product, i.e. the optimum sized product for Q-PCR. Q-PCR was performed using a Rotor-Gene 3000 instrument (Corbett Life Science) and SYBR® Green JumpStart™ *Taq* ReadyMix™ for quantitative PCR allowing PCR products to be quantified fluorescently using the double-stranded DNA binding dye SYBR green (Fig. 4.10).

The threshold cycle (Ct) indicates the fractional cycle number at which the amount of amplified target reaches a fixed threshold. Ct values for test (TPx) and control (Actin) genes were generated by Rotor-Gene Real-Time analysis software 6.0 (build 14) (Corbett Research).

The equation that describes the exponential amplification of PCR is:

$$X_n = X_0 \times (1 + E_x)^n$$

Where X_n is the number of target molecules at cycle n of the reaction, X_0 is the initial number of target molecules. E_x is the efficiency of target amplification (in this case, efficiency is 2 as the number of target molecules doubles after every cycle) and n is the number of cycles (Livak & Schmittgen, 2001). From this equation, a method for

Figure 4.9. *B. mori* TPx cDNA sequence. The shaded box shows the 585bp open reading frame. The two primer binding sites are shown underlined.

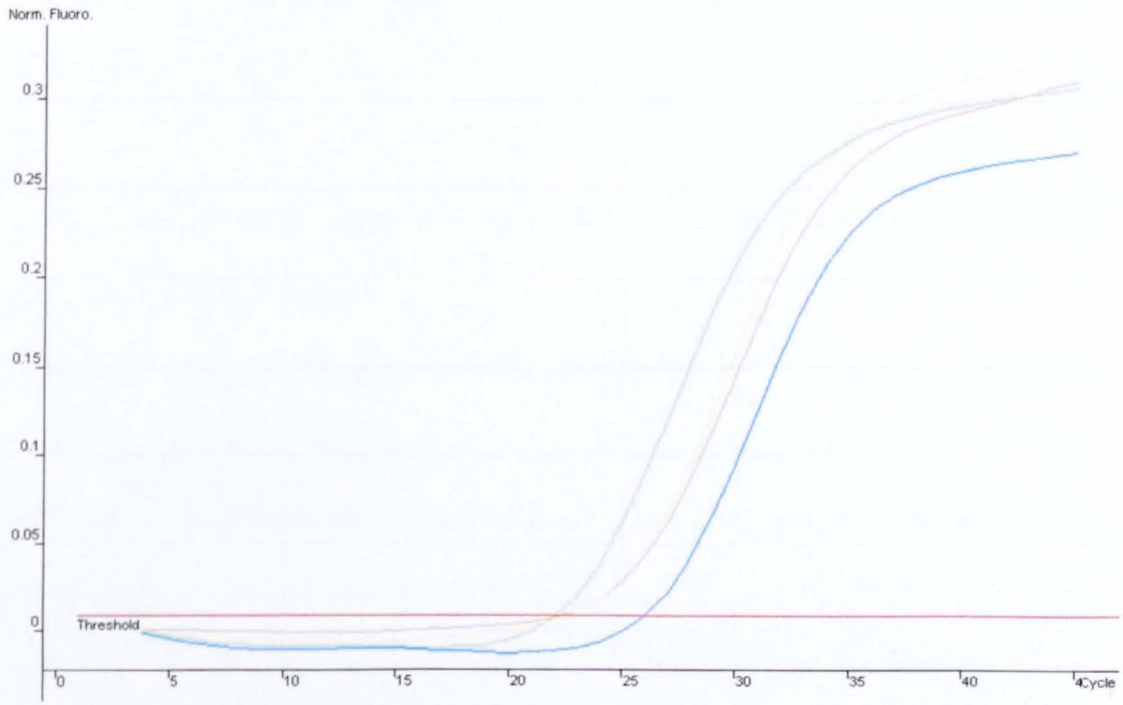

Figure 4.10. Q-PCR quantification data showing amplification of the TPx gene from *B. mori* cDNA. The threshold is a fixed level of fluorescence at which Ct (threshold cycle) values are calculated. From this, the real-time analysis software can calculate relative changes in the levels of transcripts. Yellow and green lines represent levels of TPx DNA present after each cycle, whereas magenta and blue lines represent the levels of control gene DNA (Actin) present after each cycle.

determining relative changes in amounts of transcript (R) can be derived:

$$R = 2^{\Delta Ct\ (\text{Control TPx Ct} - \text{Treated TPx Ct})} / 2^{\Delta Ct\ (\text{Control Actin Ct} - \text{Treated Actin Ct})}$$

The formula above estimates the relative change in expression of each test gene relative to the reference gene, in this case, Actin. A relative change of 1 indicates no change, anything above 1 is an increase and anything below 1 is a decrease. The results obtained for TPx indicated a relative change of approximately 1, therefore, there were no significant changes in the relative amounts of TPx transcripts.

4.2.6 Measurement of hydrogen peroxide (H_2O_2) concentrations in BM36 and Sf21 cells treated with Pyridalyl

As the main role of TPx is to remove hydrogen and alkyl-peroxides using a thiol reducing equivalent, the up-regulation of TPx has led to the hypothesis that Pyridalyl metabolism leads to the formation of peroxides, therefore, it was decided to investigate whether any hydrogen or organic peroxides could be detected in Pyridalyl-treated cells. The method used for analysis was a modification of the method of Al Mushrif *et al.* (1998). BM36 and Sf21 cells from 75cm^2 cell culture flasks (~ 1x10^6 cells) were centrifuged at 1300 x g for 10 min and the resulting supernatant removed. The cell pellets were each resuspended in 1ml of fresh medium, treated with 10µg of Pyridalyl and incubated at 27°C overnight. The reaction was stopped by the centrifugation of the cells and the removal of the culture medium. The cells were then lysed with 0.01M acetate buffer (pH 4.5). Standards containing 0.01, 0.02, 0.1, 0.3, 0.5, 1.0, 2.0, 3.0, 4.0 and 5.0µg H_2O_2/ml were prepared in 0.01M acetate buffer pH 4.5. 1ml of each standard and of each sample were added to separate centrifuge tubes, containing 0.2ml peroxidase [(0.01 mg/ml) from Horseradish; Sigma] and 20µl o-dianisidine (1% w/v; Sigma).

A blank containing 1ml 0.01M acetate buffer, 0.2ml peroxidase and 20µl o-dianisidine was also prepared. The contents of each tube were mixed well and incubated at 25°C. After 10 min 40µl of 4M HCl was added to each tube to stop the reaction and stabilise colour production. After 5 min, the absorption of standards and samples was measured at 400nm in a UV/visible spectrophotometer. A calibration curve was drawn from the readings for the standards and the concentrations of H_2O_2 in the unknown test samples calculated from this. No hydrogen peroxide could be detected in any of the samples.

4.3 Discussion

The aim of this chapter was to investigate differences in protein expression between Pyridalyl-resistant and –sensitive cell lines. Any differences between these two cell lines may well point to possible target areas for Pyridalyl action, however, differences may not be observed until the cells are challenged with the insecticide, for instance if the resistance mechanism involves the up-regulation of an enzyme that detoxifies Pyridalyl that is only induced upon treatment. It was shown in Chapter 3 that cytochrome P450-dependent metabolism is required for Pyridalyl's insecticidal activity. Thus, it was of particular interest to examine whether any differences could be detected in the expression of cytochrome P450s between Pyridalyl-sensitive and –resistant cell lines. However, hydrophobic membrane proteins (including microsomal membrane proteins such as P450s) tend to precipitate and don't run well during isoelectric focusing, making detection of differences in P450 expression almost impossible. Fig 4.7 shows the region of a 2D-gel where cytochrome P450s are likely to be located.

The initial hypothesis was that the P450 or P450s involved in Pyridalyl metabolism may be down-regulated in the resistant cell line, thus, leading to a decrease in the metabolism of the insecticide to its active metabolites. Although a cytochrome P450 that is involved in the metabolism of Pyridalyl was not identified in this study, it did yield intriguing results, most interestingly the 2.3-fold up-regulation of thiol peroxiredoxin (TPx) in Pyridalyl-resistant cells. TPx is known to eliminate H_2O_2 and alkyl hydroperoxides with use of a thiol-reducing equivalent (Lee *et al.*, 2005). Two closely related members of the TPx family were identified as being up-regulated by DeCyder (spots 1447 and 1480; Table 4.2 & 4.3)

Organisms living in aerobic environments require defence mechanisms that prevent oxidative damage caused by reactive oxygen species (ROS). ROS such as the superoxide anion, hydrogen peroxide and the hydroxyl radical are noted for their high reactivity and resultant damage to proteins, lipid membranes and DNA (Halliwell and Guterridge, 1989). To protect against the toxicity of ROS, aerobic organisms have evolved protective enzyme systems, amongst which is TPx, that is known to eliminate H_2O_2 and other ROS (Lim *et al.*, 1993). The TPx family is a large family of antioxidant proteins ubiquitously found in all living organisms, from prokaryotes to eukaryotes (Chae *et al.*, 1994). In insects, TPx genes have been isolated from *Drosophila melanogaster, Aedes aegypti, Apis mellifera* and *Bombyx mori.* (Radyuk *et al.*, 2001).

These data, coupled with the data from the live cell imaging and metabolism experiments, leads to the possible hypothesis that the metabolism of Pyridalyl (possibly by a cytochrome P450) leads to the production of H_2O_2 and/or other reactive oxygen species. These reactive species cause oxidative damage, which eventually leads to cell death. We can further hypothesise that the resistant cell line still metabolises Pyridalyl, however, TPx removes the reactive oxygen species before any damage can be done, thus, protecting the cells. Detection of H_2O_2 and other ROS in Pyridalyl treated cells has been attempted, however, no H_2O_2 could be detected in Sf21 or BM36 cells. More sensitive methods involving the use of chemiluminescense (Fossati *et al.*, 2002) have also been used, but with no success. It should be noted that as this experiment does not deal with the first hand effects of Pyridalyl i.e. direct Pyridalyl treatment, the involvement of TPx in the protection of insect cells from the action of Pyridalyl can only be implied and not definitively proven.

The fact that Q-PCR showed no significant changes in the levels of TPx transcripts between Pyridalyl-treated and –untreated *Bombyx* BM36 cells is not a negative result. It has been shown, previously that in two samples with steady mRNA levels protein levels can vary by more than 20-fold (Gygi *et al.*, 1999). There is emerging evidence which suggests that an increase in mRNA levels may not necessarily cause an increase in protein translation and *vice versa.* This evidence includes discoveries of post-transcriptional mechanisms controlling the protein translation rate (Harford and Morris, 1997), changes to the half-lives of specific proteins or mRNAs (Varshavsky, 1996) and the intracellular location and molecular association of the protein products of expressed genes (Urlinger *et al.*, 1997). Had more time been available it would have been beneficial to sequence the Q-PCR product to ensure that it is indeed the TPx cDNA sequence that has been amplified.

Another of the differentially expressed proteins that was identified is Aldehyde dehydrogenase and is up-regulated 2-fold in Pyridalyl-resistant Sf21 cells. Aldehyde dehydrogenases are enzymes that catalyse the irreversible oxidation of a wide spectrum of endogenous and exogenous aldehydes to their corresponding carboxylic acids. Aldehydes are formed during oxidative stress, being very long-lived molecules and potent electrophiles that interact with cellular macromolecules (Esterbauer *et al.*, 1991). The up-regulation of this enzyme in Pyridalyl-resistant cells again suggests that Pyridalyl metabolism leads to the production of reactive oxygen species (such as peroxides and aldehydes) and, ultimately, cell death.

Harder to explain, however, is the differential expression of the other identified proteins; one is a part of the glycolytic pathway (Phosphoglygerate kinase), one is involved in transport between cytosol and nucleus [Karyopherin alpha (Cook *et*

al., 2007)] and the final protein is involved in the production of mature tRNAs from their precursors (Pop1-like nucleolar protein).

CHAPTER 5

EFFECTS OF PYRIDALYL ON PROTEIN EXPRESSION IN *BOMBYX MORI* MIDGUT AND IN THE *B. MORI* BM36 CELL LINE

5.1 INTRODUCTION

Silkworms are amongst the best studied of all lepidopteran insects and belong to two families, Bombycidae and Saturniidae. The domesticated silkworm, *Bombyx mori*, a member of the family Bombycidae, is a well-studied lepidopteran model system with a rich repertoire of genetic information available on mutations affecting morphology, development and behaviour (Arunkumar *et al.*, 2006). Archaeological evidence indicates that *B. mori* were domesticated in China at least 5000 years ago. It is the only truly domesticated insect species, being completely dependent on humans for survival and reproduction (Goldsmith *et al.*, 2005). Silkworms are also one of the most economically important insects, being employed in the production of silk; the value of China's silk industry in 2006 alone reached $17.7 billion (Xia *et al.*, 2007).

Due to its large size, complex metabolism and the abundance of mutants, the silkworm has become one of the best-characterised models for biochemical, molecular genetic and genomic studies of the order Lepidoptera (Nagaraju & Goldsmith, 2002). Due to its position as a model Lepidopteran, the genome of *B. mori* has now been fully sequenced (Xia *et al.*, 2004) and a genome-wide microarray has been produced covering all 22,987 known and predicted genes in the genome (Xia *et al.*, 2007).

The wealth of information available for *B. mori*, i.e. genome sequence and EST databases, makes it an ideal candidate for proteome studies. Furthermore, it was shown in Chapter 2 that *B. mori* is sensitive to the cytotoxic effects of Pyridalyl and metabolises the insecticide in an apparently similar way to other Lepidopteran species.

Evidence was produced in Chapter 3 demonstrating the requirement for cytochrome P450 in the action of Pyridalyl and the suggestion was made that Pyridalyl may induce up-regulation of a cytochrome P450, possibly involved in its own metabolism. Furthermore, results of proteomic analyses (Chapter 4) of Pyridalyl-sensitive and –resistant Sf21 cells, showed the up-regulation of a number of proteins involved in removing ROS. The required cytochrome P450 may be involved in the production of such reactive oxygen species.

In view of the foregoing, it was necessary to examine directly the effects of Pyridalyl on the proteome. Firstly, it was necessary to examine whether Pyridalyl led to up-regulation of a cytochrome P450. Since most P450s are microsomal, including xenobiotic-metabolising ones, such a sub-cellular fraction (sub-proteome) was used to increase the likelihood of detecting such an up-regulated protein. For this, *Bombyx* larvae were treated and the midgut was used to provide sufficient material. It has been reported that Pyridalyl exhibits activity on *Bombyx* and we have corroborated this. For examination of the effects of Pyridalyl on the general cellular proteome, whole BM36 cells were used.

Therefore, proteomic experiments were designed to investigate differences in protein expression between Pyridalyl-treated and –untreated *B. mori* insect midgut

microsomes and in a separate, but complementary, experiment to investigate differences in protein expression between Pyridalyl-treated and –untreated whole *B. mori* BM36 cells. Differentially expressed proteins may well reflect candidate target processes for Pyridalyl action in this model lepidopteran.

Techniques for mass spectrometry-based protein identification rely strongly upon exact matching of peptides and/or peptide fragments to sequences from database entries, making the identification of proteins from organisms with unsequenced genomes difficult (eg the identification of *Spodoptera frugiperda* proteins in Chapter 4, Liska *et al.*, 2004). Using *B. mori* for these proteomics studies eliminates the need for cross-species protein identification (Habermann *et al.*, 2004) and homology-based protein identification (Shevchenko *et al.*, 2001).

5.2 Methods and Results

For both types of samples, a DIGE approach was used, after first optimising the separations by 2D-PAGE. As stated in section 2.2.3 *B. mori* larvae were treated with 10μg of Pyridalyl in 1g of artificial diet, following overnight incubation the insect larvae exhibited signs of insecticidal action.

5.2.1 2D-PAGE

5.2.1.1 B. mori midgut 2D-PAGE

It has previously been shown (section 3.2.2) that the metabolism of Pyridalyl by at least one cytochrome P450 is essential for its insecticidal action. As the expression of xenobiotic-metabolising cytochrome P450s, which are bound to the endoplasmic reticulum, is often induced by their substrate (see section 1.5), it was envisaged that a proteomic analysis of *B. mori* midgut microsomal proteins may allow the identification of an up-regulated cytochrome P450 responsible for Pyridalyl metabolism. Microsomal proteins were isolated from 10 Pyridalyl-treated and –untreated 5^{th} instar *B. mori* larvae as described in sections 2.2.1 to 2.2.4. The larvae were synchronized at the $4^{th}/5^{th}$ moult and were used at the 2^{nd} day of the 5^{th} instar. The microsomal proteins were assayed using the Bradford method (see section 2.3.1), precipitated with acetone, and 2D-PAGE was then performed using the samples as in section 2.3.4. using pH 3-10 IPG (7cm) strips and a 10% polyacrylamide gel. Initially, 100μg of each sample was analysed on separate gels in order to optimise the protocol and the gels were visualised by silver staining (Fig. 5.1).

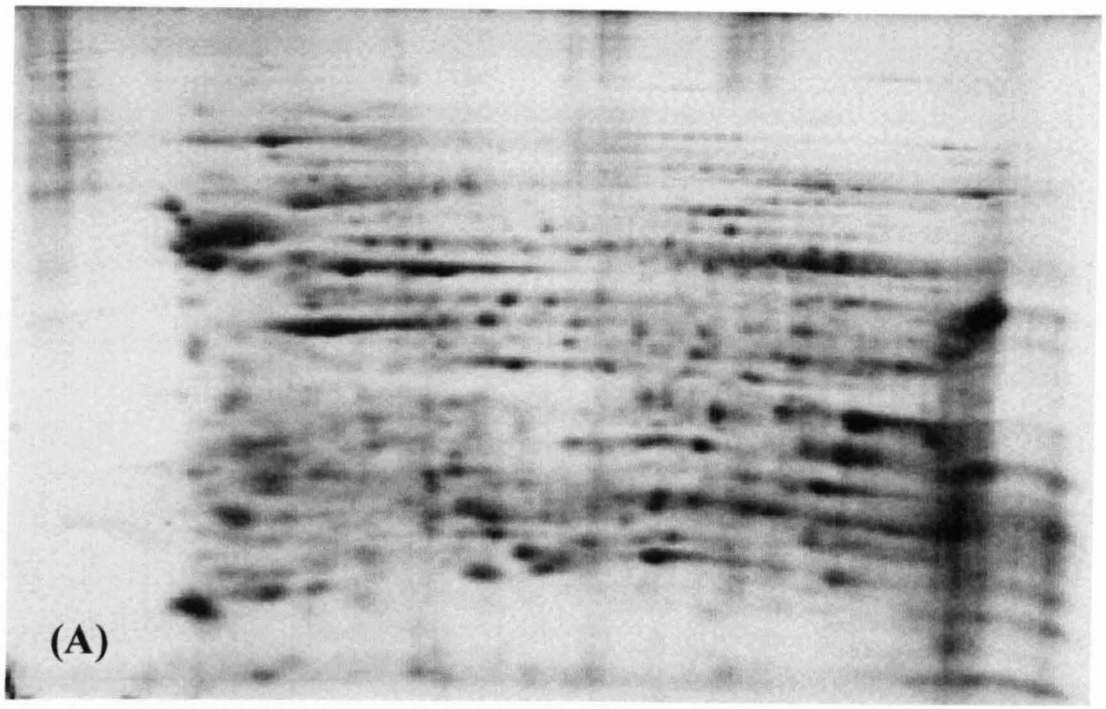

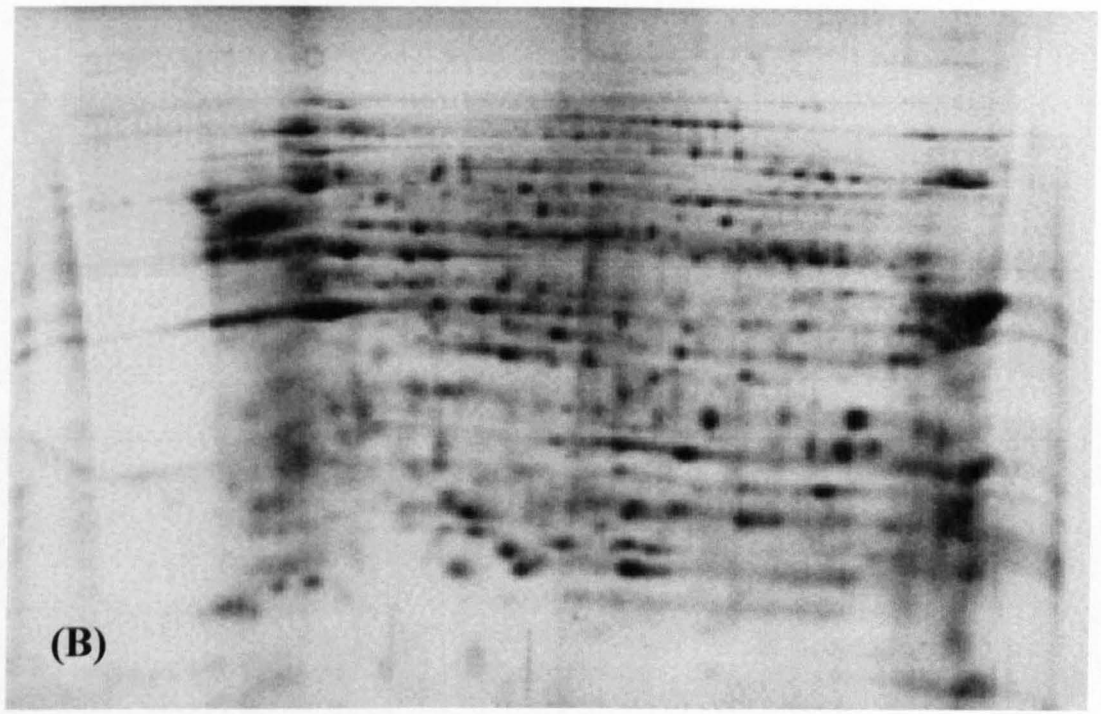

Figure 5.1. Silver stained 2D-PAGE gels showing microsomal proteins from Pyridalyl-untreated (A) and –treated (B) *B. mori* mid-gut tissue. IEF was performed using 7cm pH 3-10 non-linear IPG strips (BioRad) and a 10% polyacrylamide gel was used in the second dimension.

5.2.1.2 BM36 cell 2D-PAGE

B. mori BM36 cells were grown until confluency in eight 75cm^2 cell culture flasks (~3x10^6 cells per flask) and treated overnight with 1µg/ml (final concentration) Pyridalyl (for details see Chapter 2). The cells were aspirated from the flasks, centrifuged for 10 min at 1500 x g and the culture medium was removed. The cell pellet was washed twice in ice-cold isotonic HEPES buffer before finally being resuspended in ice-cold hypotonic HEPES buffer (see section 2.1.5); both the wash and re-suspension buffer contained a protease inhibitor cocktail (Complete protease inhibitor cocktail tablets; Roche, Sussex, UK). The cells were then lysed by homogenisation followed by brief sonication (5 x 3 sec) on ice. The resulting homogenate was centrifuged for 10 min at 1500 x g to remove any cellular debris; the supernatant was removed and transferred to a clean tube and assayed using the Bradford method (see section 2.3.1). 2D-PAGE was then performed on the acetone precipitated protein samples as in section 2.3.4. using 17cm pH 3-10 IPG strips and a 10% polyacrylamide gel. Initially, 100µg of each sample was analysed on separate gels in order to optimise the protocol and the gels were visualised by silver staining (Fig. 5.2).

5.2.2 DIGE

DIGE was performed using both sets of samples in independent experiments. Pyridalyl-treated and –untreated *B. mori* insect midgut microsomal proteins and Pyridalyl-treated and –untreated BM36 whole cell proteins were precipitated in acetone at -20°C. The precipitates were then centrifuged at 8,000 x g for 5 min, washed twice with ether and allowed to air dry. The protein pellets were then dissolved in 10µl of lysis buffer (10mM Tris, 5mM magnesium acetate, 8M urea, 2M thiourea, 4% CHAPS adjusted to pH 8.5) and centrifuged at 13,000 x g for 5

min. 1μl of fluorescent dye (Cy2, Cy3 and Cy5 in dimethyl foramide; DMF; GEHC

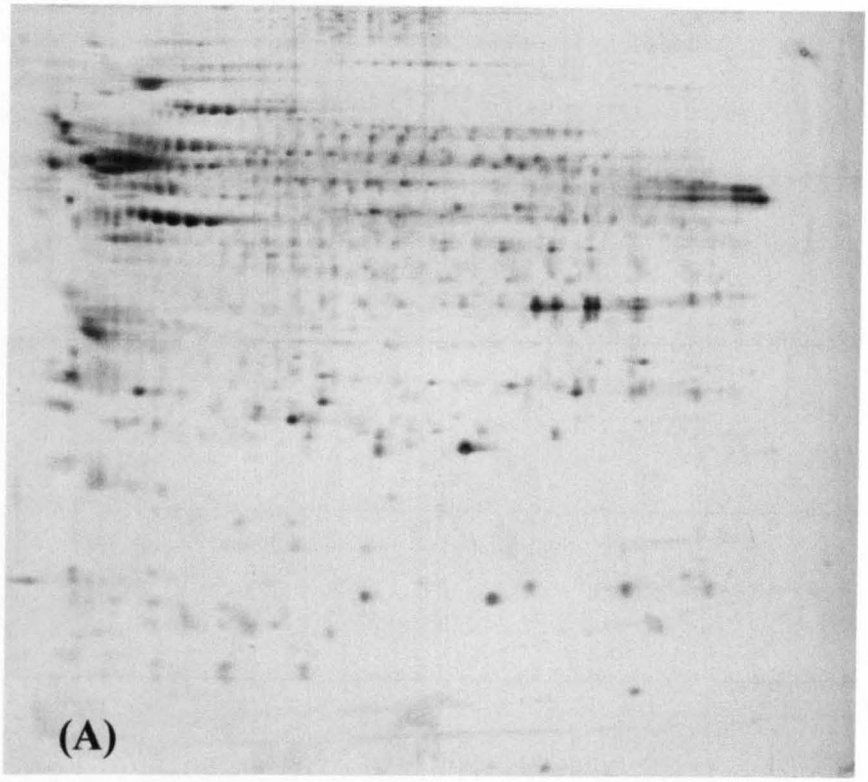

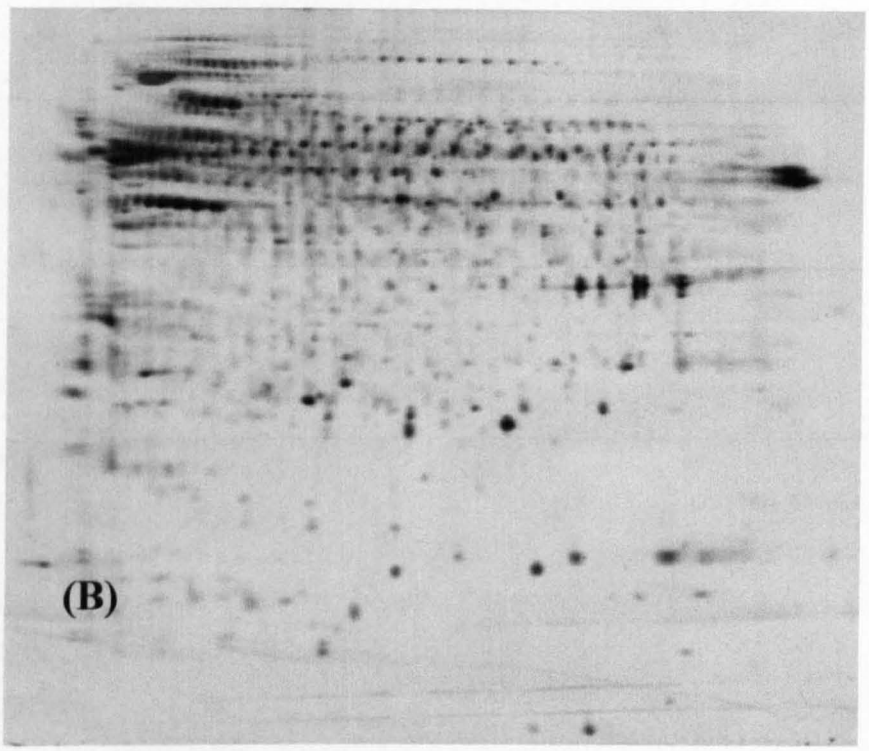

Figure 5.2. Silver stained 2D-PAGE gels showing whole cell proteins from Pyridalyl-untreated (A) and –treated (B) BM36 cells. IEF was performed using 17cm pH 3-10 non-linear IPG strips (BioRad) and a 10% polyacrylamide gel was used in the second dimension.

Biosciences) was added to each of the 3 supernatants, a different dye was used for each sample, with Cy2 being used to label the internal standard; and incubated for 30 min at 4°C in the dark. The labelling procedure was that recommended by GEHC Biosciences (www.gelifesciences.com/aptrix/upp00919.nsf/Content/Proteomics+DIGE). Unreacted linkers were then blocked by addition of 1µl 1mM lysine and incubated for 30 min at 4°C in the dark. The 3 samples were then pooled and an equal volume of 2x buffer [8M urea, 2M thiourea, 4% CHAPS, 0.2% (w/v) DTT, 0.4% (v/v) Biolytes] was added before incubation for 15 min at 4°C. Rehydration buffer (8M urea, 2M thiourea, 4% CHAPS, 0.2% Biolytes, 0.05% ASB14) was then added to a final volume of 320µl. Isoelectric focusing and SDS-PAGE were then performed as previously described on 17cm gels. Gels were produced using 4 biological replicates in both of the experiments, the labelling and separation was randomised as in Table 4.1 (Chapter 4) to eliminate the possibility of preferential labelling. The gels were then imaged using a Typhoon scanner (GEHC Biosciences) and image analysis performed using DeCyder software as in section 4.4.2 (GEHC Biosciences). The most statistically significant differentially expressed protein spots identified by DeCyder are summarised in Table 5.1 for the *B. mori* mid-gut experiment and Table 5.2 for the BM36 cell experiment. Spots exhibiting greater than 1.4-fold change and a t-test α-level of less than $1x\ 10^{-2}$ were chosen.

5.2.3 Spot excision, tryptic digestion and mass spectrometry

Proteins of interest were excised from four replicate, preparative 17cm 2D-gels (each loaded with 500µg of protein) stained with Colloidal Coomassie blue for both of the experiments (Fig. 5.3 & 5.4, see section 2.3.7). The protein spots were excised using a

Spot I.D.	Average Ratio of spot intensity Treated/Untreated ±S.E.M.	Students t test
1237	1.65 ± 0.03	$2.9x10^{-3}$
2043	-2.10 ± 0.07	$1.8x10^{-2}$
2048	1.84 ± 0.06	$1.5x10^{-2}$
2639	1.49 ± 0.05	$3.1x10^{-3}$
2983	-1.45 ± 0.04	$8.3x10^{-3}$
3743	2.64 ± 0.09	$2.7x10^{-2}$
3838	1.48 ± 0.03	$2.1x10^{-3}$
3894	2.32 ± 0.07	$2.7x10^{-3}$
3989	1.67 ± 0.03	$9.6x10^{-3}$

Table 5.1. The nine most statistically significant differentially expressed protein spots between Pyridalyl -treated and –untreated *B. mori* insect midgut tissue. Spot I.D. numbers are assigned automatically by DeCyder during spot matching between samples/gels starting from the top right corner of the gel. The average ratio of spot intensity, Treated/Untreated, represents the relative expression level of that particular protein i.e. an average ratio of 2.0 indicates that the protein is upregulated 2.0-fold in the treated sample; conversely an average ratio of -2.0 indicates that the protein is down regulated 2.0-fold in the treated sample relative to the untreated sample. Values for the average ratios of spot intensities are the mean ± S.E.M. of 4 biological replicate samples run on 8 gels.

Spot I.D.	Average Ratio of spot intensity Treated/Untreated ±S.E.M.	Students t test
426	-1.46 ± 0.05	8.9×10^{-5}
456	-1.96 ± 0.09	1.7×10^{-5}
692	4.06 ± 0.03	2.1×10^{-4}
756	1.97 ± 0.03	5.7×10^{-4}
764	-1.46 ± 0.07	5.9×10^{-5}
1185	-2.43 ± 0.06	1.7×10^{-4}
1684	1.44 ± 0.08	1.3×10^{-4}
1756	-2.17 ± 0.02	3.1×10^{-4}
1924	4.01 ± 0.04	2.3×10^{-4}
1930	5.03 ± 0.03	8.7×10^{-4}
2081	1.41 ± 0.07	8.3×10^{-4}
2256	1.54 ± 0.08	3.7×10^{-4}
2263	-3.83 ± 0.07	5.5×10^{-4}
2288	2.45 ± 0.05	3.5×10^{-4}
2366	2.12 ± 0.05	3.8×10^{-4}

Table 5.2. The fifteen most statistically significant differentially expressed protein spots between Pyridalyl –treated (1μg/ml, overnight) and control-treated (DMSO) *B. mori* BM36 cells. Spot I.D. numbers are assigned automatically by DeCyder during spot matching between samples/gels starting from the top right corner of the gel. The average ratio of spot intensity, Treated/Untreated, represents the relative expression level of that particular protein i.e. an average ratio of 2.0 indicates that the protein is upregulated 2.0-fold in the treated sample; conversely an average ratio of -2.0 indicates that the protein is down regulated 2.0-fold in the treated sample relative to the untreated sample. Values for the average ratios of spot intensities are the mean ± S.E.M. of 4 biological replicate samples run on 8 gels.

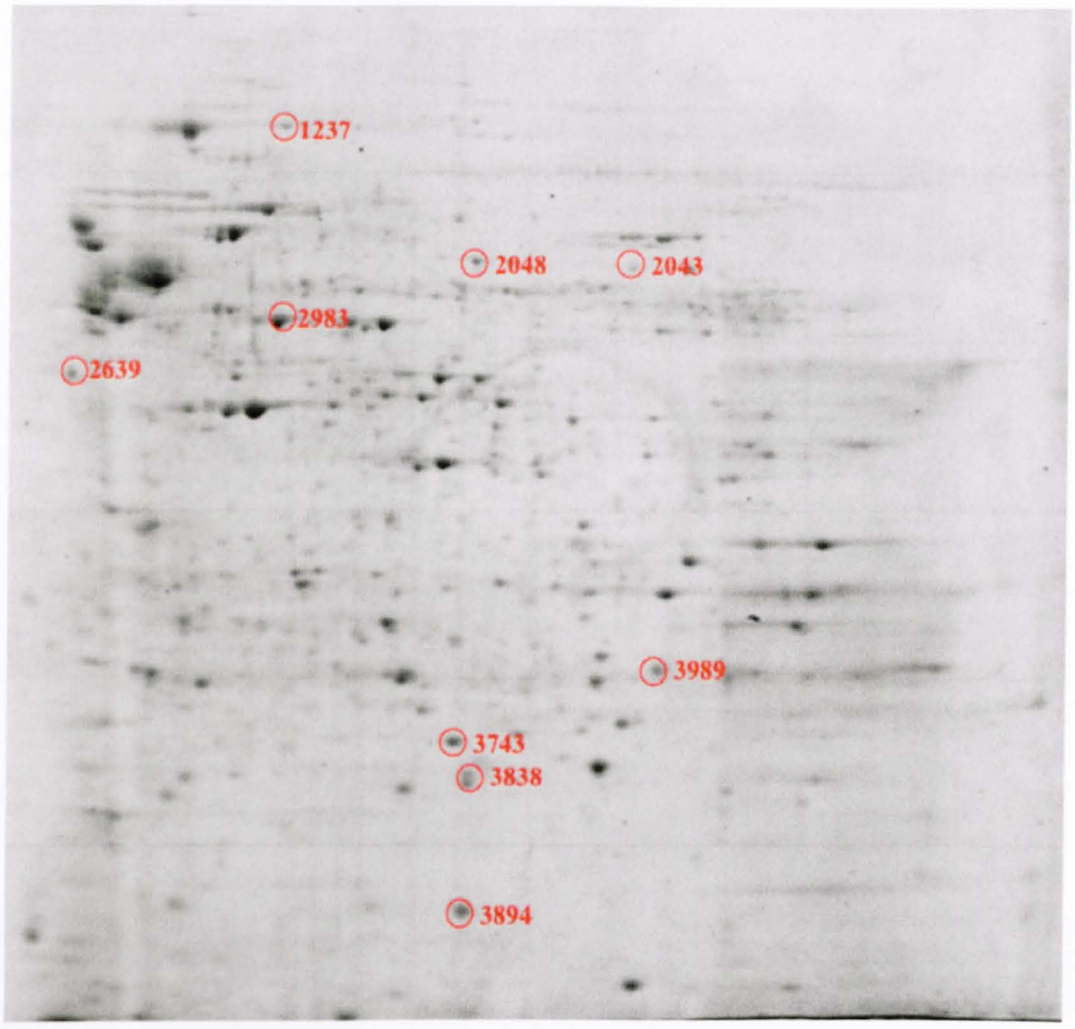

Figure 5.3. Colloidal Coomassie blue stained gel of *B. mori* midgut microsomal proteins. The 9 proteins of interest identified by DeCyder are highlighted along with their spot I.D. numbers.

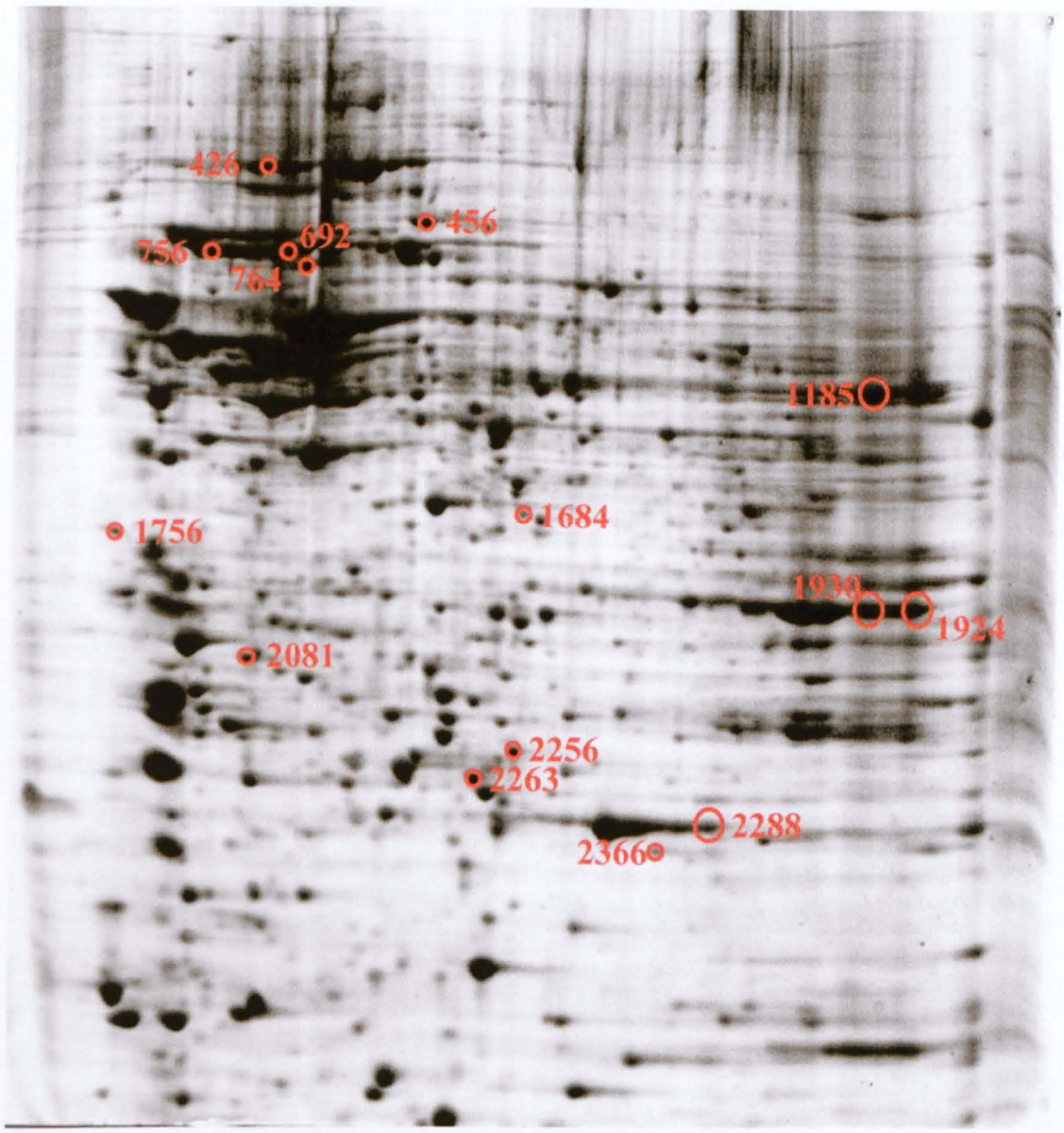

Figure 5.4. Colloidal Coomassie blue stained gel of *B. mori* BM36 whole cell proteins. The 15 proteins of interest identified by DeCyder are highlighted along with their spot I.D. numbers.

spot-picking tool and expelled into a microcentrifuge tube. This produces a gel plug of approximately $1mm^3$. The proteins in each gel plug were then digested with trypsin and extracted as described in section 2.3.9. For each gel plug, this produced a 10µl solution of peptides. The samples were then analysed using a Q-Tof mass spectrometer as described in section 2.3.10.

5.2.4 Analysis of mass spectrometric data and database searching

Mass spectrometric data for both the *B. mori* midgut DIGE experiment and the BM36 cell DIGE experiment were analysed using the InsPect database searching tool as in section 4.2.4.1 and manual sequencing as in section 4.2.4.2. However, another technique was also used when InsPect failed to provide identification and the MS/MS spectrum was of insufficient quality. This new technique is basically a MASCOT search that searches all of the available spectra for a given protein simultaneously, thereby producing a protein score rather than a peptide score as with traditional MASCOT searches. The Peak List Conversion Utility (www.proteomecommons.org/current/531/ConvertPeakList.jnlp) is used to produce a merged file containing all of the processed spectra for the protein of interest. This is then used as the input file for a standard MASCOT search (Falkner *et al.*, 2006). See Fig. 5.5 for diagram outlining protein identification methods. InsPect searches were undertaken against a local *Bombyx* protein database (21,000 entries) obtained from Professor David Heckel (Max Planck Institute for Chemical Ecology, Jena), whereas MASCOT searches were against both this database and MSDB (NCBI).

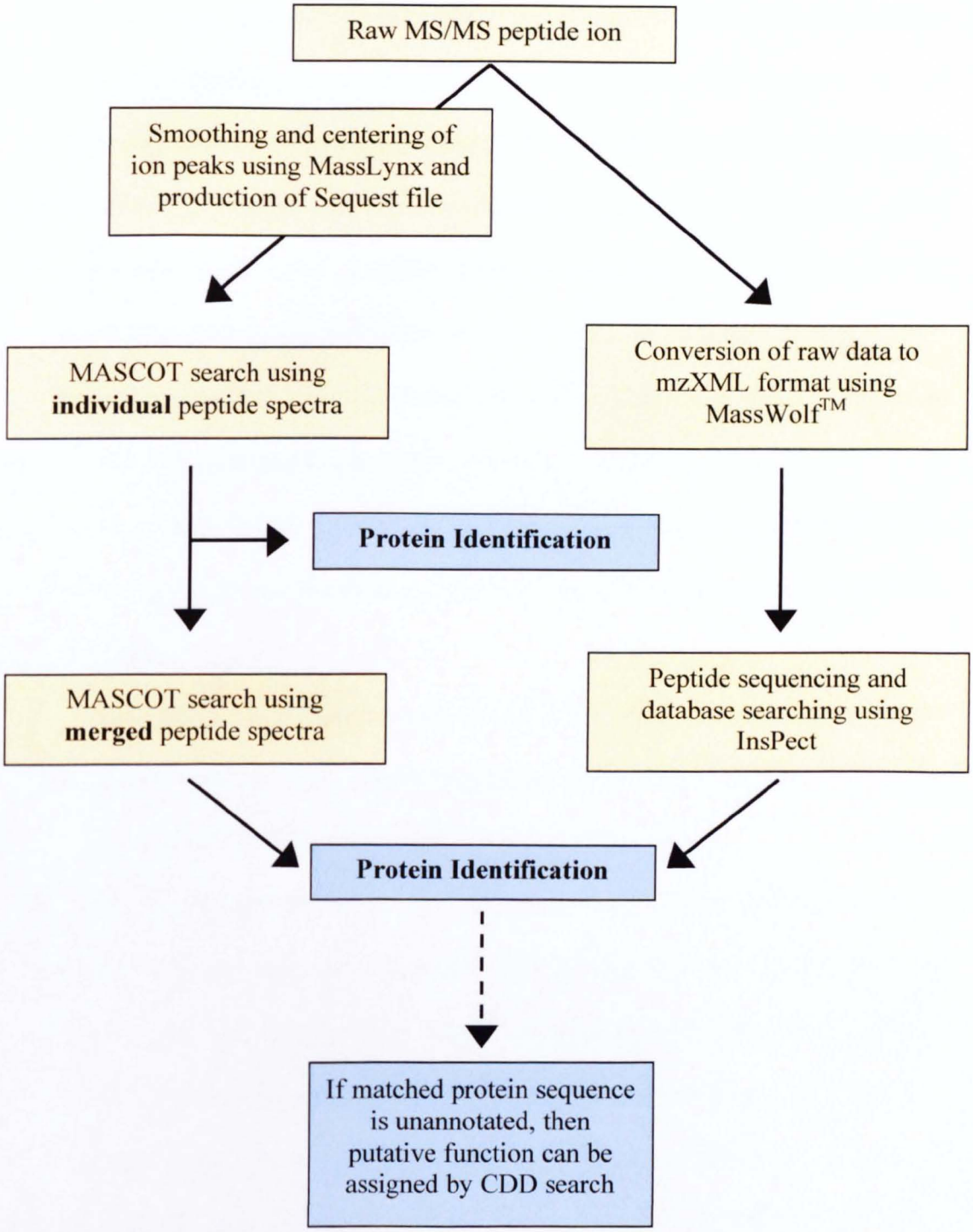

Figure 5.5. Flow diagram outlining protein identification from MS/MS spectra. The two methods shown (MASCOT searching and InsPect searching) were not used independently, but used to support each other, i.e. if Inspect failed to produce an identification, then MASCOT searching would be used or *vice versa*. The results of both methods are verified by manual sequencing using the PepSeq module of MassLynx (Waters, Mass., USA) followed by BLAST searching of the MSDB (NCBI) database (limited to *Bombyx*).

Proteins identified, using a combination of all the proteomic data analysis methods mentioned above, from the *B. mori* midgut DIGE experiment are described below and listed in Table 5.3:

- Fibroin; this is the main constituent of *B. mori* silk and forms fibres that are 10-25μm in diameter and consists primarily of glycine (43%), alanine (30%) and serine (12%). This abundant protein is expressed in the silk gland of *B. mori* and used in the formation of the cocoon. Its presence in this midgut microsomal protein sample probably suggests contamination which is inevitable during dissection and fractionation (Vepari *et al.*, 2007).
- A membrane bound alkaline phosphatase is a hydrolase enzyme responsible for the removal of phosphate groups from organic molecules such as proteins and DNA.
- A titin-like protein; this protein shows high levels of homology with the vertebrate protein Titin, which contributes to muscle assembly and resting tension (Labeit & Kolmerer, 1995).
- Actin depolymerising factor (ADF); actin filaments within cells are transient structures that continually polymerise and depolymerise and depolymerisation of actin by ADF results in prevention of actin filament elongation or even removal of actin monomers from the filament ends i.e. the shortening of the actin filament (De Ruijter & Emons, 1998). The presence of ADF in a microsomal protein sample is likely due to some of the cytoskeleton being 'pulled-down' with the endoplasmic reticulum, to which it is attached, during isolation.
- Proteasome Alpha, Beta and Beta 7 subunits; these are members of the major proteolytic system responsible for the removal of oxidised cytosolic and nuclear

proteins. The proteasome is located in the cytosol, nucleus and is attached to the endoplasmic reticulum and other membranes (Bader & Grune, 2006).

No identifications were obtained by InsPect, manual sequencing or merged MASCOT searching for two of the protein spots of interest, due to their low abundance.

Protein Spot Number	Peptides	Spectra	Average Expression Ratio Treated/Untreated	Protein Annotation	Match Quality
1237	2	2	1.65	Fibroin	2.90
2048	5	20	1.84	Membrane-bound Alkaline Phosphatase	2.30
2983	1	1	-1.45	Titin-like protein	1.02
3743	2	2	1.48	Proteasome Alpha Subunit	2.70
3838	2	40	1.48	Proteasome Beta Subunit	3.80
3894	2	9	2.32	Actin depolymerising factor	3.58
3989	1	7	1.67	Proteasome Beta 7 Subunit	1.89

Table 5.3. Protein identifications derived by InsPect database searches and confirmed by *de novo* sequencing from the nine *B. mori* midgut DIGE spots of interest. The match quality (MQ) scores for each of the peptides indicate whether the match is correct or incorrect; a value of 1 and above indicates a correct match, whereas a value less than 1 indicates an incorrect match (Tanner *et al.*, 2005).

Proteins identified in the same way from the *B.mori* BM36 cell DIGE experiment are described below and listed in Table 5.4.

- An endoplasmic reticulum ATPase; a protein involved in the translocation of misfolded proteins from the endoplasmic reticulum (Nakatsukasa & Brodsky, 2008).
- Two ATP synthases; these enzymes are responsible for the production of ATP from ADP and inorganic phosphate.
- Two members of the Hsp70 family; these 70kDa heat shock proteins are expressed during stress to protect the cell from accumulating protein damage (Morrow & Tanguay, 2003).
- Two Glyceraldehyde- 3-phosphate dehydrogenases (GAPDH); a glycolysis enzyme responsible for the conversion of glyceraldehyde-3-phosphate to D-glycerate 1,3-bisphosphate. However, GAPDH has been shown to be involved in cell death triggered by nitric oxide (NO) stress (Hara *et al.*, 2006).
- Thiol peroxiredoxin (TPx); an antioxidant enzyme (see Section 4.3).
- Proteasome 26S non-ATPase, Beta 6 and Beta 7 subunits; all are members of the previously mentioned proteasome system for the degradation of oxidatively damaged proteins.

No identifications were obtained by Inspect, manual sequencing or merged MASCOT searching for four of the protein spots of interest, due to their low abundance.

Protein Spot Number	Peptides	Spectra	Average Expression Ratio Treated/Untreated	Protein Annotation	Match Quality
426	n/a	n/a	-1.46	Endoplasmic Reticulum ATPase*	[50]+
692	4	11	1.96	Hsp70	4.02
756	6	70	1.97	Hsp70	3.60
764	9	37	-1.46	Vacuolar ATP synthase	3.58
1185	3	50	-2.43	ATP synthase	3.94
1684	3	55	1.44	Proteasome 26S non-ATPase Subunit 7	4.03
1924	3	38	4.01	Glyceraldehyde-3-Phosphate dehydrogenase	4.18
1930	3	18	5.03	Glyceraldehyde-3-Phosphate dehydrogenase	4.23
2081	3	36	1.41	Proteasome Beta 3 Subunit	4.05
2288	2	14	2.45	Thiol peroxiredoxin	3.65
2366	1	3	2.12	Proteasome Beta 6 subunit	3.09

Table 5.3. Protein identifications derived by InsPect and MASCOT ion searches, but confirmed by *de novo* sequencing from the fifteen *B. mori* BM36 cell DIGE spots of interest. The match quality (MQ) scores for each of the peptides indicate whether the match is correct or incorrect; a value of 1 and above indicates a correct match, whereas a value less than 1 indicates an incorrect match (Tanner *et al.*, 2005). *Identification obtained through MASCOT search of merged spectra (See section 5.2.4). + MOWSE based probability score.

5.2.5 Measurement of oxidatively damaged protein levels in Pyridalyl-treated and –untreated BM36 cells

All three DIGE experiments (Pyridalyl sensitive vs Pyridalyl resistant Sf21 cells, Pyridalyl-treated vs –untreated *B. mori* midgut microsomes and Pyridalyl-treated vs –untreated BM36 cells) have revealed the up-regulation of proteins involved in oxidative stress responses. Since previous experiments were unable to detect any reactive oxygen species within Pyridalyl-treated cells (see Section 4.2.6), it was decided to investigate whether there are any differences in the levels of protein oxidation between Pyridalyl-treated and –untreated BM36 cells. Such differences may well allow confirmation of the implications of the proteomics data.

The levels of oxidised proteins were measured using an Oxyblot™ kit (Millipore, Watford, Herts.). Oxidative modification of proteins by ROS and other free radicals causes the introduction of carbonyl groups into protein side chains in a site-specific manner. The Oxyblot™ kit provides the immunodetection of these carbonyl groups, which are a hallmark of the oxidation status of proteins. The carbonyl groups in the protein are derivatised to 2,4-dinitrophenylhydrazone (DNP-hydrazone) by reaction with 2,4-dinitrophenylhydrazine (DNP-H). The DNP-derivatised protein samples are separated by SDS-PAGE followed by Western blotting using a primary antibody specific to the DNP moiety of the proteins.

10µg of total protein from Pyridalyl-treated and –untreated BM36 cells were reacted with 1x dinitrophenylhydrazine (DNPH) for 15min followed by neutralisation with a solution containing glycerol and β-mercaptoethanol (www.millipore.com/techpublications/tech1/74k537). Negative controls for both

types of sample were included (underivitised protein). These samples were then separated by SDS-PAGE, and electrotransferred to a nitrocellulose membrane as described in Sections 2.2.3 and 2.2.12. The nitrocellulose membrane was incubated overnight with a rabbit anti-DNPH antibody (1:150) at 4°C followed by incubation in goat anti-rabbit antibody (1:300) for 1h at room temperature. After rinsing with buffer (TTBS), the immunocomplexes were visualised by chemiluminescence using the ECL kit (GEHC Biosciences) according to the manufacturer's instructions (Fig. 5.6). To assess for differences between the two sample groups, the intensities of the oxidatively damaged proteins were measured using Kinetic Imaging AQM Advance software (Kinetic Imaging Ltd, Notts., UK). Replicates were produced for each treatment (n=3), although mean and standard error were presented graphically (Fig. 5.7). Differences between Pyridalyl-treated and –untreated samples were assessed by ANOVA (α=0.005). ANOVA was followed by Student-Newman-Keuls *post hoc* comparisons to determine differences between Pyridalyl-treated and –untreated samples (SigmaStat; Sysstat software inc., USA). The data were both homoscedastic and normally distributed (SigmaStat) making ANOVA possible.

ANOVA (n=3, α=0.005) revealed significant differences in the levels of oxidatively damaged proteins between Pyridalyl-treated and –untreated BM36 cells. Student-Newman-Keuls *post hoc* test revealed that Pyridalyl-treated BM36 cells show 1.6-fold greater level of oxidatively damaged proteins than untreated BM36 cells.

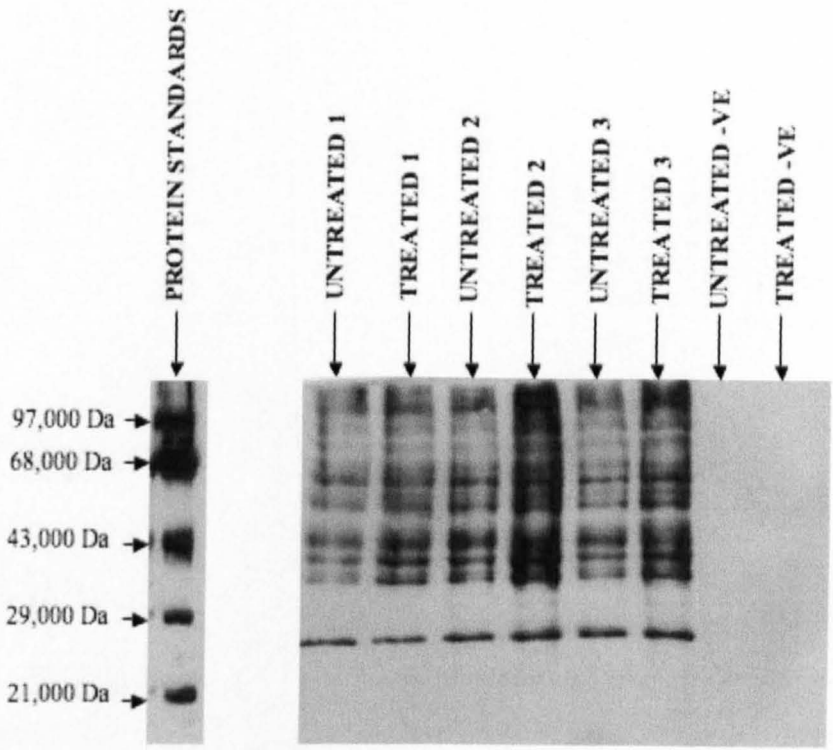

Figure 5.6. Immunoblot analysis of Pyridalyl-treated (1µg/ml, overnight) and control-treated (DMSO) BM36 cell proteins using the OxyBlot™ protein oxidation detection kit. Three biological replicates were analysed simultaneously along with a negative control for both sets of samples. The protein standards are a mixture of five proteins containing 1-3 dinitrophenyl residues per molecule.

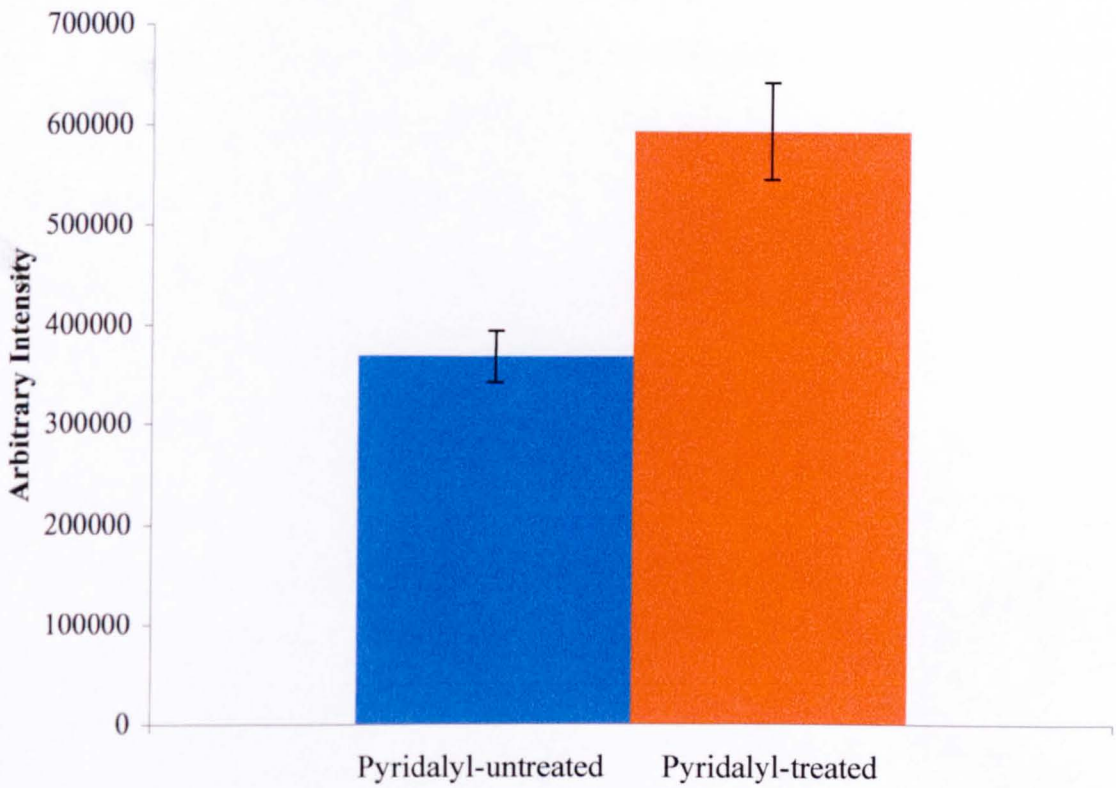

Figure 5.7. Differences in the levels of oxidatively damaged proteins between Pyridalyl-treated (1µg/ml, overnight) and control-treated (DMSO) BM36 cells. The intensity of each immunoblot was measured using Kinetic Imaging AQM Advance software (Kinetic Imaging Ltd, Notts., UK). Data analysis was performed using (SigmaStat; Sysstat software inc., USA). Data represent the mean of 3 biological replicates ± S.E.M.

5.3 Discussion

The aim of this chapter was to investigate differences in protein expression between (i) Pyridalyl-treated and –untreated *B. mori* midgut microsomes, and (ii) Pyridalyl-treated and –untreated *B. mori* BM36 cells using DIGE. Any differences in protein expression may well indicate the biochemical processes involved in the cytotoxicity of Pyridalyl. It was shown in Chapter 3 that the metabolism of Pyridalyl by cytochrome P450s is essential for its action, hence, the reason why *B. mori* midgut microsomes were chosen for this investigation, as most insecticide-metabolising P450 are microsomal. Also, whole insect midgut protein samples are very crude, containing appreciable amounts of insoluble (fatty) material and many highly abundant proteins, such as structural proteins, making 2D-PAGE very difficult and the identification of low abundance proteins practically impossible. For these reasons, the midgut proteins were fractionated to allow examination of only a sub-proteome, in this case, the microsomal proteins.

The second investigation involved Pyridalyl-treated and –untreated *B. mori* BM36 cells, this time, however, whole cell proteins would be investigated as there are no problems with insoluble material nor highly abundant proteins associated with these samples. The results of these experiments could potentially complement the results of the *B. mori* midgut microsome DIGE experiments. The main benefit of using *B. mori* tissues and cells for these experiments is the fact that the genome sequence of *B. mori* is freely available, making protein identification not just easier, but also much more reliable.

The presence of the abundant proteins, silk-gland protein Fibroin and the Titin-like protein, involved in movement are likely due to contamination during dissection

and the crude fractionation method used in the isolation of microsomes (i.e. centrifugation). Fibroin is one of the three monomers that combine to make a silk fibre, it is synthesised in the silk glands, but it is so abundant it can still be seen in the microsomal protein fraction following several fractionation steps (Altman *et al.*, 2003). The Titin-like protein could, like Fibroin, be carry-over from another tissue or, as it is homologous to a mammalian muscle cell protein, it could play some role in midgut peristalsis as muscles are present in the lepidopteran midgut wall (Audsley *et al.*, 2008).

Three of the differentially expressed protein spots in *B. mori* midgut microsomes and three in the BM36 cells have been identified as subunits of the proteasome. The degradation of proteins is a normal physiological process required to maintain normal cellular function and cells possess several pathways for general protein breakdown, the major one being the proteasome system (Rock *et al.*, 2004). The proteasome is localised in the cytosol and nucleus, as well as being attached to the endoplasmic reticulum and other cell membranes (Coux *et al.*, 1996).

Proteins, nucleic acids and membrane lipids of all aerobic organisms are constantly subjected to oxidative modifications due to the action of reactive oxygen species generated by physiological processes (Bader & Grune, 2006). Protein oxidation is, therefore, a continuously occurring process, albeit at a slow rate during normal metabolism. During times of oxidative stress, the increased formation of reactive oxygen species increases the levels of protein oxidation within the cell. If these proteins cannot be reconstituted by various heat shock proteins or the oxidised amino acids cannot be reduced by the thioredoxin reductase system (see Section 4.3), then the oxidised proteins have to be degraded. The major proteolytic system

for the removal of oxidatively damaged proteins during times of high oxidative stress is, again, the proteasome (Grune *et al.*, 1997).

The up-regulation of proteasome subunits in both Pyridalyl-treated and –untreated *B. mori* mid-gut microsomes and Pyridalyl-treated and –untreated BM36 cells, supports the hypothesis put forward in Section 4.3, that the metabolism of Pyridalyl by cytochrome(s) P450 leads to the production of reactive oxygen species, oxidative damage to cellular macromolecules and subsequent cell death. Furthermore, the antioxidant enzyme, thiol peroxiredoxin, that was found to be up-regulated in Pyridalyl-resistant Sf21 cells (see Section 4.2.4.1) was also shown to be up-regulated in Pyridalyl-treated BM36 cells, further supporting the hypothesis that Pyridalyl metabolism leads to the production of reactive oxygen species.

Two of the differentially expressed proteins in the BM36 cell DIGE experiments were identified as belonging to the Hsp70 family of stress proteins. These proteins were originally identified in *Drosophila melanogaster* cells exposed to elevated temperatures and were, therefore, called heat shock proteins (Hsp; Tavaria *et al.*, 1996). It has since been discovered, however, that a range of stresses, including heavy metals, amino acid analogues, inflammation and oxidative stress, induce the expression of Hsp genes. Consequently, the term 'stress protein' is preferred, although many of these proteins have essential roles during non-stressed conditions (Benjamin & McMillan, 1998).

The Hsp70s are a family of highly conserved ATPases of relative molecular mass around 70kDa and are found in most of the compartments of eukaryotic cells. They have essential roles in protein metabolism under both stress and non-stress

conditions, including roles in *de novo* protein folding and membrane translocation, the degradation of misfolded proteins, as well as regulatory processes. The versatility of the Hsp70s results from their basic function, which is to bind and release hydrophobic segments of an unfolded polypeptide chain in an ATP-hydrolytic reaction cycle. Binding results in the stabilisation of the unfolded state and controlled release allows progression along the folding pathway (Hartl, 1996).

During oxidative stress, the formation of oxidised amino acid products leads to the partial unfolding of proteins, exposing hydrophobic moieties on the protein surface, therefore protein hydrophobicity increases with increasing protein damage. The exposed hydrophobic regions are available for binding to an Hsp70 family member and the protein may become re-folded. If the protein is damaged beyond the ability of Hsp70 to re-fold it, then the damaged protein is proteolytically removed by the proteasome (Mary *et al.*, 2004). The up-regulation of two Hsp70 family members (1.96- and 1.97-fold) in Pyridalyl-treated BM36 cells, is consistant with the hypothesis that Pyridalyl metabolism results in the production of reactive oxygen species, which damage proteins and other cellular macromolecules, causing the up-regulation of antioxidant enzymes such as thiol peroxiredoxin, the proteasome and chaperones, such as Hsp70.

The final two differentially expressed proteins that were identified from the BM36 cell DIGE experiment came from a train of spots (Fig 5.4) and were both identified as being glyceraldehyde-3-phosphate dehydrogenase (GAPDH) and were up-regulated 4.01- and 5.03-fold in Pyridalyl-treated cells. For decades, GAPDH has been regarded as merely a housekeeping glycolytic enzyme that exists mainly in the cytoplasm. However, several studies are now suggesting that GAPDH has a

number of different functions (Sirover, 1999). GAPDH binds to microtubules and modulates microtubule bundling (Huitorel & Pantaloni, 1985) and also contributes to membrane fusion (Morero *et al.*, 1985). GAPDH has also been shown to exist in the nucleus and plays a role in gene transcription, DNA replication, DNA repair and nuclear RNA export (Hara *et al.*, 2006).

During oxidative stress, the formation of nitric oxide (NO) causes necrotic cell death via the formation of peroxynitrite, a powerful oxidant that promotes DNA breaks, lipid peroxidation and protein oxidation. In mammalian cells, a pool of GAPDH translocates to the nucleus under a variety of stressors, most of which are associated with oxidative stress. At the molecular level, a catalytic cysteine in GAPDH is *S*-nitrosylated by NO, the modified GAPDH becomes capable of binding with Siah1 (an E3 ubiquitin ligase), the GAPDH-Siah complex translocates to the nucleus and degrades Siah1's substrates leading to cytotoxicity (Hara *et al.*, 2006). It is possible that the up-regulation of GAPDH in Pyridalyl-treated BM36 cells is due to a similar mechanism i.e. Pyridalyl metabolism leads to the formation of reactive oxygen species, one of which is NO, which ultimately causes GAPDH to translocate to the nucleus and cause necrotic cell death. However, previous work in the field of GAPDH and cell death has not indicated whether any up-regulation is associated with GAPDH is this newly identified role.

The up-regulation of antioxidant enzymes (such as TPx), the proteasome, chaperones (such as Hsp70) and GAPDH all point towards Pyridalyl causing some sort of oxidative stress in treated cells. Therefore, the next logical step was to assess whether there are any other markers for oxidative stress present in Pyridalyl-treated cells. Using the antibody-based protein oxidation detection kit

(Oxyblot™), it was possible to show that the levels of total protein oxidation in Pyridalyl-treated cells was indeed higher than in untreated cells, further contributing to the hypothesis that Pyridalyl-treated cells are subjected to oxidative stress, which ultimately leads to death via necrosis.

Significantly, up-regulation of a cytochrome P450 species was not detected in midgut microsomes nor BM36 cells following Pyridalyl treatment. This does not rule out the occurrence of such a phenomenon, particularly since membrane-associated proteins are generally under-represented in 2D-PAGE separations. Such proteins are known to have a tendency to precipitate during the first isoelectric focusing step.

CHAPTER 6

A PROTEOMIC ANALYSIS OF PYRIDALYL-TREATED AND –UNTREATED *Bombyx* BM36 CELLS USING iTRAQ

6.1 INTRODUCTION

All proteins associated with membranes are considered membrane proteins. Thus, membrane proteins are a heterogeneous mixture of integral membrane proteins with many transmembrane regions and peripheral membrane proteins, which are associated with a membrane, for example via a glycolipid (Santoni *et al.*, 2000). Generally membrane proteins are hydrophobic and this is indeed true of cytochrome P450s. This makes membrane proteins such as cytochrome P450s less amenable to solubilisation in protein extraction buffers and also susceptible to precipitation during isoelectric focusing (Patton, 1999). Membrane protein analysis is also made more difficult by their low abundance in cells and low copy numbers of individual proteins (Lehner *et al.*, 2003).

In order to avoid the inherent problems of membrane protein analysis it is possible to use non gel-based proteomic techniques such as iTRAQ. This technique uses four (or eight) amine-specific isobaric reagents to label the primary amines of tryptic peptides from up to four different samples (Fig. 6.1, Ross *et al*, 2004). The labelled peptides from each sample are mixed and then fractionated by cation exchange chromatography and analysed by LC-MS/MS. Due to the isobaric nature of the reagents, the same peptide from each sample appears as a single peak in the

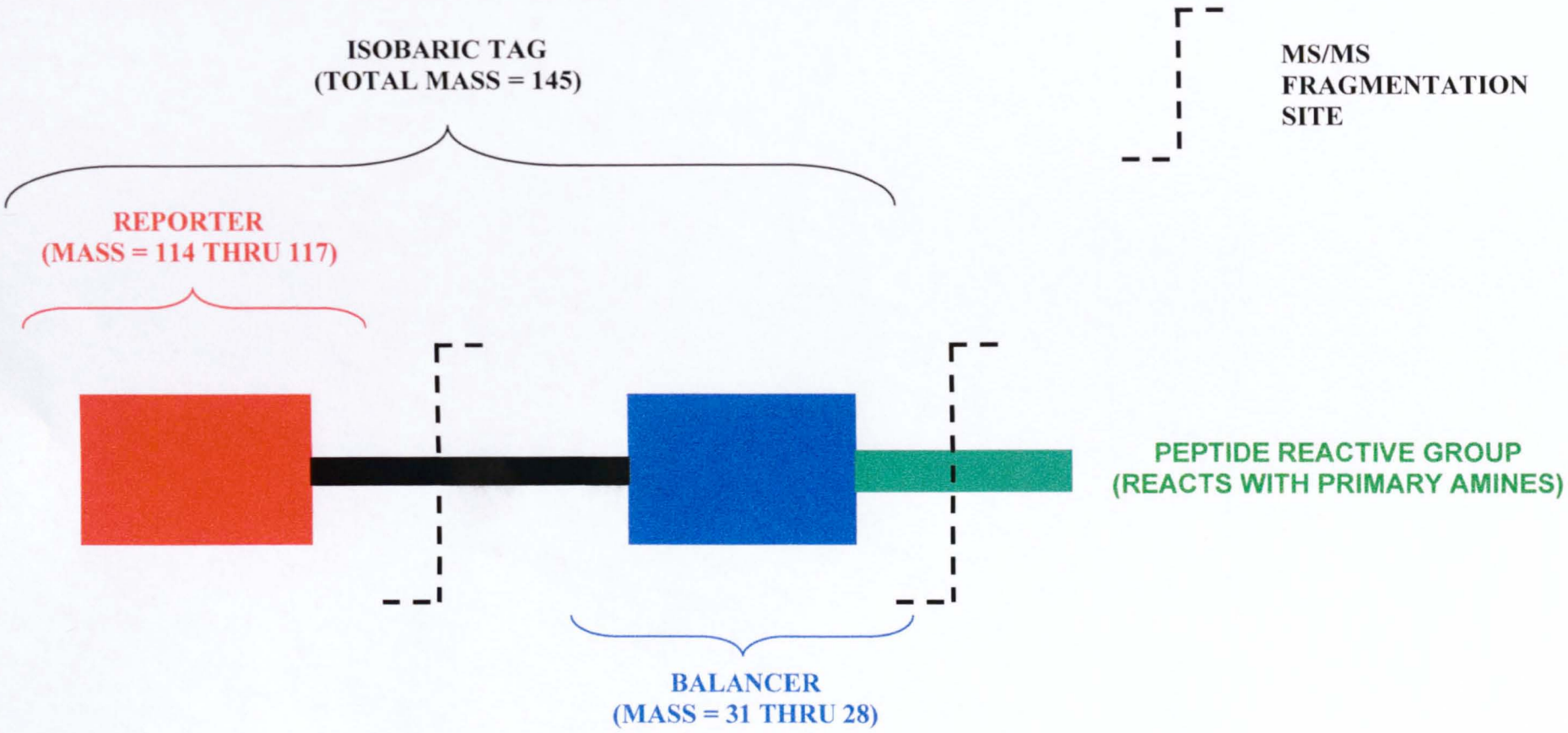

Figure 6.1. iTRAQ reagent structure. The iTRAQ reagent consists of a charged reporter group (unique to each of the four reagents), a peptide reactive group (labels all N-termini and lysine side chains) and a neutral balance region to maintain an overall mass of 145 (www.appliedbiosystems.com).

MS spectrum (Chen *et al.,* 2007). Upon collision-induced dissociation, the iTRAQ-tagged peptides fragment to release reporter ions at 114.1, 115.1, 116.1 and 117.1 m/z and *b*- and *y*-ion series (Fig. 6.2). The peak areas of the reporter ions are used to assess the relative abundance of peptides and, consequently, the proteins from which they are derived (Aggarwal *et al.*, 2006).

Evidence was produced in Chapter 3 demonstrating the requirement for cytochrome P450 in the action of Pyridalyl and it was suggested that Pyridalyl, like other insecticides that are metabolically activated by cytochrome P450 such as organophosphates, may cause the up-regulation of the cytochrome P450 species that metabolises it (Feyereisen, 1999). A 2D-PAGE and DIGE approach (Chapter 5) was unable to detect an up-regulation of any cytochrome P450, but this is likely due to the fact that many hydrophobic proteins are lost during the first isoelectric focusing step of 2D-PAGE and DIGE.

With the view of attempting to identify, amongst other things, any up-regulated cytochrome P450s, a novel iTRAQ experiment was designed. Whole cell proteins from Pyridalyl-treated and –untreated *Bombyx mori* BM36 cells would first be separated using SDS-PAGE, the region of the gel most likely to contain cytochrome P450s (55-75kDa) would be removed, the proteins digested in-gel with trypsin and the resulting peptides extracted ready for iTRAQ labelling. This SDS-PAGE step is effectively producing a sub-proteome in the size range of cytochrome P450s, hopefully increasing the likelihood of identifying the P450 species responsible for the metabolic activation of Pyridalyl. Furthermore, by avoiding isoelectric focusing, the likelihood of detecting membrane proteins is increased.

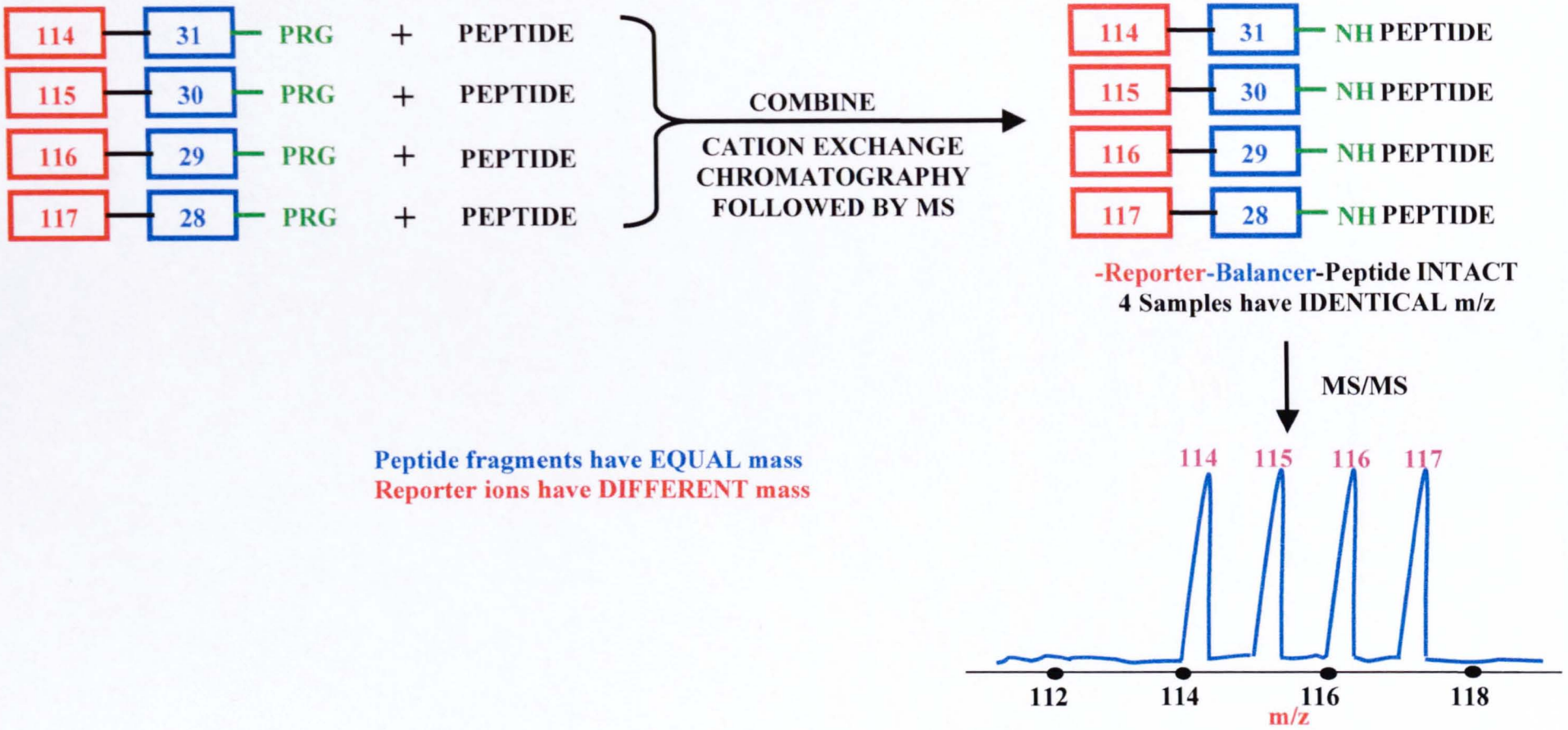

Figure 6.2 The principle of the iTRAQ technique. Up to four separate samples are digested with trypsin and labelled using one of four mass tags, these labelled samples are then combined, fractionated by cation exchange chromatography and analysed by mass spectrometry. The equivalent, derivatised peptides from each sample have equal masses and are, therefore, indistinguishable from each other, whereas the reporter ions have different masses and appear as separate peaks. Relative quantification is possible by comparing reporter ion peak areas.

6.2 Methods and Results

6.2.1 SDS-PAGE, in-gel digestion, extraction of tryptic peptides and iTRAQ labelling

B. mori BM36 cells were grown until confluency in eight 75cm^2 cell culture flasks (~3x10^6 cells per flask) and treated overnight with 1μg/ml (final concentration) Pyridalyl (for details see Chapter 5). The cells were aspirated from the flasks, centrifuged for 10 min at 1500 x g and the culture medium was removed. The cell pellet was washed twice in ice-cold isotonic HEPES buffer before finally being resuspended in ice-cold hypotonic HEPES buffer (see section 2.1.5); both the wash and re-suspension buffer contained a protease inhibitor cocktail (Complete protease inhibitor cocktail tablets; Roche, Sussex, UK). The cells were then lysed by homogenisation followed by brief sonication (5 x 3 sec) on ice. The resulting homogenate was centrifuged for 10 min at 1500 x g to remove any cellular debris; the supernatant was removed and transferred to a clean tube and the protein content assayed using the Bradford method (see section 2.3.1). Three biological replicates of cells were grown and produced. 25μl of the protein samples (approximately 150μg protein) were then separated using a 10% (w/v) SDS-PAGE gel (section 2.3.3). The region of the gel that is likely to contain cytochrome P450s (55-75kDa) was removed, cut into 1mm slices, which were each placed in separate tubes, after cutting into approximately 1mm^2 pieces. The tube contents were digested with trypsin and extracted as in section 2.3.9 with one modification; 50mM ammonium bicarbonate, which is usually used in digests is not compatible with iTRAQ and was therefore substituted with triethylammonium bicarbonate (TEAB). iTRAQ reagent vials were removed from storage at -20°C and equilibrated to room temperature before the addition of 70μl of ethanol. Each vial of iTRAQ reagent is enough to label up to 100μg of protein following trypsin

digestion. Each vial was vortexed for 1 min and the contents were transferred into the sample tubes; reagent 114 into the Pyridalyl-untreated peptides and reagent 115 into the –treated peptides (manufacturers instructions www.aplliedbiosystems.com). The samples were then mixed by vortexing and incubated at room temperature for 1h, after which the contents of both sample tubes from each biological replicate were combined in a fresh microcentrifuge tube and mixed by vortexing.

6.2.2 Preparation of samples for mass spectrometry using strong cation exchange (SCX) chromatography.

SCX chromatography was performed by Dr M C Wilkinson using an ÄKTA Purifier (GEHC Biosciences) equipped with a Waters AP minicolumn packed in-house with 5 x 115mm polysulphoethyl A resin (Western Analytical, Lake Elsinore, USA). The iTRAQ labelled peptides were loaded onto the column in 2ml 30% acetonitrile, 5mM KH_2PO_4, pH 2.7. A 90 min gradient was run from 0 to 350mM KCl in 30% acetonitrile, 5mM KH_2PO_4, pH 2.7 (Fig. 6.3) with a flow rate of 0.25ml/min. Seventeen 1.0ml fractions were collected from each of the three biological replicates.

6.2.3 Analysis of cation exchange fractions by mass spectrometry

100µl of each SCX fraction was removed and desalted using a ZipTip^{TM} (Millipore). The ZipTips were first wetted with 100% acetonitrile and then equilibrated with 0.1% trifluoroacetic acid (TFA) in ultra pure water. Each sample was aspirated through the ZipTip and dispensed 10 times to bind the peptides and the tip washed using 0.1% TFA in ultra pure water three times to remove the salts. The bound peptides were then

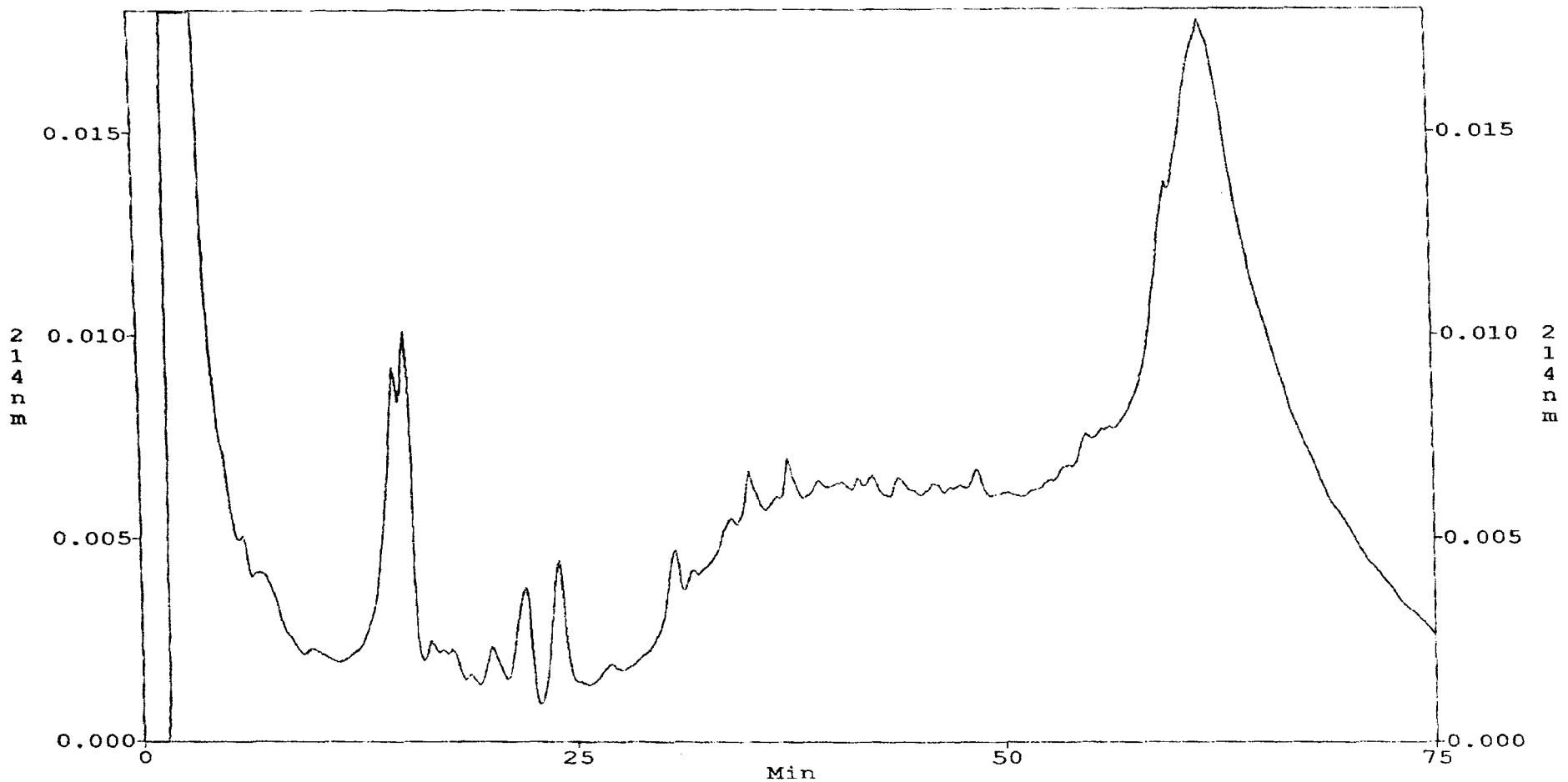

Figure 6.3 UV trace showing a typical strong cation exchange chromatography run. Tryptic peptides are eluted from the column after approximately 20 mins.

eluted in 5µl of 0.1% TFA in 50% acetonitrile. The samples were then analysed using MALDI-TOF mass spectrometry to identify which SCX fractions contained the most peptides (MALDI conditions; matrix: α-cyano-4-hydroxycinnamic acid, pulse voltage: 3400V, source voltage: 15,000V, reflectron voltage: 500V and a mass scan range of 800-4000Da). Fractions 5, 6, 7, 8 and 9 were found to contain the majority of peptides and were retained for MS/MS analysis, whereas the fractions containing few peptides were pooled into three (fractions 1-4, 10-13 and 14-17) and retained for MS/MS.

In order to produce good expression data, it is vital to obtain high quality spectra for the iTRAQ reporter ions themselves. To facilitate this, 25% of each fraction (from each biological replicate) was removed and analysed by MS/MS using a high collision energy (40-65V depending on peptide mass) to produce strong reporter ions. The resulting data were analysed and an inclusion list was produced containing all differentially expressed peptides from each fraction. As replicate data are only needed for expression analysis and not protein identification, the remaining 75% of each biological replicate fraction was pooled together in order to give a greater chance of identifying low abundance proteins. Half of the pooled fractions was then analysed by MS/MS using lower collision energy (30-55V depending on peptide mass), in order to obtain good quality fragmentation spectra.

6.2.4 Analysis of mass spectrometric data

The raw mass spectrometry data were processed using MASCOT 'Distiller' (www.matrixscience.com/distiller.html), a unique algorithm, which fits each peak in the MS/MS spectra to a calculated isotope distribution, processing the raw data into high quality, de-isotoped peak lists. The resulting MASCOT generic files

(.mgf) were merged to create a single file containing all of the labelled peptides using a web-based peak list conversion utility (www.proteomecommons.org). This merging was undertaken, since the labelled individual Tryptic peptides from each protein will be distributed in different fractions from ion-exchange chromatography. This allows the subsequent database search algorithm, MASCOT, to utilize several derived peptides in the search. Thus, the combined file was searched against a protein database from *B. mori* using an in-house MASCOT algorithm (Matrix Science). MASCOT performs quantification based on the iTRAQ reporter ions and provides accurate protein identification (Table 6.1).

Proteins identified in this way include:

- A myosin homologue; myosins are actin-based motors that play fundamental roles in eukaryotic cell motility (Berg *et al.*, 2001).
- A member of the Hsp70 family; these 70kDa heat shock proteins are expressed during stress to protect the cell from accumulating protein damage (Morrow & Tanguay, 2003).
- Elongation factor 1 alpha; involved in protein production; this family of enzymes is responsible for the delivery of aminoacyl tRNAs to the ribosome (Reed *et al.*, 1995).
- A member of the tubulin family of structural proteins.

Protein I.D.	Ratio of m/z 115:114 Reporter ions*	MOWSE Score	Number of peptides matched in identification
Myosin	0.496	48	1
Hsp70	1.553	41	2
Elongation factor 1 alpha	0.788	42	2
Tubulin	0.500	37	1

* The proteins from 'control' cells were labelled with iTRAQ reagent yielding Reporter ion m/z 114, whereas the proteins from Pyridalyl-treated cells were labelled with Reporter ion m/z 115.

Table 6.1 Table of proteins showing differential expression between Pyridalyl-treated (1µg/ml, overnight) and control-treated (DMSO) BM36 cells. A ratio of reporter ions of 1 indicates no change in the relative expression levels of that protein whereas a ratio less than 1 indicates a down-regulation in Pyridalyl-treated cells and a ratio greater then 1 indicates an up-regulation in Pyridalyl-treated cells. A MOWSE-based probability score indicates the quality of the match; all four proteins show MOWSE scores that indicate good identifications (for details see Appendix 5).

6.3 Discussion

The main aim of this chapter was to identify any microsomal cytochrome P450 species that might be up-regulated by Pyridalyl. Such cytochrome P450 species may be responsible for the metabolic activation of Pyridalyl. The non-gel-based technique, iTRAQ, was chosen for this purpose as it gives a greater chance of identifying hydrophobic, membrane proteins, such as cytochrome P450s, than conventional proteomics techniques that rely on gels, as hydrophobic proteins tend to precipitate during isoelectric focusing.

Unfortunately, no cytochrome P450s were identified in this work, possibly due to their relative low abundance within the cell. Several of the proteins that were identified are of interest and further support the hypothesis that the metabolism of Pyridalyl by a cytochrome P450 produces a reactive metabolite that then goes on to cause oxidative stress within the cell and ultimately necrotic cell death.

A member of the Hsp70 family of heat shock proteins was identified as being up-regulated 1.5-fold in Pyridalyl-treated cells. The Hsp70s are a family of highly conserved ATPases of approximate relative molecular mass 70kDa and are found in most of the compartments of eukaryotic cells. They have essential roles in protein metabolism under both stress and non-stress conditions, including roles in *de novo* protein folding and membrane translocation, the degradation of misfolded proteins, as well as regulatory processes. The versatility of the Hsp70s results from their basic function, which is to bind and release hydrophobic segments of an unfolded polypeptide chain in an ATP-hydrolytic reaction cycle. Binding of

protein results in the stabilisation of the unfolded state and controlled release allows progression along the folding pathway (Hartl, 1996).

An elongation factor 1 alpha homologue was shown to be down-regulated 0.7-fold in Pyridalyl-treated cells. When viewed alone this result seems uninteresting, however, it has been shown that Pyridalyl reduces the net amount of protein, as measured by ^{3}H-leucine incorporation, in lepidopteran cells and the authors implied inhibition of protein synthesis (Moriya *et al.*, 2008). Since elongation factor 1 alpha is responsible for the delivery of aminoacyl tRNAs to the ribosome, the down-regulation of this protein is likely to reduce the level of protein synthesis within the treated cell. When this result is viewed alongside previous results (Chapter 5) showing an up-regulation of the proteasome, it becomes clear that the reduction in protein synthesis resulting from a down-regulation of elongation factor 1 alpha coupled to the increase in protein degradation that results from an up-regulation of the proteasome could be the cause of the reduction in total protein observed by Moriya *et al.* upon Pyridalyl treatment.

In this work, some difficulty was experienced in processing some of the mass spectrometric MS/MS output files for database searching; the reason for this is obscure. Due to this problem, coupled with mass spectrometer sensitivity isssues, the hits listed in table 6.1 represent all of the hits that it was possible to obtain from this data rather than the most significant, in terms of fold-change between treatments, as in previous chapters. The low number of proteins identified during this work is also likely due to the limited protein loading capacity of the first SDS-PAGE step. Mini-gels were used for this purpose with a loading capacity of 100µg protein, roughly 50% of the total protein was discarded due to it being outside of

the size range of interest and then protein losses during cation-exchange chromatography would mean that the amount of protein available for mass spectrometry would be relatively low. With this in mind, future work using this 1D-PAGE coupled to iTRAQ technique would be well advised to run large SDS-PAGE gels with a greater loading capacity, in excess of 2mg in some cases.

CHAPTER 7

GENERAL DISCUSSION

The main aim of this work was to elucidate the mode of action of the insecticide, Pyridalyl. When the project was initiated, very little was known about Pyridalyl apart from the fact that it showed extremely high specificity for lepidopteran pests (Sakamoto *et al.*, 2003). It has been demonstrated that Pyridalyl shoes high specificity towards Lepidoptera and hypothesised that the metabolism of Pyridalyl by a cytochrome P450 may be responsible for the production of a reactive metabolite, but it has proven difficult to produce definitive evidence for this.

It has been demonstrated that Pyridalyl exhibits excellent insecticidal activity against lepidopteran pests by contact and ingestion, it shows no cross-resistance with synthetic pyrethroids or organophosphates and the impact of the insecticide on various beneficial arthropods and the environment is minimal (Saito *et al.*, 2004). A dose of 100ng of Pyridalyl applied directly to the cuticle of lepidopteran larvae is enough to be lethal within 6h of application and lower doses show symptoms similar to burns at the site of application (Saito *et al.*, 2006).

Studies into the effects of Pyridalyl on insect cell lines have shown high levels of cytotoxicity towards lepidopteran cells, lower levels of cytotoxicity towards other insect cell lines (including, *Drosophila, B. terrestris* and *O. stringicollis* cell lines; Isayama *et al.*, 2005) and almost no cytotoxicity to mammalian cell lines (Isayama *et al.*, 2005), again demonstrating Pyridalyl's high specificity towards lepidoptera. Previous work has also demonstrated that the cytotoxic effects of Pyridalyl do not involve the disruption of mitochondrial respiration or RNA and protein synthesis

(Saito *et al.*, 2005), however, work in this thesis and published by others has suggested that Pyridalyl does affect protein synthesis (Chapter 6, Moriya *et al.*, 2008).

During the current work, it was demonstrated, using live cell imaging, that Pyridalyl causes cytotoxicity in a dose-dependent manner (section 3.2.1.1) and that none of the cell morphology changes characteristic of apoptotic cell death, such as cell shrinkage, membrane blebbing and the formation of apoptotic bodies (Miller *et al.*, 2002) are observed in Pyridalyl-treated cells (section 3.2.1.1). These results lead to the hypothesis that Pyridalyl-treated cells die via necrotic cell death rather than apoptosis. Live cell imaging also allowed further investigation into some of initial findings, most notably the involvement of a cytochrome P450 in the metabolic activation of Pyridalyl. It was found that the pre-incubation of *B. mori* cells with the general cytochrome P450 inhibitor, 1-ABT, before Pyridalyl treatment prevents the cytotoxic action of the insecticide, whereas pre-incubation with the general caspase inhibitor, VAD (effectively an apoptosis inhibitor as caspases are essential in apoptotic cell death), does not prevent the cytotoxic action (section 3.2.1.2). These data gave further validity to the hypothesis that Pyridalyl-treated cells die via necrosis rather than apoptosis. Had more time been available, it would have been advisable to carryout several experiments to determine whether BM36 cells can indeed undergo apoptosis, as some cell lines cannot. Once that had been determined, further studies could then determine whether VAD can block apoptosis caused by compounds known to induce cell death.

Complementary experiments using radiolabelled Pyridalyl proved that at least one, possibly several, cytochrome P450s are involved in the metabolism of Pyridalyl

(section 3.2.2). It was demonstrated that the pre-incubation of *B. mori* cells with the cytochrome P450 inhibitors, 1-ABT and PBO, completely prevents the metabolism of Pyridalyl. When the two experiments are viewed together, namely the inhibition of Pyridalyl action by P450 inhibitors and metabolism studies, that cytochrome P450 enzymes are responsible for metabolising Pyridalyl and without this metabolic step, Pyridalyl is unable to cause cytotoxicity. The metabolic activation of some organophosphate insecticides by P450s is well documented. For example, parathion and fenitrothion both contain a P=S grouping and are poor insecticides until they are metabolised by P450 enzymes to produce oxygen analogs (P=O), which are potent inhibitors of acetylcholinesterase (Hardstone *et al.*, 2007, Hodgson & Rose, 2006). It would appear that, like parathion and fenitrothion, Pyridalyl requires bioactivation by a cytochrome P450 to exhibit cytotoxic effects.

Comparisons of the proteomes of Pyridalyl-sensitive and –resistant *S. frugiperda* cells, using Difference Gel Electrophoresis (DIGE, section 4.2), showed the up-regulation of thiol peroxiredoxin (TPx, 2.3-fold) and aldehyde dehydrogenase (2.0-fold) in the Pyridalyl-resistant cell line. Both of these enzymes play important roles in the response of cells to oxidative stress. The TPx family of antioxidant enzyme removes H_2O_2 and alkyl hydroperoxides with the use of a thiol-reducing equivalent (Lee *et al.*, 2005), whereas aldehyde dehydrogenases catalyse the irreversible oxidation of endogenous and exogenous aldehydes to their corresponding carboxylic acids. Such aldehydes are potent electrophiles that interact with cellular macromolecules and are formed during oxidative stress (Esterbauer *et al.*, 1991). These data suggest that the long-term exposure of the Pyridalyl-resistant *S. frugiperda* cells to low levels of Pyridalyl has caused an

increase in the level of expression of these antioxidant enzymes, therefore leading to the hypothesis that Pyridalyl, or a reactive metabolite of the insecticide, following metabolism by a cytochrome P450 enzyme, causes the production of reactive oxygen species (ROS). It is possible that it is these ROS that ultimately cause the cytotoxic effects of Pyridalyl and that the Pyridalyl-resistant cell line has up-regulated several antioxidant enzyme systems in order to deal with the oxidative stress induced by Pyridalyl treatment.

Further proteomic studies were carried out using DIGE, however, this time the direct effects of Pyridalyl were investigated. In two separate studies, midguts from either Pyridalyl-treated or –untreated *B. mori* larvae and Pyridalyl-treated or –untreated *B. mori* BM36 cells were analysed (section 5.2). Three of the up-regulated protein spots in the *B. mori* midgut DIGE experiment were identified as subunits of the proteasome. As previously mentioned (section 5.3), the proteasome is the major system within a cell for general protein breakdown (Rock *et al.*, 2004). When proteins become oxidatively damaged and cannot be reconstituted by various heat shock proteins or the oxidised amino acids cannot be reduced using the previously mentioned thioredoxin (thiol peroxiredoxin) system, then the oxidised proteins have to be degraded. The major system for the removal of oxidatively damaged proteins is again, the proteasome system (Grune *et al.*, 1997), further reinforcing the hypothesis that Pyridalyl treatment leads to the production of reactive oxygen species. The DIGE study comparing the proteomes of Pyridalyl-treated and –untreated *B. mori* BM36 cells also showed an up-regulation of various proteasome subunits giving further validity to the previously mentioned hypothesis.

The antioxidant enzyme, thiol peroxiredoxin (TPx), was also identified as being up-regulated (3.65-fold) in Pyridalyl-treated BM36 cells as was the glycolytic enzyme glyceraldehyde-3-phosphate dehydrogenase (GAPDH). More than merely being a glycolytic enzyme, GAPDH has been shown to play a role in many different biological processes (see section 5.3; Hara *et al.*, 2006). More relevant, however, is the fact that GAPDH has been shown to be involved in necrotic cell death following oxidative stress. A common reactive oxygen species formed during the time of oxidative stress is nitric oxide (NO), which causes the formation of peroxynitrite, a powerful oxidant that promotes DNA breaks, lipid peroxidation and protein oxidation. In mammalian cells, it has been demonstrated that in response to nitric oxide stress, GAPDH can translocate to the nucleus, form a complex with the E3 ubiquitin ligase, Siah1, which then causes the polyubiquitination of proteins, marking them for degradation by the proteasome which eventually leads to necrotic cell death (Hara *et al.*, 2006). It is possible that a similar mechanism exists in insect cells and that the up-regulation of GAPDH is due to an increase in oxidative stress, namely nitric oxide stress.

Also up-regulated in Pyridalyl-treated BM36 cells are two members of the Hsp70 family of stress proteins. These are a family of highly conserved ATPases that have essential roles in protein metabolism under both stress and non-stress conditions. A range of stresses can induce the expression of Hsp70 genes, including heavy metals, amino acid analogues, inflammation and heat shock. Therefore, the up-regulation of Hsp70 proteins is less definitive than the up-regulation of thiol peroxiredoxin in giving clues as to Pyridalyl's mode of action, but it has been previously demonstrated that Hsp70 proteins can be induced by oxidative stress (Kukreja *et al.*, 1994). Oxidation of amino acids during oxidative

stress leads to the partial unfolding of proteins, the binding of Hsp70 to the unfolded protein results in stabilisation of the unfolded state and controlled release allows progression along the folding pathway and ultimately the refolding of the damaged protein (Hartl, 1996). If the protein is damaged beyond the ability of Hsp70 to repair, then the protein is removed by the proteasome system (Mary *et al.*, 2004).

Work by others supports the results within this thesis. Moriya *et al.* have demonstrated that Pyridalyl reduces the net amount of protein, as measured by ^{3}H-leucine incorporation in lepidopteran cells (Moriya *et al.*, 2008). At least three cellular mechanisms affect total protein synthesis within cells: transcription, translation and protein degradation. The Pyridalyl-mediated up-regulation of cellular protein degradation machinery, i.e. the proteasome, has already been discussed, however, the study comparing the proteomes of Pyridalyl-treated and control BM36 cells using iTRAQ (Chapter 6) revealed the down-regulation of Elongation factor 1 alpha. This protein is responsible for the delivery of aminoacyl tRNAs to the ribosome and is essential for protein translation, thus, evidence is now available for Pyridalyl effecting two out of the three mechanisms controlling protein synthesis: the down regulation of elongation factor 1 alpha, reducing the level of protein translation and the up-regulation of the proteasome, increasing the level of protein degradation. These two factors, when coupled together, may explain the reduced incorporation of ^{3}H-leucine into protein in Pyridalyl-treated cells.

Since all of the proteomics data pointed towards Pyridalyl inducing oxidative stress within treated cells, attempts were made to measure the levels of reactive oxygen species within Pyridalyl-treated cells using an enzyme assay (section 4.2.6)

and a luminometry-based assay to no success. It was possible, however, to measure the levels of oxidatively damaged proteins within Pyridalyl-treated and –untreated *B. mori* cells using the Oxyblot™ antibody-based protein oxidation detection kit (section 5.2.5). Essentially, the levels of protein oxidation reflect the levels of ROS within a given sample. Pyridalyl-treated cells showed a 1.6-fold increase in protein oxidation levels compared to Pyridalyl-untreated cells adding even more weight to the hypothesis that Pyridalyl is causing oxidative stress within treated cells.

When viewed as a whole, it is possible to produce a hypothesis as to the mode of action of the insecticide, Pyridalyl, from the work within this thesis. Live cell imaging and metabolism studies were able to show that the metabolism of Pyridalyl by cytochrome P450(s) is essential for it to have any cytotoxic effects and cytochrome P450 inhibitors can completely protect cells from the action of the insecticide. The results of numerous proteomics studies showed an up-regulation of several antioxidant enzyme systems in Pyridalyl-resistant and Pyridalyl-treated cells and also general stress response proteins (Hsp70s) that have been shown to be induced by oxidative stress. Therefore, the current working hypothesis is that Pyridalyl is metabolically activated by one, possibly several, cytochrome P450s and the resulting active metabolite then goes on to cause the production of reactive oxygen species which cause oxidative damage to cellular macromolecules and ultimately necrotic cell death (Fig. 7.1).

As indicated in the Introduction (section 1.4) previous work produced some evidence that Pyridalyl or metabolite(s) bound (covalently?) to some proteins, as revealed by 2D-PAGE autoradiography. However, it was not possible to pursue

this line of investigation in the current work, due to the low amount of radioactive Pyridalyl available and the apparently low level of binding. The foregoing hypothesis is not incompatible with the notion that Pyridalyl metabolite(s) could conceivably bind to protein during oxidative damage. However, it is not clear how specific is this binding of Pyridalyl metabolite(s) to proteins.

Recent work (Moriya *et al.,* 2008) published following the completion of this project concerning the effects of Pyridalyl on the levels of protein synthesis in lepidopteran cells, showed that during their studies Pyridalyl appeared to show no insecticidal effects in *B. mori.* These data, produced by Moriya *et al*, are contradictory to the BM36 cell dose response shown in chapter 3 and to the observed insecticidal symptoms in chapter 5 when *B. mori* larvae were fed Pyridalyl in their diet, however, a dose response in *B. mori* larvae was not produced. The reason for the differing results remains obscure.

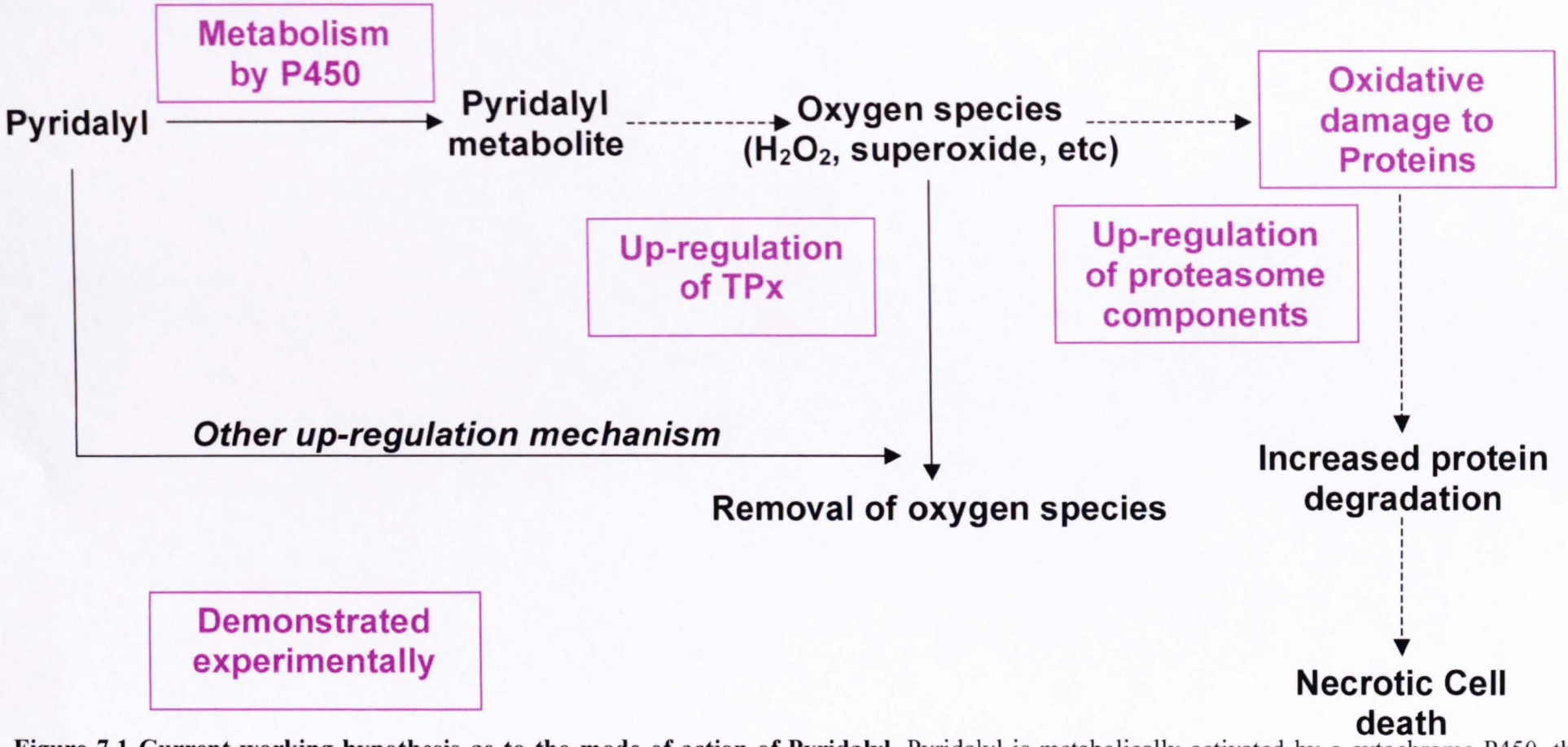

Figure 7.1 Current working hypothesis as to the mode of action of Pyridalyl. Pyridalyl is metabolically activated by a cytochrome P450, the reactive metabolite then leads to the production of reactive oxygen species, which in resistant cells are removed by antioxidant enzymes such as TPx and the cells survive, or in the case of sensitive cells, damage to cellular macromolecules leads to necrotic cell death. Steps highlighted in colour have been demonstrated experimentally during the course of this work.

Attempts have been made during the course of this work to identify the exact cytochrome P450 responsible for the metabolic activation of Pyridalyl. Unfortunately, no modulated (up-regulated) P450 enzymes were identified in any of the proteomics studies and is likely due to the fact that these enzymes are hydrophobic membrane-bound proteins which are generally under-represented in 2D-PAGE separations due to their tendency to precipitate during the isoelectric focusing step. A genome-wide microarray for *B. mori* has been produced covering all 22,987 known and predicted genes in the genome (Xia *et al.*, 2007) and presumably contains all *B. mori* cytochrome P450 sequences. This microarray would therefore be the ideal starting place for any future work attempting to identify the P450 enzyme responsible for the metabolic activation of Pyridalyl assuming that the enzyme's expression is induced by the insecticide (Feyereisen, 1999).

APPENDIX 1

Statistical analyses

Effects of inhibitors of caspases and cytochrome P450s

Normality Test: Passed (P=0.274)

Equal Variance Test: Passed (P=0.061)

Group	Number of replicates	Mean Slope	Std Dev	S.E.M.
Control (1)	6	0.0047	0.0037	0.0015
Pyridalyl (2)	6	0.0516	0.0269	0.0110
Pyridalyl + VAD (3)	6	0.0357	0.0142	0.0058
Pyridalyl + 1-ABT (4)	6	0.0122	0.0086	0.0035

All pairwise multiple comparison procedures (Student-Newman-Keuls Method):

Comparison	Diff of Means	p	q	P	P<0.05
2 vs 1	0.046	4	7.195	<0.001	Yes
2 vs 4	0.039	3	6.059	0.001	Yes
2 vs 3	0.015	2	2.440	0.100	No
3 vs 1	0.030	3	4.755	0.008	Yes
3 vs4	0.023	2	3.619	0.019	Yes
4 vs 1	0.007	2	1.135	0.432	No

P values of less than 0.05 indicate statistically significant differences between the groups being compared whereas P values greater than 0.05 indicate no statistical difference between the groups that are being compared.

Measurement of oxidatively damaged protein levels in Pyridalyl-treated and –untreated BM36 cells

Normality Test: Passed (P=0.657)

Equal Variance Test: Passed (P=0.151)

Group	Number of replicates	Mean	Std Dev	S.E.M.
Untreated (1)	3	368117	52236.17	26118.08
Treated (2)	3	594015	136325.06	68162.53

All pairwise multiple comparison procedures (Student-Newman-Keuls Method):

Comparison	Diff of Means	p	q	P	P<0.05
2 vs 1	225897	2	4.377	0.021	Yes

P values of less than 0.05 indicate statistically significant differences between the groups being compared whereas P values greater than 0.05 indicate no statistical difference between the groups that are being compared.

APPENDIX 2

Sf21 cell DIGE experiment InsPect database search results

DIGE spot 321

Accession Number: Bmb027345

Protein: Karyopherin alpha 3

Peptides: 2

Spectra: 5

Coverage: 11.9%

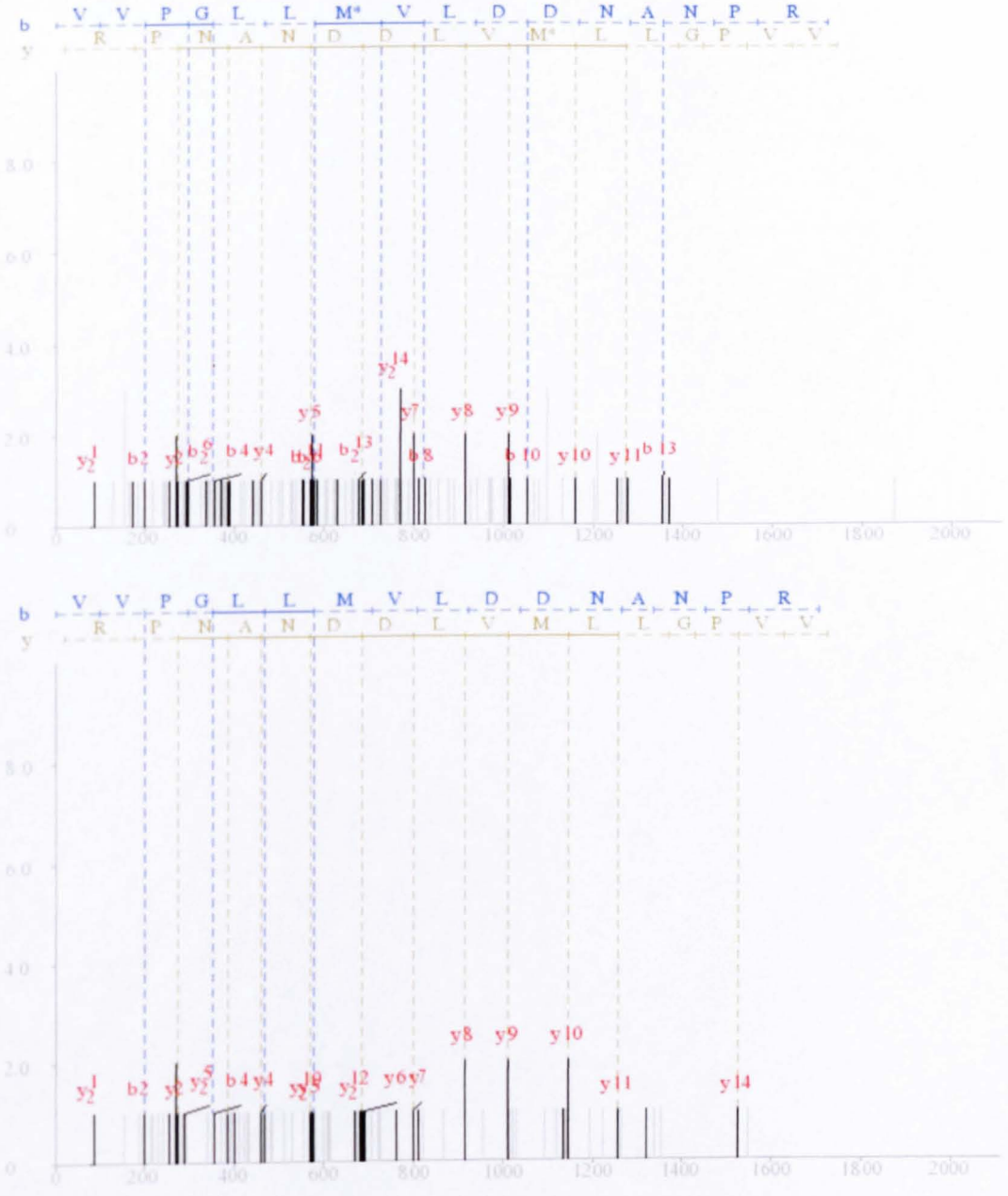

DIGE spot 873

Accession Number: Bmb023984

Protein: Aldehyde dehydrogenase

Peptides: 1

Spectra: 2

Coverage: 3.0%

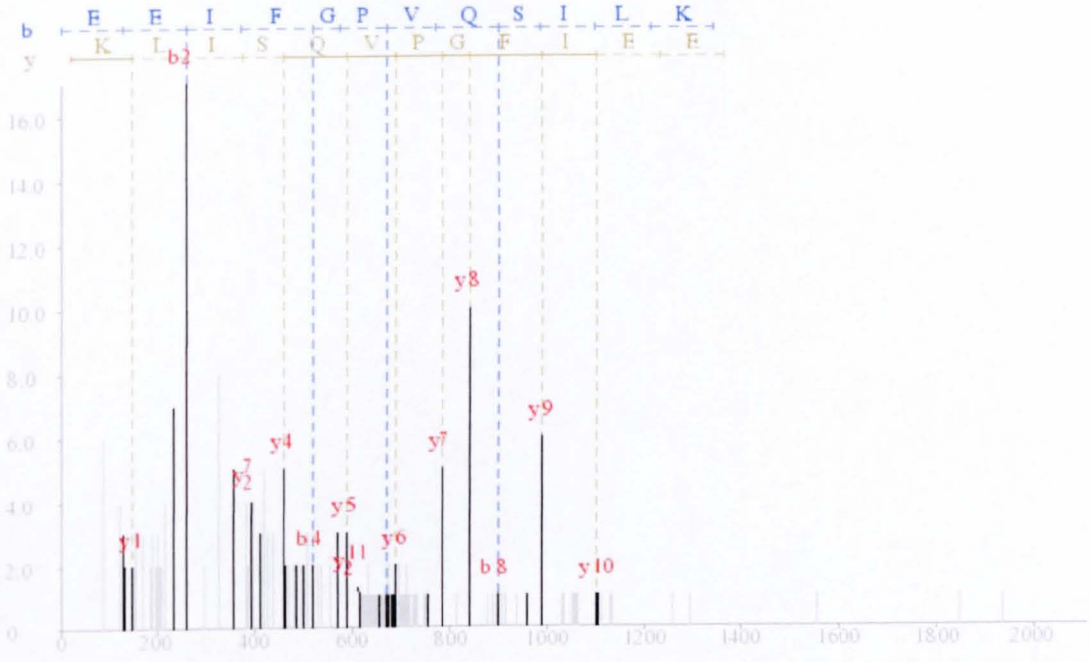

DIGE spot 1043

Accession Number: Bmb038842

Protein: Phosphoglycerate kinase

Peptides: 1

Spectra: 8

Coverage: 11.2%

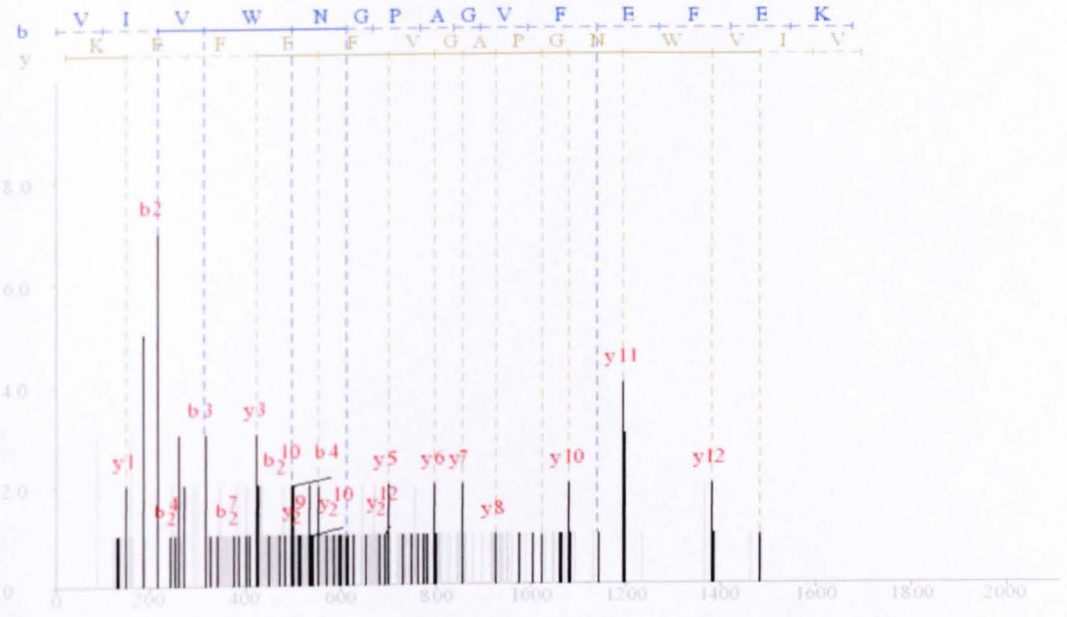

DIGE spot 1447

Accession Number: Bmb002691

Protein: Thiol peroxiredoxin

Peptides: 2

Spectra: 4

Coverage: 14.3%

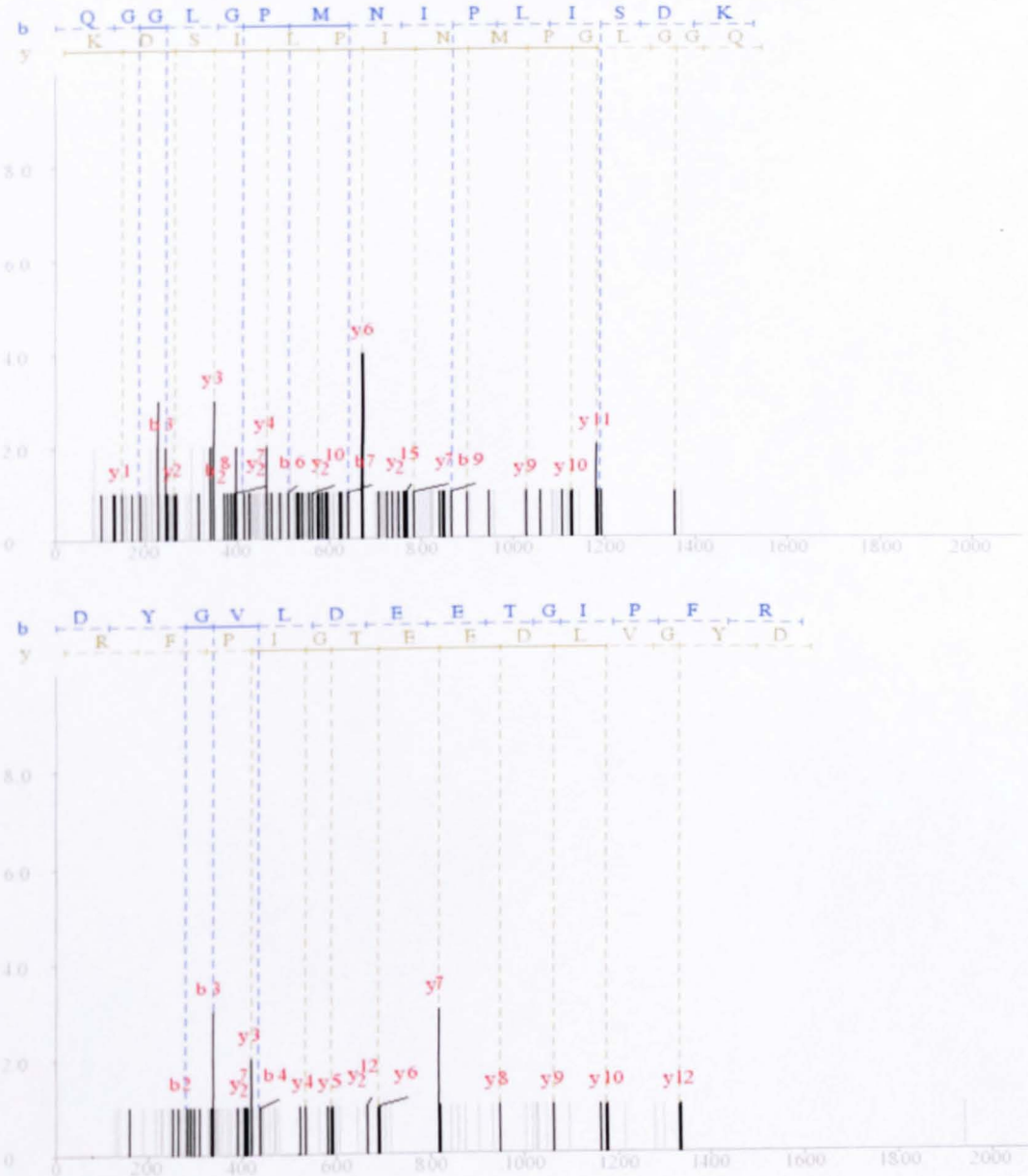

DIGE spot 1466

Accession Number: Bmb031228

Protein: POP1-like nucleolar protein

Peptides: 1

Spectra: 2

Coverage: 7.3%

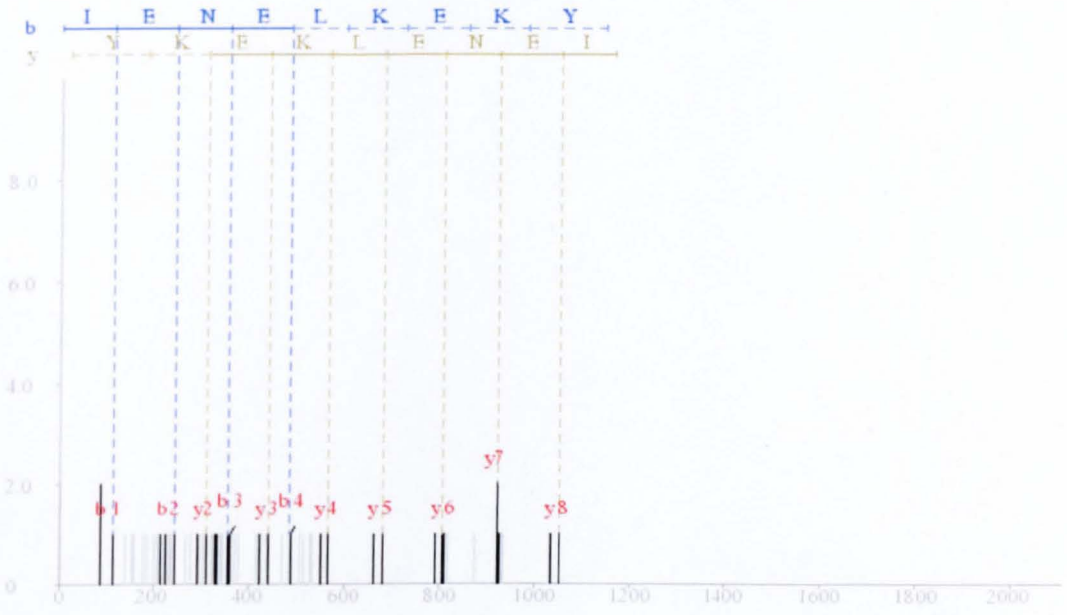

DIGE spot 1480

Accession Number: Bmb038389

Protein: Thiol peroxiredoxin

Peptides: 1

Spectra: 19

Coverage: 10.4%

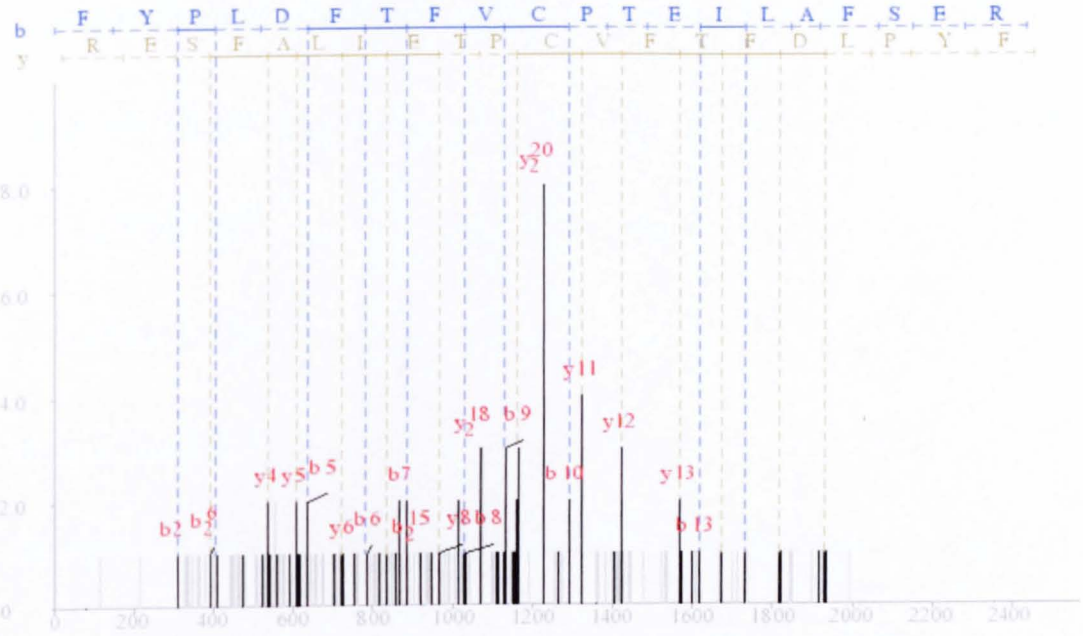

APPENDIX 3

Bombyx mori midgut microsomes DIGE experiment InsPect database search results

DIGE spot 1237

Accession Number: Bmb000423

Protein: Fibroin

Peptides: 2

Spectra: 2

Coverage: 14.2%

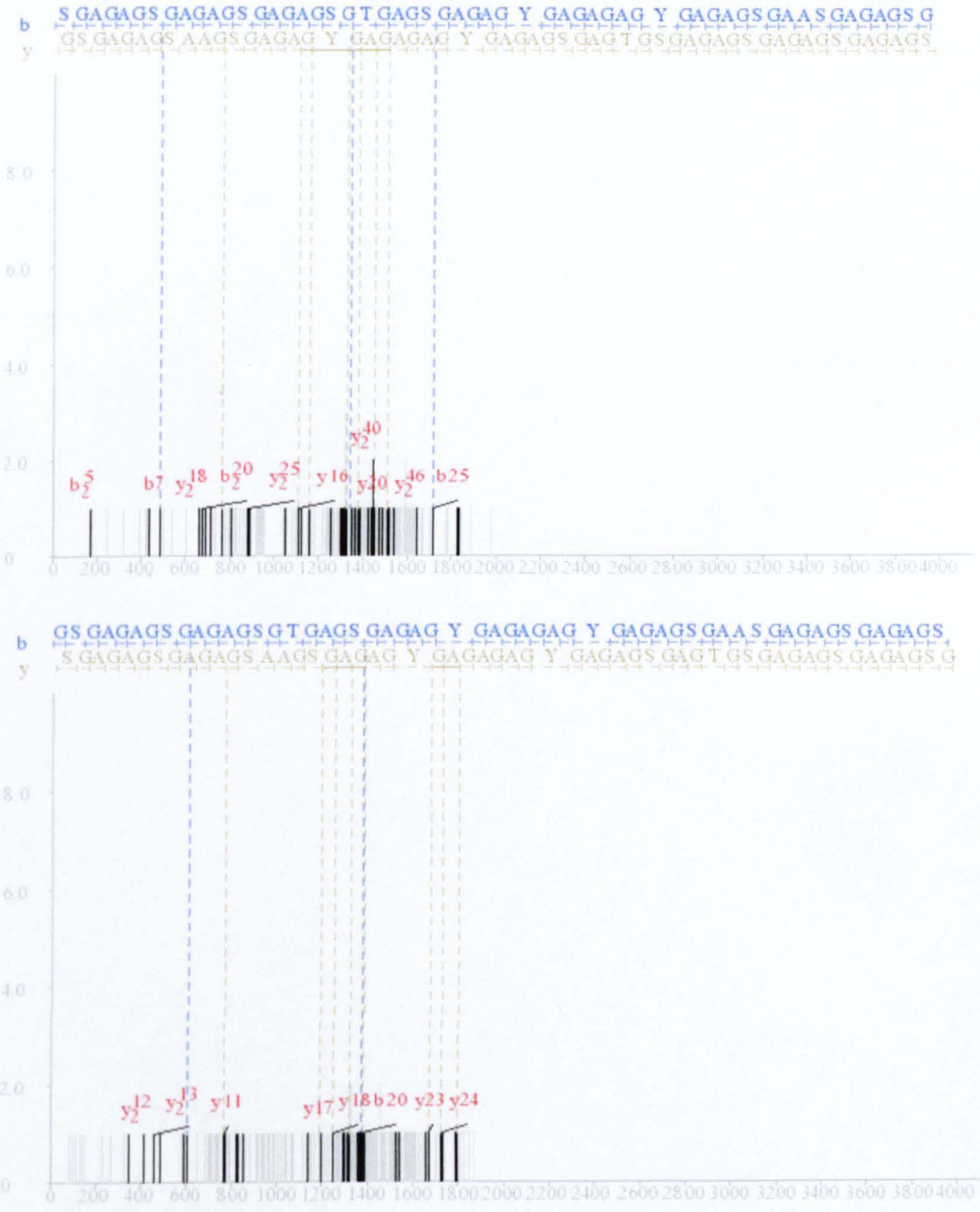

DIGE spot 2048

Accession Number: Bmb026932

Protein: Membrane-bound Alkaline phosphatase

Peptides: 5

Spectra: 20

Coverage: 11.1%

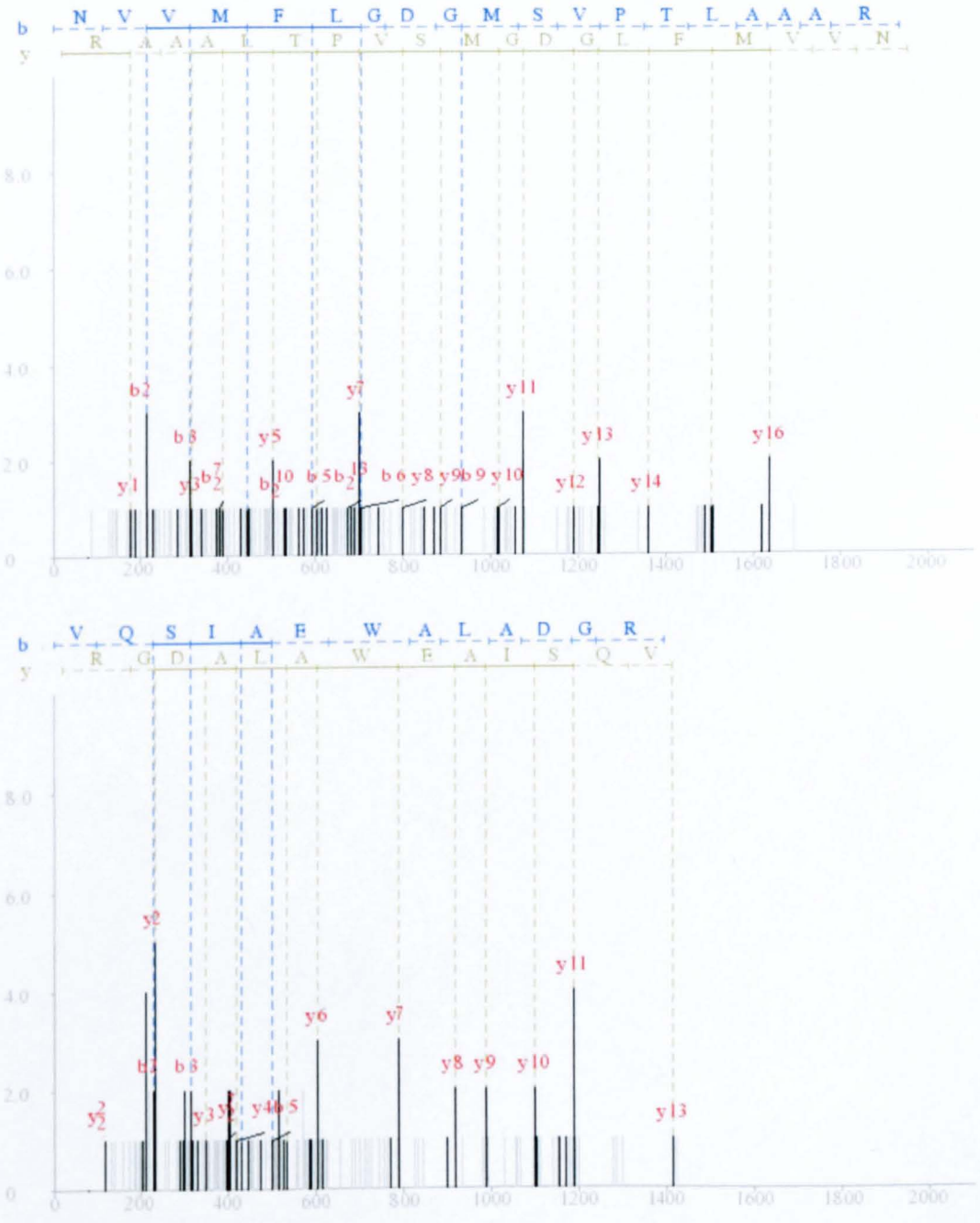

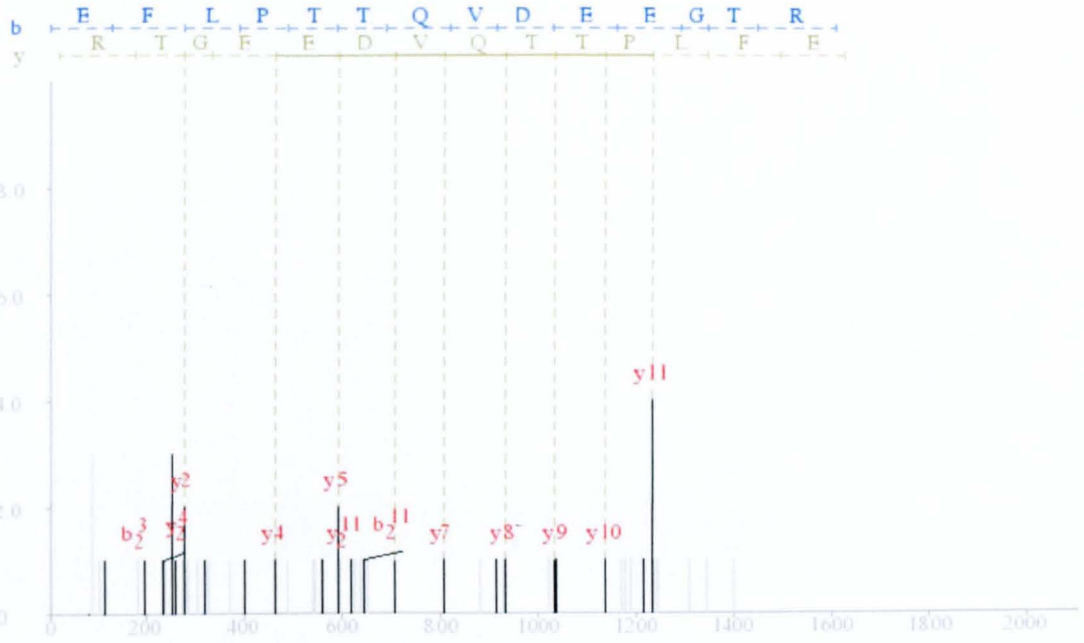
b E F L P T T Q V D E E G T R
y R T G F F D V Q T T P L F F
y11
y2
y5
y4
y7
y8
y9
y10
0
2.0
4.0
6.0
8.0
0
200
400
600
800
1000
1200
1400
1600
1800
2000

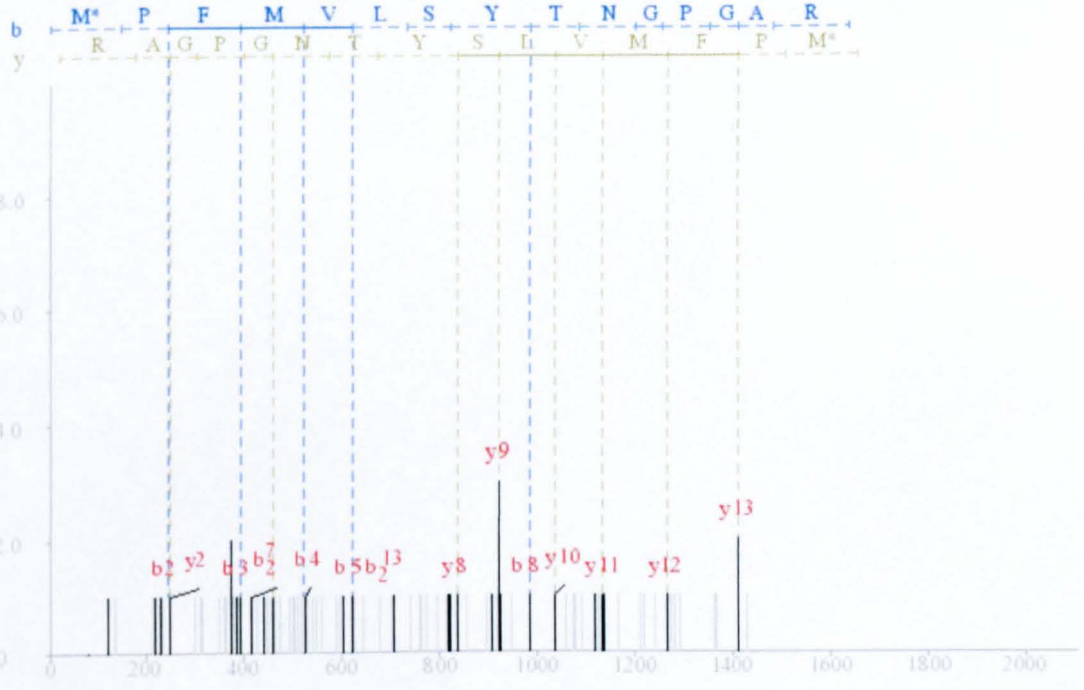
b M* P F M V L S Y T N G P G A R
y R A G P G N T Y S L V M F P M*
y9
y13
y2
y8
y10
y11
y12
0
2.0
4.0
6.0
8.0
0
200
400
600
800
1000
1200
1400
1600
1800
2000

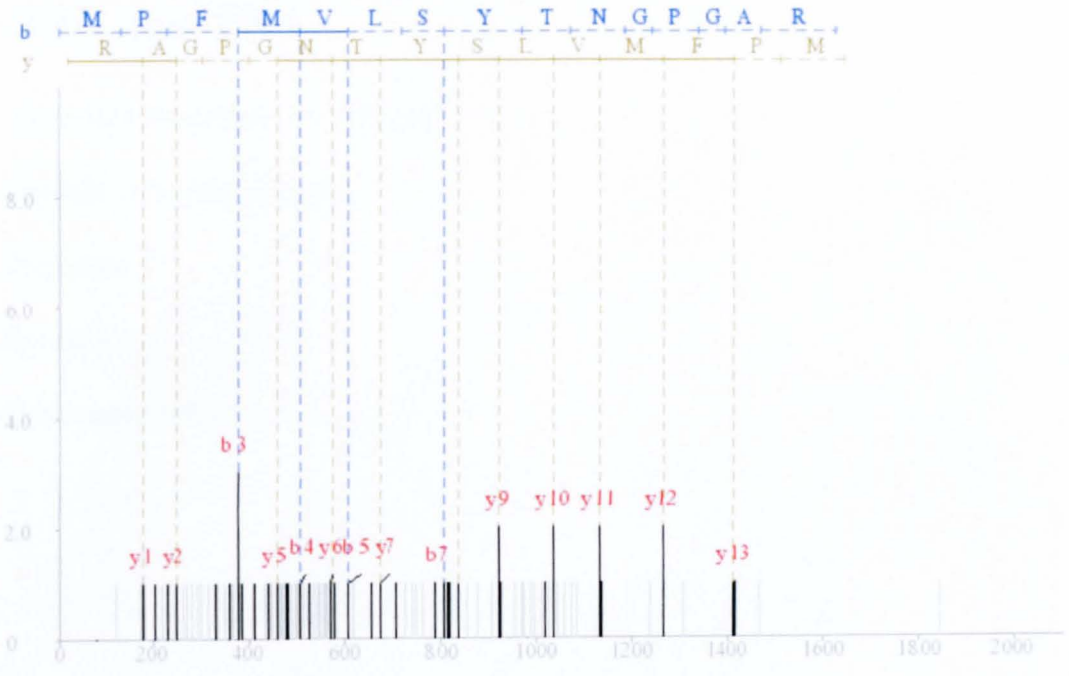
b
y
M P F M V L S Y T N G P G A R
R A G P G N T Y S L V M F P M
8.0
6.0
4.0
2.0
0
b3
y1 y2
y5 b4 y6 b5 y7
b7
y9 y10 y11 y12
y13
0 200 400 600 800 1000 1200 1400 1600 1800 2000

DIGE spot 2983

Accession Number: Bmb002778

Protein: Titin-like protein

Peptides: 1

Spectra: 1

Coverage: 7.6%

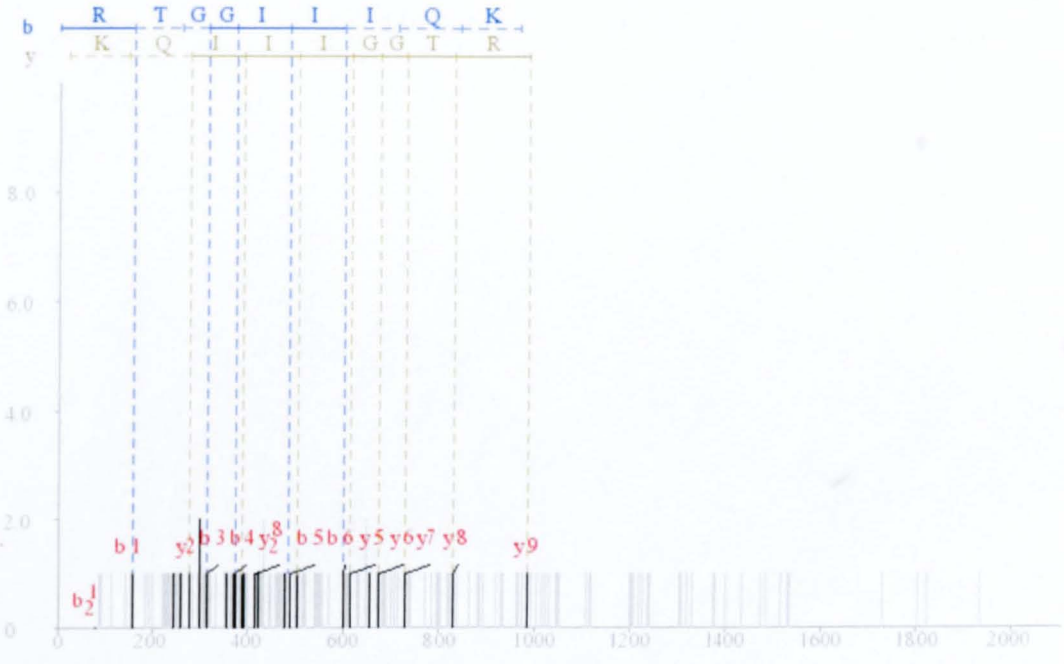

DIGE spot 3743

Accession Number: Bmb022778

Protein: Proteasome alpha subunit

Peptides: 2

Spectra: 2

Coverage: 20.2%

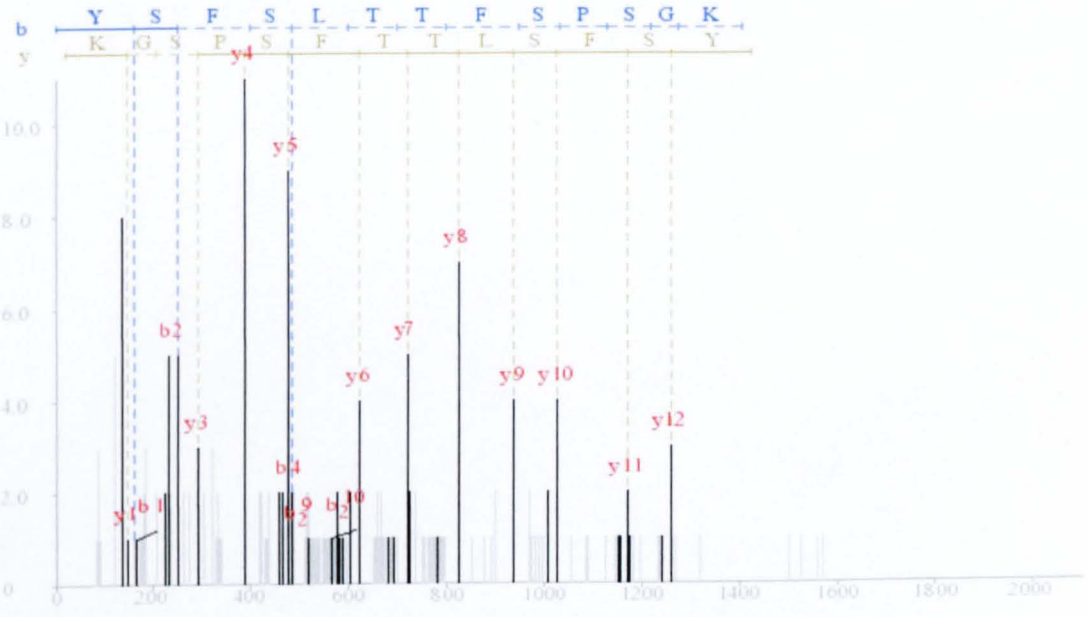

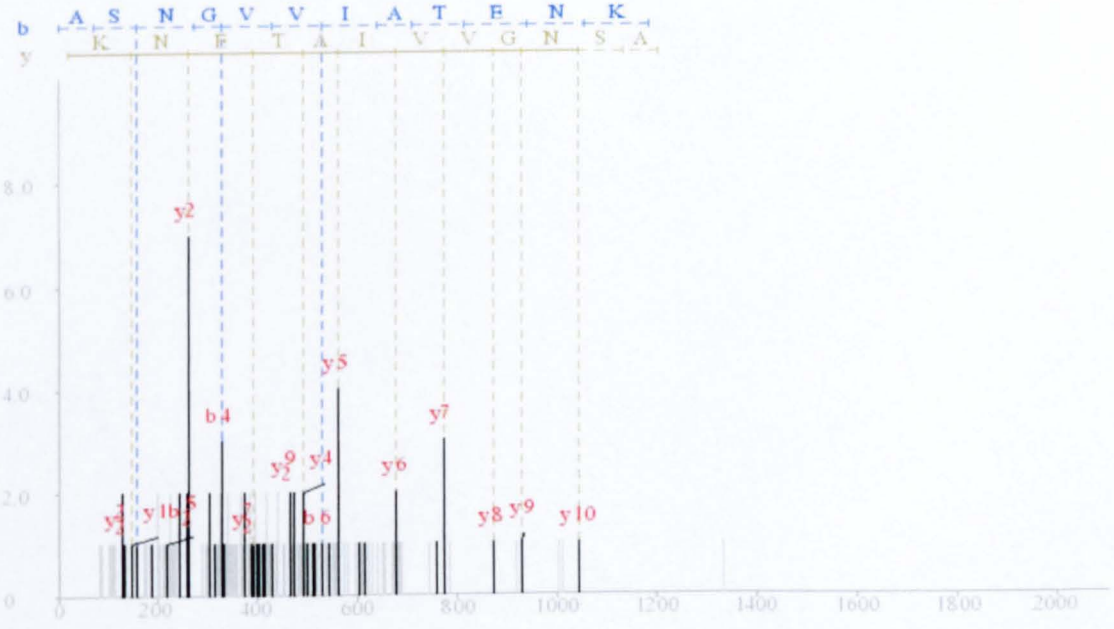

DIGE spot 3838

Accession Number: Bmb020455

Protein: proteasome beta subunit

Peptides: 2

Spectra: 40

Coverage: 23.8%

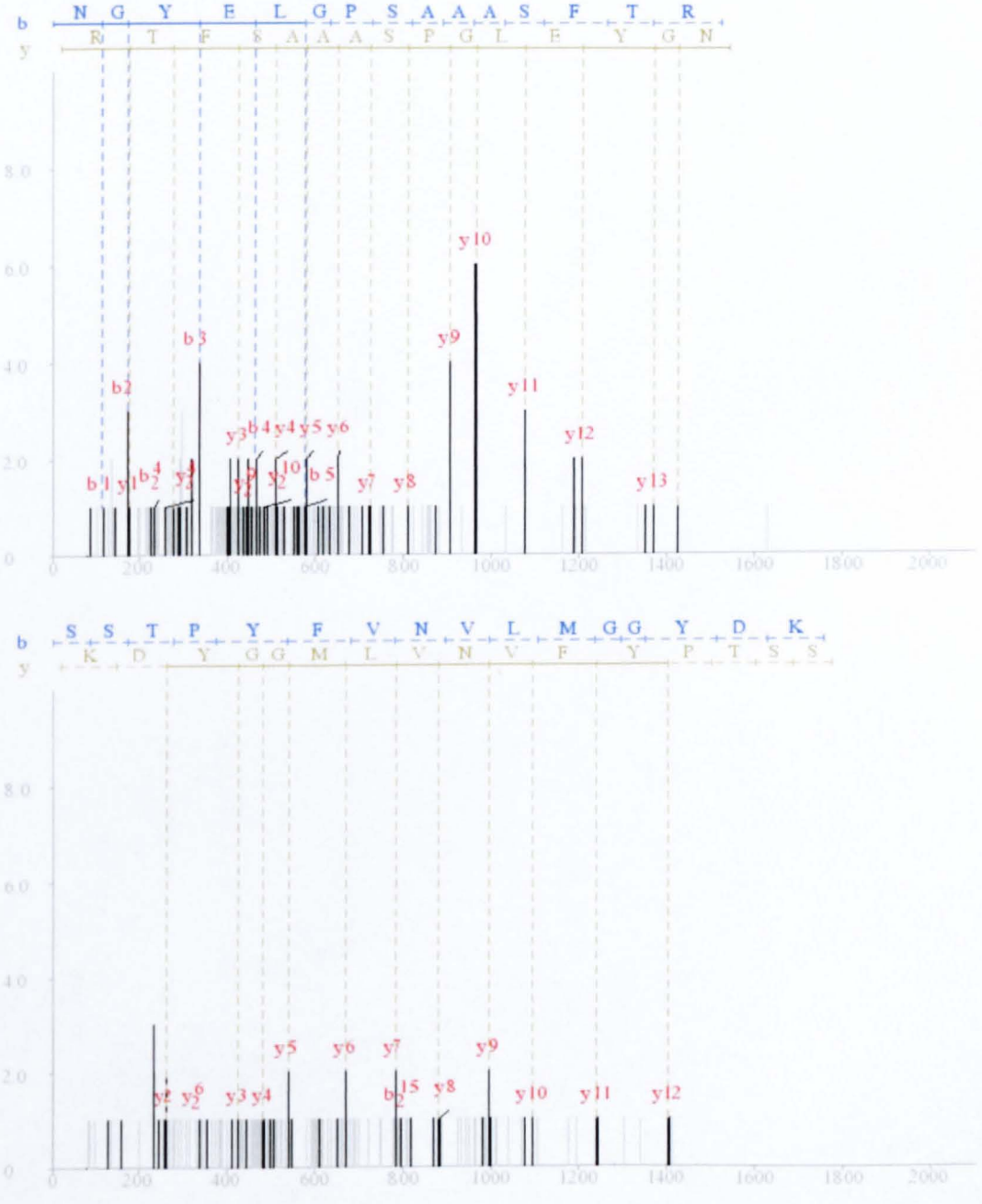

DIGE spot 3894

Accession Number: Bmb034978

Protein: Actin depolymerising factor

Peptides: 2

Spectra: 9

Coverage: 19.8%

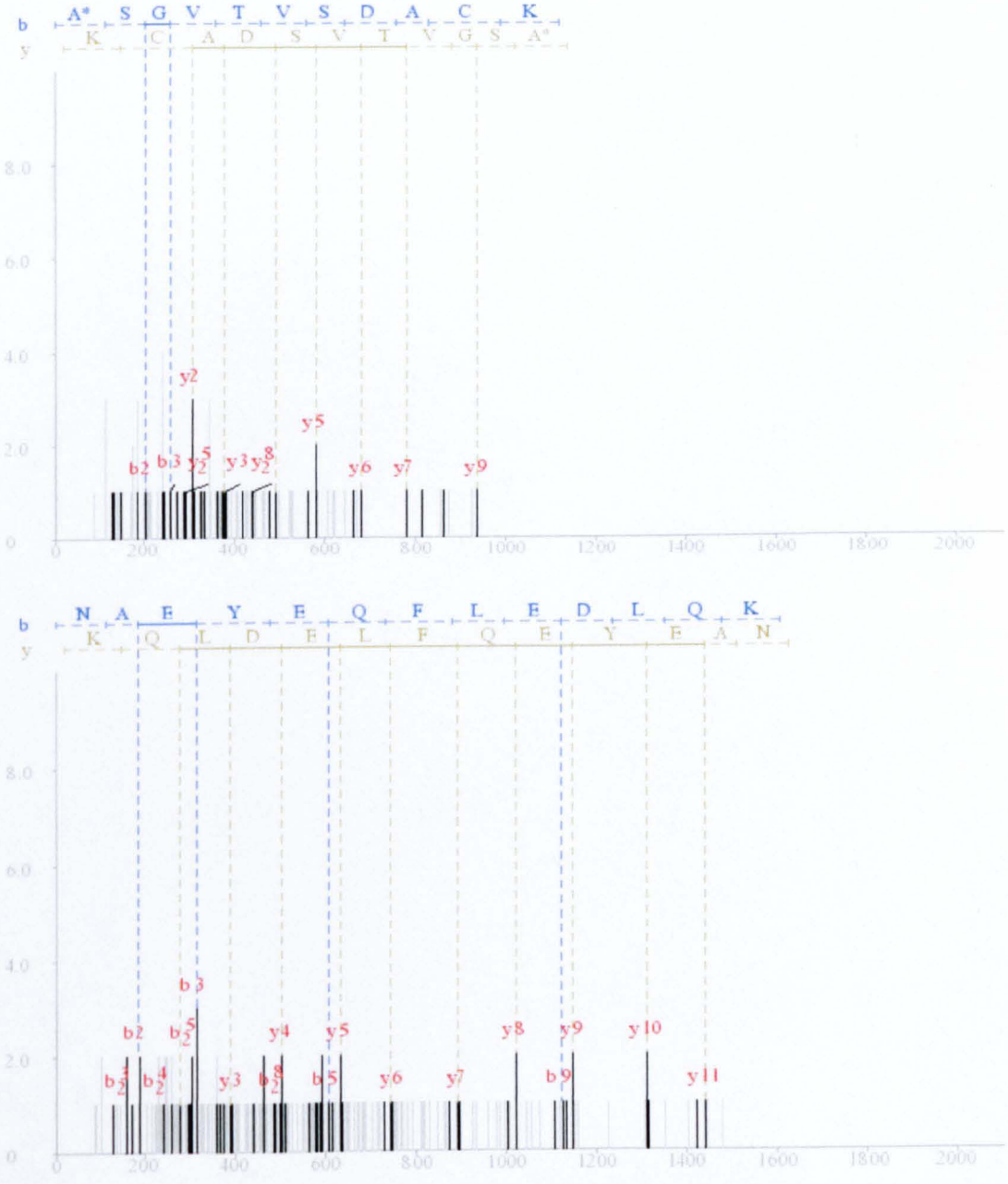

DIGE spot 3989

Accession Number: Bmb026932

Protein: Proteasome beta 7 subunit

Peptides: 1

Spectra: 7

Coverage: 4.2%

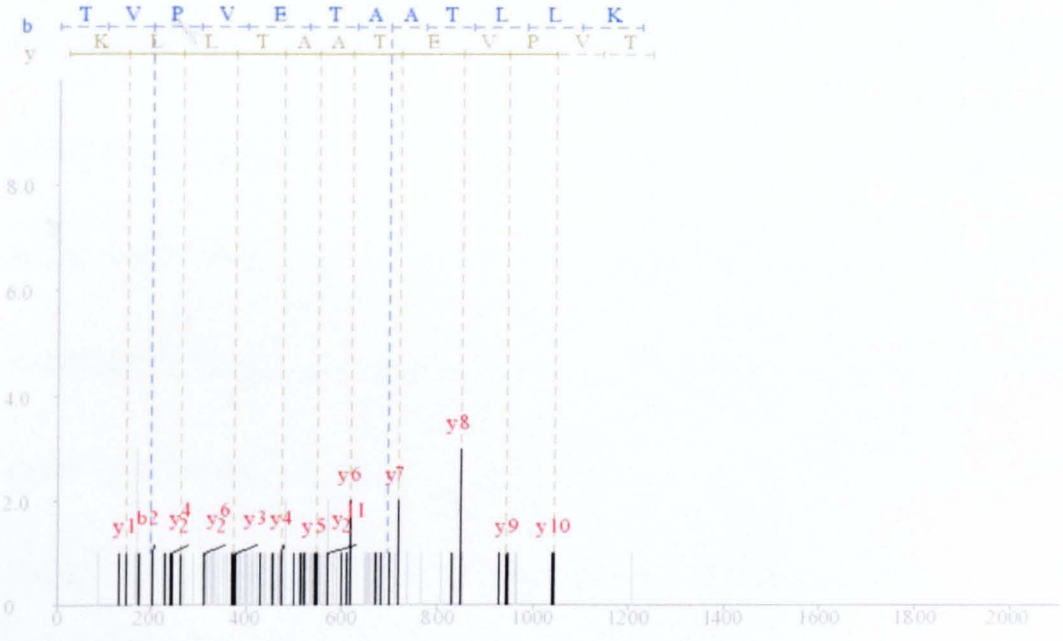

APPENDIX 4

Bombyx mori BM36 cell DIGE experiment InsPect database search results

DIGE spot 692

Accession Number: Bmb009360

Protein: Hsp70

Peptides: 4

Spectra: 11

Coverage: 10.3%

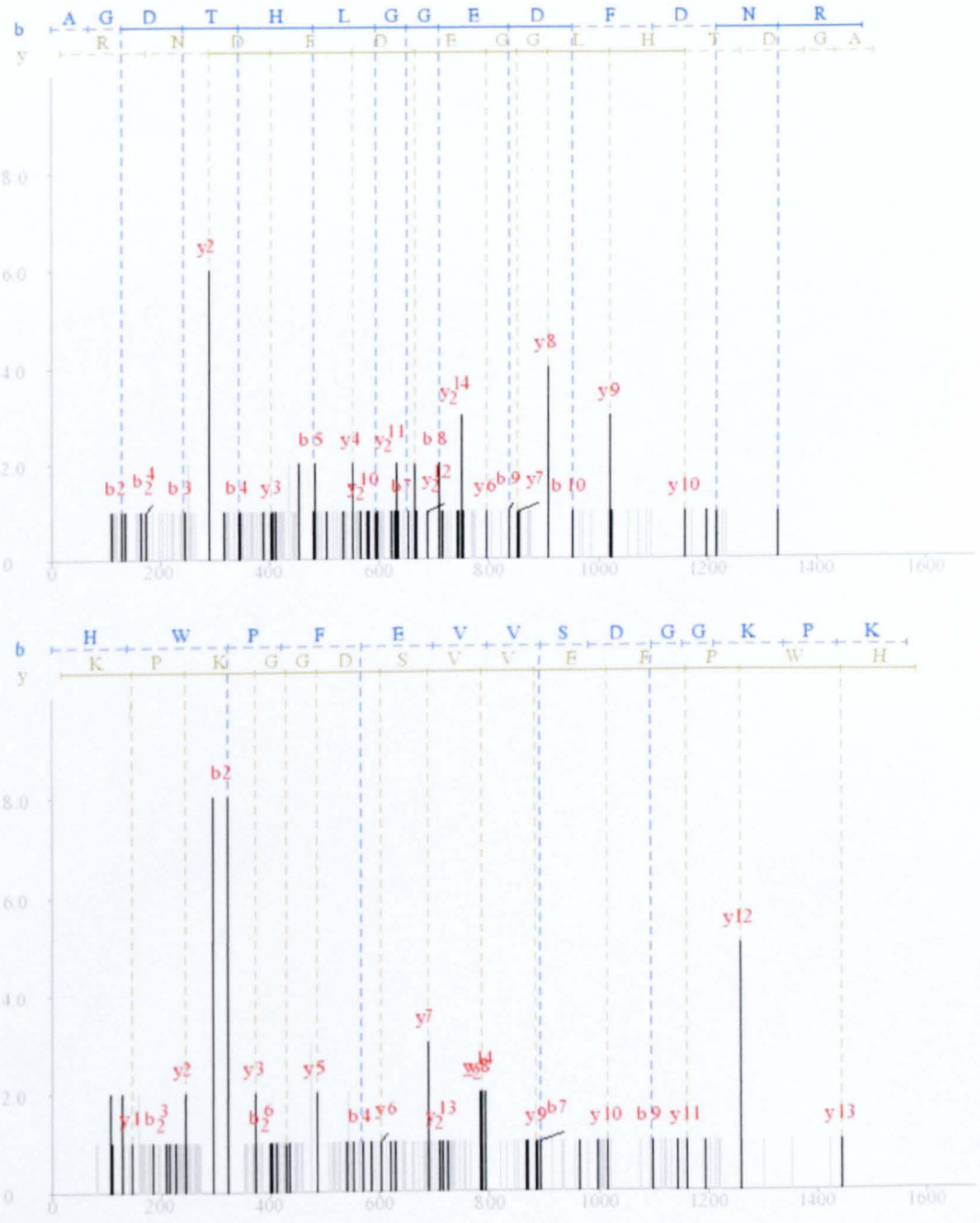

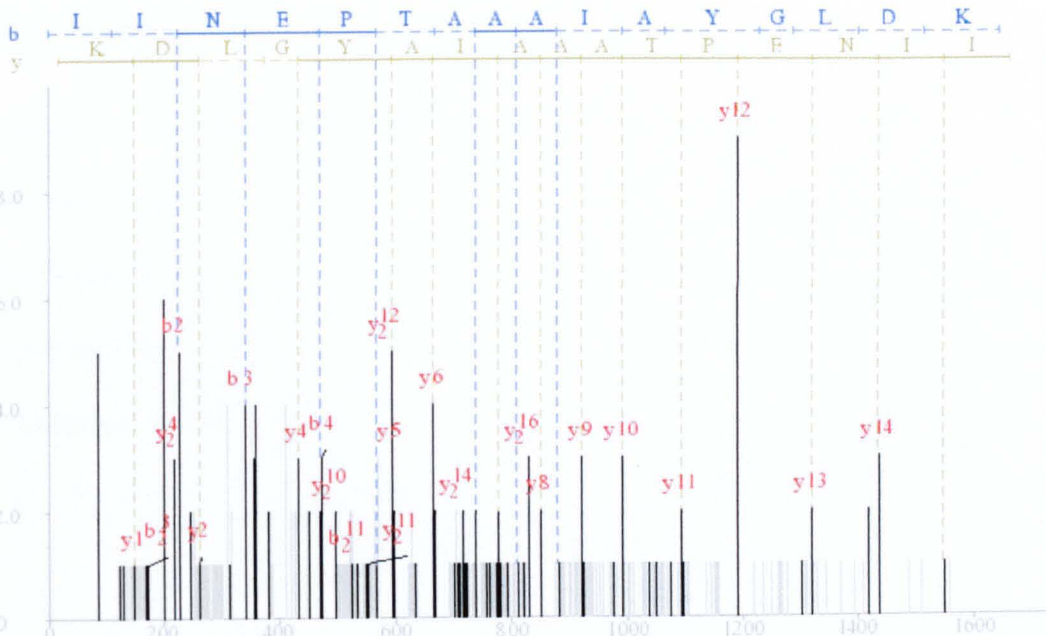
b I I N E P T A A A I A Y G L D K
y K D L G Y A I A A A T P E N I I
y12
b2
b3
y6
y4
b4
y5
y9
y10
y14
y8
y11
y13
y1
8.0
6.0
4.0
2.0
0
200
400
600
800
1000
1200
1400
1600

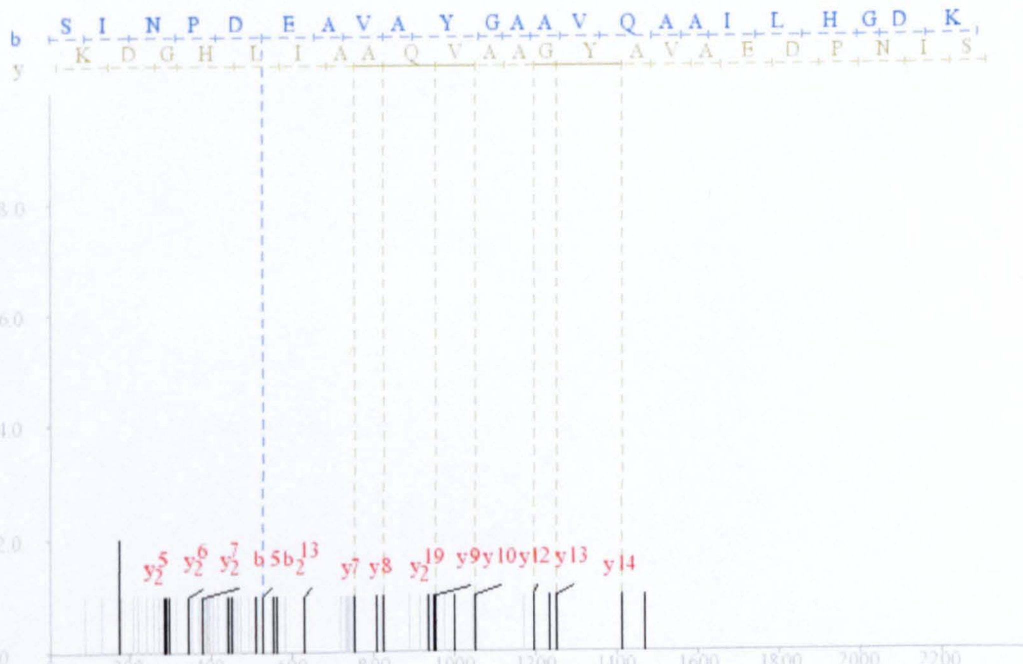
b S I N P D E A V A Y G A A V Q A A I L H G D K
y K D G H L I A A Q V A A G Y A V A E D P N I S
y7
y8
y9
y10
y12
y13
y14
8.0
6.0
4.0
2.0
0
200
400
600
800
1000
1200
1400
1600
1800
2000
2200

DIGE spot 756

Accession Number: Bmb009360

Protein: Hsp70

Peptides: 6

Spectra: 70

Coverage: 14.6%

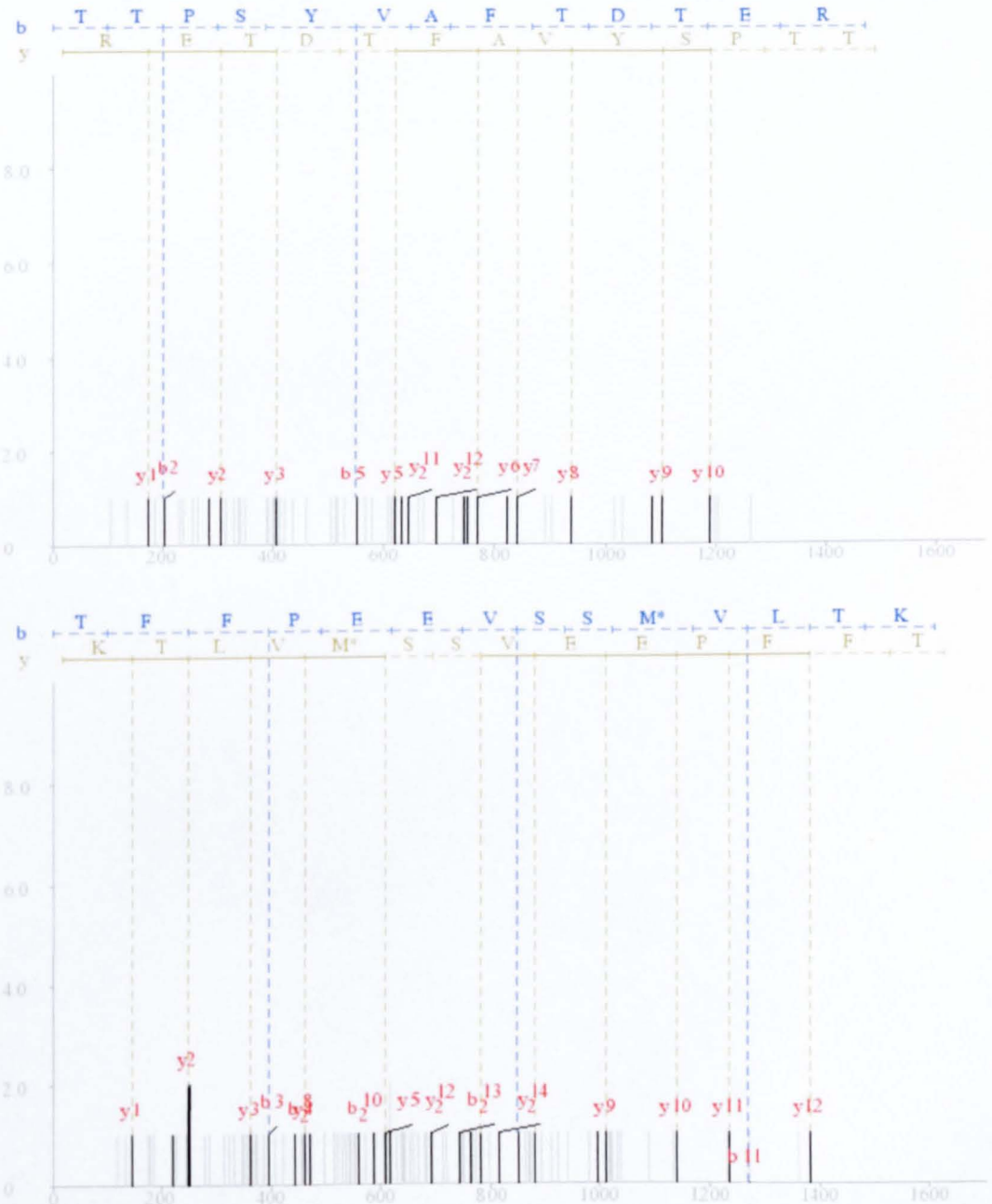

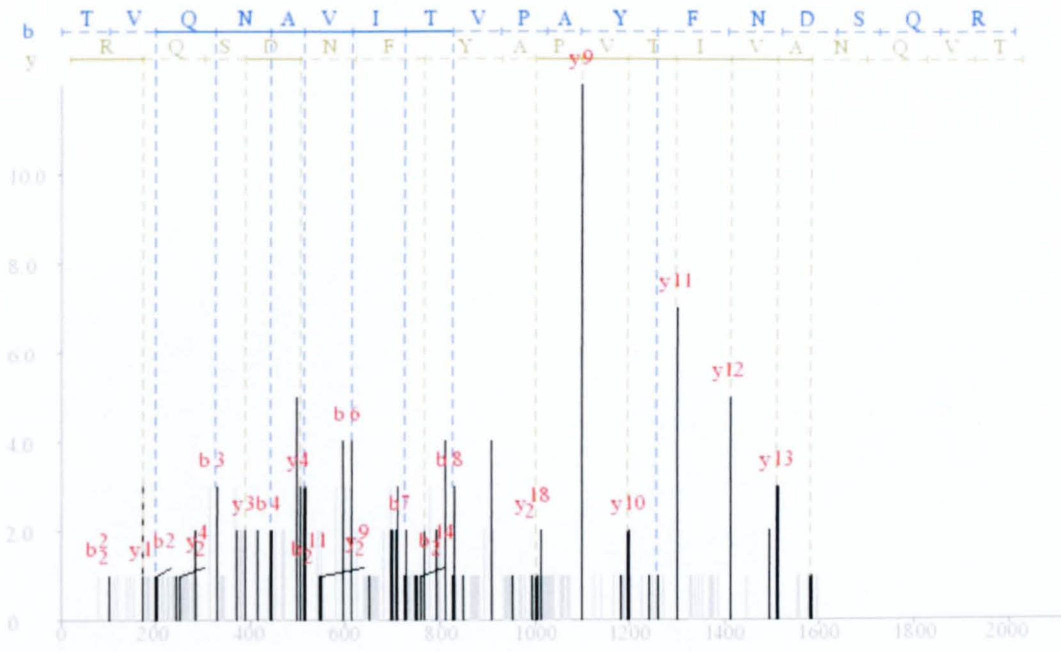
b T V Q N A V I T V P A Y F N D S Q R
y R Q S D N F Y A P V T I V A N Q V T
y9
y11
y12
y13
y10
b6
b3
b8
y4
y3b4
b7
b2
y1
0
2.0
4.0
6.0
8.0
10.0
0 200 400 600 800 1000 1200 1400 1600 1800 2000

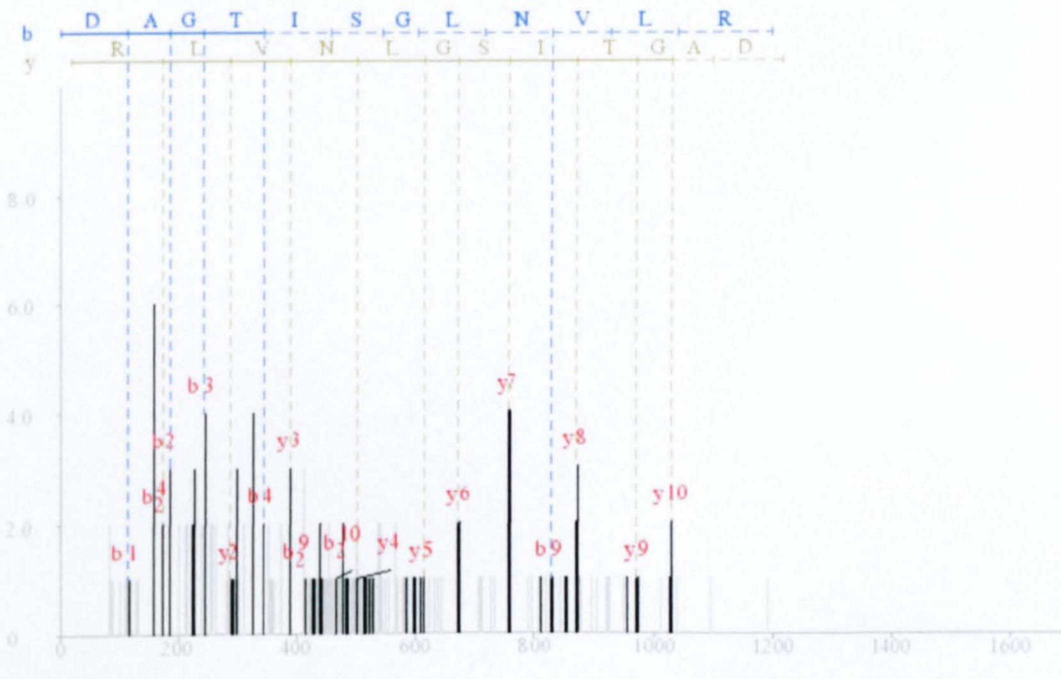
b D A G T I S G L N V L R
y R L V N L G S I T G A D
y7
b3
b2
y3
y8
y6
b4
y10
b1
y2
y4
y5
b9
y9
0
2.0
4.0
6.0
8.0
0 200 400 600 800 1000 1200 1400 1600

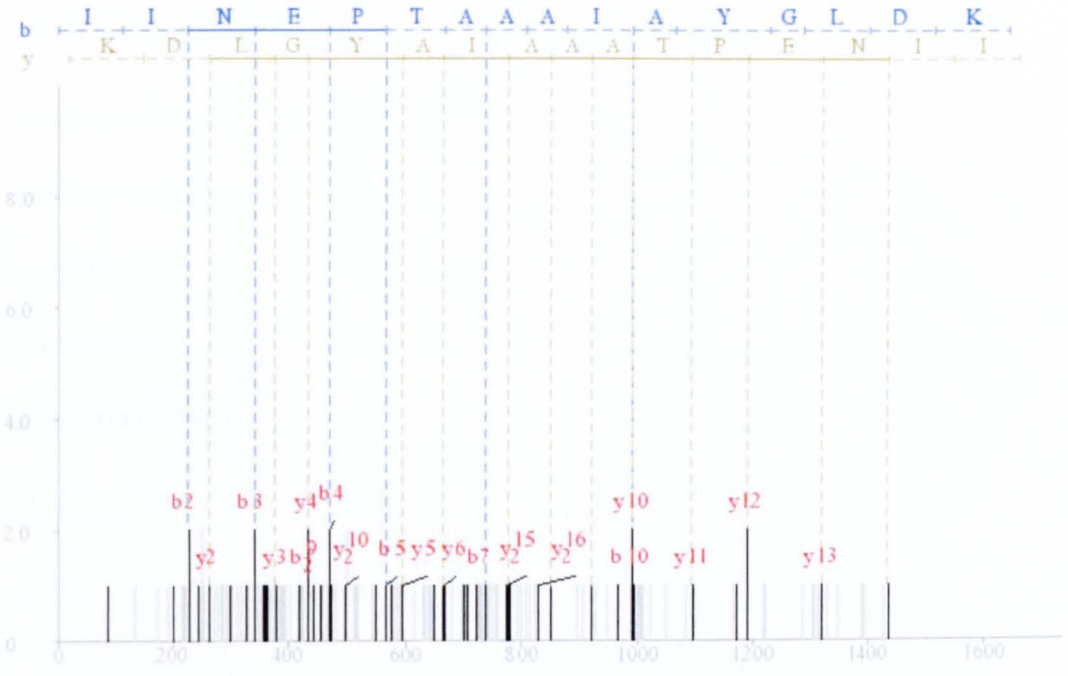
b I I N E P T A A A I A Y G L D K
y K D L G Y A I A A A T P E N I I
8.0
6.0
4.0
2.0
0
b2 b3 y4 b4 y10 y12
y2 y3 b5 y5 y6 b7 y15 y16 b10 y11 y13
0 200 400 600 800 1000 1200 1400 1600

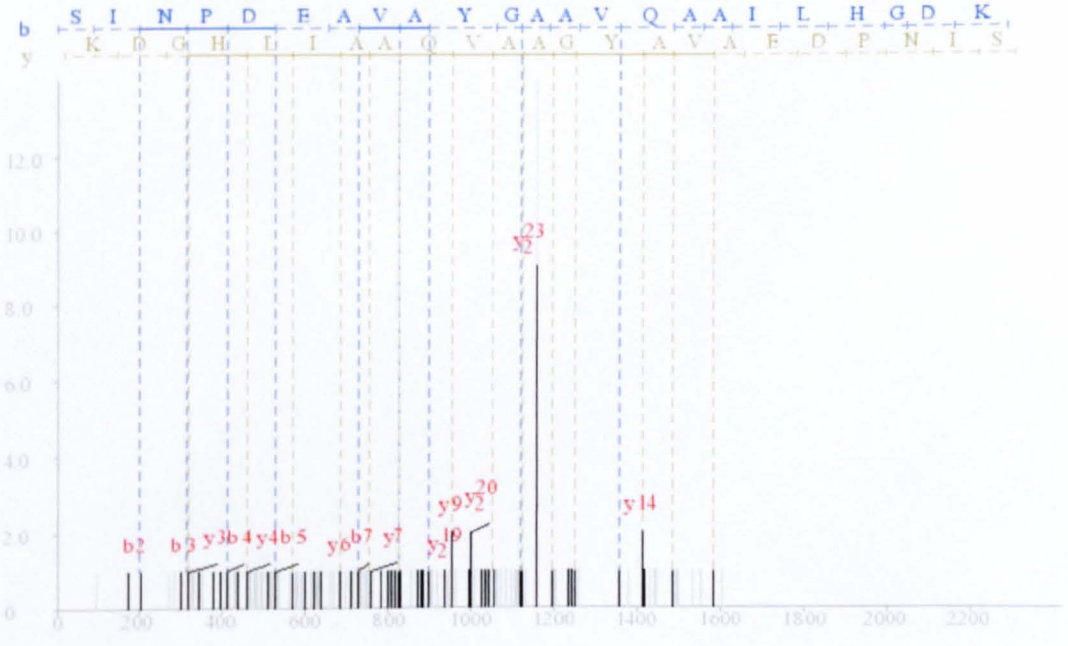
b S I N P D E A V A Y G A A V Q A A I L H G D K
y K D G H D I A A Q V A A G Y A V A E D P N I S
12.0
10.0
8.0
6.0
4.0
2.0
0
y23
y9 y20 y14
b2 b3 y3 b4 y4 b5 y6 b7 y7 y10
0 200 400 600 800 1000 1200 1400 1600 1800 2000 2200

DIGE spot 764

Accession Number: Bmb008836

Protein: Vacuolar ATP synthase

Peptides: 9

Spectra: 37

Coverage: 15.6%

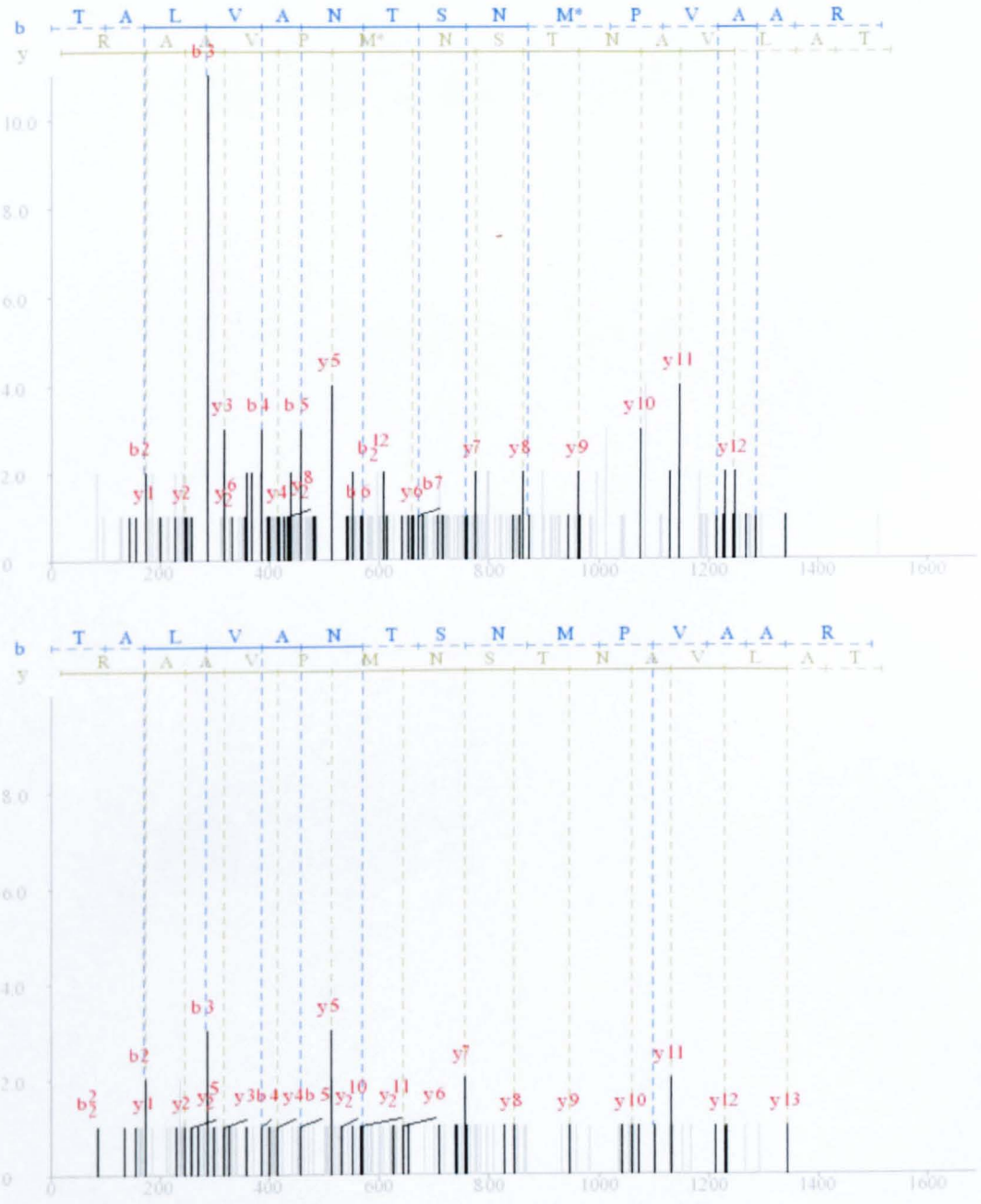

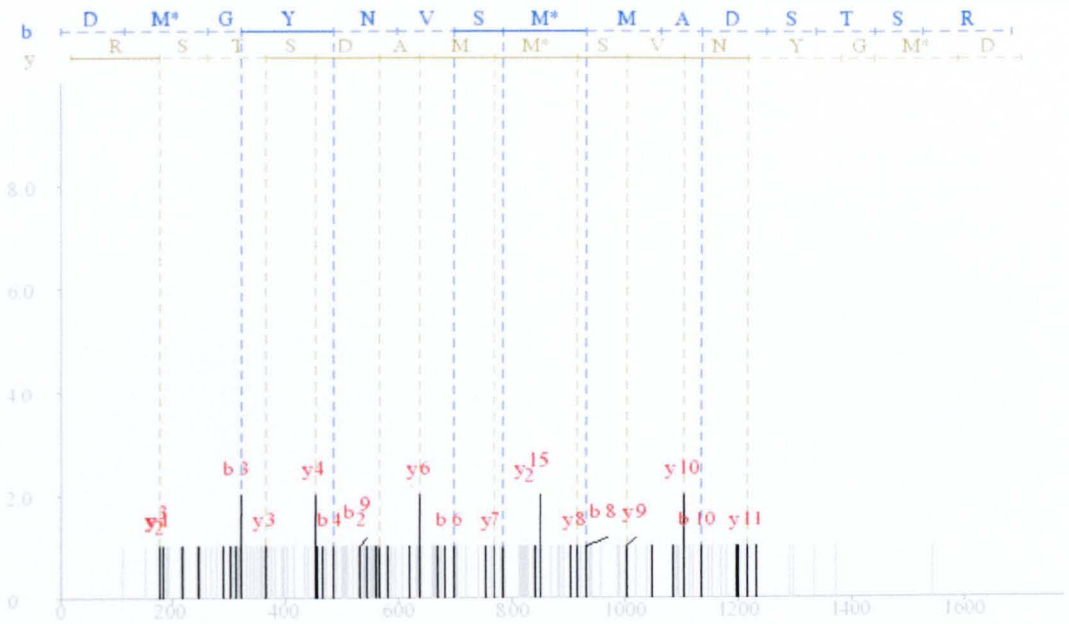
b
y
D M* G Y N V S M* M A D S T S R
R S T S D A M M* S V N Y G M* D
8.0
6.0
4.0
2.0
0
200
400
600
800
1000
1200
1400
1600


b
y
D M* G Y N V S M M A D S T S R
R S T S D A M M S V N Y G M* D
8.0
6.0
4.0
2.0
0
200
400
600
800
1000
1200
1400
1600

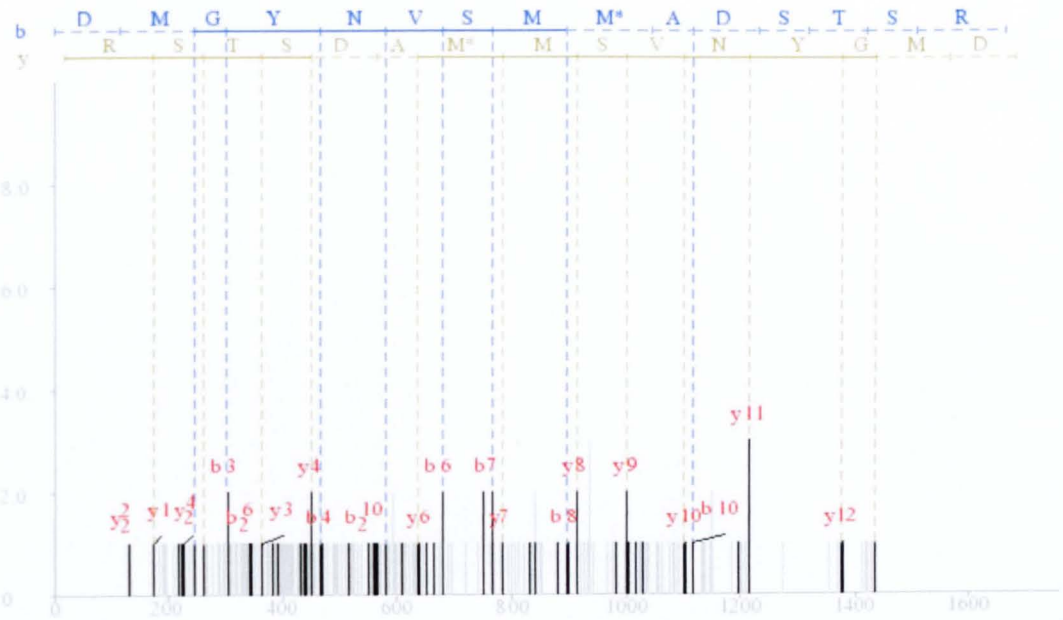
b D M G Y N V S M M* A D S T S R
y R S T S D A M* M S V N Y G M D
y11
b3 y4 b6 b7 y8 y9
y2 y1 y2 b2 6 y3 b4 b2 10 y6 y7 b8 y10 b 10 y12
0 200 400 600 800 1000 1200 1400 1600


b E I L Q E E E D L S E I V Q L V G K
y K G V L Q V I E S L D E E E Q L I E
y5 y2 18 y12
y2 b2 y3 b3 y4 b2 10 b 5 b 13 y2 15 y9 y11 b 12 y13
0 200 400 600 800 1000 1200 1400 1600 1800 2000

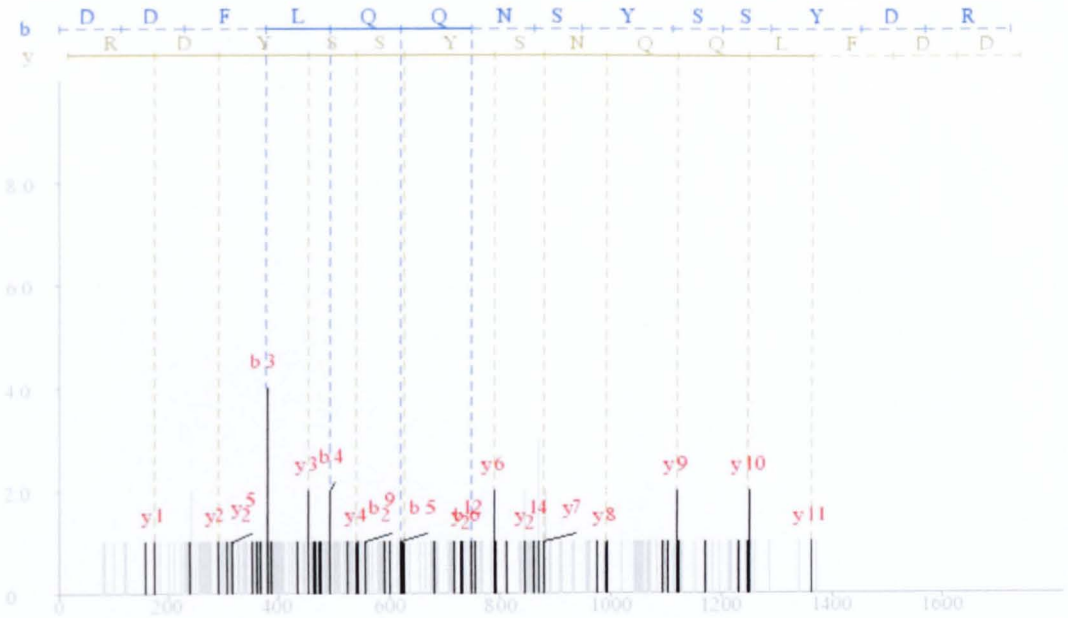
b
y
D D F L Q Q N S Y S S Y D R
R D Y S S Y S N Q Q L F D D
b3
y3 b4
y6
y9
y10
y1
y2 y2 5
y4 b2 9
b 5
y2 12
y2 14
y7
y8
y11
8.0
6.0
4.0
2.0
0
0 200 400 600 800 1000 1200 1400 1600

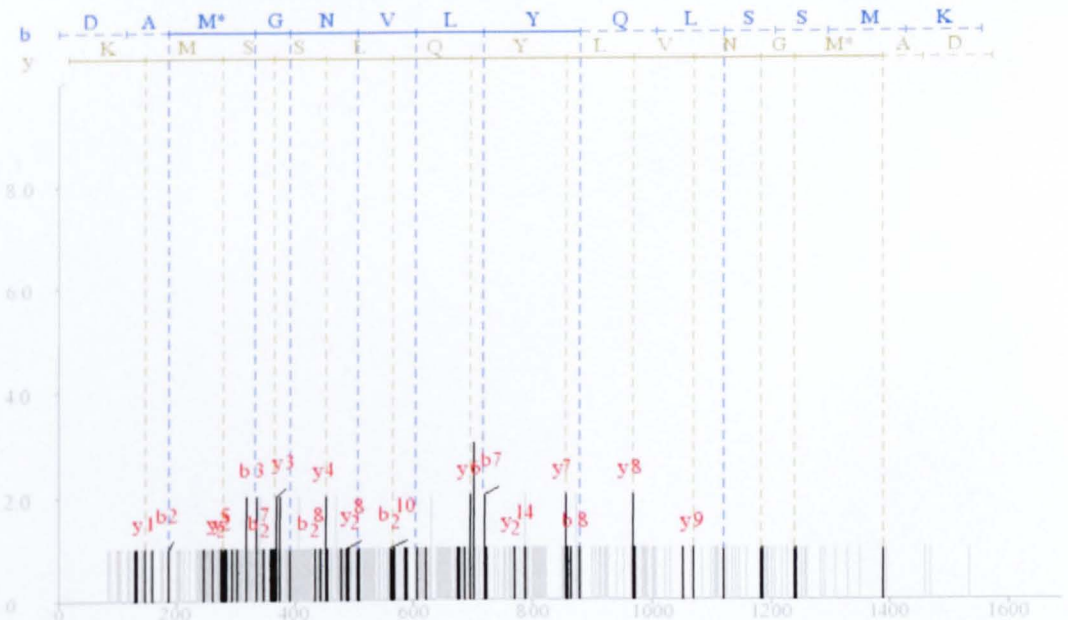
b
y
D A M* G N V L Y Q L S S M K
K M S S E Q Y L V N G M* A D
b3 y3
y4
y6 b7
y7
y8
y1 b2
y9
8.0
6.0
4.0
2.0
0
0 200 400 600 800 1000 1200 1400 1600

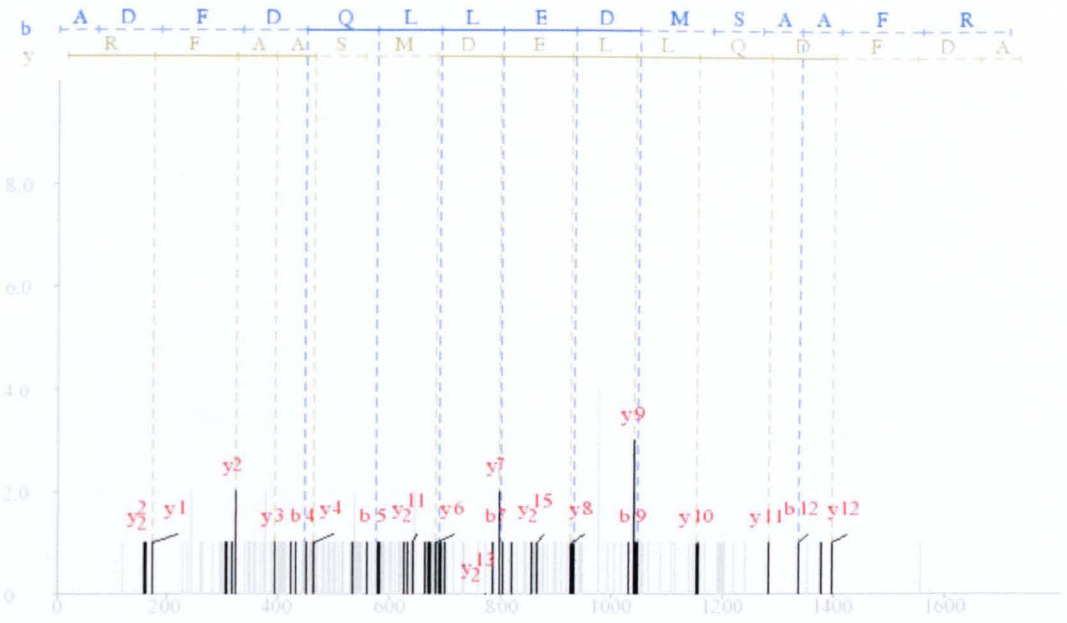
b
A D F D Q L L E D M S A A F R
y
R F A A S M D E L L Q D F D A
8.0
6.0
4.0
2.0
0
y9
y2
y7
y1
y3
b4
y4
b5
y11
y6
b7
y15
y8
b9
y10
y11
b12
y12
y13
0
200
400
600
800
1000
1200
1400
1600

DIGE spot 1185

Accession Number: Bmb005542

Protein: ATP synthase

Peptides: 3

Spectra: 50

Coverage: 8.0%

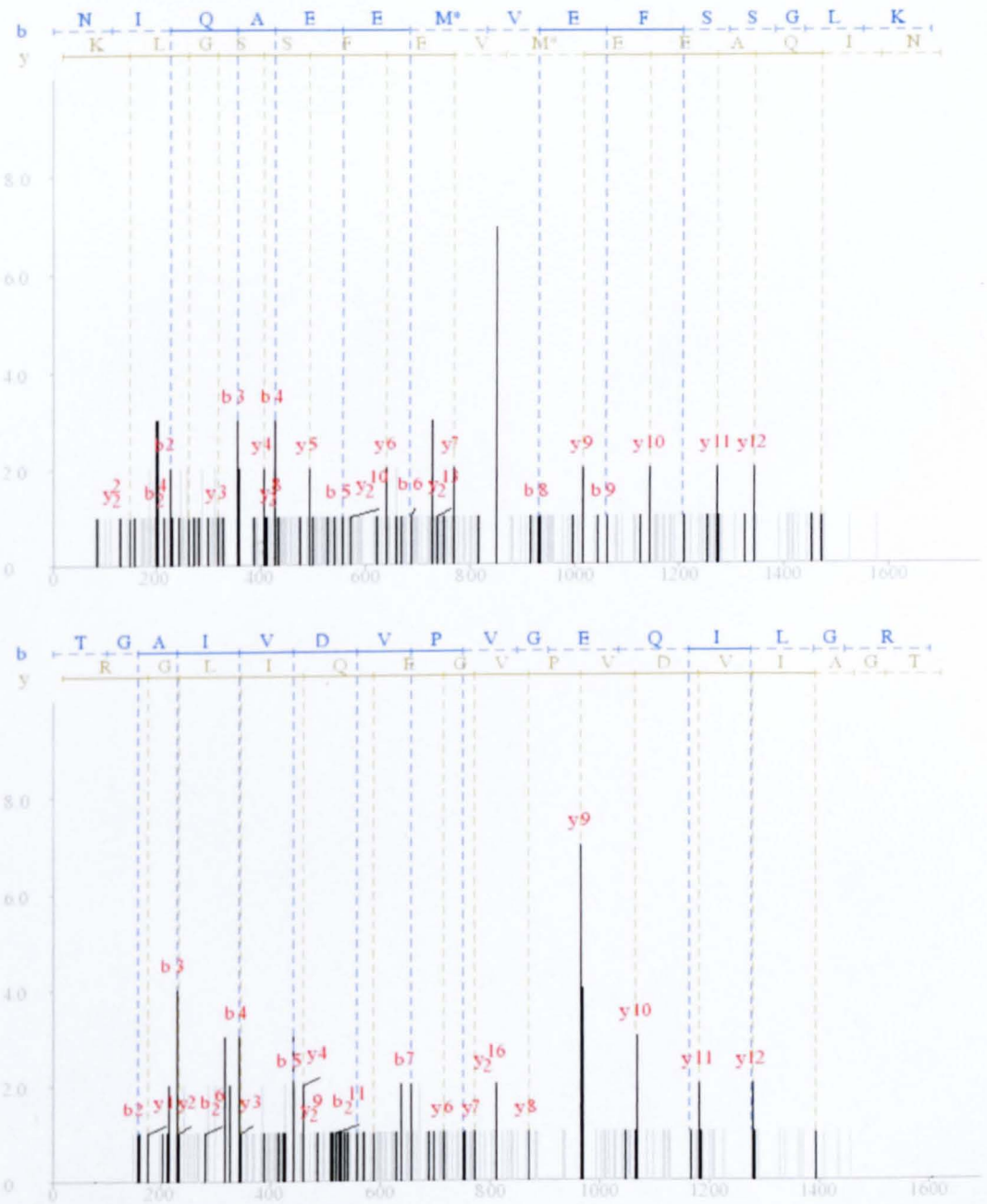

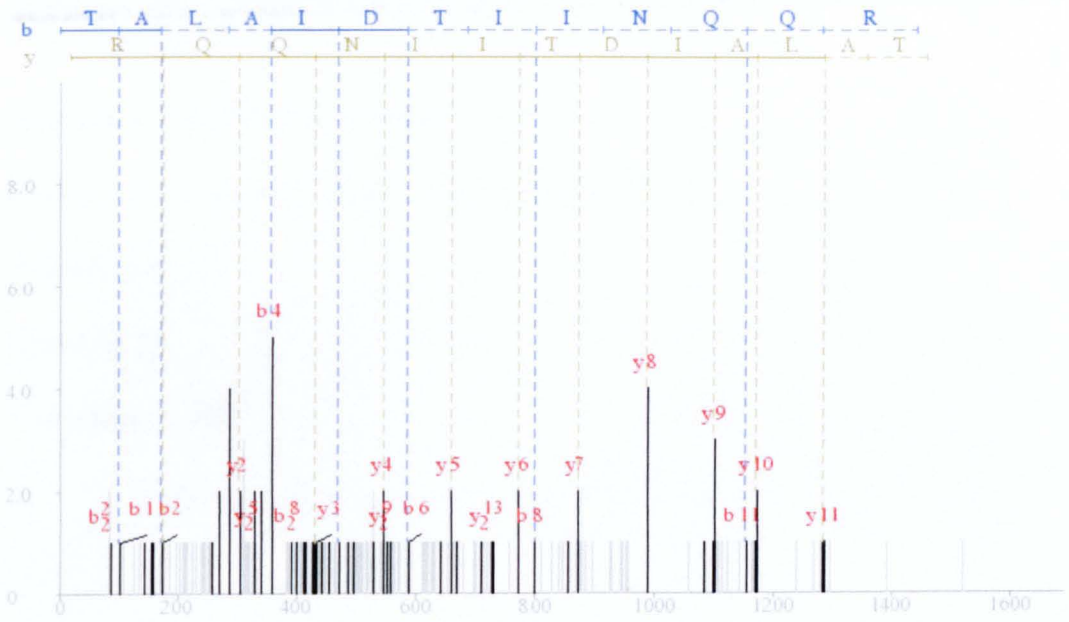
b
y
T A L A I D T I I N Q Q R
R Q Q N I I T D I A L A T
8.0
6.0
4.0
2.0
0
b4
y8
y9
y2
y4
y5
y6
y7
y10
b1 b2
y3
b6
b8
y11
0
200
400
600
800
1000
1200
1400
1600

DIGE spot 1684

Accession Number: Bmb013403

Protein: Proteasome 26S non-ATPase subunit 7

Peptides: 3

Spectra: 55

Coverage: 9.7%

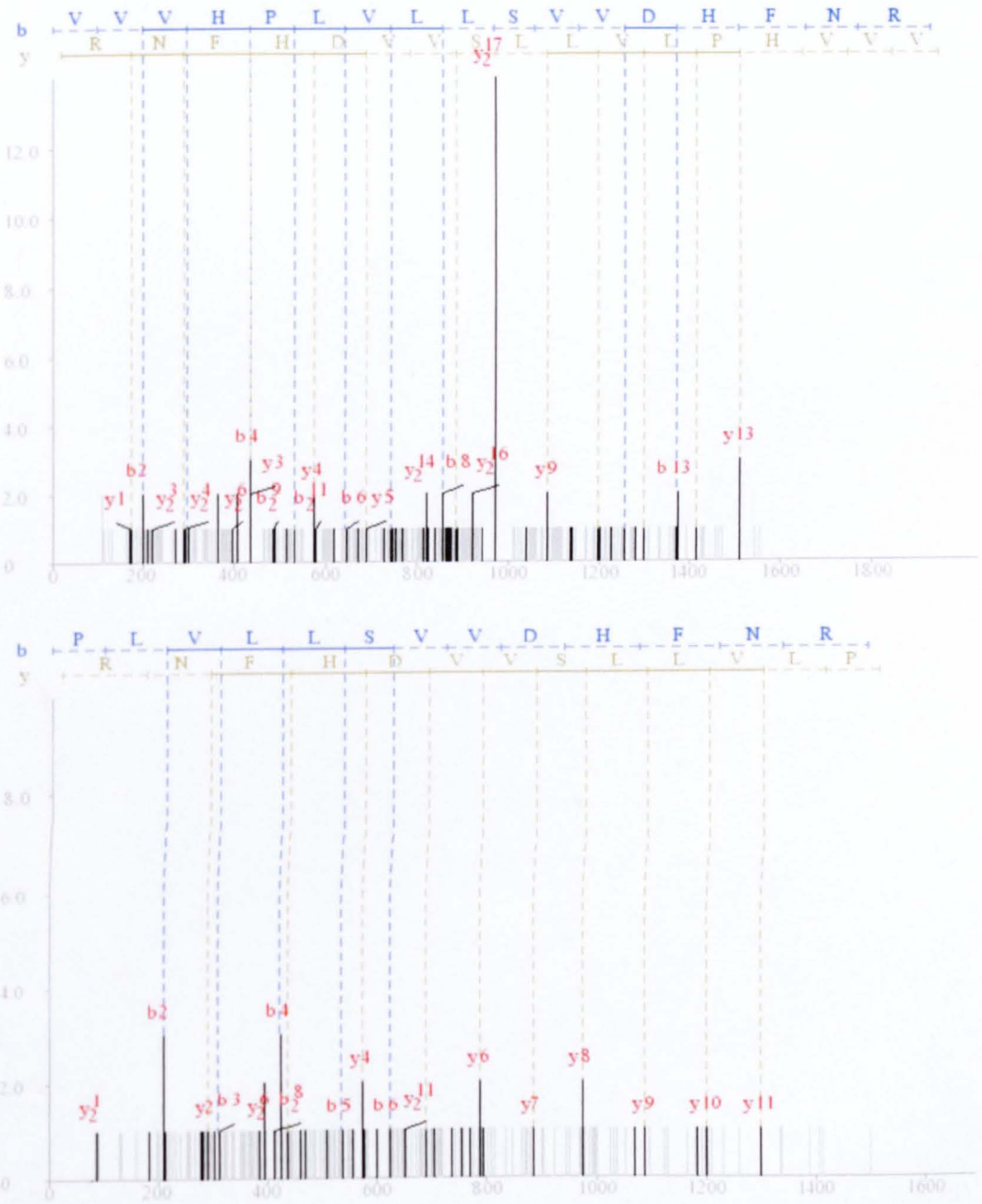

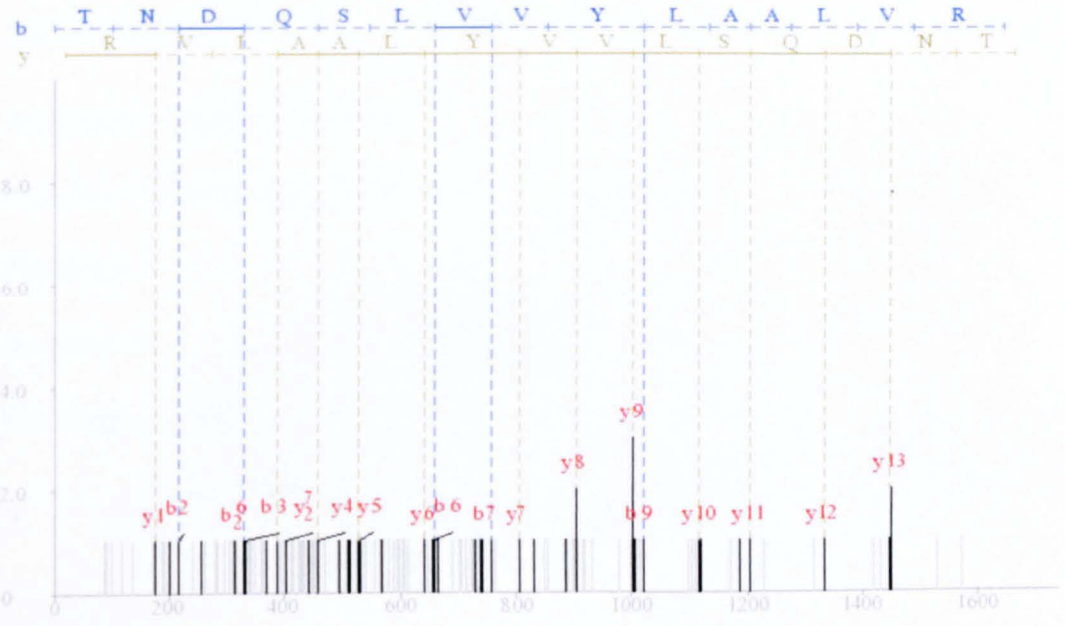
b T N D Q S L V V Y L A A L V R
y R N L A A L Y V V L S Q D N T
8.0
6.0
4.0
2.0
0
y1 b2 b2 b3 y2 y4 y5 y6 b6 b7 y7 y8 y9 b9 y10 y11 y12 y13
0
200
400
600
800
1000
1200
1400
1600

DIGE spot 1924

Accession Number: *Bmb006175*

Protein: Glyceraldehyde-3-Phosphate dehydrogenase

Peptides: 3

Spectra: 38

Coverage: 13.6%

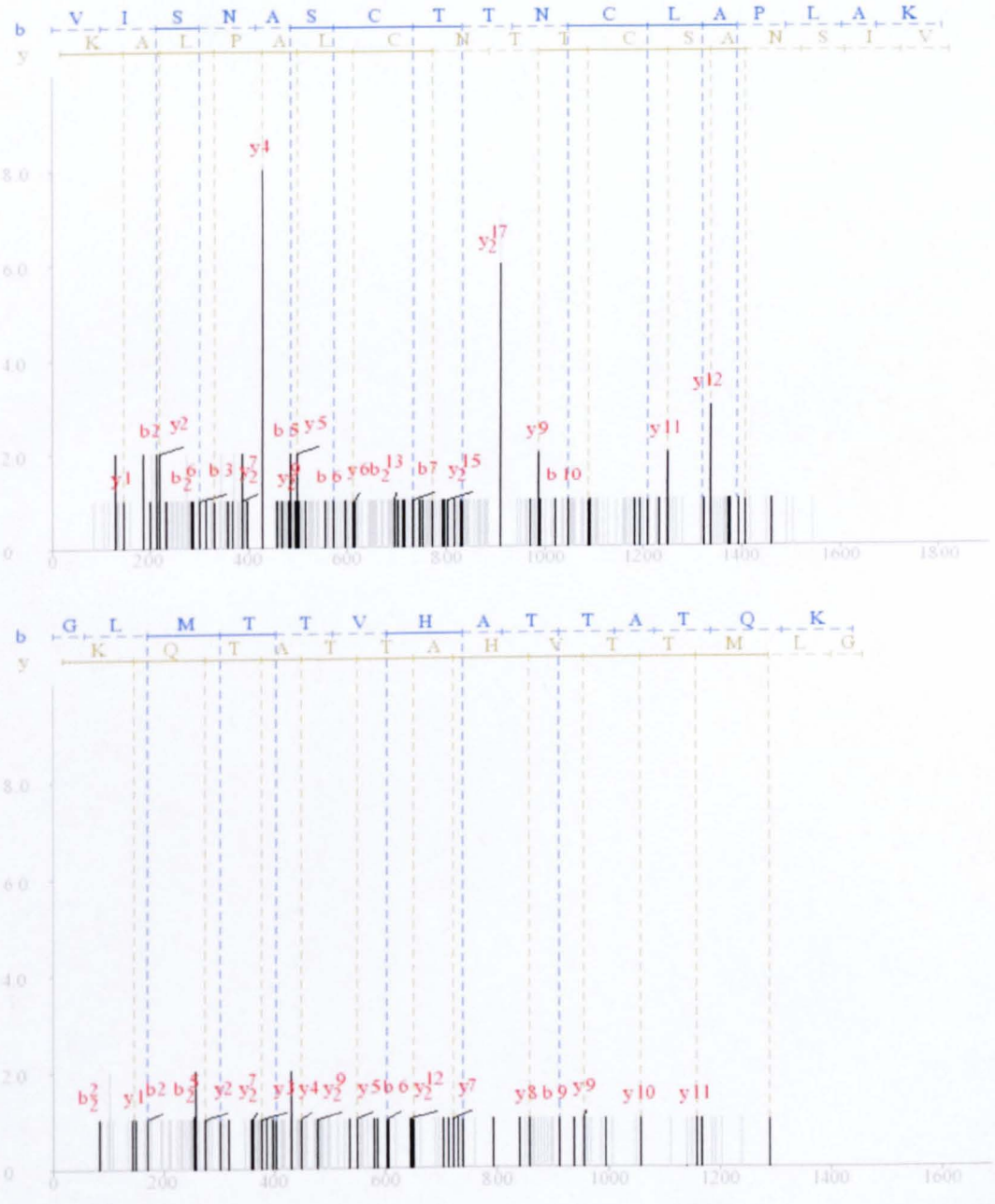

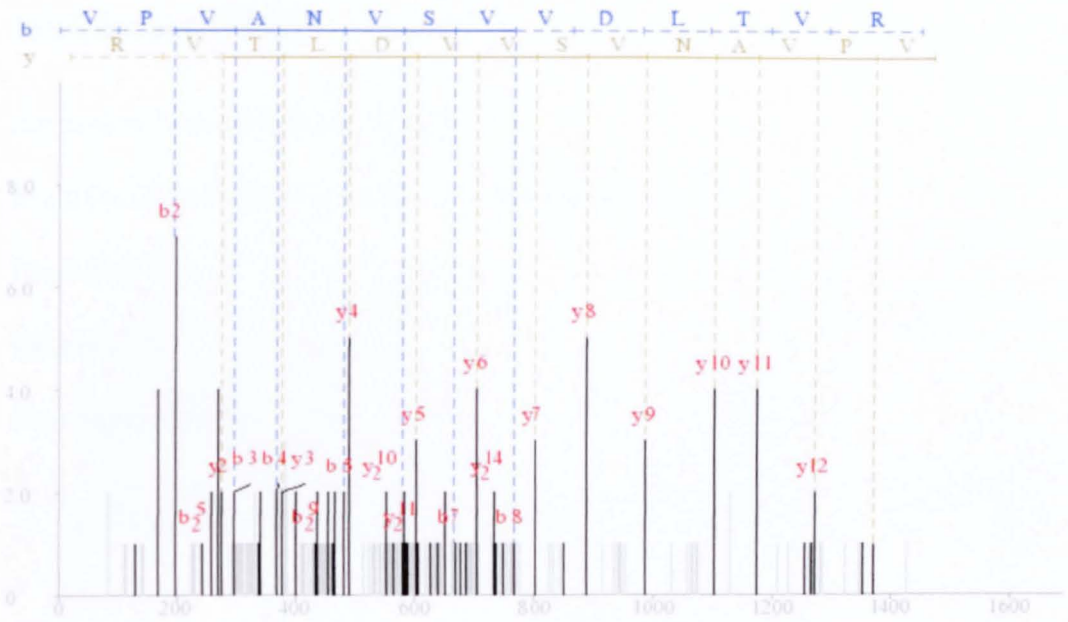
b V P V A N V S V V D L T V R
y R V T L D M M S V N A V P V
b2
y4
y8
y6
y10 y11
y5
y7
y9
y12
b3 b4 y3
b5
b8
0
200
400
600
800
1000
1200
1400
1600

DIGE spot 1930

Accession Number: Bmb006175

Protein: Glyceraldehyde-3-Phosphate dehydrogenase

Peptides: 3

Spectra: 18

Coverage: 13.9%

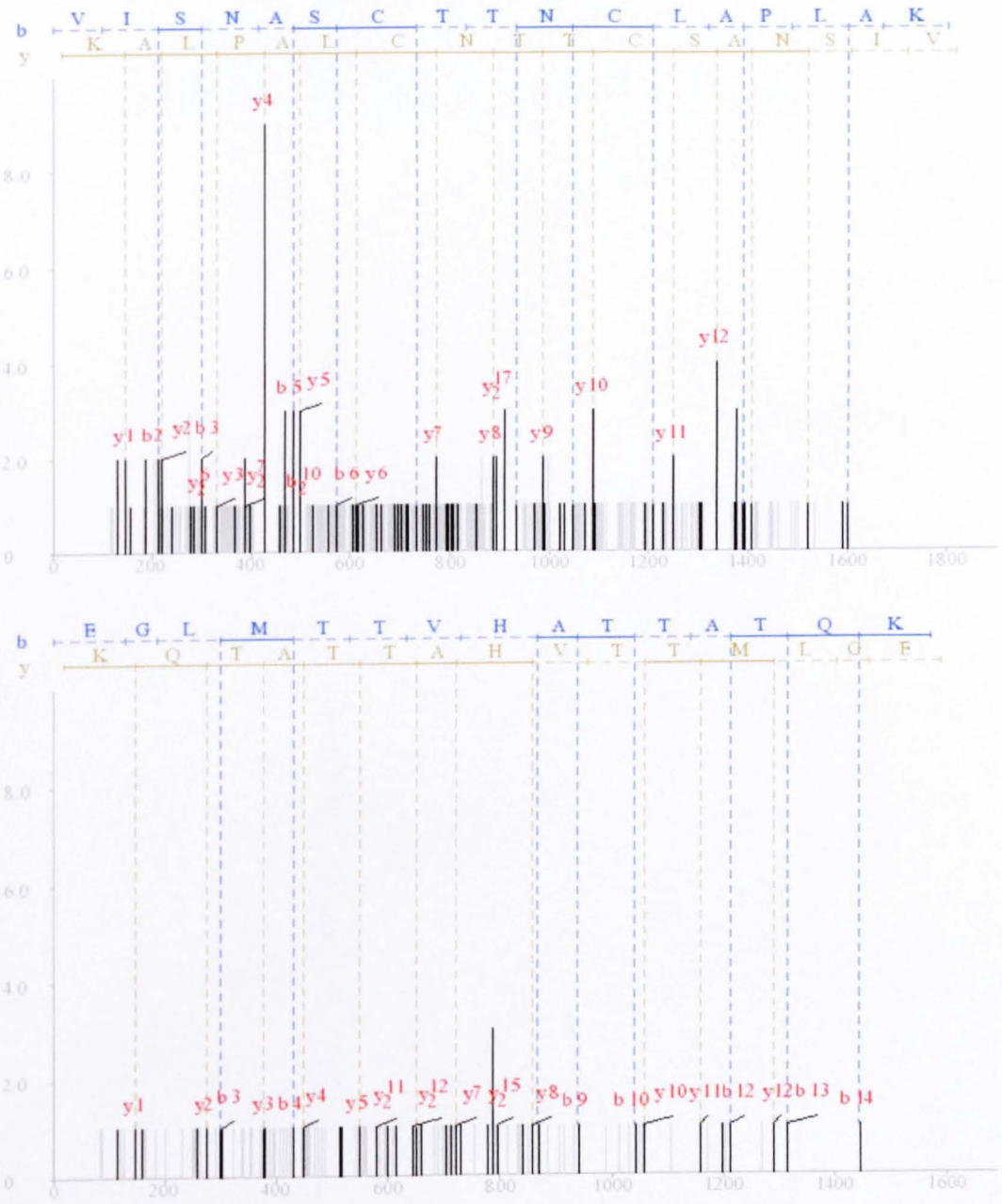

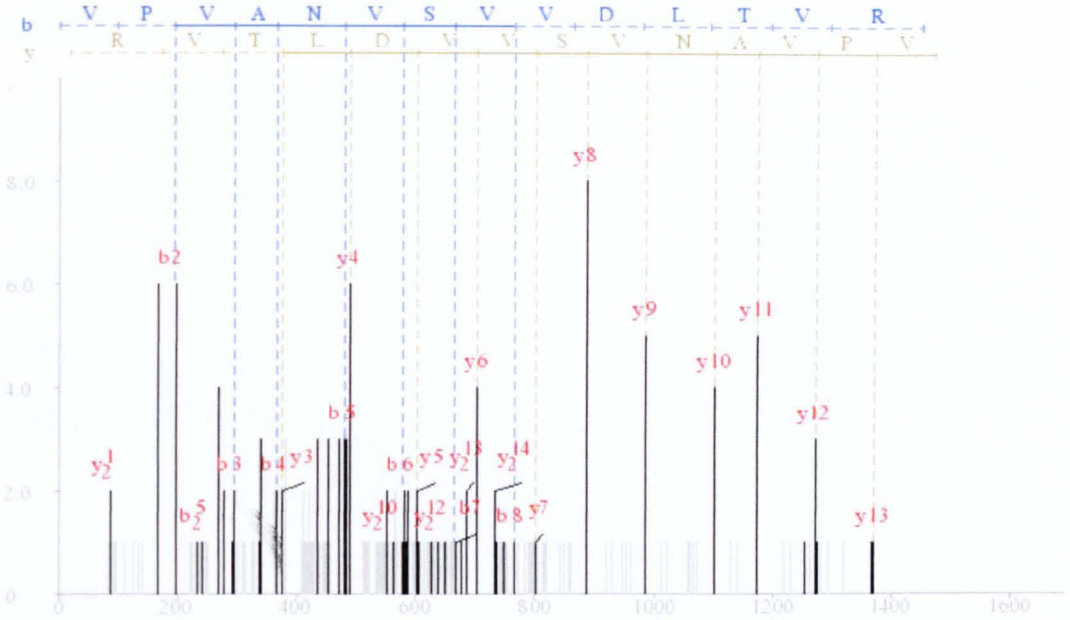
b
y
V P V A N V S V V D L T V R
R V T L D M M S V N A V P V
y8
b2
y4
y9
y11
y6
y10
b5
y12
y2 1
b3
b4
y3
b6
y5
y2 13
y2 14
b2 5
y2 10
y2 12
b7
b8
y7
y13
8.0
6.0
4.0
2.0
0
0
200
400
600
800
1000
1200
1400
1600

DIGE spot 2081

Accession Number: Bmb017629

Protein: Proteasome beta 3 subunit

Peptides: 4

Spectra: 36

Coverage: 22.4%

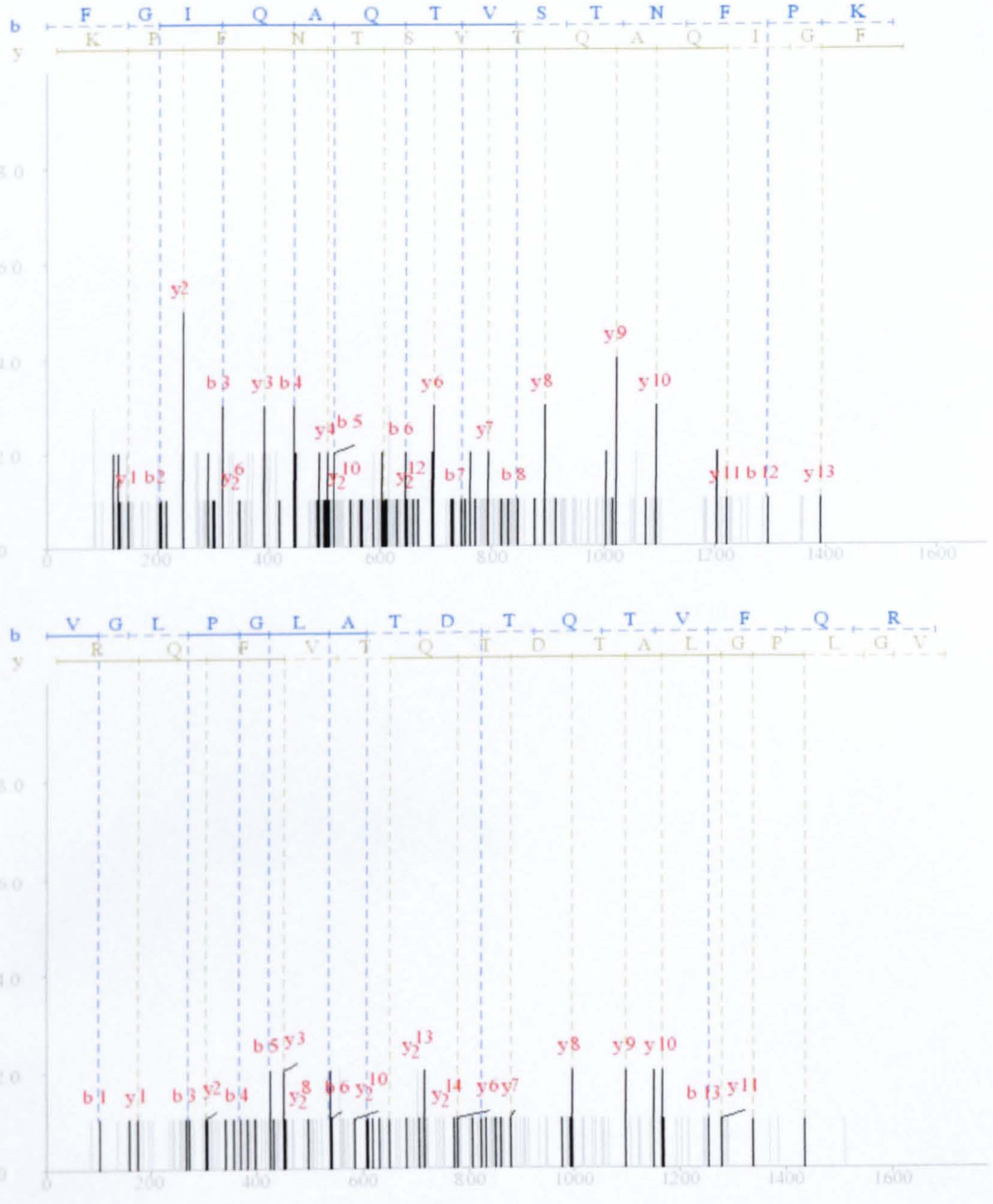

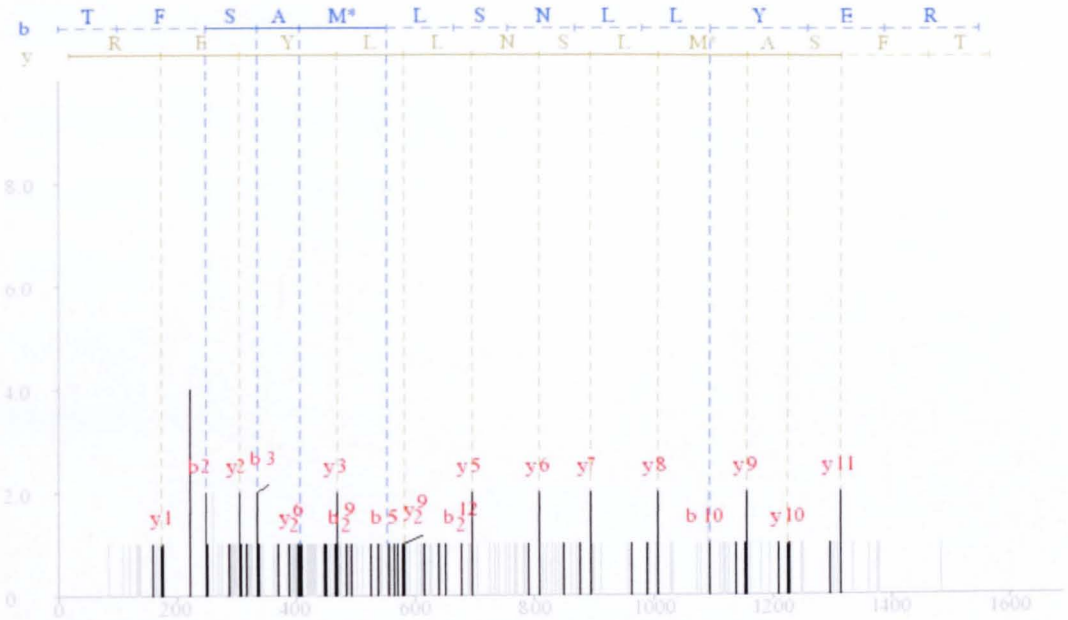
b T F S A M* L S N L L Y E R
y R E Y L L N S L M A S F T
8.0
6.0
4.0
2.0
0
0 200 400 600 800 1000 1200 1400 1600
b2 y2 b3 y3 y5 y6 y7 y8 y9 y11
y1 b5 b10 y10

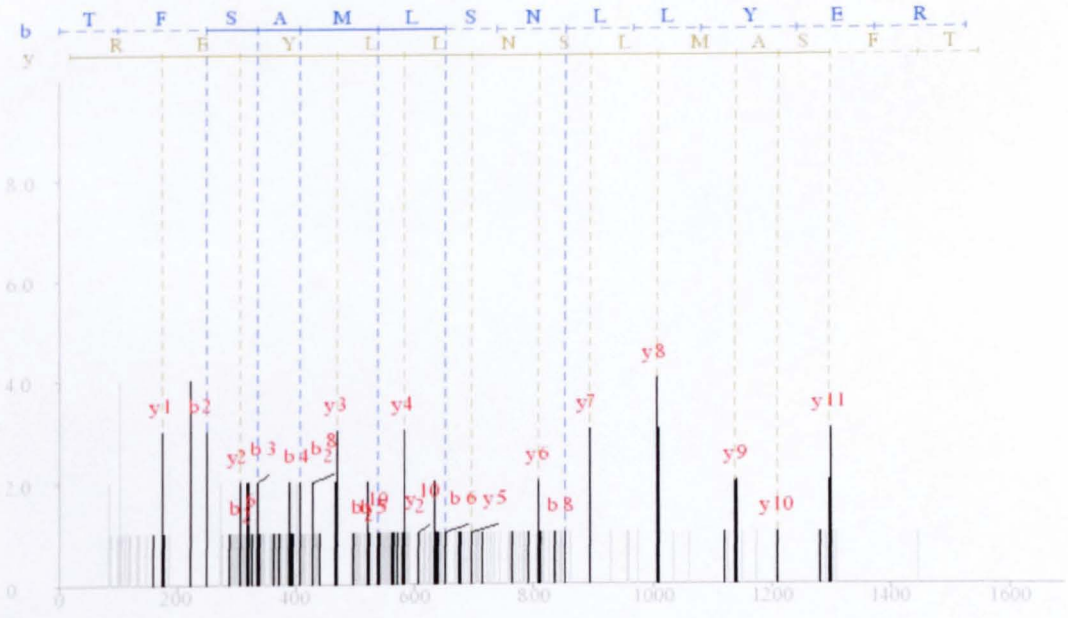
b T F S A M L S N L L Y E R
y R E Y L L N S L M A S F T
8.0
6.0
4.0
2.0
0
0 200 400 600 800 1000 1200 1400 1600
y8
y1 b2 y3 y4 y7 y11
y2 b3 b4 y6 y9
y10 b6 y5 b8

DIGE spot 2288

Accession Number: Bmb002691

Protein: Thiol peroxiredoxin

Peptides: 2

Spectra: 1

Coverage: 14.3%

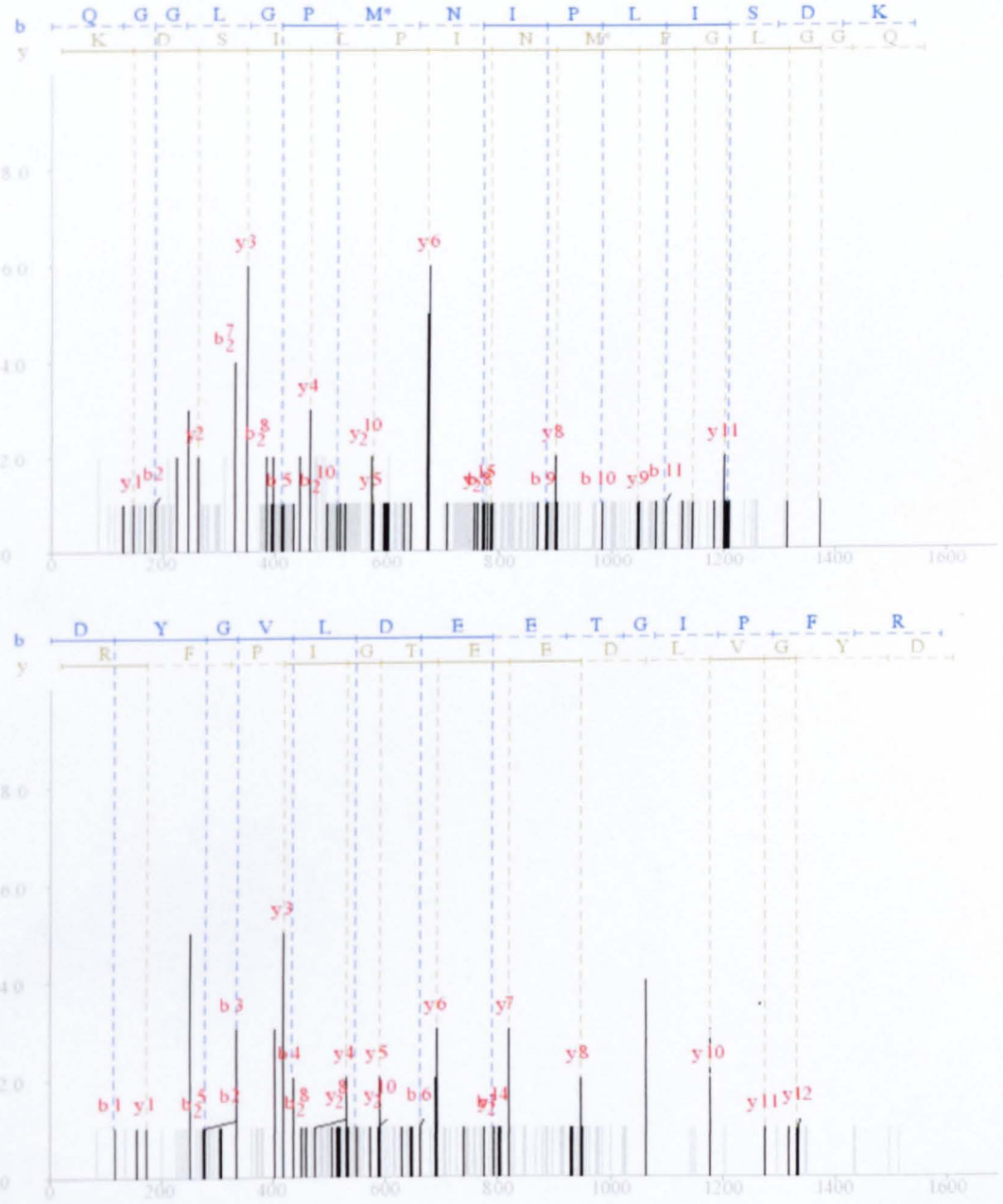

DIGE spot 2366

Accession Number: Bmb030447

Protein: Proteasome beta 6 subunit

Peptides: 1

Spectra: 3

Coverage: 4.9%

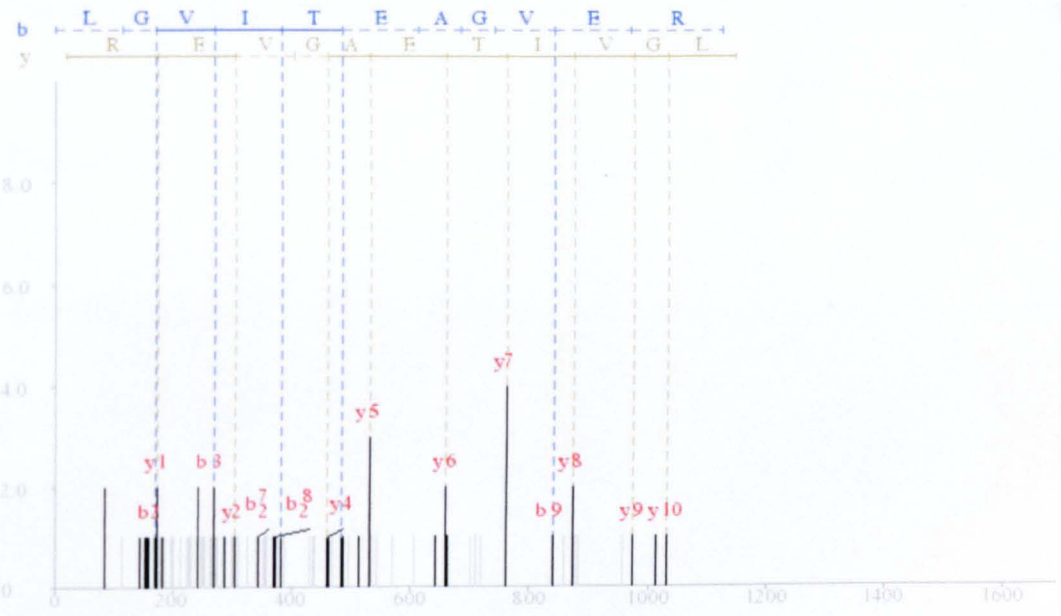

§

APPENDIX 5

Bombyx mori BM36 cell iTRAQ MASCOT results

Protein: Myosin

Peptide sequence: KAPDFVFFAPR

MOWSE score indicating identity: 31

Actual MOWSE score: 48

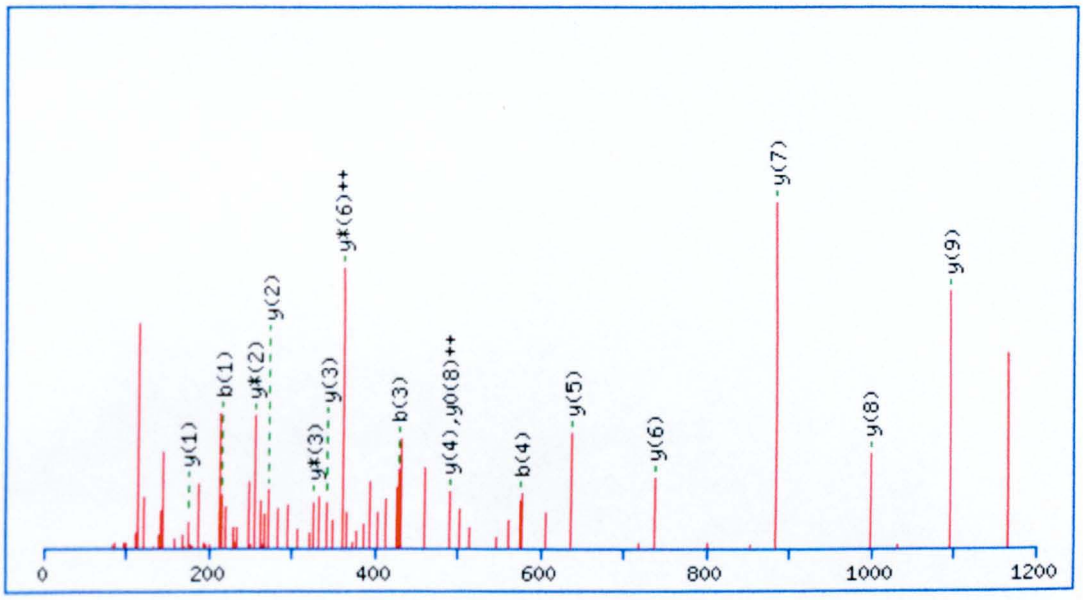

Protein: Hsp70

Peptide sequence: KFELTGIPPARG

MOWSE score indicating identity: 31

Actual MOWSE score: 41

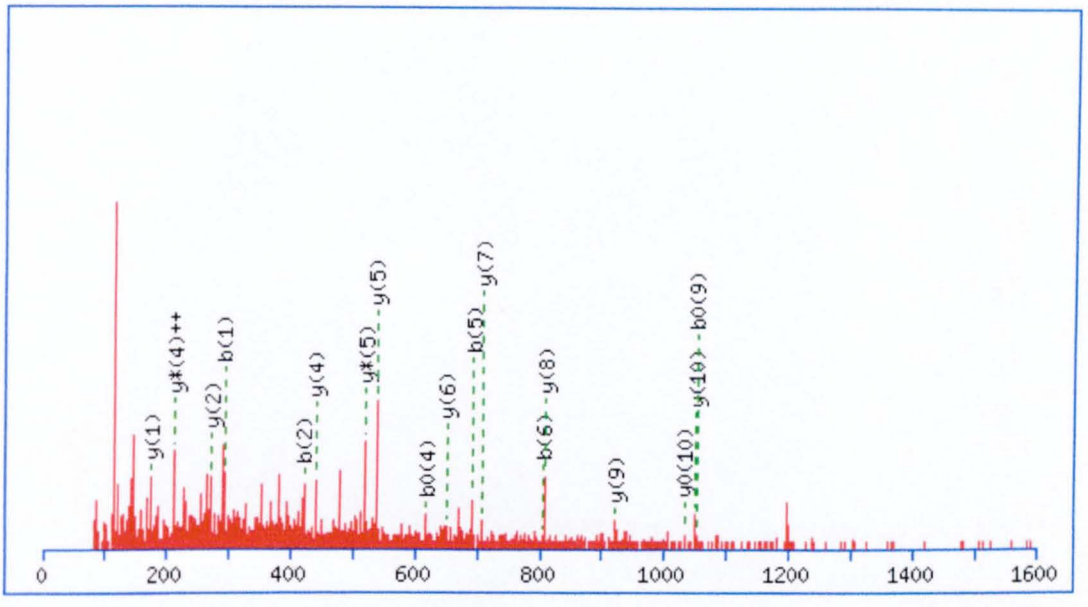

Protein: Hsp70

Peptide sequence: KDAGTISGLLNVLRI

MOWSE score indicating identity: 31

Actual MOWSE score: 32

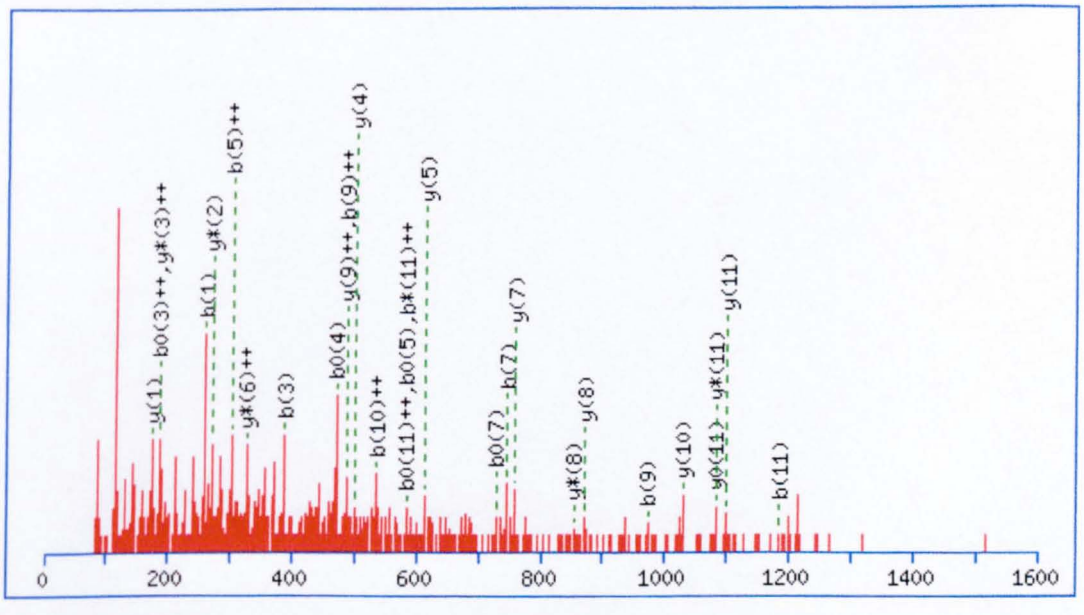

Protein: Elongation factor 1 alpha

Peptide sequence: KGWTIDRK

MOWSE score indicating identity: 31

Actual MOWSE score: 32

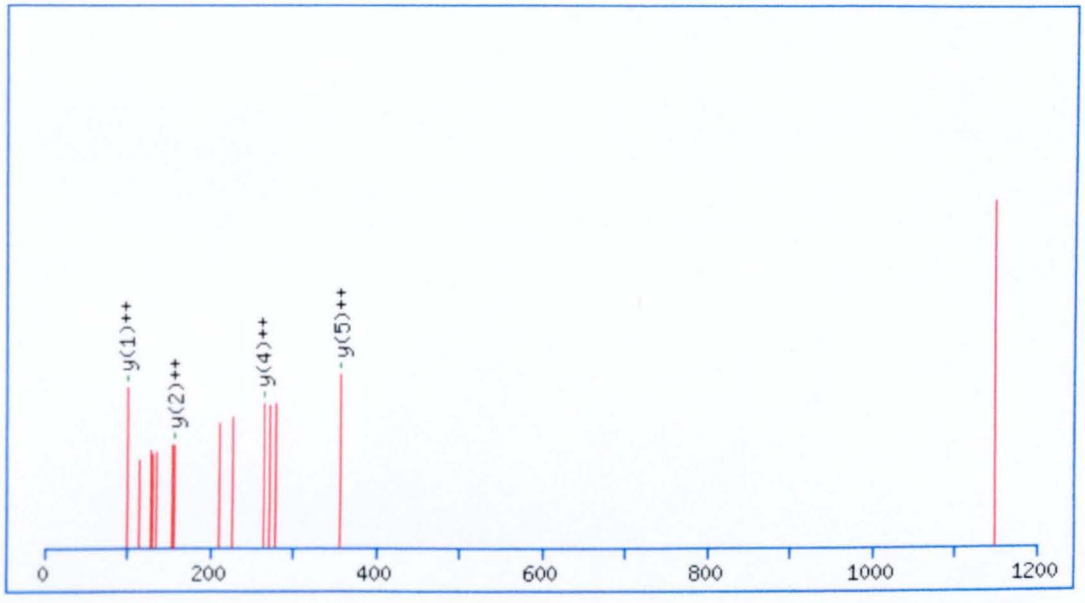

Protein: Elongation factor 1 alpha

Peptide sequence: KIGGIGTPVPGRV

MOWSE score indicating identity: 31

Actual MOWSE score: 42

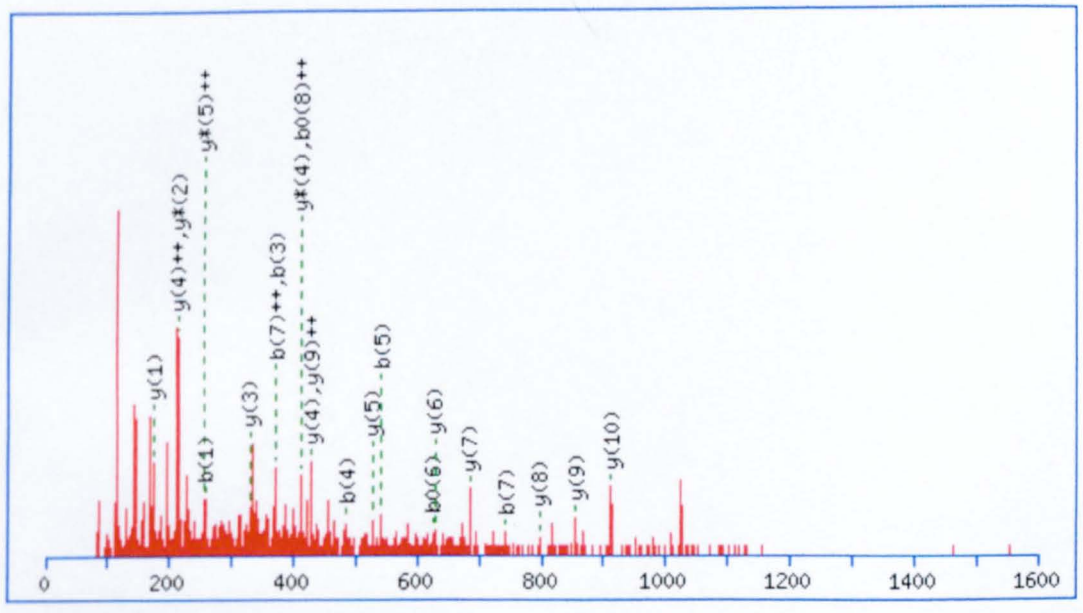

Protein: Tubulin

Peptide sequence: RLIGQIVSSITASLR

MOWSE score indicating identity: 31

Actual MOWSE score: 55

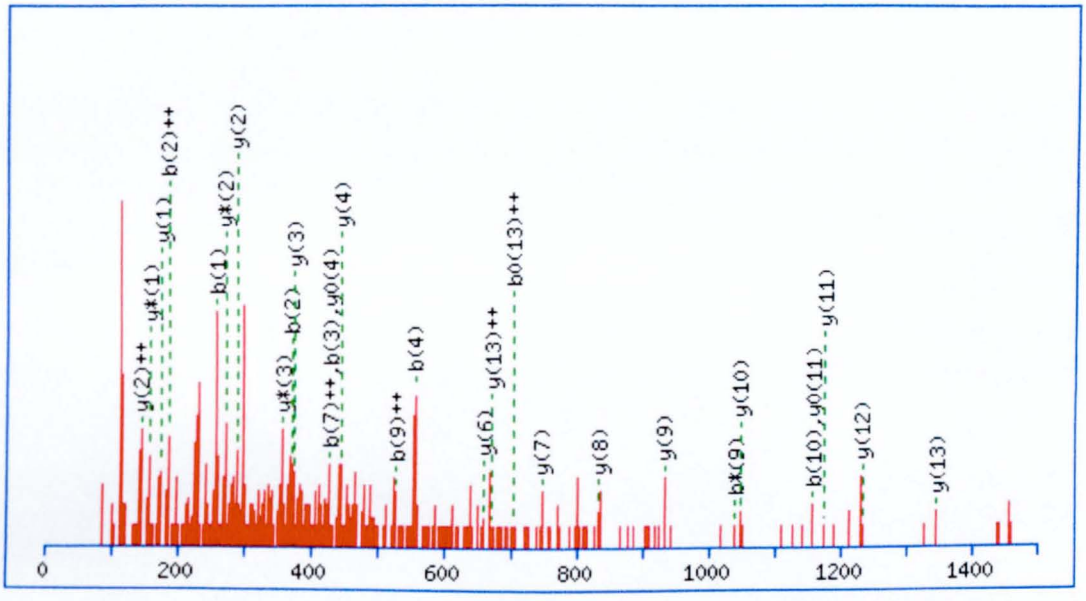

REFERENCES

Aggarwal, K., Choe, L. H. and Lee, K. H. (2006) Shotgun proteomics using the iTRAQ isobaric tags. Brief Funct Genomic Proteomic. **5**, 112-120

Alban, A., David, S. O., Bjorkesten, L., Andersson, C., Sloge, E., Lewis, S. and Currie, I. (2003) A novel experimental design for comparative two-dimensional gel analysis: two-dimensional difference gel electrophoresis incorporating a pooled internal standard. Proteomics. **3**, 36-44

Al-Mushrif, S. and Jones, B. M. (1998) A study of the prevalence of hydrogen peroxide generating Lactobacilli in bacterial vaginosis: the determination of H2O2 concentrations generated, in vitro , by isolated strains and the levels found in vaginal secretions of women with and without infection. J Obstet Gynaecol. **18**, 63-67

Alnouti, Y. and Klaassen, C. D. (2008) Tissue distribution, ontogeny, and regulation of aldehyde dehydrogenase (Aldh) enzymes mRNA by prototypical microsomal enzyme inducers in mice. Toxicol Sci. **101**, 51-64

Altman, G. H., Diaz, F., Jakuba, C., Calabro, T., Horan, R. L., Chen, J., Lu, H., Richmond, J. and Kaplan, D. L. (2003) Silk-based biomaterials. Biomaterials. **24**, 401-416

Altschul, S. F., Gish, W., Miller, W., Myers, E. W. and Lipman, D. J. (1990) Basic local alignment search tool. J Mol Biol. **215**, 403-410

Arunkumar, K. P., Metta, M. and Nagaraju, J. (2006) Molecular phylogeny of silkmoths reveals the origin of domesticated silkmoth, Bombyx mori from Chinese Bombyx mandarina and paternal inheritance of Antheraea proylei mitochondrial DNA. Mol Phylogenet Evol. **40**, 419-427

Audsley, N., Matthews, J., Nachman, R. J. and Weaver, R. J. (2008) Transepithelial flux of an allatostatin and analogs across the anterior midgut of Manduca sexta larvae in vitro. Peptides. **29**, 286-294

Bader, N. and Grune, T. (2006) Protein oxidation and proteolysis. Biol Chem. **387**, 1351-1355

Bar-Nun, S., Kreibich, G., Adesnik, M., Alterman, L., Negishi, M. and Sabatini, D. D. (1980) Synthesis and insertion of cytochrome P-450 into endoplasmic reticulum membranes. Proc Natl Acad Sci U S A. **77**, 965-969

Beer, J., Muschler,R., Kass,D. and Somarriba,E. (1998) Shade managment in coffee and cacao planatations. Agyoforesty systems. **38**, 139-164

Benjamin, I. J. and McMillan, D. R. (1998) Stress (heat shock) proteins: molecular chaperones in cardiovascular biology and disease. Circ Res. **83**, 117-132

Berg, J. S., Powell, B. C. and Cheney, R. E. (2001) A millenium myosin census. Mol. Biol. Cell **12**, 780-794

Black, B. C., Hollingworth, R.M., Ahammadsahib, K.I., Kukel, C.D. and Donovan, S. (1994) Insecticidal action and mitochondrial uncoupling activity of AC-303,630 and related halogenated pyrroles. Pestici. Biochem. Phys. **50**, 115-128

Blank, M. and Shiloh, Y. (2007) Programs for cell death: apoptosis is only one way to go. Cell Cycle. **6**, 686-695

Bradford, M. M. (1976) A Rapid and Sensitive Method for the Quantitation of Microgram Quantities of Protein Utilizing the Principle of Protein-Dye Binding. Anal. Biochem. **72**:248-254.

Bustin, S. A. (2000) Absolute quantification of mRNA using real-time reverse transcription polymerase chain reaction assays. J Mol Endocrinol. **25**, 169-193

Cappellozza, L., Cappellozza, S., Saviane, A. and Sbrenna, G. (2005) Artificial diet rearing system for the silkworm Bombyx mori (Lepidoptera: Bombycidae): effect of vitamin C deprivation on larval growth and cocoon production. Appl. Entom. Zoo. **40**, 405-412.

Chae, H. Z., Chung, S. J. and Rhee, S. G. (1994) Thioredoxin-dependent peroxide reductase from yeast. J Biol Chem. **269**, 27670-27678

Chang, H. Y. and Yang, X. (2000) Proteases for cell suicide: functions and regulation of caspases. Microbiol Mol Biol Rev. **64**, 821-846

Chen, X., Sun, L., Yu, Y., Xue, Y. and Yang, P. (2007) Amino acid-coded tagging approaches in quantitative proteomics. Expert Rev Proteomics. **4**, 25-37

Cook, A., Bono, F., Jinek, M. and Conti, E. (2007) Structural biology of nucleocytoplasmic transport. Annu Rev Biochem. **76**, 647-671

Copping, L. G. and Duke, S. O. (2007) Natural products that have been used commercially as crop protection agents. Pest Manag Sci. **63**, 524-554

Coux, O., Tanaka, K. and Goldberg, A. L. (1996) Structure and functions of the 20S and 26S proteasomes. Annu Rev Biochem. **65**, 801-847

De Ruijter, N. C. A. E. (1998) Actin-binding proteins in plant cells. Plant Biol. **1**, 26-35

Denholm, I. and Rowland, M. W. (1992) Tactics for managing pesticide resistance in arthropods: theory and practice. Annu Rev Entomol. **37**, 91-112

Devine, G. J. (2007) Insecticide use: Contexts and ecological consequences. Agriculture and human values. **24**, 281-306

Dierks, E. A., Davis, S. C. and Ortiz de Montellano, P. R. (1998) Glu-320 and Asp-323 are determinants of the CYP4A1 hydroxylation regiospecificity and resistance to inactivation by 1-aminobenzotriazole. Biochemistry. **37**, 1839-1847

Edman, P. (1949) A method for the determination of the amino acid sequence in peptides. Arch. Biochem. Biophys. **22**, 475–476

Esterbauer, H., Schaur, R. J. and Zollner, H. (1991) Chemistry and biochemistry of 4-hydroxynonenal, malonaldehyde and related aldehydes. Free Radic Biol Med. **11**, 81-128

Falkner, J. A., Falkner, J. W. and Andrews, P. C. (2007) ProteomeCommons.org IO Framework: reading and writing multiple proteomics data formats. Bioinformatics. **23**, 262-263

Fenn, J. B., Mann, M., Meng, C. K., Wong, S. F. and Whitehouse, C. M. (1989) Electrospray ionization for mass spectrometry of large biomolecules. Science. **246**, 64-71

Feyereisen, R. (1999) Insect P450 enzymes. Annu. Rev. Entom. **44,** 507-533.

Feyereisen, R., Langry, K.C. and Oritz de Montellano, P.R. (1984) Self-catalyzed destruction of insect cytochrome P-450. Insect Biochem **14**, 19-26

Field, L. M., Devonshire, A. L. and Forde, B. G. (1988) Molecular evidence that insecticide resistance in peach-potato aphids (Myzus persicae Sulz.) results from amplification of an esterase gene. Biochem J. **251**, 309-312

Fossati, G., Bucknall, R. C. and Edwards, S. W. (2002) Insoluble and soluble immune complexes activate neutrophils by distinct activation mechanisms: changes in functional responses induced by priming with cytokines. Ann Rheum Dis. **61**, 13-19

Fothergill-Gilmore, L. A. M. (1993) Evolution of glycolysis. Progr. Biophys. Mol. Biol. **59**, 105-235

Frank, A., Tanner, S., Bafna, V. and Pevzner, P. (2005) Peptide sequence tags for fast database search in mass-spectrometry. J. Proteome Res. **4**, 1287-1295

Fujisawa, T. a. K., T. (2005) Oxidative activation and degredation of organophosphorus pesticides mediated by iron porphyrins. J. Pestic. Sci. **30**, 103-110

Gencsoylu, I., Liu, W., Usmani, K. A. and Knowles, C. O. (2004) Toxicological studies of the carbamates methomyl and bendiocarb in the bulb mite Rhizoglyphus echinopus. Exp. App. Acar. **22,** 157-166.

Ginzinger, D. G. (2002) Gene quantification using real-time quantitative PCR: an emerging technology hits the mainstream. Exp Hematol. **30**, 503-512

Goldsmith, M. R., Shimada, T. and Abe, H. (2005) The genetics and genomics of the silkworm, Bombyx mori. Annu Rev Entomol. **50**, 71-100

Gorg, A., Boguth, G., Obermaier, C. and Weiss, W. (1998) Two-dimensional electrophoresis of proteins in an immobilized pH 4-12 gradient. Electrophoresis. **19**, 1516-1519

Goyret, J. and Raguso, R. A. (2006) The role of mechanosensory input in flower handling efficiency and learning by Manduca sexta. J Exp Biol. **209**, 1585-1593

Graham, S. E. and Peterson, J. A. (1999) How similar are P450s and what can their differences teach us? Arch Biochem Biophys. **369**, 24-29

Graham-Lorence, S. and Peterson, J. A. (1996) P450s: structural similarities and functional differences. FASEB J. **10**, 206-214

Grant, D. F. and Hammock, B. D. (1992) Genetic and molecular evidence for a trans-acting regulatory locus controlling glutathione S-transferase-2 expression in Aedes aegypti. Mol Gen Genet. **234**, 169-176

Graves, P. R. and Haystead, T. A. (2002) Molecular biologist's guide to proteomics. Microbiol Mol Biol Rev. **66**, 39-63

Grune, T., Reinheckel, T. and Davies, K. J. (1997) Degradation of oxidized proteins in mammalian cells. Faseb J. **11**, 526-534

Grune, T., Reinheckel, T. and Davies, K. J. (1997) Degradation of oxidised proteins in mammalian cells. FASEB J. **11**, 526-534

Gygi, S. P., Rochon, Y., Franza, B. R. and Aebersold, R. (1999) Correlation between protein and mRNA abundance in yeast. Mol. Cell Biol. **19**, 1720-1730.

Habermann, B., Oegema, J., Sunyaev, S. and Shevchenko, A. (2004) The power and the limitations of cross-species protein identification by mass spectrometry-driven sequence similarity searches. Mol Cell Proteomics. **3**, 238-249

Halliwell, B. and Gutteridge, JM. (1989) Role of free radicals and catalytic metal ions in human disease: an overview. *Methods Enzymol.* **186**, 1–85

Hara, M. R., Cascio, M. B. and Sawa, A. (2006) GAPDH as a sensor of NO stress. Biochim Biophys Acta. **1762**, 502-509

Hardstone, M. C., Leichter, C., Harrington, L.C., Kasai, S., Tomita, T. and Scott, J.G. (2007) Cytochrome P450 monooxygenase-mediated permethrin resistance confers limited and larval specific cross-resistance in the southern horse mosquito, *Culex pipiens quinquefasciatus.* Pestisci biochem phys. **89**, 175-184

Harford, J. B. and Morris, D. R. (1997) mRNA metabolism and post-transcriptional gene regulation. Wiley-Liss, UK.

Hartl, F. U. (1996) Molecular chaperones in cellular protein folding. Nature. **381**, 571-579

Hemingway, J. (2000) The molecular basis of two contrasting metabolic mechanisms of insecticide resistance. Insect Biochem Mol Biol. **30**, 1009-1015

Hemingway, J., Hawkes, N. J., McCarroll, L. and Ranson, H. (2004) The molecular basis of insecticide resistance in mosquitoes. Insect Biochem Mol Biol. **34**, 653-665

Hemingway, J. and Karunaratne, S. H. (1998) Mosquito carboxylesterases: a review of the molecular biology and biochemistry of a major insecticide resistance mechanism. Med Vet Entomol. **12**, 1-12

Hodgson, E. and Rose, R. L. (2006) Organophosphorus chemicals: potent inhibitors of the human metabolism of steroid hormones and xenobiotics. Drug Metab Rev. **38**, 149-162

Holloway, J. D., Bradley, J. D. and Carter, D. J. (1987) 1. Lepidoptera. Wallingford, C.A.B. International, British Museum Natural History

Hughes, I. and Hunter, D. (2001) Techniques for analysis and purification in high-throughput chemistry. Curr Opin Chem Biol. **5**, 243-247

Huitorel, P. and Pantaloni, D. (1985) Bundling of microtubules by glyceraldehyde-3-phosphate dehydrogenase and its modulation by ATP. Eur J Biochem. **150**, 265-269

Isayama, S., Saito, S., Kuroda, K., Umeda, K. and Kasamatsu, K. (2005) Pyridalyl, a novel insecticide: potency and insecticidal selectivity. Arch Insect Biochem Physiol. **58**, 226-233

Karp, N. A. and Lilley, K. S. (2005) Maximising sensitivity for detecting changes in protein expression: experimental design using minimal CyDyes. Proteomics. **5**, 3105-3115

Karp, N. A., Spencer, M., Lindsay, H., O'Dell, K. and Lilley, K. S. (2005) Impact of replicate types on proteomic expression analysis. J Proteome Res. **4**, 1867-1871

Klingenberg, M. (1958) Pigments of rat liver microsomes. Arch Biochem Biophys. **75**, 376-386

Kukreja, R. C., Kontos, M. C., Loesser, K. E., Batra, S. K., Qian, Y. Z., Gbur, C. J., Jr., Naseem, S. A., Jesse, R. L. and Hess, M. L. (1994) Oxidant stress increases heat shock protein 70 mRNA in isolated perfused rat heart. Am J Physiol. **267**, H2213-2219

Kumar, S., Thomas, A., Sahgal, A., Verma, A., Samuel, T. and Pillai, M. K. (2002) Effect of the synergist, piperonyl butoxide, on the development of deltamethrin resistance in yellow fever mosquito, Aedes aegypti L. (Diptera: Culicidae). Arch Insect Biochem Physiol. **50**, 1-8

Labeit, S. and Kolmerer, B. (1995) Titins: giant proteins in charge of muscle ultrastructure and elasticity. Science. **270**, 293-296

Lee, K. S., Kim, S. R., Park, N. S., Kim, I., Kang, P. D., Sohn, B. H., Choi, K. H., Kang, S. W., Je, Y. H., Lee, S. M., Sohn, H. D. and Jin, B. R. (2005) Characterization of a silkworm thioredoxin peroxidase that is induced by external temperature stimulus and viral infection. Insect Biochem Mol Biol. **35**, 73-84

Lehner, I., Niehof, M. and Borlak, J. (2003) An optimized method for the isolation and identification of membrane proteins. Electrophoresis. **24**, 1795-1808

Levi, P. E., Hollingworth, R.M. and Hodgson, E. (1988) Differences in oxidative dearylation and desulfuration of Fenitrothion by cytochrome *p*-450 isozymes and in the subsequent inhibition of monooxygenase activity. Pestisci biochem phys. **32**, 224-231

Li, X., Schuler, M. A. and Berenbaum, M. R. (2007) Molecular mechanisms of metabolic resistance to synthetic and natural xenobiotics. Annu Rev Entomol. **52**, 231-253

Lilley, K. S. and Friedman, D. B. (2004) All about DIGE: quantification technology for differential-display 2D-gel proteomics. Expert Rev Proteomics. **1**, 401-409

Lim, Y. S., Cha, M. K., Kim, H. K., Uhm, T. B., Park, J. W., Kim, K. and Kim, I. H. (1993) Removals of hydrogen peroxide and hydroxyl radical by thiol-specific antioxidant protein as a possible role in vivo. Biochem Biophys Res Commun. **192**, 273-280

Liska, A. J., Popov, A. V., Sunyaev, S., Coughlin, P., Habermann, B., Shevchenko, A., Bork, P., Karsenti, E. and Shevchenko, A. (2004) Homology-based functional proteomics by mass spectrometry: application to the Xenopus microtubule-associated proteome. Proteomics. **4**, 2707-2721

Livak, K. J. and Schmittgen, T. D. (2001) Analysis of relative gene expression data using real-time quantitative PCR and the 2(-Delta Delta C(T)) Method. Methods. **25**, 402-408

Lygerou, Z., Mitchell, P., Petfalski, E., Seraphin, B. and Tollervey, D. (1994) The POP1 gene encodes a protein component common to the RNase MRP and RNase P ribonucleoproteins. Genes Dev. **8**, 1423-1433

Mackey, A. J., Haystead, T. A. and Pearson, W. R. (2002) Getting more from less: algorithms for rapid protein identification with multiple short peptide sequences. Mol Cell Proteomics. **1**, 139-147

Marchler-Bauer, A., Panchenko, A. R., Shoemaker, B. A., Thiessen, P. A., Geer, L. Y. and Bryant, S. H. (2002) CDD: a database of conserved domain alignments with links to domain three-dimensional structure. Nucleic Acids Res. **30**, 281-283

Marouga, R., David, S. and Hawkins, E. (2005) The development of the DIGE system: 2D fluorescence difference gel analysis technology. Anal Bioanal Chem. **382**, 669-678

Mary, J., Vougier, S., Picot, C. R., Perichon, M., Petropoulos, I. and Friguet, B. (2004) Enzymatic reactions involved in the repair of oxidized proteins. Exp Gerontol. **39**, 1117-1123

McGinnis, S. and Madden, T. L. (2004) BLAST: at the core of a powerful and diverse set of sequence analysis tools. Nucleic Acids Res. **32**, W20-25

Miller, M. L., Andringa, A., Dixon, K. and Carty, M. P. (2002) Insights into UV-induced apoptosis: ultrastructure, trichrome stain and spectral imaging. Micron. **33**, 157-166

Morero, R. D., Vinals, A. L., Bloj, B. and Farias, R. N. (1985) Fusion of phospholipid vesicles induced by muscle glyceraldehyde-3-phosphate dehydrogenase in the absence of calcium. Biochemistry. **24**, 1904-1909

Moriya, K., Setsuko, H., Kobayashi, J., Ozoe, Y., Saito, S. and Utsumi, T. (2008) Pyridalyl inhibits cellular protein synthesis in insect, but not mammalian, cell lines. Arch. Ins. Bio. Chem. Phys. **69**, 22-31

Morrow, G. and Tanguay, R. M. (2003) Heat shock proteins and aging in Drosophila melanogaster. Semin Cell Dev Biol. **14**, 291-299

Nagaraju, J. M. R. (2002) Silkworm genomics- progress and prospects. Curr Sci. **83**, 415-425

Nakatsukasa, K. and Brodsky, J. L. (2008) The recognition and retrotranslocation of misfolded proteins from the endoplasmic reticulum. Traffic. **9**, 861-870

Nelson,D.R., Kamataki,T., Waxman,D.J., Guengerich,F.P., Estabrook,R.W., Feyereisen,R., Gonzalez,F.J. Coon,M.J., Gunsalus,I.C., Gotoh,O., Okuda,K. and Nebert,D.W.(1993) The P450 superfamily: update on new sequences, gene mapping, accession numbers, early trivial names of enzymes and nomenclature. *DNA and Cell Biol.* 12:1- 51.

Nicholson, D. W. and Thornberry, N. A. (1997) Caspases: killer proteases. Trends Biochem Sci. **22**, 299-306

Ochou, G. O., Mathews, G. A. and Mumford, J. D. (1998) Farmers knowledge and perception of cotton insect pest problems in Cote d'Ivoire. Int. J. Pest Manag. **44**, 5-9

O'Farrell, P. H. (1975) High resolution two-dimensional electrophoresis of proteins. J Biol Chem. **250**, 4007-4021

Omura, T. (1999) Forty years of cytochrome P450. Biochem Biophys Res Commun. **266**, 690-698

Oppenoorth, F. J. (1984) Biochemistry of insecticide resistance. Pestici biochem phys. **22**, 187-193

Oppenoorth, F. J. and Van, A. (1960) Allelic genes in the housefly producing modified enzymes that cause organophosphate resistance. Science. **132**, 298-299

Ortiz de Montellano, P. R. and Mathews, J. M. (1981) Autocatalytic alkylation of the cytochrome P-450 prosthetic haem group by 1-aminobenzotriazole. Biochem. J. **195**, 761-764.

Pan, G. and Dutta, H. M. (1998) The inhibition of brain acetylcholinesterase activity of juvenile largemouth bass Micropterus salmoides by sublethal concentrations of diazinon. Environ Res. **79**, 133-137

Patton, W. F. (2002) Detection technologies in proteome analysis. J Chromatogr B Analyt Technol Biomed Life Sci. **771**, 3-31

Patton, W. F. (1999) Proteome analysis. II. Protein subcellular redistribution: linking physiology to genomics via the proteome and separation technologies involved. J Chromatogr B Biomed Sci Appl. **722**, 203-223

Perkins, D. N., Pappin, D. J., Creasy, D. M. and Cottrell, J. S. (1999) Probability-based protein identification by searching sequence databases using mass spectrometry data. Electrophoresis. **20**, 3551-3567

Pimental, D. (2005) Environmental and economic costs of the application of pesticides primarily in the United States. Environ Develop Sustainabil. **7**, 229-252

Poullet, P., Carpentier, S. and Barillot, E. (2007) myProMS, a web server for management and validation of mass spectrometry-based proteomic data. Proteomics. **7**, 2553-2556

Potter, H. H. (1943) The effects of war gases on water supplies decontamination. J. New Eng. W. W. Assc. **57**, 137-162

Putz, S., Reinders, J., Reinders, Y. and Sickmann, A. (2005) Mass spectrometry-based peptide quantification: applications and limitations. Expert Rev Proteomics. **2**, 381-392

Radyuk, S. N., Klichko, V. I., Spinola, B., Sohal, R. S. and Orr, W. C. (2001) The peroxiredoxin gene family in Drosophila melanogaster. Free Radic Biol Med. **31**, 1090-1100

Raghu, S. C. (2007) Understanding the ghost of *Cactoblastis* past: Historical clarifications on a poster child of classical biological control. Bioscience. **57**, 699-705

Ray, D. E. and Fry, J. R. (2006) A reassessment of the neurotoxicity of pyrethroid insecticides. Pharmacol Ther. **111**, 174-193

Reed, V. S., Wastney, M. E. and Yang D. C. (1994) Mechanisms of the transfer of aminoacyl-tRNA from aminoacyl-tRNA synthetase to the elongation factor 1 alpha. J. Biol. Chem. **269**, 32932-32936

Rees, H. H. (1995) Ecdysteroid biosynthesis and inactivation in relation to function. Eur. J. Entomol. **92**, 9-39

Rock, K. L., Gramm, C., Rothstein, L., Clark, K., Stein, R., Dick, L., Hwang, D. and Goldberg, A. L. (1994) Inhibitors of the proteasome block the degradation of most cell proteins and the generation of peptides presented on MHC class I molecules. Cell. **78**, 761-771

Roepstorff, P. and Fohlman, J. (1984) Proposal for a common nomenclature for sequence ions in mass spectra of peptides. Biomed. Mass Spectrom. **11,** 601

Ross, P. L., Huang, Y. N., Marchese, J. N., Williamson, B., Parker, K., Hattan, S., Khainovski, N., Pillai, S., Dey, S., Daniels, S., Purkayastha, S., Juhasz, P., Martin, S., Bartlet-Jones, M., He, F., Jacobson, A. and Pappin, D. J. (2004) Multiplexed protein quantitation in Saccharomyces cerevisiae using amine-reactive isobaric tagging reagents. Mol Cell Proteomics. **3**, 1154-1169

Saito, S. (2005) Effects of pyridayl on ATP concentrations in cultured Sf9 cells. J Pestic Sci. **30**, 403-405

Saito, S., Sakamoto, N. and Umeda, K. (2005) Effects of Pyridayl, a novel insecticidal agent, on cultured Sf9 cells. J Pestic Sci. **30**, 17-21

Saito, S., Isayama, S., Sakamoto, N. and Umeda, K. (2004) Insecticidal activity of Pyridalyl: Acute and sub-acute symptoms in *Spodoptera litura* larvae. J Pestic Sci. **29**, 372-375

Saito, S., Yoshioka, T. and Umeda, K. (2006) Ultrastructural effects of Pyridayl, an insecticidal agent, on epidermal cells of *Spodoptera Litura* larvae and cultured insect cells Sf9. J Pestic Sci. **31**, 335-338

Sakamoto, N., Saito, S., Hirose, T., Suzuki, M., Matsuo, S., Izumi, K., Nagatomi, T., Ikegami, H., Umeda, K., Tsushima, K. and Matsuo, N (2003) The discovery of Pyridalyl: a novel insecticidal agent for controlling lepidopterous pests. Pest Manag. Sci. **60,** 25-34.

Sambrook, J. and Russel, D. (2001) Molecular cloning: a laboratory manual. 3rd Edition. Cold Spring Harbour Laboratory Press, USA.

Santoni, V., Molloy, M. and Rabilloud, T. (2000) Membrane proteins and proteomics: un amour impossible? Electrophoresis. **21**, 1054-1070

Sargison, N., Roger, P., Stubbins, L., Baber, P. and Morris, P. (2007) Controlling sheep scab by eradication. Vet. Rec., 491-492

Scott, J. G. (1999) Cytochromes P450 and insecticide resistance. Insect Biochem Mol Biol. **29**, 757-777

Scott, J. G., Liu, N. and Wen, Z. (1998) Insect cytochromes P450: diversity, insecticide resistance and tolerance to plant toxins. Comp Biochem Physiol C Pharmacol Toxicol Endocrinol. **121**, 147-155

Shevchenko, A., Sunyaev, S., Loboda, A., Shevchenko, A., Bork, P., Ens, W. and Standing, K. G. (2001) Charting the proteomes of organisms with unsequenced genomes by MALDI-quadrupole time-of-flight mass spectrometry and BLAST homology searching. Anal Chem. **73**, 1917-1926

Sirover, M. A. (1999) New insights into an old protein: the functional diversity of mammalian glyceraldehyde-3-phosphate dehydrogenase. Biochim Biophys Acta. **1432**, 159-184

Sogorb, M. A. and Vilanova, E. (2002) Enzymes involved in the detoxification of organophosphorus, carbamate and pyrethroid insecticides through hydrolysis. Toxicol Lett. **128**, 215-228

Soranno, T. M. and Sultatos, L. G. (1992) Biotransformation of the insecticide parathion by mouse brain. Toxicol Lett. **60**, 27-37

Stetter, J. and Lieb, F. (2000) Innovation in Crop Protection: Trends in Research. Angew Chem Int Ed Engl. **39**, 1724-1744

Sultatos, L. G. (1991) Metabolic activation of the organophosphorus insecticides chlorpyrifos and fenitrothion by perfused rat liver. Toxicology. **68**, 1-9

Tanner, S., Pevzner, P. A. and Bafna, V. (2006) Unrestrictive identification of post-translational modifications through peptide mass spectrometry. Nat Protoc. **1**, 67-72

Tanner, S., Shu, H., Frank, A., Wang, L. C., Zandi, E., Mumby, M., Pevzner, P. A. and Bafna, V. (2005) InsPecT: identification of posttranslationally modified peptides from tandem mass spectra. Anal Chem. **77**, 4626-4639

Tavaria, M., Gabriele, T., Kola, I. and Anderson, R. L. (1996) A hitchhiker's guide to the human Hsp70 family. Cell Stress Chaperones. **1**, 23-28

Teh, C., . Pang, J. and Ho, C. (2006) Variation of the response of clonal cocoa to attack by cocoa pod borer *Conopomorpha cramerella* (Lepidoptera: Gracillariidae) in Sabah. Crop Protection. **25**, 712-717

Tsur, D., Tanner, S., Zandi, E., Bafna, V. and Pevzner, P. A. (2005) Identification of post-translational modifications by blind search of mass spectra. Nat Biotechnol. **23**, 1562-1567

UN. (1999) The world at six billion. www.un.org/esa/populations/sixbillion/sixbilpart1.pdf

Urlinger, S., Kuchler, K., Meyer, T. H., Uebel, S. and Tampe, R. (1997) Intracellular location, complex formation, and function of the transporter associated with antigen processing in yeast. Eur J Biochem. **245**, 266-272

Vais, H., Williamson, M. S., Devonshire, A. L. and Usherwood, P. N. (2001) The molecular interactions of pyrethroid insecticides with insect and mammalian sodium channels. Pest Manag Sci. **57**, 877-888

Van den Bergh, G. and Arckens, L. (2005) Recent advances in 2D electrophoresis: an array of possibilities. Expert Rev Proteomics. **2**, 243-252

Varshavsky, A. (1996) The N-end rule: functions, mysteries, uses. Proc Natl Acad Sci U S A. **93**, 12142-12149

Vepari, C. K. D.L. (2007) Silk as a biomaterial. Prog. Polym. Sci. **32**, 991-1007

Vermes, I., Haanen, C. and Reutelingsperger, C. (2000) Flow cytometry of apoptotic cell death. J Immunol Methods. **243**, 167-190

Waxman, D. J. (1999) P450 gene induction by structurally diverse xenochemicals: central role of nuclear receptors CAR, PXR, and PPAR. Arch Biochem Biophys. **369**, 11-23

Werck-Reichhart, D. F. R. (2000) Cytochrome P450: a success story. Genome Biol. **1**, 1-9

Whalon, M. E. and Wingerd, B. A. (2003) Bt: mode of action and use. Arch Insect Biochem Physiol. **54**, 200-211

Wheelock, G. E., Shan, G. and Ottea, J. (2005) Overview of carboxylesterases and their role in the metabolism of insecticides. J Pestic Sci. **30**, 75-83

Wiemeyer, S. N., Lamont, T. G., Bunck, C. M., Sindelar, C. R., Gramlich, F. J., Fraser, J. D. and Byrd, M. A. (1984) Organochlorine pesticide, polychlorobiphenyl, and mercury residues in bald eagle eggs--1969-79--and their relationships to shell thinning and reproduction. Arch Environ Contam Toxicol. **13**, 529-549

Wiseman, V., Hawley, W. A., ter Kuile, F. O., Phillips-Howard, P. A., Vulule, J. M., Nahlen, B. L. and Mills, A. J. (2003) The cost-effectiveness of permethrin-treated bed nets in an area of intense malaria transmission in western Kenya. Am J Trop Med Hyg. **68**, 161-167

Wu, A., Ying, Z. and Gomez-Pinilla, F. (2006) Dietary curcumin counteracts the outcome of traumatic brain injury on oxidative stress, synaptic plasticity, and cognition. Exp Neurol. **197**, 309-317

Xia, Q., Cheng, D., Duan, J., Wang, G., Cheng, T., Zha, X., Liu, C., Zhao, P., Dai, F., Zhang, Z., He, N., Zhang, L. and Xiang, Z. (2007) Microarray-based gene expression profiles in multiple tissues of the domesticated silkworm, Bombyx mori. Genome Biol. **8**, R162

Xia, Q., Zhou, Z., Lu, C., Cheng, D., Dai, F., Li, B., Zhao, P., Zha, X., Cheng, T., Chai, C., Pan, G., Xu, J., Liu, C., Lin, Y., Qian, J., Hou, Y., Wu, Z., Li, G., Pan, M., Li, C., Shen, Y., Lan, X., Yuan, L., Li, T., Xu, H., Yang, G., Wan, Y., Zhu, Y., Yu, M., Shen, W., Wu, D., Xiang, Z., Yu, J., Wang, J., Li, R., Shi, J., Li, H., Li, G., Su, J., Wang, X., Li, G., Zhang, Z., Wu, Q., Li, J., Zhang, Q., Wei, N., Xu, J., Sun, H., Dong, L., Liu, D., Zhao, S., Zhao, X., Meng, Q., Lan, F., Huang, X., Li, Y., Fang, L., Li, C., Li, D., Sun, Y., Zhang, Z., Yang, Z., Huang, Y., Xi, Y., Qi, Q., He, D., Huang, H., Zhang, X., Wang, Z., Li, W., Cao, Y., Yu, Y., Yu, H., Li, J., Ye, J., Chen, H., Zhou, Y., Liu, B., Wang, J., Ye, J., Ji, H., Li, S., Ni, P., Zhang, J., Zhang, Y., Zheng, H., Mao, B., Wang, W., Ye, C., Li, S., Wang, J., Wong, G. K. and Yang, H. (2004) A draft sequence for the genome of the domesticated silkworm (Bombyx mori). Science. **306**, 1937-1940

Yan, J. X., Wait, R., Berkelman, T., Harry, R. A., Westbrook, J. A., Wheeler, C. H. and Dunn, M. J. (2000) A modified silver staining protocol for visualization of

proteins compatible with matrix-assisted laser desorption/ionization and electrospray ionization-mass spectrometry. Electrophoresis. **21**, 3666-3672

Yang, J., McCart, C., Woods, D. J., Terhzaz, S., Greenwood, K. G., ffrench-Constant, R. H. and Dow, J. A. (2007) A Drosophila systems approach to xenobiotic metabolism. Physiol Genomics. **30**, 223-231

Yates, J. R., 3rd. (1998) Mass spectrometry and the age of the proteome. J Mass Spectrom. **33**, 1-19

Zhang, W., Ramamoorthy, Y., Kilicarslan, T., Nolte, H., Tyndale, R. F. and Sellers, E. M. (2002) Inhibition of cytochromes P450 by antifungal imidazole derivatives. Drug Metab Dispos. **30**, 314-318

Zieske, L. R. (2006) A perspective on the use of iTRAQ reagent technology for protein complex and profiling studies. J Exp Bot. **57**, 1501-1508